UNIVERSITY OF SOUTHAMPTON

THE INTERACTION OF SEQUENCE-SPECIFIC LIGANDS WITH THE NUCLEOSOME

Kristofer David Leslie

SUBMITTED FOR THE DEGREE OF DOCTOR OF PHILOSOPHY

FACULTY OF SCIENCE
SCHOOL OF BIOLOGICAL SCIENCES

APRIL 2001

UNIVERSITY OF SOUTHAMPTON

ABSTRACT

FACULTY OF SCIENCE

SCHOOL OF BIOLOGICAL SCIENCES

Doctor of Philosophy

THE INTERACTION OF SEQUENCE-SPECIFIC LIGANDS WITH THE NUCLEOSOME

By Kristofer David Leslie

The interaction of sequence specific ligands with DNA has been widely studied and the majority of this research has focused up on the binding of these drugs to free DNA. However, a therapeutic compound that targets DNA must interact with chromatin *in vivo*. Previous work with nucleosomes using reconstituted TyrT DNA, from *E.coli*, demonstrated that in the presence of sequence selective ligands the DNA appeared to rotate by 180° relative to the histone octamer. Since these studies utilised natural DNA, which contains many drug binding sites, only the gross effect of ligand binding could be observed. This work utilises DNA constructs containing drug-binding sites at defined rotational and translational positions, with respect to the histone octamer. Therefore it is possible to assess changes in nucleosome structure in the presence of a defined number of ligand molecules binding at a defined region of the DNA superhelix. The ligands used in this study are the minor groove binder Hoechst 33258 and the bis-intercalator echinomycin. It is observed that Hoechst molecules can bind to sites on the outer surface of the DNA superhelix without altering the structure of the core particle. Echinomycin does not appear to recognise targets in this rotational setting. The interaction of Hoechst and echinomycin with single target sites located on the inner surface of the DNA helix also has little effect up on the structure of the nucleosome. However, it has been observed that the binding of two or three Hoechst molecules to the inner surface appears to alter the rotational position of the DNA superhelix, with respect to the histone octamer, by 180°. This is not observed with echinomycin. However, experiments in which ligand is added during nucleosome reconstitution show that echinomycin inhibits this process with constructs containing two or three inner facing target sites and the level of nucleosome disruption appears to be dependent upon the translational position of the targets. In contrast Hoechst 33258 does not.

Abbreviations

A	adenine
bp	base pairs
BSA	bovine serum albumin
bz	benzimidazole
C	cytosine
dCTP	deoxycytosine triphosphate
CD	circular dichroism
G	guanine
Kda	kilo daltons
9-DAM	9-deoxydoxorubicin
DAP	2,6,-diaminopurine
4-DDM	4-demethoxydaunorubicin
dATP	deoxyadenosine triphosphate
dCTP	deoxycytosine triphosphate
DEPC	diethylpyrocarbonate
dGTP	deoxyguanine triphosphate
dHAT	histone Acetyl-detransferase
DHFR	dihydrofolate reductase
DNA	deoxyribonucleic acid
DNaseI	deoxyribonuclease I
4'-DMA	4'-deoxydoxorubicin
DMSO	dimethylsulfoxide
dTTP	deoxythymidine triphosphate
EDTA	Ethylediaminetetraacetic acid
HAT	histone Acetyl-Transferase
H33258	hoechst 33258
H1	histone H1
H2A	histone H2A
H2B	histone H2B
H3	histone H3
H4	histone H4
H5	histone H5
His	histidine
4'- IAM	4'-deoxy, 4'-iodo-doxorubicin
IPTG	isopropyl ∃-D-thioglactopyranoside
NMR	nuclear magnetic resonance
NOE	nuclear overhauser electron spin
nt	nucleotide
MNase	micrococcal Nuclease
MPE	methidiumpropyl-EDTA
PAGE	polyacrylamide gel electrophoresis
PCR	polymerase chain reaction
PMSF	Phenylmethylsulphonylfluoride
phe	Phenol
rpm	revolutions per minute
T	thymine
TBE	Tris-Borate-EDTA buffer

TE	Tris-EDTA buffer
TEMED	N, N, N', N'-tetramethylethylenediamine
T*m*	melting temperature
X-gal	5-bromo-4-chloro-3-indolyl ß-galactosidase

Preface

The work in this thesis was completed between the dates of October 1997 and November 2000 at the University of Southampton, School of Biological Sciences, Division of Biochemistry and Molecular Biology, Basset Crescent East, Southampton.

I'd like to pass on a special thank you to Claire, James, Bruce, Sarah and Rene for their help and incredible support. Thank you for being such wonderful friends.

Claire I'd like to say that you have my deepest respect...you are, quite simply, the bravest person that I have ever met. Thank you for being who you are.

McBroon thanks for everything! You know what I'm talking about.

Rene, you mad Dutch person, thanks for the constant ideas, discussion and the occasional late night pizza! We should have opened a credit account with Dominos...

Sarah, thanks for letting me ask you constant questions about life the universe and everything. You were very patient oh wise one.

Paul...thanks for being a constant source of amusement!

A special thanks to my wife Natalie. I don't know how you managed to put up with me! I'm very lucky to have you.

Additional thanks go to Dr Markus Winter (*University of Auckland, New Zealand*) and Dr Thierry Lacombe (*University of Geneva, Switzerland*).

Finally, I would also like to thank the remaining people in the lab past and present and my supervisor Prof. Keith Fox. In addition, thank you to the Association for International Cancer Research for funding my PhD.

Contents

1 Introduction

1.1 Why Study the Interaction of Small Ligands with the Nucleosome?

There is an extensive body of literature relating to the binding of small ligands with free DNA. Many of these ligands are potent antibiotics and by virtue of their DNA sequence selectivity, effective anti-tumour compounds. To evaluate the role small ligands might play as potential therapeutic agents, it is necessary to study their interaction in an environment, which mimics that of the cell. The eucaryotic genome is packaged into the cell nucleus as chromatin. In this state the DNA is highly supercoiled and interacts extensively with histone proteins. The conformation of the DNA *in vivo* is vastly different to that of free DNA and hence represents an altered binding substrate for sequence selective ligands. In addition, the interaction of the DNA with histone proteins will mask potential ligand binding sites and alter the manner by which the ligand interacts. This study focuses on the interaction of sequence selective ligands with the nucleosome. Off course, *in vivo* the DNA helix will contain on average, one nucleosome every 200bp, but for simplicity, ligand binding to one nucleosome has been carried out. Previous studies of this type, see below, used DNA containing many ligand binding sites at undefined positions, with respect to the histone octamer. Hence, it was possible only to assess the overall consequences of ligand binding to the nucleosome. This study attempts to clarify some of the issues raised from previous work by using 1-3 ligand binding sites at a defined position on the nucleosome core particle. It is then possible to assess not only the consequences of ligand binding to this complex but also the contribution made by 1-3 ligands at a defined position on the DNA. To this end, the ligands used for this work where the minor groove binder Hoechst 33258 and the naturally occurring bis-intercalator echinomycin.

1.2 Chromatin

Approximately two metres of DNA are compacted into the eucaryotic cell nucleus in the form of chromatin that consists of a fibrous nucleoprotein network containing

genomic DNA and protein. Formally, there are two types of chromatin: heterochromatin and euchromatin. In heterochromatin, the nucleoprotein fibres are densely packed together while in euchromatin the structure is open. Isolated chromatin gives the appearance of what has commonly been described as "beads on a string". These "beads" correspond to nucleosomes, fig 1.1. The nucleosome is the fundamental unit of chromatin and is responsible for the binding of 146bp of DNA in 1.65 left-handed superhelical turns. It is composed of four proteins, the core histones, called H2A, H2B, H3 and H4. *In vivo*, a linear chain of nucleosomes is folded further into a 30nm fibre, which is the basic structure of mitotic chromosomes and requires the presence of a fifth histone, H1, which stabilises the fibre (McGhee & Felsenfeld, 1980; Pruss *et al.*, 1995). DNA between nucleosomes is known as linker DNA and is usually 30-40bp long to allow for the additional binding of H1/H5 (forming a chromatosome) and therefore, on average there is one nucleosome per 200bp.

1.3 The Structure of the Nucleosome

The nucleosome is the elementary unit of eucaryotic chromatin. Since most eucaryotic DNA is complexed with histone proteins this represents the template on which gene regulation and DNA replication occur. The X-ray crystal structure of the nucleosome has recently been resolved at 2.8Å (Luger *et al.*, 1997) and 2.2Å (Harp *et al.* 2001) and has provided the long awaited structural detail of this important complex. In addition the structure of the nucleosome containing the histone variant H2A.Z has also been solved at 2.6Å resolution (Suto *et al.* 2000).

146bp of DNA is wrapped around the central protein core in 1.65 turns in a flat left-handed superhelix. The psuedo- symmetrical point of the complex, the dyad, passes directly through a single DNA base-pair thus dividing the superhelix into a 72 and 73bp half. The superhelix has a diameter of 41.8Å and is not uniformly bent; rather it is kinked along its path that contributes to a final overall axis of super helical curvature, figs 1.2 and 1.3. The protein core is composed of two copies each of the histones H2A, H2B, H3 and H4 that assemble to form an octamer on which the DNA

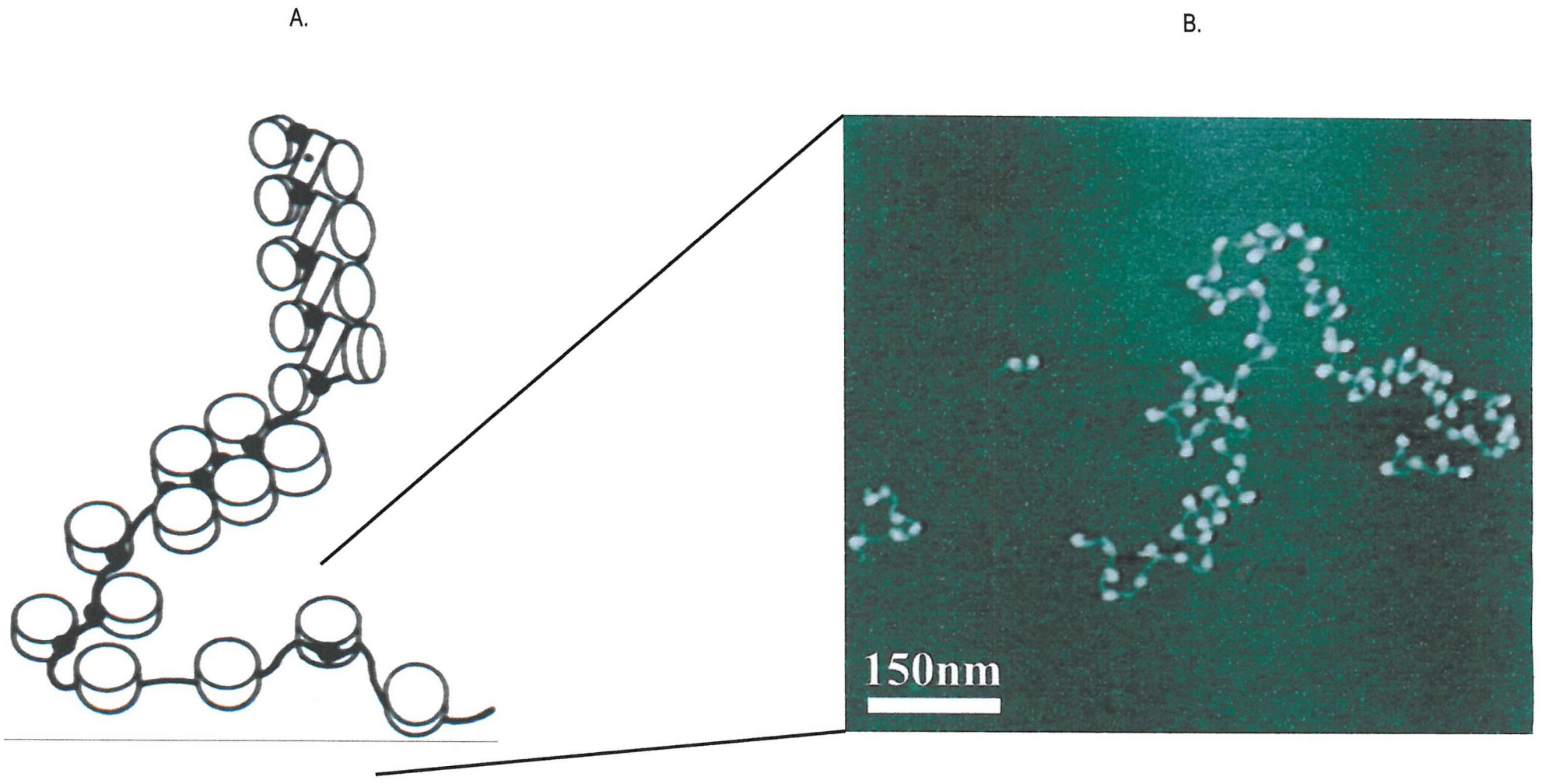

Figure 1.1 The higher order structure of chromatin. A, shows a model for cooperative interaction within the30nm fibre, resulting in a folded nucleosome array. Near the bottom of this figure, the array has an open structure. The DNA is shown as a black line and individual nucleosomes are shown as 3-D circles. Image taken from Pruss *et al.* 1995. B, cryo-AMF (atomic force microscopy) image of chicken erythrocyte chromatin. Individual nucleosomes are white dots and the DNA, white line, can be seen weaving through the structure. This image was reproduced with the kind permission of Sitong Sheng (unpublished data).

is bound. The histone protein sequences are highly conserved from species to species, illustrating the fundamental importance of this remarkable multi-subunit DNA-binding complex. The N-terminal histone tails make up approximately 28% the total mass of the protein, 206KDa, but were not resolved in the crystal structure due to their high mobility.

1.3.1 The Histone-fold pairs

Based upon the assignment of helical and looped regions in the protein core each histone-fold has the structure: α1-α2-L1-L2. This forms a crescent shaped hetrodimer in which two-fold symmetry passes through the intersectional cross-over between the α2 helices from each histone in the pair. One dimer binds approximately 2.5 turns of DNA, inducing a 140° bend, fig 1.4. Each histone-fold-binding domain contacts the DNA at three points where the minor groove of the double helix faces the protein core. The arrangement between each histone subunit in the pair creates the L1-L2 and the α1-α1 binding sites at the edge and centre of the dimer. However, some differences are evident in the manner in which α1-"1 helices and L1-L2 sites interact within each pair. Structural alignment of the four histones, based on the "2 helices, reveals that the H4 and H2A loops are slightly shorter, by 1-2 amino acids, than their H3 and H2B counterparts. The L2 loops in the C-terminal half of the histone fold show a high degree of structural homology between histones. A three amino acid stretch in the L2 loop of one histone in the pair and the L1 loop of the other histone run in parallel beta conformation at the end of the dimer. The conformation of these loop motifs might be dependent upon the local DNA sequence (Luger *et al.*, 1997).

1.3.2 Histone-fold DNA Interactions

The histone-fold domain binds 121bp of DNA with 4bp regions between each domain. Each histone fold is associated with 27bp (ca. 2.5 turns) of DNA. Binding is primarily through the interaction with charged phosphate groups with the DNA backbone and only two such groups are available for binding per helical turn. Notice that three principle binding sites are evident in the histone-fold. The α1-α1 site binds the centre of the DNA segment across the histone domain while the L1-L2 loops

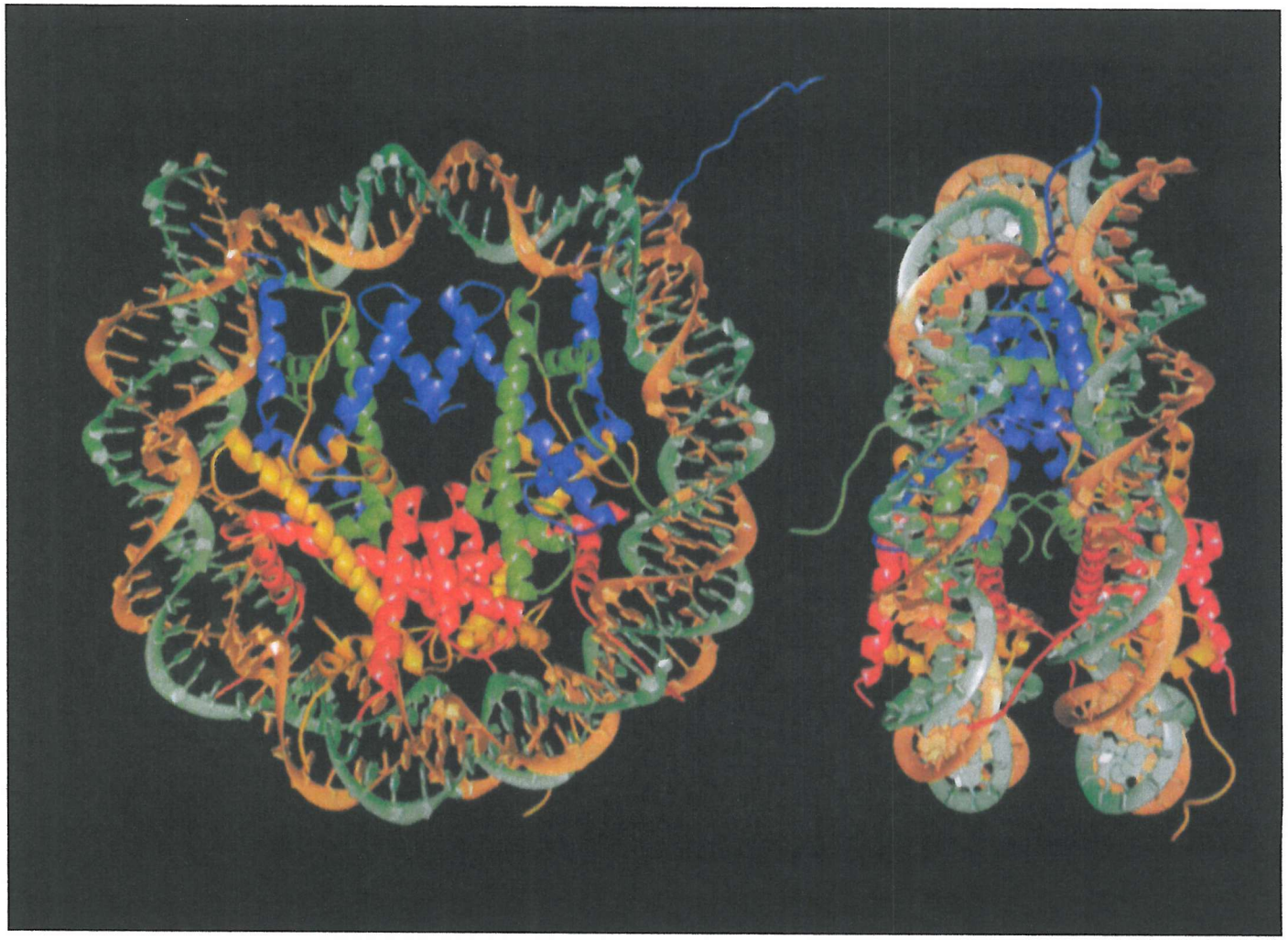

Figure 1.2, The crystal structure of the nucleosome at 2.8Å resolution. The 146bp of DNA (coloured brown and turquoise) and the histone core proteins (H2A: yellow, H2B: red, H3: blue and H4; green) are shown as a ribbon structure. The left image is a view looking down the DNA superhelix axis and the right image is a view looking perpendicular to the superhelix axis. Image taken from Luger *et al.* 1997.

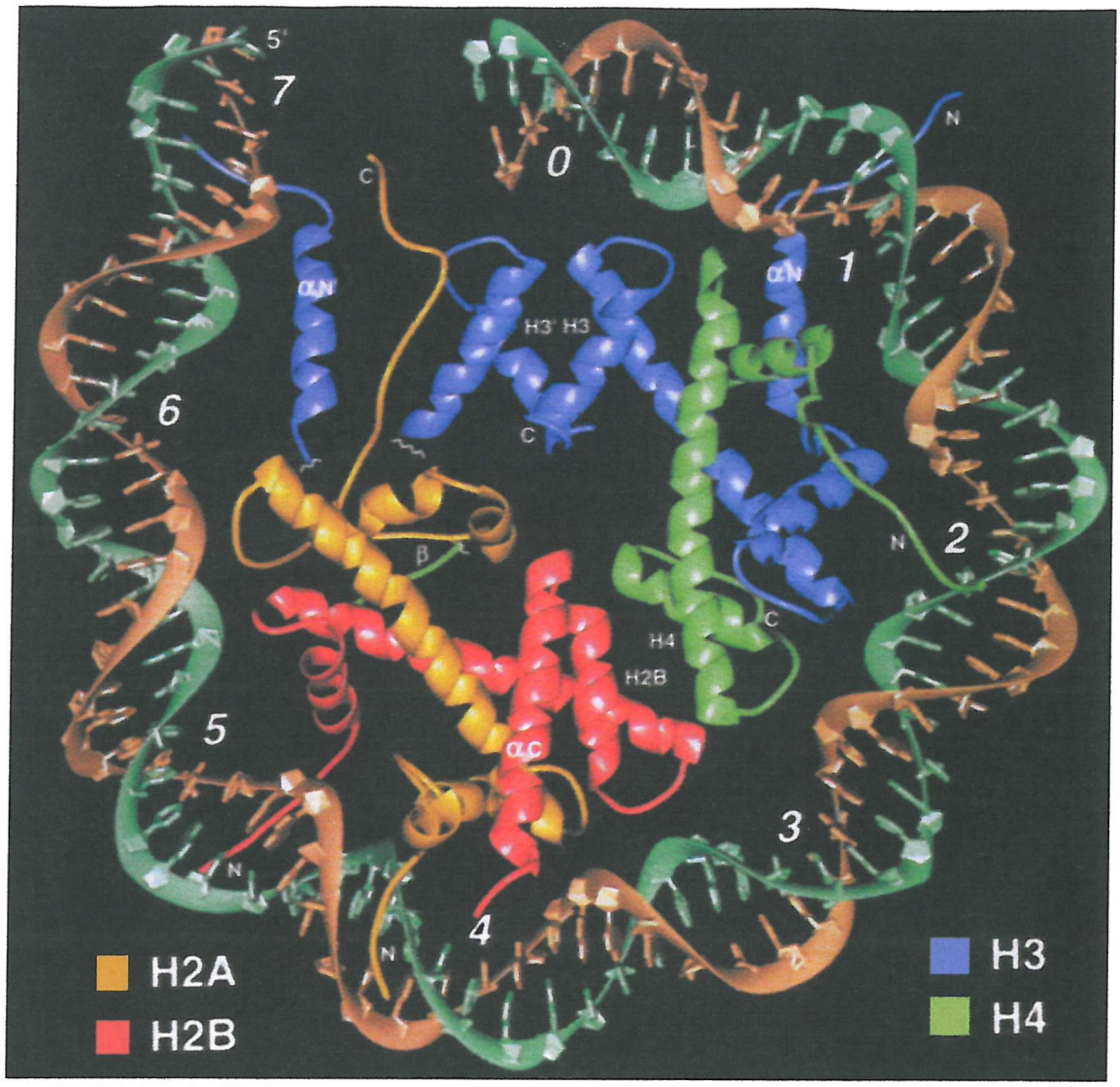

Figure1.3, A cross-section of the nuclesome core particle showing the 73bp half. The complex is presented as a ribbon structure and is coloured as in fig 1.2. The view is looking down the DNA superhelix axis. The dyad is positioned at the top of the image and the central base pair though which it passes is labelled SHL 0 (super helix location). Each SHL label represents an addition helical turn of the DNA. Duplicate copies of the histone proteins are indicated either as primed or unprimed. Taken from Luger *et al.* 1997.

A.

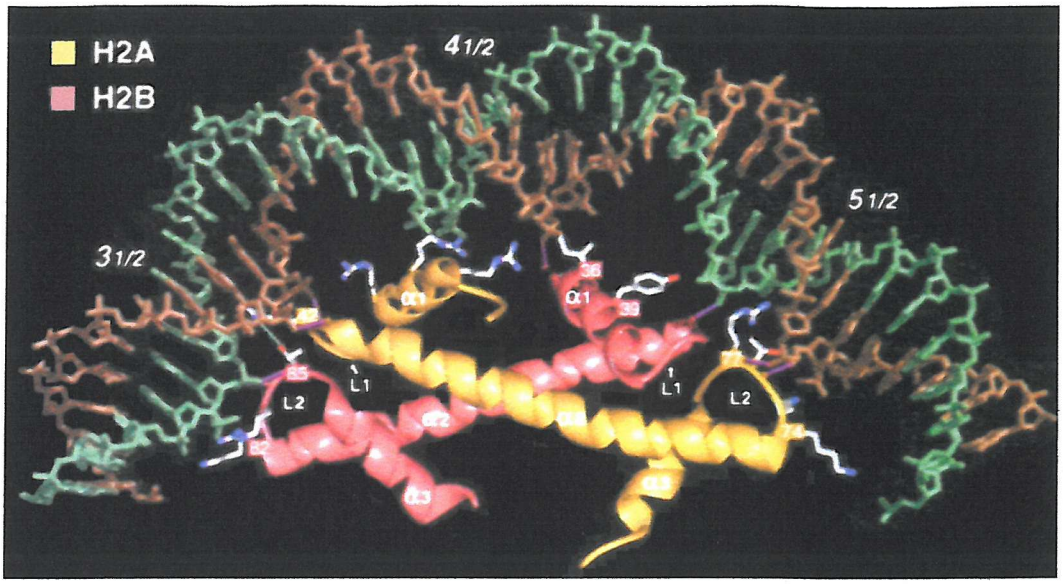

B.

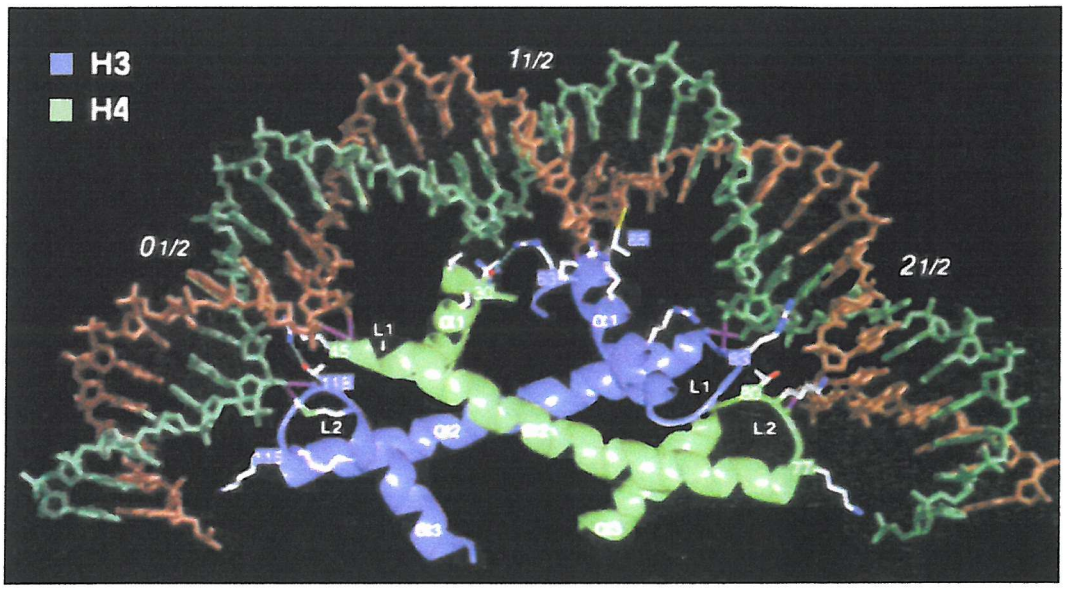

Figure 1.4, The histone fold pairs. The DNA is shown as a ball and stick structure while histone proteins are shown as ribbons. Each image is coloured as in fig 1.2. A, theH2A-H2B fold pair. The SHL is indicated and side chains which make contact with theDNA superhelix are shown. B, as in (A) but showing the H3-H4 fold pair. Image taken from Luger *et al.* 1997.

bind at the edges of each DNA segment. Luger *et al.* (1997) have observed five principle features in binding:

1. The N-termini of helices α1 ∀1 in histones H3, H4 and H2B interact with a single phosphate group in the DNA backbone.

2. Hydrogen bonds to phosphates are made from main-chain amide nitrogen atoms either near or in the last turn of the α1 and α2 helices.

3. An arginine side-chain from each histone fold enters the DNA minor groove 10 out of the 14 times it faces the octamer. The last four such interactions are made from tail regions penetrating the minor groove.

4. Extensive non-polar contacts are made with deoxyribose groups.

5. Hydrogen bonds and salt-links occur frequently between DNA phosphate atoms and protein basic and hydroxyl side chain groups. These side chains approach the inward facing DNA backbone from both the minor and major grooves.

(Luger *et al.*, 1997)

The H3, H4 and H2B α1-α1 binding sites all have their N-termini focused on a single phosphate group of the DNA backbone and there are no specific interactions with the double helix although the residue isoleucine 65 of histone H3 was found to reach into the major groove and make a nonpolar contact with the 5-methyl group of thymidine. It is unclear whether this represents a standard histone-DNA contact or whether it is due to the DNA sequence used in the structure. Arginine residues inserted at each inward facing minor groove are restricted from making base-specific contacts with the DNA due to hydrogen bonds with the core protein residues.

1.3.3 The NH2-Nucleosome "Tails"

The histone tails account for approximately 25% the mass of the nucleosome (Wolffe & Hayes, 1999). They are located at the amino termini of histones H2A, H2B, H3, and H4 and additionally in the carboxyl terminus of histone H2A. Trypsinized mono-nucleosomes produce identical positioning patterns on *Lytechinus variegates* and *X. borealis* 5s rRNA DNA constructs compared to non-trypsinized controls (Dong *et al.*, 1990a; Hayes *et al.*, 1991a). DNaseI and hydroxyl radical footprinting data have also shown that removal of the histone tails appears to have no effect on the structure of DNA and does not contribute to the helical periodicity found in histone-reconstituted *X. borealis* 5s rRNA gene constructs (Hayes *et al.*, 1991a). Hence, proteolytic digestion of the nucleosome, which removes the histone tails, appears to have little influence up on nucleosome positioning; neither does it appear to significantly modify the conformation of the core particle, fig 1.5.

Although the conformation of the histone tails was not resolved in the crystal structure, because of molecular disorder (Luger *et al.*, 1997), it is known that these domains interact with both the DNA superhelix and the protein octamer. It has been previously documented that loss of the histone tails can effect the super coiled structure of the bound DNA causing it to uncoil (Diaz & Walker, 1983). Early NMR experiments have reported that the tails dissociate with increases in ionic strength. This dissociation is highly cooperative with no intermediate stage, i.e. the tails are either bound or unbound (Walker, 1984). When unbound from the core complex, the tails are thought to lack a coherent secondary structure. However, they are not random coils and particular conformational restraint is found at arginine residues. At approximately 600mM NaCl, changes in the conformation of the nucleosome core particle have been attributed not to unfolding of the complex but to an apparent increase in molecular size, and anisotropy (Ausio *et al.*, 1984). Removal of the tails, by proteolysis, has little affect upon the hydrodynamic frictional properties of the particle and DNaseI digestion assays show little change in the cleavage pattern of these complexes (Ausio *et al.*, 1989). Alterations are observed at elevated ionic strength. At 600mM NaCl, DNaseI cleavage patterns become less distinct and there

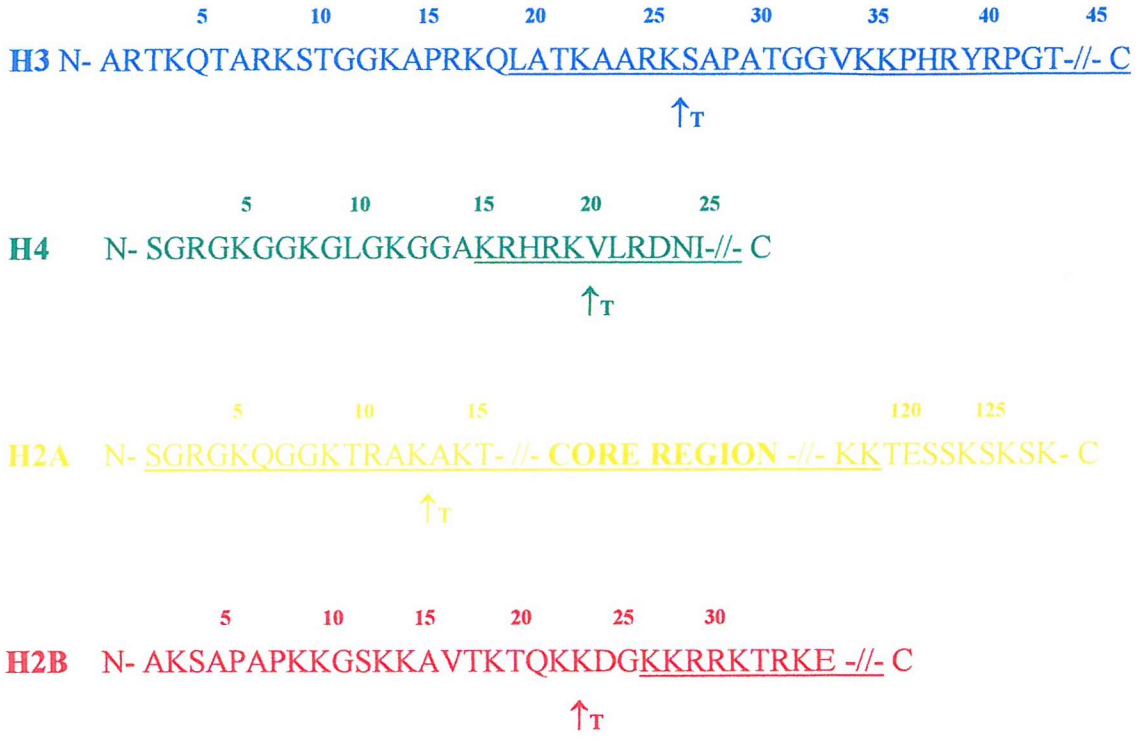

Figure 1.5, Histone tail sequences of *X. borealis*. The residue number is shown above each sequence, regions underlined represent areas that were solved in the crystal structure and ↑T indicates trypsin cleavage sites. Adapted from Luger *et al.* 1997.

is a loss in the average 10bp/turn nucleosome-phasing pattern so that it begins to resemble that of free DNA (Dong *et al.*, 1990b). This has been accredited to a loosening in the supercoiled nature of the bound DNA and was also confirmed by sedimentation analysis (Yager & Van Holde, 1984). In addition, changes in the frictional characteristics of the complex are also apparent but with a constant radius of gyration (Ausio et al., 1984).

1.3.4 Interaction between the histone "tails" and the DNA superhelix

Cross-linking studies (Pruss & Wolffe, 1993), have mapped the binding of the H2A carboxyl terminal tail across the dyad of the nucleosome in reconstituted *X. borealis* 5S rRNA gene constructs. These results have been confirmed using mixed sequence chicken DNA purified as nucleosomes after MN*ase* digestion to produce H1-stripped chromatin (Usachenko *et al.*, 1994). The carboxyl terminal tail of H2A contacts the DNA superhelix at position nt 77 (dyad axis) by virtue of the residue His123. The amino terminal domain of H4 contacts the DNA at position nt 93 via residue His18 and weakly at nt 57 and 66. At increased ionic strength, 400-600mM NaCl, or after proteolytic digestion, these contacts are greatly reduced, further supporting the conclusion that this is due to the interaction of the histone tails with the bound DNA. The H2A contact across the dyad axis is lost in the presence of linker DNA depleted of linker histones. It is suggested that the C-terminal domain of H2A may be arranged along the linker DNA in this system. Removal of the linker DNA by MNase causes the H2A C-terminal domain to rearrange to the closest site on the core nucleosomal DNA, the dyad. A more recent study, using recombinant histone proteins, has also identified binding of the H2A tail ~40bp to ether side of the dyad, primarily to one of the two strands of DNA and an additional set of two cross-links approximately 5bp symmetrically disposed to either side of this single cross-linking site (Lee & Hayes, 1997). It has been suggested that the inner most portion of the H2A tail is anchored to the structural core domain so that interactions with the DNA are restricted to a single location. Since the pattern of observed cross-links is highly localised, it appears that the H2A tails do not bind the DNA superhelix as a random

coil or in multiple conformations but that a degree of conformational restraint exists in these domains.

1.4 Nucleosome Positioning

(Chao *et al.*, 1979) first observed core histone proteins binding to the *E.coli* lac control region in an asymmetric manner and, of many possible arrangements, the formation of only two nucleosomes was favoured. This phenomenon is now known as nucleosome positioning and there are numerous examples of DNA sequences which position in a defined manner with core histone proteins (Clarke *et al.*, 1985; Cockell *et al.*, 1983; Costanzo *et al.*, 1990; Drew & Calladine, 1987; Eisfeld *et al.*, 1997; Flaus *et al.*, 1996; Flaus & Richmond, 1998; Kralovics *et al.*, 1995; Patterton & Hapgood, 1996; Pennings *et al.*, 1991; Pennings *et al.*, 1989; Ramsay *et al.*, 1984; Roberts *et al.*, 1995). Nucleosome positioning can be defined in terms of two components: rotational positioning and translational positioning. Rotational positioning refers to the unique orientation of the DNA relative to the protein surface while translational positioning refers to where along the DNA the histone octamer sits, fig 1.6.

The association of the histone octamer with a large number of sequences demonstrates that a specific interaction between histone core proteins and the DNA may not be a significant factor in nucleosome positioning. Rather it appears more likely that positioning is determined by the overall flexibility and conformation of the DNA. So, although the histone octamer does not recognise a specific DNA sequence it does recognise the DNA structure, which is ultimately determined by the sequence. Sequence-dependent preferences have been observed in rotational positioning where it was found that AAA/TTT and AAT/ATT sequences were orientated so that the minor groove tended to face the histone octamer while GGC/GCC and ACG/CGT sequences were found to face away from the histone octamer (Drew & Travers, 1985; Fitzgerald & Anderson, 1998; Satchwell *et al.*, 1986; Staffelbach *et al.*, 1994; Travers & Klug, 1987; Travers & Klug, 1990). This model of binding was first proposed by (Zhurkin *et al.*, 1979) and took into account a

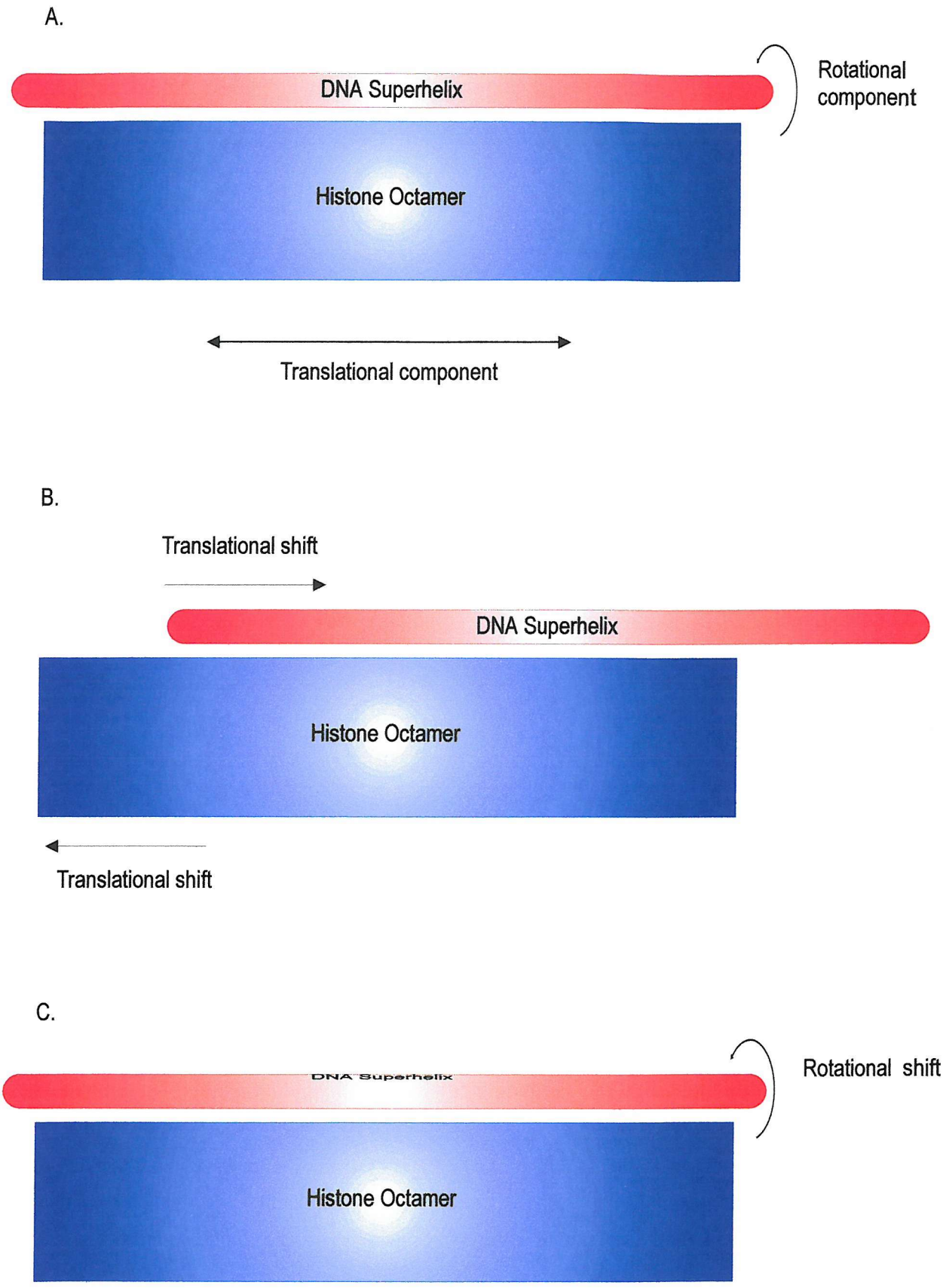

Figure 1.6, The two components of nucleosome positioning. The Histone octamer is shown as a blue box and the DNA superhelix is shown in red. (A), highlights each component. (B), shows a change in translational positioning and (C) shows a change in the rotational positioning, where the DNA has been turned at an angle around its axis.

property of DNA known as anisotropic flexibility. Therefore, DNA sequences that are intrinsically bent will tend to form nucleosomes more readily than sequences, which are not although both types of sequence are equally stable once complexed with core histone proteins (Pennings *et al.*, 1989).

Studies with DNA sequences that exhibit anisotropic flexibility and have sequence elements in phase with the helical repeat have been found to incorporate strongly into nucleosomes (Anselmi *et al.*, 1999; Buttinelli *et al.*, 1995; Lowman & Bina, 1990; Pennings et al., 1989; Shrader & Crothers, 1989; Shrader & Crothers, 1990) and support the model of rotational positioning based upon the curvature of DNA. Genomic sequences isolated from mouse *Ehrlich asceites* cells show an occurrence of molecules with phased runs of AAA and AAAA, CA repeats and TATA tetranucleotides which form highly stable nucleosomes (Widlund *et al.*, 1997) and DNA sequences isolated from a large selection of randomly produced sequences show a high degree of intrinsic curvature (Lowary & Widom, 1998). Periodic sequence elements, which could serve as nucleosome positioning signals, have also been observed in human exons and introns (Baldi *et al.*, 1996). CTG triplets, which are associated with several human diseases such as myotonic dystrophy, spinal and bulbar muscular atrophy and Huntington's disease, have also been found to form highly stable nucleosomes, and it has been observed that these repeats are preferentially found around the nucleosome dyad (Godde & Wolffe, 1996). Repeating units of the "TG sequence" (5'-TCGGTGTTAGAGCCTGTAAC-3') also have a higher affinity for the histone octamer relative to nucleosomally derived DNA and exhibit a stable rotational position (Shrader & Crothers, 1989) but further studies demonstrated that the translational position is random (Patterton & Simpson, 1995). In addition, the positioning of this sequence *in vivo* was not confirmed (Tanaka *et al.*, 1992; Wallrath *et al.*, 1994). It has been suggested that this is because the local helical repeat of DNA across the nucleosome dyad does not match that of the TG sequence (Tanaka *et al.*, 1992).

In addition, it has been found that modification of the exocyclic groups of DNA alter

its positioning properties with the histone octamer. This was carried out by the substitution of cytosine and adenine with inosine-5-methylcytosine and 2,6,-diaminopurine. The rotational positioning of the DNA was found to be sensitive to the number of modified exocyclic groups incorporated into the sequence under study, which was the tyrT fragment from *E. coli.* Therefore it was deduced that the exocyclic groups of DNA impose steric constraints on binding to the histone octamer and are important in setting the rotational position of the DNA (Buttinelli *et al.*, 1998). It has also been suggested that the translational position of nucleosomes may also be directed by the anisotropic flexibility of the DNA molecule (Fitzgerald & Anderson, 1998; Sivolob & Khrapunov, 1995). Therefore it appears likely that the rotational and translational position of a DNA molecule will be governed by the interplay of many different factors associated with the conformation of the DNA molecule and recognised "positioning sequences" which ultimately impart this conformational information. The length of the DNA is also important since it has been observed that the central 40bp of a 145bp sequence is essential for the positioning of the DNA and that this central 40bp is bound symmetrically across the nucleosome dyad (Ramsay, 1986).

In contrast, there are a number of sequences, which inhibit nucleosome formation. The repeating motif $[(G/C)_3NN]_n$ excludes the formation of nucleosomes and this is thought to be due to fact that molecules containing repeating units of this sequence are found to bend into the major and not the minor groove of the DNA (Wang & Griffith, 1996). This sequence has also been found in the control region of the DHFR gene, which is not complexed with core histone proteins *in vivo* (Shimada *et al.*, 1986). In addition, repeating units (>50) of the sequence CCG, found in fragile X syndrome, are also found to exclude the formation of stable nucleosomes (Wang *et al.*, 1996). Telomeric DNA sequences have less affinity for the histone octamer and this is thought to be due to the telomeric repeat length, which is 6-8bp long and is hence out of phase with the helical repeat of nucleosomal DNA, which is ca. 10.17bp (Cacchione *et al.*, 1997; Rossetti *et al.*, 1998).

The structure of the DNA superhelix appears to be similar when different sequences are successfully complexed with core histone proteins. The average periodicity of free DNA in solution is ca. 10.5bp $turn^{-1}$ while that of nucleosomal DNA is 10.17 bp $turn^{-1}$, as derived from statistical sequencing (Drew & Travers, 1985), 10.21bp $turn^{-1}$, from the direct sequencing of a small sample from the same molecular population (Satchwell et al., 1986) and 10.18bp $turn^{-1}$, as assayed by hydroxyl radical digestion of the *X. borealis* 5S gene complexed as a nucleosome (Hayes *et al.*, 1990). Hayes *et al.* 1990 observed that the same sequence, when bound to a calcium phosphate surface, had a periodicity of 10.49bp $turn^{-1}$ demonstrating that these changes in helical repeat are directly attributed to the binding of the histone octamer. In addition, it was observed that the periodicity of DNA crossing the nucleosome dyad, corresponding to the central three turns of the DNA sequence, was increased from 10.05bp turn-1, across positions +15 to +75 if the *X. borealis* 5S gene, to 10.7bp $turn^{-1}$. After crossing the dyad, the periodicity of the DNA returns to 10.05bp $turn^{-1}$. Therefore this increase in period at the dyad accounts for the average periodicity of 10.18bp $turn^{-1}$ in nucleosomal DNA. Drew and Travers 1985 and Satchwell *et al.* 1986 previously observed similar results and attributed this change in helical repeat to the departure of the DNA across the dyad from a uniform superhelix between the two adjacent turns of the supercoil, fig 1.7. Studies in which different DNA sequences, each displaying altered conformational properties, have been incorporated into nucleosome core particles show that there is little difference on the organisation of these sequences when associated with the histone octamer which demonstrates that the core histone proteins constrain the DNA, regardless of the source, after successful reconstitution (Hayes *et al.*, 1991b).

1.5 Post-translational Histone Modifications

Post-translational modifications of histone proteins appear to play a key role in the control and initiation of events such as transcription, DNA replication, repair, recombination, mitosis, meiosis and chromosomal condensation and segregation. Identified modifications of histone proteins include acetylation, phosphorylation, ADP-ribosylation, methylation and ubiquitination which take place on the histone

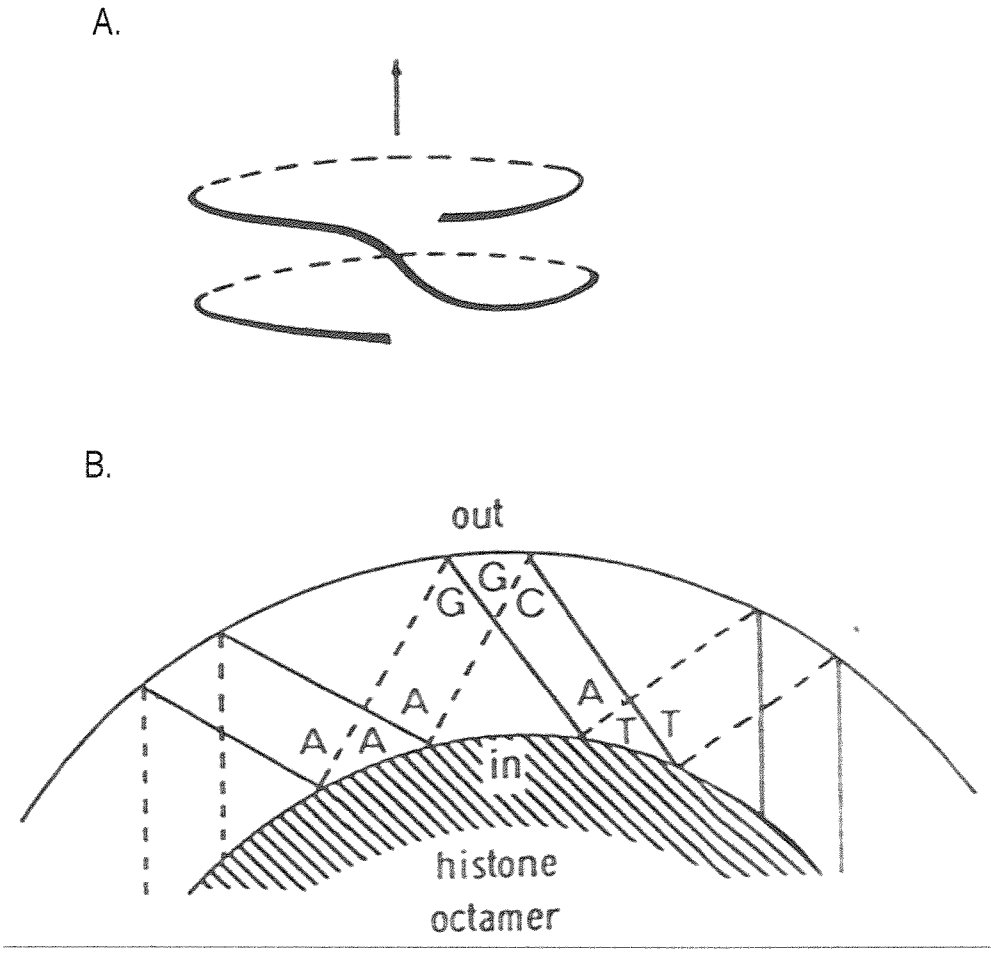

Figure 1.7 (A), the path of the DNA superhelix across the dyad axis of the nucleosome as it departs from a uniform superhelix which is thought to account for an increase in the DNA helical repeat across this region. (B), the orientation of AT and GC steps in the rotational positioning of DNA with respect to the minor groove. From Travers and Klug 1990.

tails domains.

Phosphorylation of histone proteins has long been associated with chromatin condensation. Histone H1 is phosphorylated at S-phase in the cell cycle and reaches a state of hyper-phosphorylation before the final stage of mitosis and is then rapidly dephosphorylated to a level comparable to that of S-phase (Bradbury, 1992). However, chromatin condensation can occur in the absence of phosphorylated H1 since histone H3 also undergoes phosphorylation (Ajiro *et al.*, 1996a; Guo *et al.*, 1995; Ohsumi *et al.*, 1993; Shen *et al.*, 1995). Modification at serines 10 and 28 of H3, is linked to the transcriptional competence of *c-fos* and *c-myc* immediate early genes and mitotic chromosome condensation. (Ajiro *et al.*, 1996b; Chadee *et al.*, 1999; Goto *et al.*, 1999; Guo et al., 1995; Houssier *et al.*, 1983; Thomson *et al.*, 1999; Wei *et al.*, 1998; Wei *et al.*, 1999).

Histone acetylation was first observed in calf thymus nuclei in 1964 (Alffrey *et al.*, 1964) and has been associated with transcription for some time. Some transcriptional activators are histone acetylases (HATs) while some transcriptional repressors are histone deacetylases (dHATS). The process of acetylation occurs on histone lysine residues and helps the binding of the transcriptional apparatus to the target regions on the nucleosome since this modification is thought to relax histone-DNA contacts (Kimura & Horikoshi, 1998; Wolffe & Hayes, 1999). Examples of HATs include GCN5p, which acetylates histones H3 and H4 (Kuo *et al.*, 1996; Sternglanz & Schindelin, 1999; Tanner *et al.*, 1999; Trievel *et al.*, 1999), PCAF which acetylates histone H3 and other proteins involved in transcription (Clements *et al.*, 1999) and HAT1, which only acetylates free H4 (Verreault *et al.*, 1998). Enzymes involved in acetylation and deacetylation carry these processes out on the N-terminal tails of histone proteins and many contain a unique structural motif known as the bromodomain (Winston & Allis, 1999).

Of the remaining three modifications much less is known. Ubiquitination may correspond to transcriptionally active regions in the genome since the level of this

modification has been found to increase with transcription. ADP-ribosylation has been linked to DNA repair since the enzyme poly(ADP-ribose) polymerase which carries out this modification, is activated after DNA damage and it may also be implicated in DNA replication (Althaus, 1992; Boulikas, 1990; Realini & Althaus, 1992). The role of histone methylation is unclear although it may have a link to transcriptional activation; this has been implicated in the ciliate Tetrahymena (Strahl *et al.*, 1999). Recent thoughts have focused on the concept of a "histone code" (Strahl & Allis, 2000). In this model, covalent modifications may be read by other proteins, which would ultimately bring about a specific effect, i.e. transcription. Rather than a single modification event, it could be possible that multiple modifications act in concert to produce the desired effect. This is the essence of the "Histone-Code" hypothesis. Multiple modifications on the same histone tail could become extremely complex and it has been proposed that covalent modification by one histone-modifying enzyme may affect the efficiency of another factor interacting with the now modified tail.

1.6 Echinomycin

The quinoxaline, echinomycin, is a naturally occurring compound derived from *Streptomyces echinatus*. It has potent antibiotic and anti-tumour activity which is in contrast to the minor groove binder Hoechst 33258 which is principally used as a chromosome/DNA dye. Echinomycin is composed of a cyclic octapeptide linked centrally by a thioacetal cross-bridge. Two quinoxaline-2-carboxylic acid chromophores project out from the octapeptide on each side of the molecule, fig 1.8. Examples of related compounds include [N-MeCys3,N-MeCys7]TANDEM and Triostin A (Addess & Feigon, 1994a; Addess & Feigon, 1994b; Addess & Feigon, 1994c; Addess *et al.*, 1993; Alfredson *et al.*, 1994; Bailly & Waring, 1998; Fox *et al.*, 1983; Lee & Waring, 1978a; Lee & Waring, 1978b; Low *et al.*, 1986b; Low *et al.*, 1984b; Portugal *et al.*, 1988; Singh *et al.*, 1986; Ughetto *et al.*, 1985; Viswamitra *et al.*, 1981).

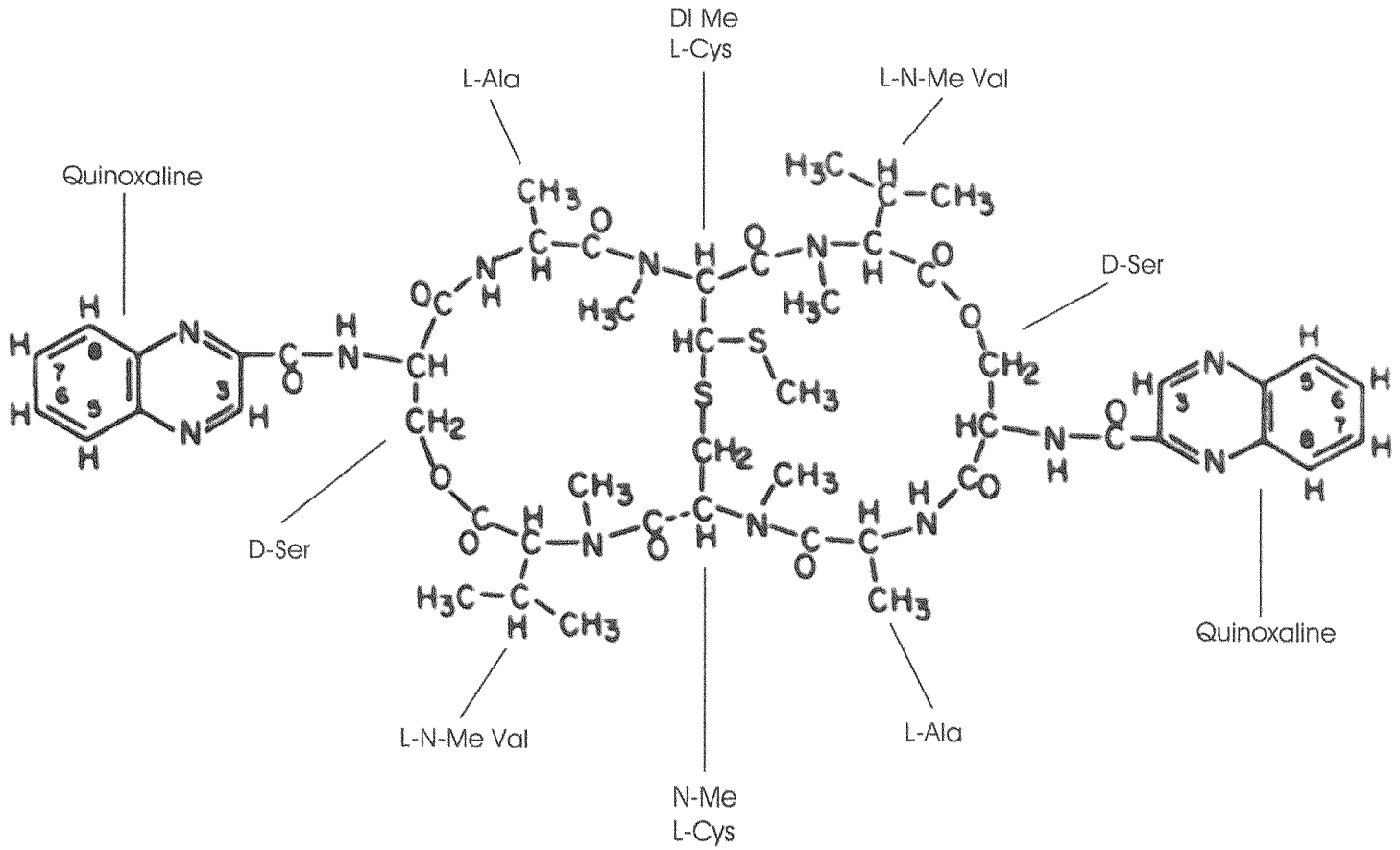

Figure 1.8, The chemical structure of echinomycin. The quinoxaline chromophores and the identity of amino acids in the drug are indicated.

Echinomycin binds by the mode of bifunctional intercalation, which subsequently unwinds the DNA by almost twice that of ethidium bromide, and interestingly chemical modification of the quinoxaline chromophores also has implications for ligand binding (Fox *et al.*, 1980; Fox *et al.*, 1981a; Wakelin & Waring, 1976; Waring, 1979; Waring & Wakelin, 1974). Each quinoxaline chromophore intercalates into the double helix, disrupting local base staking across the target site and bracketing the CG step, while the octapeptide ring makes extensive non-bonding interactions across the surface of the minor groove which is now open and unwound by the binding of the ligand. Intercalation is an electrostatically unfavourable interaction, as measured by stacking interaction energies of the quinoxaline chromophores, the sandwiched CG base pairs and flanking bases to the central site. Since echinomycin binds strongly to its target sequence, this is balanced by the favourable interactions between the octapeptide and the minor groove of DNA (Gallego *et al.*, 1994). The mode of intercalation is also dependent upon the ionic strength of solution. In high ionic strength intercalation is thought to be monofunctional moving to sesquifunctional and finally bifunctional as the salt concentration is reduced, as deduced from measurements of the helix unwinding angle and sedimentation analysis (Wakelin & Waring, 1976; Waring & Wakelin, 1974). The rate of dissociation is also increased in the presence of elevated ionic strength. Echinomycin has dissociation half-lives ranging from 1-40 mins at 20°C, which appears to be dependent upon the sequences flanking the CG step, and, as expected, the dissociation of the drug is slower from ACGT than it is from TCGA (Fletcher & Fox, 1996a; Fletcher & Fox, 1996b). The drug has a clear preference for mix sequence DNA richer in G+C rather than A+T (Wakelin & Waring, 1976) although two modes of binding have been observed (Fox *et al.*, 1981b; Fox & Waring, 1984; Fox & Waring, 1985). These results can be explained by the fact that, when presented with alternating CpG and GpC, the ligand initially binds to both targets and then consequently redistributes to the superior target site: 5'-CpG-3'. This would result in a kinetic profile that is described by the sum of two exponentials. This is not observed with mixed sequence natural DNA because the spectral properties of echinomycin are very similar when bound to different DNA

targets (Fox & Waring, 1985).

The ligand has a high affinity for 5'-NCGN-3' tetranucleotide steps of double stranded DNA, with particular affinity for ACGT and ACGG which have a corresponding C_{50} value, the ligand concentration required to decrease the band intensity by 50% on DNaseI sequencing gels, of <0.3uM. The sequences flanking the 5'-CG-3' step have important consequences for binding due to differences in the DNA conformation (Low *et al.*, 1984a). For example, the target sites GCGG and CCGG are poor substrates for this ligand with C_{50} values of 4.2∀1.7μM and 35∀7μM respectively (Lavesa & Fox, unpublished observations).

1.6.1 The Echinomycin-DNA Complex: Footprinting Studies

Although the undisputed primary recognition site of echinomycin is the 5'-NCGN-3' step there is evidence to suggest that this ligand may also have secondary binding sites. In an elegant series of experiments, Fox and co-workers have deduced that the drug also interacts with alternating AT (Fox & Kentebe, 1990; Fox *et al.*, 1991; Waterloh & Fox, 1991). This form of binding is observed in the echinomycin analogue [N-MeCys3,N-MeCys7]TANDEM (Waterloh *et al.*, 1992). Changes in DNaseI, DNaseII and MPE-Fe^{2+} cleavage in AT flanking regions, flanking CpG steps have also been reported by other groups (Bailly *et al.*, 1994; Low *et al.*, 1984a; Van Dyke & Dervan, 1984).

Echinomycin-DNA complexes have also been footprinted with the chemical probe diethylpyrocarbonate (DEPC), which is very sensitive to alterations in the conformation of DNA, and $KMnO_4$. DECP is a base specific chemical probe, which targets purine bases, and will react with adenine over guanine. The compound reacts in the major groove and interacts on the side of the bases not involved in hydrogen bonding (Bailly *et al.*, 1994). The N7 group of adenine or guanine undergoes electrophilic attack with the probe and becomes carbethoxylated. Consequently, DEPC reactions are not a measure of base pair disruption but are a result of conformational changes in the DNA, via the accessibility of the N7 group. DEPC

reacts weakly with native B-form DNA since the N7 group is not very accessible in this conformation. KMnO4 reacts on the 5,6-double bond of thymine. When echinomycin binds its target, bases adjacent to the central CG step become less stacked and hence are more accessible to reaction with these footprinting reagents (Bailly *et al.*, 1994).

In the presence of echinomycin, several enhancements are evident in AT regions flanking the central CG recognition motif when using DECP as a footprinting probe suggesting that secondary binding has occurred, which alters the DNA conformation at these sites rendering adenine N7 more accessible to DEPC. Bailly *et al.*, 1994 also observed DECP enhancements that suggested that these were indicative of the DNA adopting an altered conformation in the presence of the ligand. Similar results were obtained for KMnO4 in AT flanking regions of the duplex. However, the authors suggested that these enhancements did not represent the ligand interacting with AT flanking regions since these sequences were not considered long enough for such an interaction to occur. Changes in conformation, transmitted from the central binding site were thought to be the principle reason for enhancements in DECP and KMnO4 some distance from the binding site. It has also been argued that this increased DECP reactivity to the N7 group is due to the formation of Hoogsteen base pairing in which the glycosidic bond of adenine moves into the *syn* conformation upon binding of the ligand, see below.

Crystallographic and NMR studies have strongly implicated the 2-amino group of guanine to be critical in determining the affinity of echinomycin for the recognition motif 5'-NCGN-3'. The idea of that this group may interact with the drug was first proposed by Laurence *et al.* 1976. The 2-amino group is the only hydrogen bond donor in the minor groove, it sterically inhibits access to the floor of the minor groove and it disrupts the spine of hydration (Larsen *et al.*, 1991). Studies in which guanine is replaced with inosine, where this functional group is missing, have

confirmed the importance of the 2-amino moiety by DNaseI footprinting, (Marchand *et al.*, 1992). Stacking interactions in the helix are also known to be important in determining the binding of echinomycin to DNA and it is quite probable that inosine stacks in a different manner thus directly altering the binding characteristics of the ligand via this mechanism (Alfredson & Maki, 1990; Alfredson *et al.*, 1991). However, further importance for the role of the 2-amino group comes from base analogue studies in which it was reallocated to adenine to form 2,6-diaminopurine (DAP) and where inosine was used to replace guanine (Bailly *et al.* 1993; Waring and Bailly 1994; Bailly *et al.* 1995; Bailly *et al.* 1995; Bailly and Waring 1995). In these studies, echinomycin recognises TpDAP steps with very high affinity, with an observed IC_{50} of ca. <1μM. It has been suggested that the ligand may recognise the 2-amino group by virtue of the conformation properties conferred to the DNA duplex by its presence. These properties would include things such as groove width and other alterations in the DNA structure.

1.6.2 The Crystal Structure of Echinomycin bound to DNA

Figure 1.9, shows the crystal structure of the echinomycin-DNA complex (Ughetto *et al.*, 1985) and a comparison is made to that of Triostin A, fig 1.10. The two carboxylic acid chromophores stack over the central CG site and project into the major groove and the peptide portion of the ligand can divided amino acids that project towards the DNA duplex and those that face away. The principle components that stabilize the complex are hydrogen bonding between alanine and guanine, extensive van der waals interactions and favourable stacking interactions between the ligand chromophores and the terminal DNA bases of the binding site.

The importance of the 2-amino group is also highlighted in this crystal structure. Hydrogen bonds are present between the alanine and the G12 N3 atom and between the alanine carbonyl group and the G12 N2-amino group. The hydrogen bond lengths for these are 2.68Å for ala-NH-N-G12 and 3.38Å for ala-CO-H-G12. The third hydrogen bond is between alanine 1 and the N3 group of G2; it has a corresponding bond length of 3.6Å. There is no evidence of any hydrogen bond

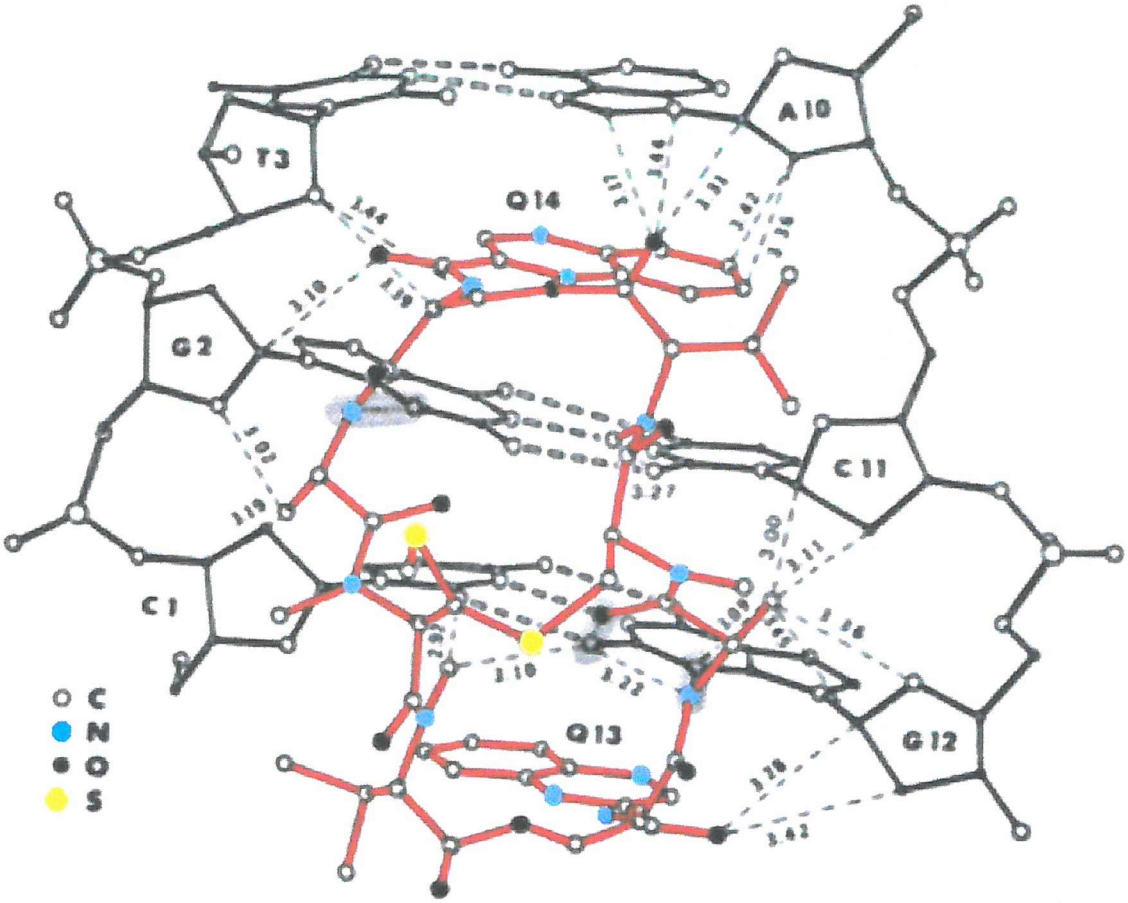

Figure1.9, The crystal structure of echinomycin. The ligand is traced in red and the DNA target site is shown in black. Hydrogen bonds between the drug and the DNA are indicated by flat shaded ovals. Image taken and modified from Ughetto *et al* 1985.

A.

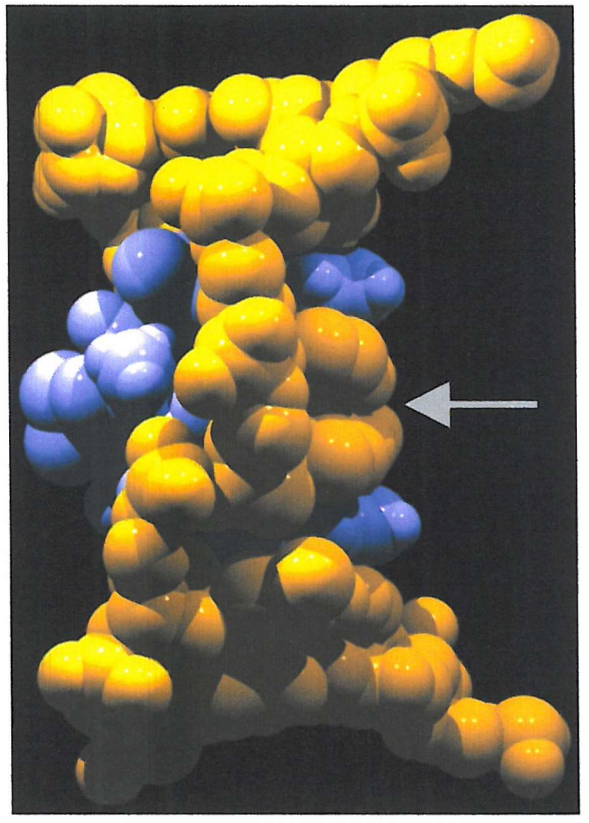

B.

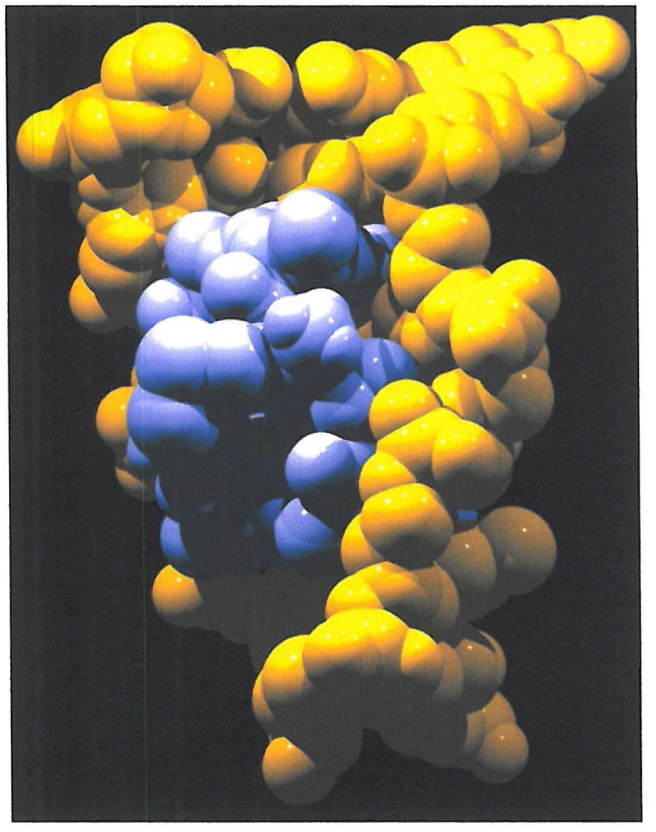

Figure 1.10, The crystal structure of Triostin A is presented as a comparison to fig 1.8. (A), the complex is shown as a space-filled model where the DNA is coloured yellow and the drug is coloured light purple. The arrow indicates the CpG step which is compressed by the binding of the ligand. (B), as in (A), a rotated view of the complex which highlights structural deviations in the DNA duplex when the drug binds.

network involving water in this structure since steric occlusion would make this impossible. This interaction is clearly very significant as judged by the work of others but could this importance also be due to other structural features derived from having the N2-amino group in the minor groove?

The complex shows substantial conformational change in the DNA helix when complexed with the ligand. Alanine is responsible for much of this by virtue of its methyl side chains, which wedge between the sugar groups of C1 and G2 and, in the second helical chain, of G12 and C11. This causes an increase in tilt between these base pairs but does not affect the hydrogen bonding between them (Ughetto et al., 1985). Further helical distortion occurs from intercalation of the quinoxaline chromophores, which taken together with the above cause internal destabilisation in the helix by disruption of base stacking interactions. The standard axial rise between bases is approximately 3.4Å, in a B-form helix, but in the echinomycin-DNA complex this increases to 3.97Å. However, favourable stacking interactions occur between the chromophores and the terminal adenine of each binding site. This is brought about by a change in the torsion angle of the glycosidic bond which is now found in the syn conformation making the central AT base pairs of the oligonucleotide bond in Hoogsteen fashion, fig 1.11, this has also been confirmed by NMR, see below. The chromophore stacks with A10 but not with T3. Due to the short length of the polynucleotide under study it was not possible to speculate on how far these Hoogsteen interactions may spread from the binding site when the ligand binds and NMR cannot be used to answer such questions since a short DNA length is also a requirement for successful results.

A final feature of the structure is extensive van der waal interactions which stabilise the complex. Examples include the interaction with the alanine side chain and the sugar of C11, methyl groups and the deoxyribose (e.g. the N-methyl group of valine and the O2 atom of C1). In addition, the formation of Hoogsteen base interactions causes the opposite C1 and C1' atoms of the bases involved to move 2Å closer to each other, compared to standard Watson-Crick. This has the affect of bringing the

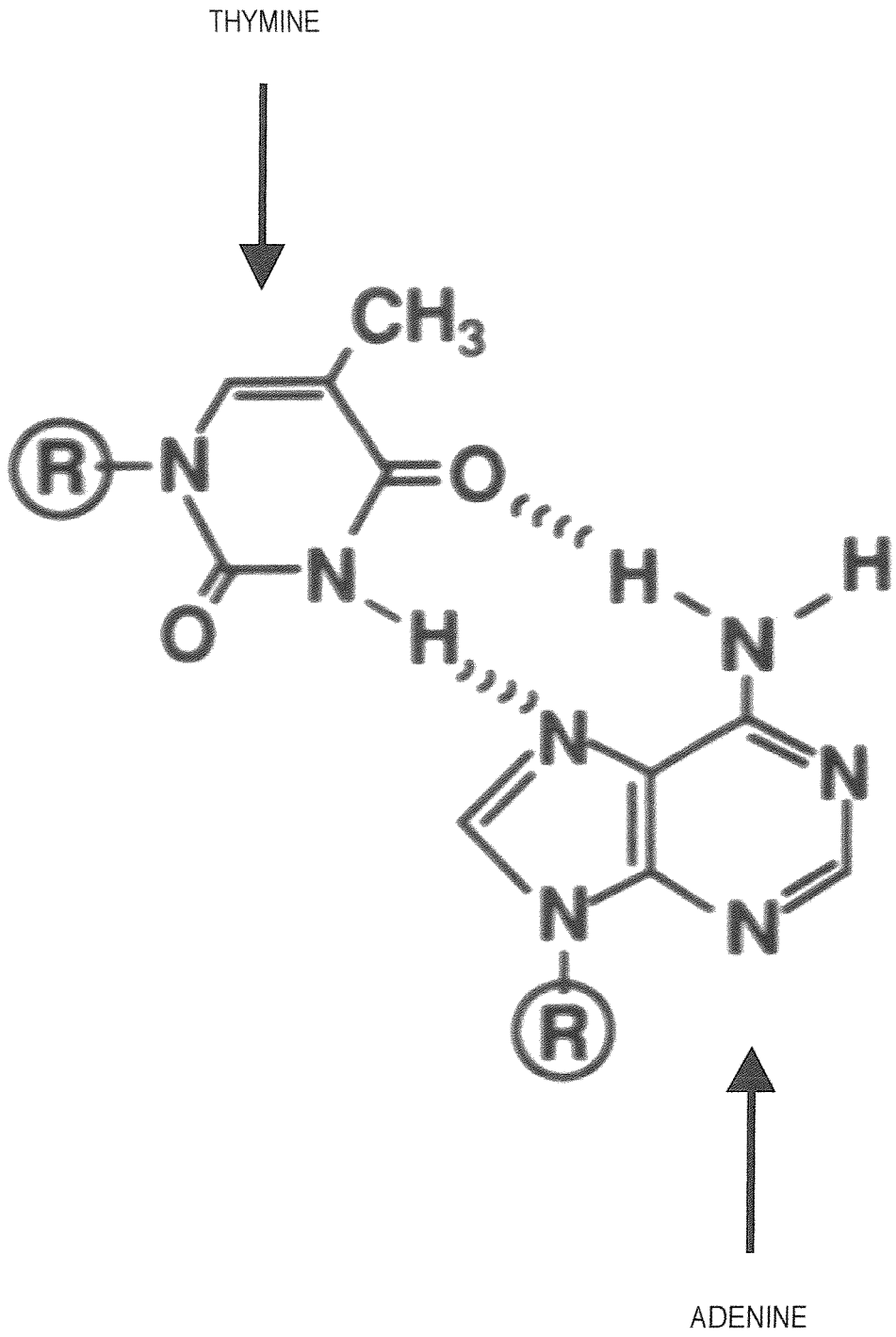

Figure 1.11, The structure of a Hoogsteen base pair. "R" indicates deoxyribose.

DNA closer to the intercalated chromophore rings (Ughetto *et al.*, 1985).

1.6.3 NMR Studies of Echinomycin-DNA Complexes

The solution structure of echinomycin bound to a number of different DNA templates has been studied and confirms the intercalative mode of binding by this ligand and the critical alanine-2-amnio group interaction (Feigon *et al.*, 1984a; Feigon *et al.*, 1984b; Gao & D.J., 1988; Gao & Patel, 1989; Gilbert & Feigon, 1991; Gilbert & Feigon, 1992; Gilbert *et al.*, 1989; Park & Choi, 1995; Waring, 1979). Another interesting observation is that the drug appears to bind to two closely spaced target sites in a cooperative fashion. Cooperative binding has also been confirmed by quantitative DNaseI footprinting experiments (Bailly *et al.*, 1996). However, the exact mechanism behind this cooperativity remains unclear. It is possible that direct drug-drug contacts may be involved when CG sites are closely spaced or an alternative explanation is that changes in the conformation of the DNA helix, as a result of ligand binding, may enhance the binding of a second drug. Arguably, a number of different factors acting in concert is plausible depending up on the nature of the binding sites, separation and the environment of the solution.

There is also strong evidence supporting the formation of Hoogsteen base pairing in Echinomycin-DNA complexes, as assessed by strong NOE signals between the H8 and H1' protons, of the A•T base pairs flanking the central CG site, indicating that the glycosidic bond is now in the *syn* conformation (Gilbert *et al.*, 1989). It has been suggested that the formation of either Hoogsteen or Watson-Crick base pairing might be a consequence of stacking interactions once the quinoxaline rings intercalate into the DNA helix (Gallego *et al.*, 1993; Gao & D.J., 1988). The orientation of adenine with the glycosidic bond in *syn* provides very favourable stacking interactions to occur between it and the quinoxaline ring.

1.6.4 Hoogsteen Base Pairing: A Controversy?

The formation of Hoogsteen base pairing in sequences flanking the central CG site of echinomycin has been strongly implied from footprinting, NMR and X-ray crystallography studies. This unusual structure is also seen with the closely related compound Triostin A where it was found that crystals formed more readily at low pH, perhaps reflecting the requirement for cytosine to become protonated to form Hoogsteen bonds (Quigley *et al.*, 1986; Wang *et al.*, 1986).

The reaction of DEPC with echinomycin-DNA complexes shows hyperreactivity on base pairs flanking the CG site and it has been proposed that this may reflect the existence of Hoogsteen bonds at these positions. Under these circumstances, DECP would have to react with either N3 or N1 of adenine since N7 would now be involved in hydrogen bonding (Mendel & Dervan, 1987). Waring and co-workers dispute this conclusion and alternatively suggest that hyperreactivity of flanking bases to DEPC and other chemical probes is not a result of the glycosidic bond rotating but due to unwinding of the DNA helix which would make targets on the base pairs more susceptible to chemical cleavage (McLean *et al.*, 1989). DNA in which adenine has been replaced by 7-deaza-2-deoxyadenosine and footprinted with DNaseI and OsO_4 shows that echinomycin still binds relative to unmodified DNA and the same enhancements are observed (McLean *et al.*, 1989). The important thing about 7-deaza-2=deoxyadenosine is that it cannot form fully hydrogen bonded Hoogsteen bonds. There is nothing to stop this group rotating about the glycosidic bond so that it may reside in *syn*. However, the hydrogen bond between N7 and the N3-H of the pyrimidine cannot be formed thus logically this base pair would not be as stable as native AT Hoogsteen bonds. In extended work (Sayers & Waring, 1993), experiments were carried out on the TyrT fragment, from *E. Coli*, where adenine and guanine had been substituted with 7-deaza-2=-deoxyadenosine and 7-deaza-2=-deoxyguanine respectively. Footprinting and further analysis showed that the

incorporation of these residues did not significantly affect the binding of echinomycin to DNA. However these experiments could not rule out the possibility that 7-deaza-2=-deoxyadenosine and 7-deaza-2=deoxyguanine had still rotated into the *syn* conformation, but with one less hydrogen bond. It is possible that since the formation of Hoogsteen bonds brings the DNA duplex 2Å closer to the ligand, relative to standard Watson-Crick, that this would still be favoured and it has been suggested that Hoogsteen base pairs may be a structural consequence of the DNA attempting to accommodate a highly invasive ligand (Sayers & Waring, 1993).

1.7 Hoechst 33258

Hoechst 33258 belongs to a family of ligands referred to as the nonintercalating minor groove binders. It is a crescent-shaped synthetic molecule made from four rings in the order phenol, benzimidazole 1, benzimidazole 2, piperazine (phe-bz1-bz2-pip) with free rotation about the bonds connecting each ring, fig 1.12. Other related compounds include netropsin, distamycin, DAPI and berenil which all bind in similar ways. All of these compounds are structurally similar and are isohelical. Minor groove binders have a preference for AT*n* DNA and usually bind four to five consecutive AT base pairs without significant distortion in the DNA helix. The binding preference for these ligands has been attributed to the nature of the AT minor groove which is very narrow and hence promotes the formation of close van der waal contacts between the aromatic rings of the drug and the wall of the groove. Molecular dynamics studies indicate that the structure of AT regions is not completely pre-organised and hence ligand binding may incur a significant amount of "induced-fit" (Bostock-Smith *et al.*, 1999; Bostock-Smith & Searle, 1999). However, recent NMR data of the Hoechst-DNA complex shows that there is little difference between the structure of free and ligand-bound DNA (Gavathiotis *et al.*, 2000). Previous molecular dynamics simulations of the *Eco*RI recognition sequence, showed a trend for a narrowing in the AATT minor groove, although the groove dimensions were capable of undergoing significant breathing over the time-scale studied (Young *et al.*, 1997). The accommodation of a ligand into the AT minor groove requires movement of the bases at the bottom of the groove to resolve steric

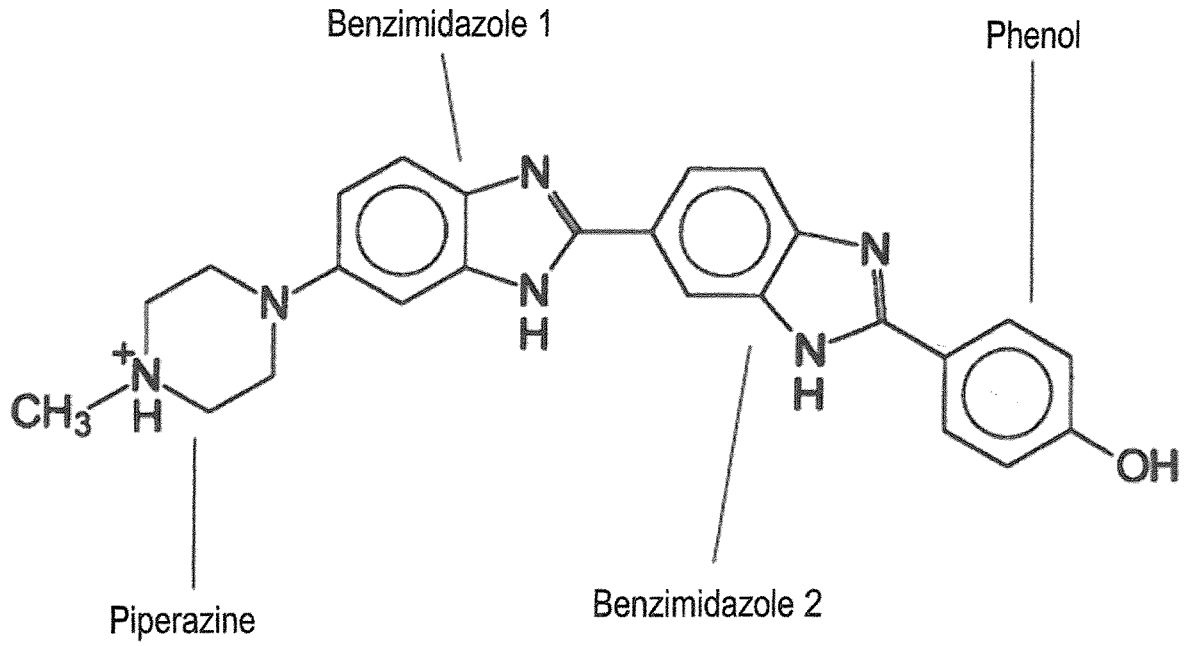

Figure 1.12, The chemical structure of Hoechst 33258.

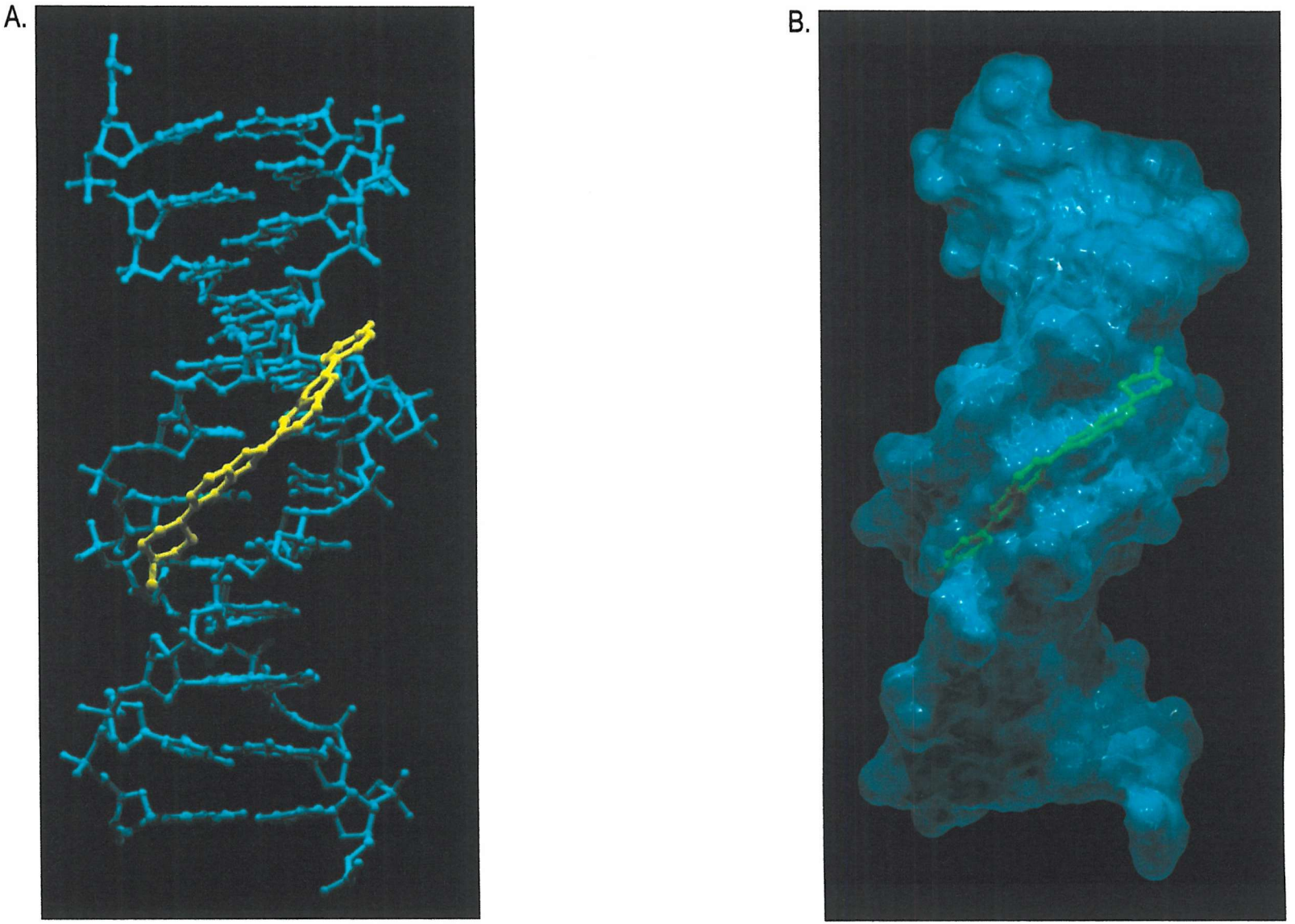

Figure 1.13, The crystal structure of Hoechst 33258 at 2.25Å resolution bound to the DNA sequence d(CGCGAATTCGCG) (A), the model is shown as a ball and stick structure. DNA is coloured teal and the drug is shown in yellow. (B), a molecular surface image of (A) which highlights the close contacts between the ligand and the minor groove of AATT. Image created in Swiss Pdb Viewer, from the pdb file of Teng *et al.* 1988, and rendered in Pov-ray for Windows.

clash from the v-shaped walls of the structure. This widens the groove near the bases, and provides a complementary hydrogen bonding surface to the drug. Conformational changes in the sugar phosphate backbone then take place to "seal" the upper region of the minor groove to the ligand, which optimises non-bonding interactions (Laughton & Luisi, 1998).

CG minor grooves are wider and would presumably not provide the same level of non-bonded interactions; the presence of the 2-amino group of guanine would also sterically block the interaction of these ligands with the DNA (Heinemann *et al.*, 1992). In addition, the negative electropotential of the AT minor groove is attractive to these positively charged ligands. Once the initial ligand-DNA complex is formed, hydrogen bonds are made between the aromatic rings of the drug and the AT bases. These hydrogen bonds stabilise the complex but are not thought to be involved in the recognition process.

Like others in its class, Hoechst 33258 binds selectively to AT rich DNA with a high preference for AATT and AAAA. The drug binds tightly between the sugar-phosphate walls of the minor groove, replacing the spine of hydration and may disrupt local hydration patterns close to the binding site. The spine of hydration was first observed in the crystal structure of the Eco*RI* restriction sequence $[GAATTC]_2$ (Drew *et al.*, 1981). First shell water molecules hydrogen bond to purine N3 and pyrimidine O2 atoms and second shell waters bridge between shell one. Recently it has been demonstrated that sodium ions act as a third shell and bridge over shell two (Shui *et al.*, 1998). Hydration around base pairs tends to be very well ordered but the patterns around other groups in the helix, such as phosphate are more random (Berman & Schneider, 1999; Bonvin *et al.*, 1998; Sunnerhagen *et al.*, 1998). It is these hydration structures that are displaced when Hoechst 33258 binds to the DNA and the ligand conserves the hydrogen bonds originally held between water and the base pairs. A detailed visualisation between a ligand and hydration patterns comes from the crystal structure of the minor groove binding drug ethyl-furamideine in which 220 water molecules were resolved (Guerri *et al.*1998).

One of the principle drives for the binding reaction is the removal of the hydrophobic surface of the drug from solvent upon complex formation with the double helix; this interaction is entropically driven (Haq *et al.*, 1997). At relatively low concentrations of hoechst sequence specific binding of the drug is observed (type I binding). At greater concentrations non-specific modes of binding are observed which are mediated through electrostatic interactions between the positively charged ligand and the negatively charged sugar-phosphate backbone of the DNA (type II binding). Positioning the 2-amino group in the sequence AATT by incorporation of the base DAP abolishes Hoechst binding to this sequence (Loontiens *et al.*, 1991).

Increases in ionic strength dissociate non-specifically bound Hoechst molecules, as do relativity low concentrations of ethanol. Absorption fluorescent studies show that one Hoechst molecule is bound per 6bp in poly d[(A-T)]. In addition, GC binding has also been observed, and it was suggested that Hoechst could be binding in the major groove at low levels (Loontiens *et al.*, 1990).

1.7.1 Footprinting Studies of the Hoechst 33258-DNA Complex

The interaction of Hoechst with A/T sites was originally proposed by Mikhailov *et al.*, 1981. Before the crystal structure of Hoechst 33258 was available, footprinting studies had already identified the primary recognition sites of this ligand as four consecutive A•T base pairs (Martin & Holmes, 1983). AATT and AAAA are strong binding sites while TAAA and ATTA were weak binding sites. This reflects the fact that the position and order of the AT bases in the DNA sequence is important since Hoechst recognises not so much the DNA sequence but the conformation of the DNA (Murray & Martin, 1988; Murray & Martin, 1994). More recently, it has been demonstrated that Hoechst discriminates between alternating AT and runs of AT and binds to the later with 50 fold greater affinity, for example binding is much stronger to AATT than to TATA. These variations in affinity were attributed to differences in minor groove width between TpA and ApT steps (Abu-Daya *et al.*, 1995; Abu-Daya & Fox, 1997).

Footprinting studies using methidiumpropyl-EDTA. Fe(II) (MPE.Fe(II)) allowed an accurate determination of the size of the binding site. DNaseI cleavage produces footprints approximately 2-3bp larger than the size of the actual binding site and it is very sensitive to changes in DNA conformation. Chemical cleavage agents such as hydroxyl radicals and MPE are not affected to the same extent by the conformation of DNA and due to their smaller size, map the size of the site with greater accuracy. Using MPE, binding site sizes for Hoechst of approximately 4-6bp are observed (Harshman & Dervan, 1985). Larger binding sites were observed in longer stretches of A and T base pairs and presumably reflect the binding of the ligand to overlapping sites. In addition, it was also found that the ligand could tolerate guanine residues at the end of a binding site (e.g. AAAAG or AAAG) but these were not found inside the AT region and the presence of a TpA step within the target site was found to greatly attenuate drug binding (Portugal & Waring, 1988).

1.7.2 The Crystal Structure of Hoechst 33258-DNA Complex

The crystal structure of Hoechst 33258 has been determined by a number of groups (Pjura *et al.*, 1987; Quintana *et al.*, 1991; Sriram *et al.*, 1992; Teng *et al.*, 1988; Vega *et al.*, 1994). In all structures, the ligand binds to target sequences via the minor groove, displacing the spine of hydration. However, although the recognition motif for Hoechst 33258 has been highlighted as AT*n* sequences, binding has been observed to the sites ATTC and GATA (Carrondo *et al.*, 1989; Pjura et al., 1987). The binding of the drug to AATT appears not to be affected by temperature although there are slight changes in the torsion angles between the benzimidazole rings (Quintana et al., 1991). In all crystal structures, Hoechst is observed to follow the spiral of the minor groove (i.e. the drug is isohelical) and there are good non-bonded interactions between the walls of the narrow groove and the benzimidazole rings of the ligand. The benzimidazole rings of Hoechst fit tightly into narrow AT minor groove which is barely wide enough for this interaction, see fig 1.13. For these contacts to occur, the carbon-carbon torsion angles between the rings are extremely important so that the drug can remain isohelical. However, the phenol ring remains

coplanar with bezimidazole 1 and is hence twisted out of the curve of the minor groove. It has been suggested that this is a consequence of resonance stabilisation between the two ring systems. Despite this, the phenol group still protects the AT base pair, even although it does not bond directly to it. In addition, there is an electrostatic contribution to the binding between the negatively charged DNA and the positively charged ligand by virtue of the piperazine ring.

It is the piperazine group that is thought to explain the one base pair slip observed by Pjura *et al.* 1987 and Carrondo *et al.* 1989. Steric clash prevents the piperazine and benzimidazole 2 lying in co-planar orientation, hence they tend to reside at right angles to each other. Under these circumstances the piperazine ring is 60° removed from parallism with the AT minor groove and it is hence impossible for it to be accommodated within this very narrow region. Therefore, it is then forced to interact with the wider GC region and this explains why the drug appears to be recognising the sequence ATTC. This allows Hoechst 33258 to tolerate either a GC or AT at the piperazine end of the binding site and it is thought that piperazine will orientate towards the region where the minor groove begins to widen.

The binding of Hoechst does not significantly distort the double helix. In summary, there are two minor changes in DNA conformation:

1. The minor groove, where the drug binds, is widened with a corresponding compression of the major groove.

2. The DNA helix undergoes an axial bend by approximately 6-8°. There is a slight increase in base pair buckle across the target site.

Base pair buckle is expected since the ligand effectively increases the helical repeat of the DNA across the binding site. This is because Hoechst is 20% longer than the distance between one base pair and the next (Goodsell & Dickerson, 1986; Quintana *et al.*, 1991).

The affinity of Hoechst for the AT minor groove can be accounted for by a number of factors. The 2-amino group of guanine would hinder binding of the drug not just because of steric occlusion but also because of its electropositive nature. Besides this, the GC minor groove is wider than that of AT, since one of the principle stabilising factors in the complex are a tight fit and van der waals interactions between ligand aromatic groups and the walls of the minor groove it is logical to deduce that a narrow groove width is more attractive for ligand binding. The bifurcated hydrogen bonds present in the structure appear to act in a stabilising manner rather than providing specificity for the interaction. These bonds could occur equally well, if the 2-amino group of guanine was not there to hinder the drug. This is in contrast to echinomycin where hydrogen bonding acts as the major recognition factor.

1.7.3 NMR studies of the Hoechst 33258-DNA Complex

The solution structure of Hoechst 33258 bound to a number of different DNA templates has been studied (Embrey *et al.*, 1993; Fede *et al.*, 1991; Gavathiotis *et al.*, 2000; Parkinson *et al.*, 1990; Searle & Embrey, 1990). NMR studies have shown that Hoechst binds to the central AT region in duplexes containing sites such as AATT and AAAA, as in the Teng *et al.* (1988) crystal structure (Fede *et al.*, 1991; Parkinson *et al.*, 1990; Searle & Embrey, 1990). Embrey and Searle (1990) observed the ligand binding in a cooperative manner to a sequence containing two closely spaced AAAA sites. In a later study this was confirmed where binding of Hoechst to the DNA was found with only the 2:1 complex of drug:DNA (Gavathiotis *et al.*, 2000). However, it is presently unclear as to how this cooperativity is mediated.

Crystal studies suggested that the piperazine ring of Hoechst would prefer to lie in a region where the minor groove becomes wider. No contacts were observed between the piperazine groups and the GC base pairs, as judged by NOE spectra (Parkinson et al., 1990; Searle & Embrey, 1990). However, a hydrogen bond was inferred between piperazine and guanine via water (Gavathiotis et al., 2000). Taking the previously

observed degeneracy of the binding site into account, i.e. the inclusion of G or C, Embrey *et al.* (1993), studied the interaction of Hoechst with a sequence which offers the ligand 5 potential binding sites. Hoechst was observed to bind across the central AATT step and concluded that the bulky piperazine group was accommodated in the narrow region of the A/T minor groove. In sequences containing two Hoechst binding sites, piperazine is orientated towards the wider GC region of the duplex (Gavathiotis *et al.*, 2000; Searle & Embrey, 1990). Dynamic behaviour in the phenol group via a mechanism of "ring-flipping", i.e. rotating 180° about the C-C bond has also been observed in Hoechst-DNA complexes. It is thought that the ability of the group to do this may reflect "breathing" of the structure in solution (Fede *et al.*, 1991; Searle & Embrey, 1990).

The binding of Hoechst, as judged by NMR, does not significantly alter the structure of the DNA duplex and this confirms all previous models for the ligand binding. Sugars are in the standard C2'-endo pucker, as observed in classic B-form DNA and glycosidic bonds are in *anti*. Minor changes were also detected in the major groove and presumable reflect minor changes in helical parameters, such as base pair buckle when the ligand binds (Fede *et al.*, 1991). The nature of the sequences under study, large propeller twists were observed across AT sites. Hence the minor groove width of these duplexes is extremely narrow, which renders it attractive for Hoechst binding. This narrowness was found to promote extensive van der waal contacts between the ligand and the DNA, especially along the floor of the groove. The helical parameters observed in the complex are also found in free DNA and this favours a model in which sequence dependent DNA conformation is attractive for ligand binding rather than these parameters arising as a result of induced fit drug binding. Bifurcated hydrogen bonds were confirmed between the NH groups of the benzimidazole rings and the adenine N3 and thymine O2 atoms on the edges of the base pairs. In addition, it was proposed that the electrostatic difference between the floor of the AT minor groove and the piperazine ring would impart further stabilisation to the complex (Parkinson *et al.*, 1990; Searle & Embrey, 1990).

1.8 Nucleosome-Ligand Interactions

To be used therapeutically, any sequence selective DNA binding ligand must interact not with free DNA but with chromatin and ultimately the nucleosome. Early studies using platinum compounds showed that there was little difference in the binding of these molecules to extracts of chromatin compared to free DNA. However, the formation of DNA-protein cross-links was inferred and could have significant consequences for the chemotherapeutic action of these drugs (Houssier *et al.*, 1983). Cross-linking of this nature could be visualised with trans-Platinum but is more difficult to see how this might occur with cis-Platinum. In contrast, the anthracycline intercalator daunomycin was found to bind to chromatin with a lower affinity relative to free DNA. The affinity of the drug was greater for nucleosomes containing 175bp of DNA than for particles with 146bp, perhaps reflecting the ligand's preference for linker sequences rather than binding to the supercoiled duplex of the central nucleosome core. However, at saturating concentrations, the drug caused unfolding and aggregation of nucleosome core particles (Chaires *et al.*, 1983). Ethidium bromide has also been demonstrated to bind to nucleosomes with a weaker affinity for the core particle than for free DNA (Taquet *et al.*, 1998). The intercalator actinomycin binds to the nucleosome in a manner comparable to that of free DNA, as judged by absorption spectra, but requires greater ligand saturation in solution to achieve this (Cacchione *et al.*, 1986). There was a significant decrease in the number of strong binding sites for this drug and it was deduced that approximately four ligand molecules were bound per nucleosome. Actinomycin also causes a change in the conformation of the nucleosome, which Cacchione *et al.* (1986) attributed to unfolding of the particle, from data obtained from sedimentation studies. This transition was found to be reversible. The nucleosomes used in this study contained ca. 170bp of DNA, and hence it remains unclear as to whether actinomycin targeted to regions of the sequence unbound to the protein octamer or whether it interacted across the surface of the central 146bp of the DNA superhelix. Actinomycin has also been found to create sites, which are hyperreactive to hydroxyl radicals, but does not yield a footprint on nucleosomes (Churchill *et al.*, 1990). Later work studying the interaction of the anthracyclines 4'-deoxy, 4'-iodo-doxorubicin (4'-IAM), 9-

deoxydoxorubicin (9-DAM), 4- demethoxydaunorubicin (4-DDM) and 4'-deoxydoxorubicin (4'-DMA) with 175bp nucleosomes showed that the drugs' spectroscopic and CD profile was similar to that of binding to free DNA (Cera *et al.*, 1991; Cera & Palumbo, 1991). However, it was observed that 4'-IAM appeared to prefer binding to the ordered conformation of nucleosomal DNA than to free DNA. (9-DAM), (4-DDM) and (4'-DMA) were thought to interact with linker DNA and not bound to the central nucleosome core.

The interaction of the intercalators echinomycin, nogalamycin, actinomycin, and the minor groove binders berenil, netropsin and distamycin with reconstituted nucleosomes have been subject to a detailed series of studies which yielded interesting results. Using the probe DNaseI, novel cleavage products were observed approximately halfway between the original cleavage maxima in drug-free controls. The hypothesis to account for these observations was that the DNA superhelix had rotated on the surface of the protein octamer in the presence of a bound ligand. This phenomenon was not observed with the mono- intercalators actinomycin and nogalamycin and at high drug concentrations the superhelix was displaced from the protein core (Portugal & Waring, 1986). To account for these results, Waring and co-workers have suggested that ligands bound first to sites exposed on the outer surface of the particle and then caused those sites to be rotated by 180° so that they would lie on the inner surface of the superhelix. The driving force for this reaction was suggested to be the optimisation of non-bonded interactions between the ligand and the DNA (Low *et al.*, 1986a; Portugal & Waring, 1986; Portugal & Waring, 1987a; Portugal & Waring, 1987b). Molecular modelling studies indicated that this conformational change in the nucleosome would be favoured after the addition of the ligand netropsin (Perez & Portugal, 1990). DNaseI and hydroxyl radical work studying the interaction of the drug mithramycin with nucleosome core particles showed that this ligand did not produce novel cleavage products inherent of superhelix location (Fox & Cons, 1993). Later work studying the interaction of the minor groove binding ligands Hoechst 33258, distamycin, netropsin and berenil with DNA fragments reconstituted with core histone proteins confirmed the rotation of the

DNA by 180° in the presence of these ligands (Brown & Fox, 1996). However, there was one important difference: the drug target sites were rotationally positioned so as to face the histone core. Therefore, these sites were occluded by the histone octamer and yet rotation of the DNA superhelix was still observed. It was concluded that the drugs had interacted with their target sites but it was unclear as to how this was achieved.

1.9 The Site Exposure Model

The problem presented for ligand access to occluded target sites on the nucleosome is one that has been previously encountered with studies concerning the binding of regulatory proteins to chromatin. *In vitro* studies have shown that many such proteins have access to their target sites even when those sites appear to be occluded by the structure of the nucleosome. Most genes are organised in the eucaryotic genome as nucleosome arrays and since many such sequences have important biological activity regulatory proteins must have some form of access to their DNA target sites. It has remained unexplained as to how target sites are recognised under such circumstances. A model has been proposed which accounts for the binding of proteins to target sites occluded by the nucleosome and is referred to as "Site Exposure", fig 1.14, panel I (Polach & Widom, 1995).

The nucleosome is viewed as a repressive component of the genome but the key to site exposure lies in the suggestion that these complexes may be dynamic structures which transiently expose regions of DNA so that regulatory proteins and other molecules can bind to target sites as though they were free in solution. Evidence for such dynamic processes have already been observed at the ends of the DNA superhelix (Clarke *et al.*, 1985). The mechanism for site exposure is that the DNA superhelix detaches from the histone octamer at the ends of the nucleosome. Therefore any target may become accessible by the dissociation of up to half of the superhelix. However, more energy is required to remove a larger portion of the DNA superhelix from the protein core and hence target sites that are close to the ends of the nucleosome will be exposed for longer periods of time, i.e. will be more

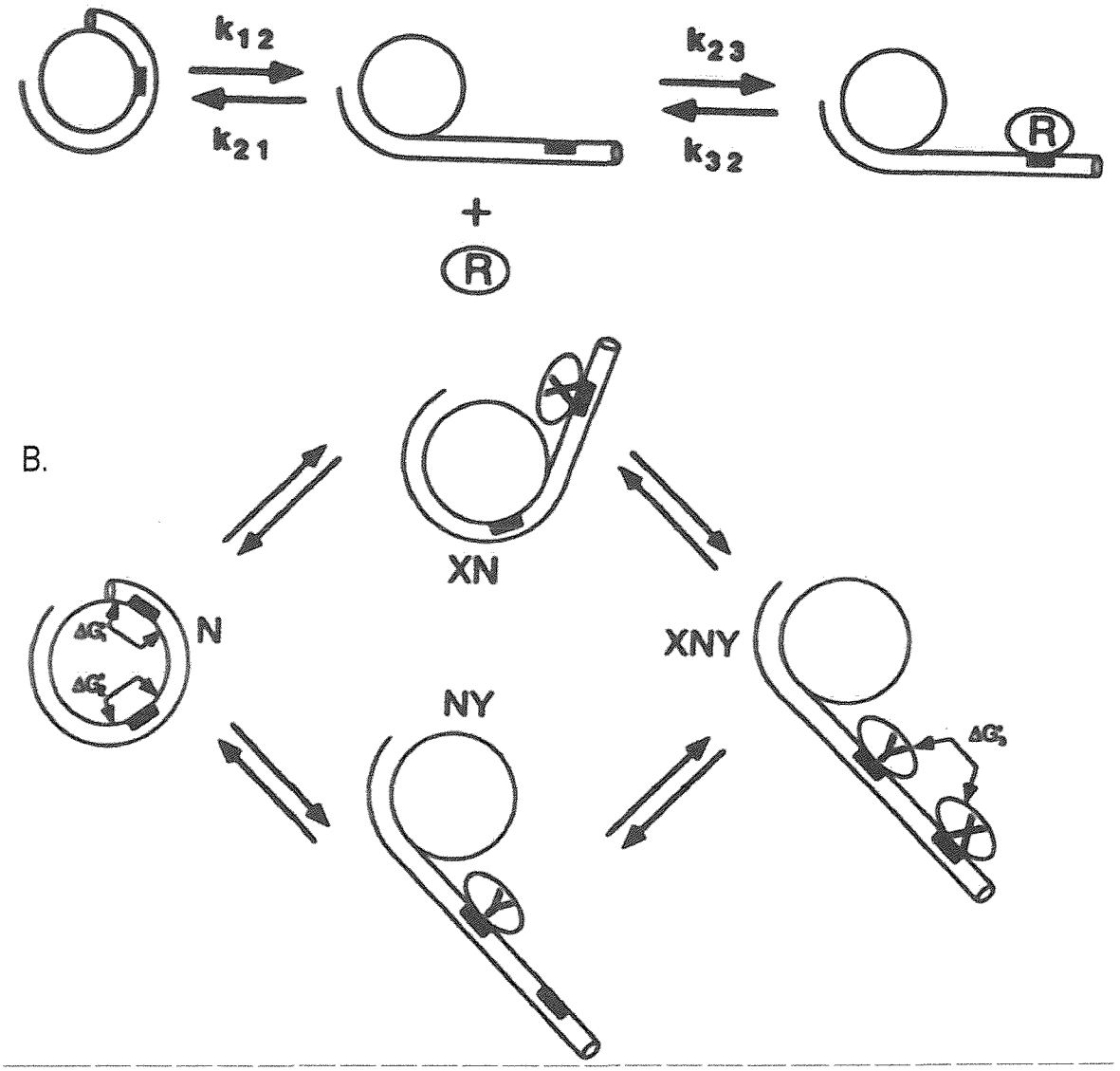

Figure 1.14, The site exposure model as presented for a single nucleosome. The histone octamer is shown as a disk with the DNA wrapping around it. (A), the target, black box, is inaccessible to protein (R). Unwrapping of the DNA from the surface allows binding. (B), Cooperativity in the binding of proteins (X) and (Y). After exposure of the target site for (X) the binding of (Y) is increased and vice versa. See text for details. Taken from Widom 1998.

accessible, than target sites that are located near the dyad, which will be less accessible. Since histone-DNA contacts occur at every inward-facing minor groove, there will be a further energetic cost to displace an additional helical turn of the DNA from the histone octamer. In an elegant series of experiments, Polach and Widom 1995 demonstrated that the equilibrium constant for a series of endonuclease target sites was related to their translational position on the nucleosome and observed a decrease in the equilibrium constant from the ends of the superhelix moving towards the dyad. It is also of interest that removal of the histone tail domains leads to a slight increase in the position-dependent equilibrium constants for site exposure (Polach *et al.*, 2000).

The site exposure model also has important implications for the binding of more than one molecule to the nucleosome and presents a novel method of cooperatively (Anderson & Widom, 2000; Polach & Widom, 1996; Widom, 1998) fig 1.14b. As illustrated in the figure, once protein Y has bound, protein X may bind without having to pay the energetic cost of site exposure, ΔG^{0}_{conf}, which without the binding of Y would normally occur. Alternatively, the binding of X will assist the binding of Y and the level of cooperatively between X and Y will equal minus one times the energetic cost for exposing a site. Therefore, this model has important ramifications for crucial biological systems such as the initiation of transcription, replication and any system that requires binding to "occluded" target sites on the nucleosome.

1.10 DNaseI

The glyco-protein DNaseI produces single nicks in double stranded DNA by cleaving at the O3'-P bond in the helix. The enzyme binds in the minor groove by the introduction of an exposed loop region, which inserts a tyrosine residue into the helix (Suck & Oefner, 1986). This interaction causes the minor groove to widen by approximately 3Å and generates a 21.5° bend in the DNA helix in a direction towards the major groove and away from the binding surface of the enzyme. This mechanism suggests that regions of DNA where the minor groove is narrow, such as A/T, would be cut less efficiently by the enzyme (Hogan *et al.*, 1989; Lahm & Suck,

1991; Oefner & Suck, 1986; Suck *et al.*, 1988). Cleavage is thought to be brought about by two histidine side chains which are in close proximity to the phosphate group in the O3'-P bond (Weston *et al.*, 1992) Although the enzyme does not exhibit any apparent sequence selectivity, the enzyme does cleave some sequences with greater efficiency than others (Herrera & Chaires, 1994), which explains why DNaseI footprinting gels do not show an even ladder of cleavage products. The enzyme binds to ca. 10bp of DNA, which is why ligand footprints are larger than expected. In addition, due to the geometry of DNA, all footprints produced with DNaseI are staggered in the 3' direction by approximately 2-3bp, fig 1.15 (Fox, 1997). DNaseI footprinting relies on the fact that the binding of a protein or small ligand to DNA will cleavage by the enzyme in the vicinity of the target site. The technique was first employed to demonstrate the binding of the lac repressor to the lac operator (Galas & Schmitz, 1978). Approximately 200bp of 3'-labelled DNA are used in a given footprinting reaction, so that cleavage products can be easily resolved by denaturing PAGE. If the molecule under study binds to its target site, DNaseI cleavage is attenuated relative to the control where the compound binds, fig 1.15. The conditions of each footprinting experiment insure that on average each DNA molecule is cut only once, i.e. single-hit kinetics. Although an ideal footprinting probe should not express any form of DNA sequence selectivity, this property of DNaseI makes it extremely useful at detecting changes in the conformation of DNA after binding of a molecule.

1.11 Hydroxyl Radicals

Hydroxyl radicals are produced by the Fenton reaction:

$$Fe^{2+} + H_2O_2 \Rightarrow Fe^{3+} + OH + OH$$

These radicals have little sequence preference, make an ideal footprinting probe and, due to their small size, provide a good estimation of the size of binding sites in DNA-drug and DNA-protein complexes. The exact cleavage site of the radical on DNA is

A.

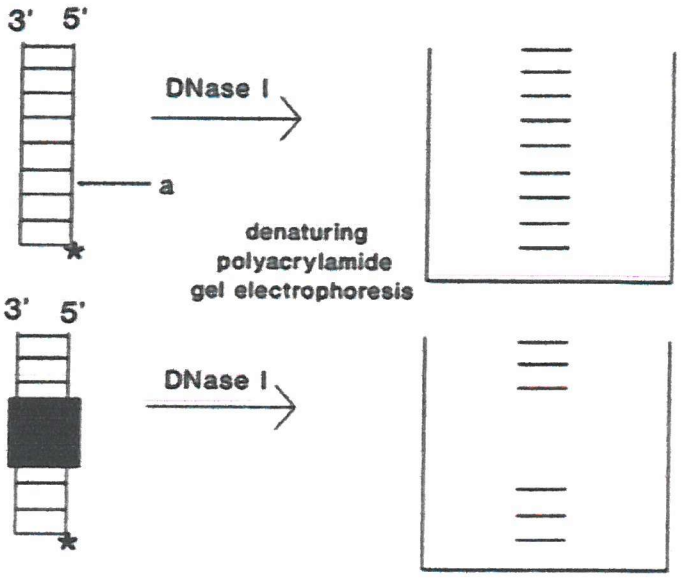

B.

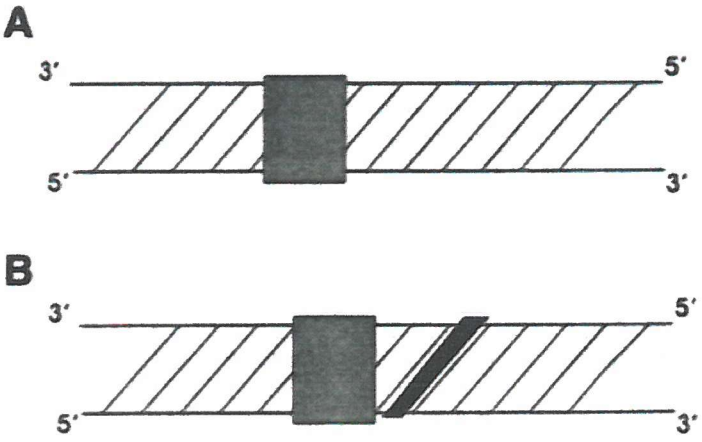

Figure 1.15, A representation of DNaseI footprinting. (A), cleavage products, where the DNA is 3'-end labelled are visualized on a sequencing gel exposing a footprint where the ligand binds to its target site. (B), the 3'-stagger of DNaseI footprints. The DNA is shown in 2D and is viewed along the minor groove. The hashed box corresponds to DNaseI and the filled diagonal is the bound ligand. Taken from Fox 1997.

not clearly defined although it is thought to react with hydrogen at position 5' in the deoxyribose and has less reactivity with other hydrogen atoms in the order H4'>H3'>H2'/H1' (Tullius & Dombroski, 1986). This cleavage probe has been used in the study of DNA-protein complexes (Draganescu *et al.*, 1995; Lee & Hahn, 1995; Tullius & Dombroski, 1986), DNA structure (Balasubramanian *et al.*, 1998; Price & Tullius, 1992; Tullius & Dombroski, 1985) and DNA-drug complexes (Cons & Fox, 1989). In this study, hydroxyl radicals have been used to map the rotational position of histone-bound DNA, see below.

1.12 DNaseI and Hydroxyl Radicals as Footprinting Probes for the Nucleosome

DNA bound to the surface of the histone octamer will be protected by the nature of the complex to footprinting probes such as DNaseI and hydroxyl radicals. Minor grooves facing the protein surface are therefore not readily accessible to these agents and only exposed regions of the double helix, across the surface of the supercoil, will be cleaved by the action of DNaseI and the hydroxyl radical. Therefore, data generated and visualised on a sequencing gel in such experiments produces what is known as a nucleosome phasing pattern, fig 1.16. Since both agents cleave DNA in the minor groove, regions of maximal cleavage represent areas where the DNA is facing away from the histone octamer, while regions of attenuated cleavage represent areas where the DNA is facing towards the protein core. Phasing patterns can be difficult to interpret with DNaseI since the enzyme exhibits a slight sequence selectivity, which makes the use of hydroxyl radicals more desirable.

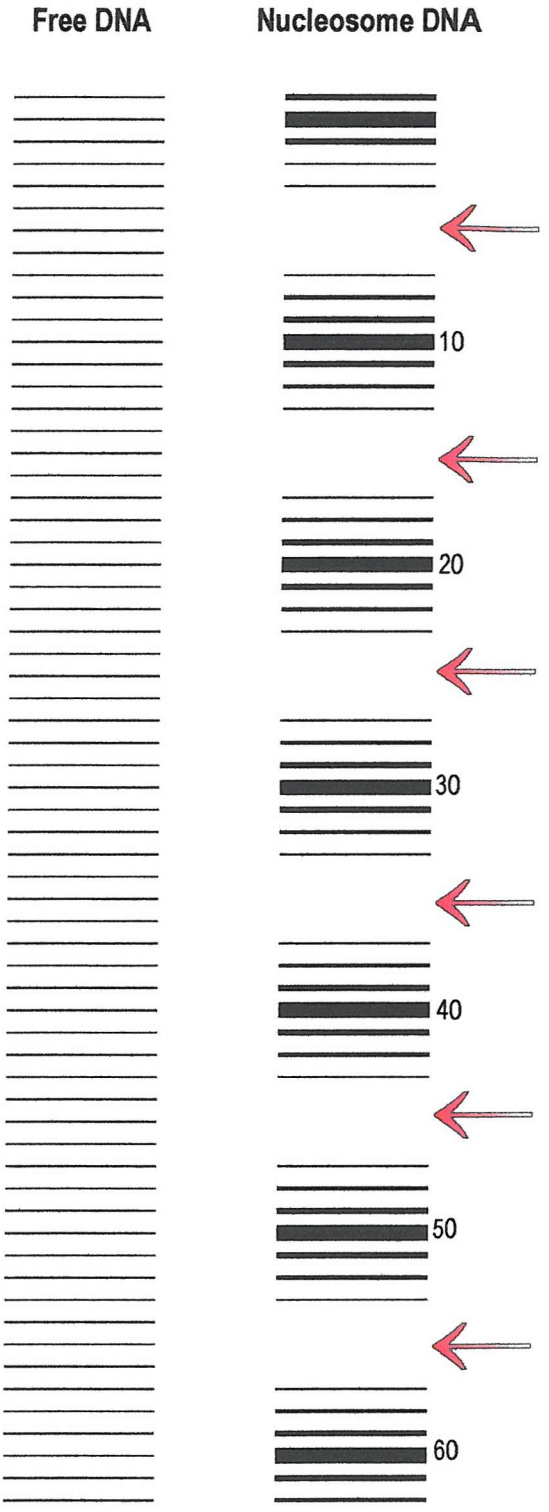

Figure 1.16, A cartoon gel demonstrating nucleosome phasing. The free DNA is represented as even ladder of cleavage products while in the nucleosome DNA attenuation of cleavage occurs where a minor groove faces the surface of the histone octamer. This is indicated with arrows.

2 Materials and Methods

2.1 Enzymes and Chemicals

All chemicals were purchased from Sigma and restriction enzymes were purchased from Promega. [∀-^{32}P]dATP was purchased from Amersham Biotech at a concentration of 3000Ci mmol-1. *Pfu Turbo* DNA Polymerase was purchased from Stratagene at a concentration of 2500 U ml-1 and was stored –20°C.

AMV reverse transcriptase was purchased from Sigma. The enzyme was stored at -20°C at a concentration of 12000 units ml^{-1}. DNaseI was also purchased from Sigma. It was stored at –20°C at a concentration of 7200 units ml^{-1} in 0.15 M NaCl containing $MgCl_2$. MNase was also purchased from Sigma and stored at a stock concentration of 170000 units ml^{-1} (absorbance units released) at –20°C.

pUC19, fig 2.1, was purchased from Pharmacia Biotech and stored at –20°C at a concentration of 25 mg ml^{-1} in 10 mM Tris-HCl, pH 7.5.

Construct tem, fig 2.2, was a gift from Professor Keith Fox and was cloned into pUC19 polylinker between the *Eco*RI and *Ava*I restriction sites.

All oligonucleotides were purchased from Oswell DNA Service and were synthesized on a scale of 40 nmoles. They were stored at –20°C in Millipore H_2O at a concentration of approximately 16 mg ml^{-1}. dNTPs were purchased from Promega and stored at –20°C at a concentration of 100 mM.

Echinomycin was a gift from Professor Keith Fox. The drug was dissolved in 100% DMSO to a final concentration of 5mM. Hoechst 33258 was purchased from Sigma and was dissolved in AnalaR® water to a stock concentration of 10mM. This stock was then aliquoted to avoid constant freeze-thaw of the ligand. Both ligands were stored at –20°C until use.

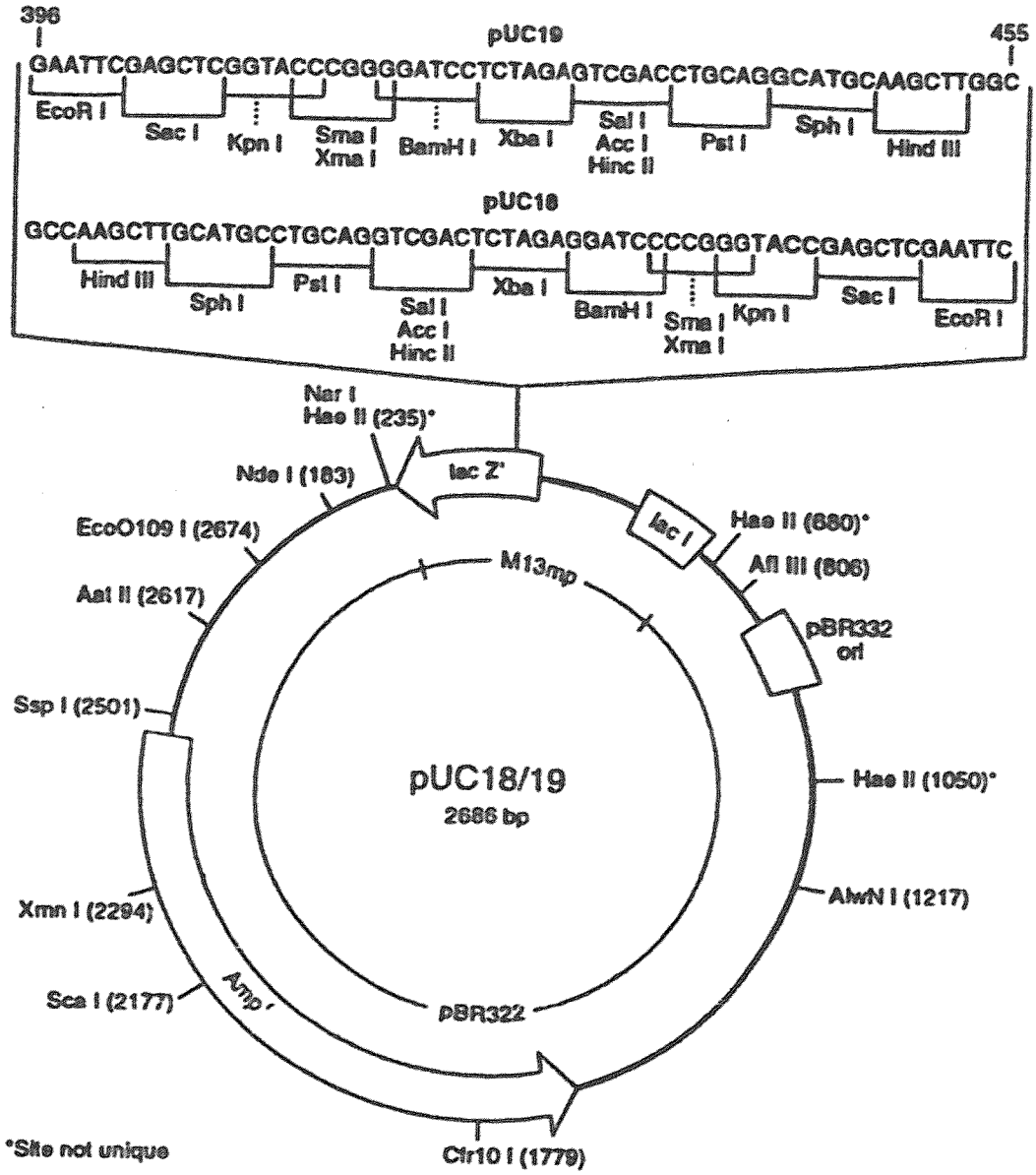

Fig 2.1. Diagram of the pUC19 vector. PCR products were cloned into the polylinker cloning site by the action of the restriction enzymes *Eco*RI and *Ava*I. Image taken from the Pharmacia Biotech Catalogue 1999.

tem:

```
5′-AATTCTGGTCACCTTCAGTCTGTTGTGGATGAAGATCACACAACCAGTTCTTCTTCCTCTTCCTGACACTCTACAGTGGTGTGTCATCTGATGTGATGTGTCCCACTTCCCAACAAGGGAGTAGGTCAGTAGAGAACATCACCCTGTCCC-3′
          10        20        30        40        50        60        70        80        90        100       110       120       130       140       150
3′-AAGACCAGTGGAAGTCAGACAACACCTACTTCTAGTGTGTTGGTCAAGAAGAAGGAGAAGGACTGTGAGATGTCACCACACAGTAGACTACACTACACAGGGTGAAGGGTTGTTCCCTCATCCAGTCATCTCTTGTAGTGGGACAGGGCC-5
```

Fig 2.2 sequences of construct *tem* which contains no CpG or (A/T)n sites and does therefore not bind with echinomycin or Hoechst 33258.

2.2 Fusion PCR Site Directed Mutagenisis

Construct tem was derived from the naturally occurring sequence TyrT, from E. coli, which contains randomly distributed binding sites for Hoechst and echinomycin. It was mutated so as to remove all CpG and (A/T)*n* sequences and therefore does not contain any target sites for the ligands echinomycin and Hoechst 33258. Mutagenisis was then used to introduce target sites for these ligands at defined locations in the sequence. These differed from the binding sites in natural TyrT in respect that all echinomycin binding sites were defined as 5'-ACGT-3' while all Hoechst sites were defined as 5'-AATT-3' (except in construct H3 where one Hoechst site was 5'-AAAA-3').

This mutagenisis method utilises the polymerase chain reaction (PCR). The method described here is a modified version (Landt *et al.*, 1990). PCR was conducted in three stages. Stage one produces the required mutation, stage two produces a full-length fragment and stage three amplifies the mutated products prior to cloning, fig 2.3.

Stage 1 reaction conditions:

2.5 µl dNTP mix (10mM stock solution)

10 µl Pfu TurboTM x10 reaction buffer (200mM Tris-HCl (pH 8.8), 100mM KCl, 100 mM $(NH_4)_2SO_4$, 20 mM $MgSO_4$, 1% Triton® X-100, 1 mg ml^{-1} nuclease-free bovine serum albumin (BSA))

175 ng Primer 1

175 ng Mismatch Primer

1 µl DNA template* (tem fragment)

Sterile H_20 to final volume of 100 µl

* This was restricted prior to use by the action of *Eco*RI and *Ava*I, in the polylinker-cloning site of pUC19, for 2 hrs at 37°C. Restriction enzymes were then heat-inactivated at 65°C for 15 mins and the DNA precipitated and resuspended in 50ul

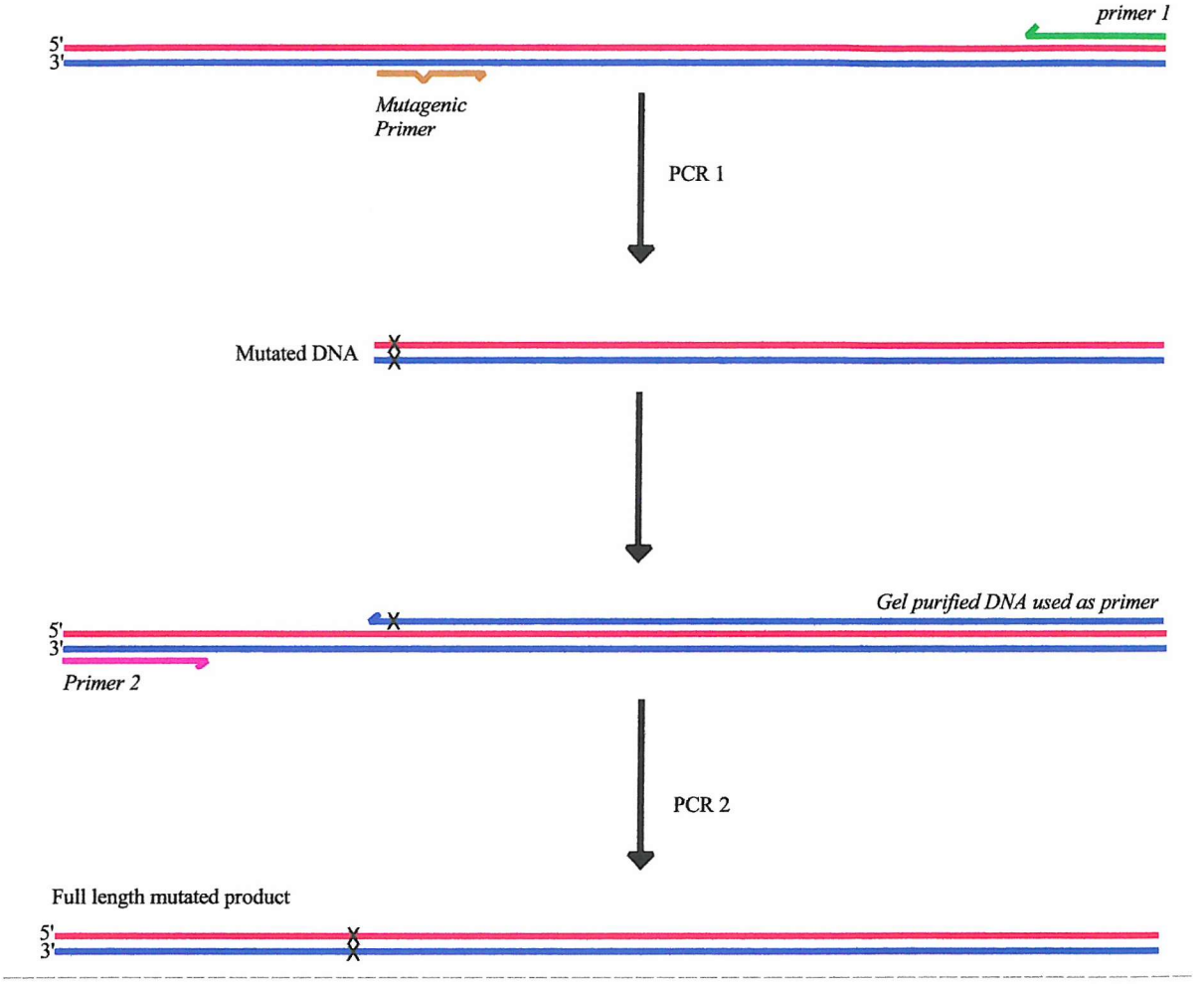

Fig 2.3, diagram of PCR mutagenisis. Stage 1 produces a fragment containing the desired mutation. Stage 2 then produces a full length fragment Taken with permission and modified from Brown 1997 (PhD Thesis).

sterile water. The template was stored at – 20°C until use.

"Hot-start" at 95°C for 1 min then add:

1 µl of Pfu TurboTM DNA polymerase (2.5 U/µl).

This was then subjected to the following PCR cycle in a Techne GeneAmp 2000 thermal cycler:

Segment	*Cycles*	*Description*	*Temperature*	*Time*
1	1	denaturation	95°C	30 s
2	30	denaturation	95°C	45 s
		primer annealing	55°C	1 min
		polymerisation	72°C	2 min 30 s

A final hold step at 72°C for 5 mins was carried out before cooling the reaction mixture to 4°C.

For each reaction, segment 2 (primer annealing) was usually altered depending upon the average Tm of the annealed primer and if non-specific polymerisation products were observed after the reaction. The average T*m* was calculated using the following formula:

$Tm = 81.5 + 0.41(\%GC) - 675/N - \%$ mismatch

Where N is the length of the primer in base pairs.

Provided the reaction is optimised, stage one should produce sequences containing the desired mutations. However, it is necessary to remove primer one before continuing on to the next stage. The DNA fragments from stage one were ethanol

precipitated, see below, and resuspended in 10 µl 10 mM Tris-HCl (pH 7.5), 0.1 mM EDTA (TE buffer). This was then run on a 1% agarose gel containing 10 µg ml^{-1} ethidium bromide. At this stage it is also possible to assess the extent of amplification. Bands corresponding to mutated product from stage one were cut out from the gel under UV light and the DNA extracted using Qiagen Qiaex II DNA extraction kit. The procedure was followed as detailed in the manufactures instructions.

Stage 2 reaction conditions:
2.5 µl dNTP mix (10 mM stock solution)
10 µl *Pfu* Turbo™ x10 reaction buffer
175 ng Primer 2
3 µl gel purified product from stage 1
1 µl DNA template (tem fragment)
Sterile H_20 to final volume of 100 µl

"Hot-start" at 95°C for 1 min then add:

1 µl of *Pfu* TurboTM DNA polymerase (2.5 U ml^{-1}).

This was then subjected to the same reaction temperature cycle indicated above and the resulting product, was gel purified and extracted from agarose in the same manner as described for stage one. If low product yields were evident from stage 2 the product was subjected to a final round of PCR in stage three to amplify mutagenic sequences.

Stage 3 reaction conditions:
2.5 µl dNTP mix (10 mM stock solution)
10 µl *Pfu* Turbo™ x10 reaction buffer
175 ng Primer 1

175 ng Primer 2

35 µl gel purified product from stage 2

Sterile H_20 to final volume of 100µl

"Hot-start" at 95°C for 1 min then add:

1 µl of *Pfu* Turbo™ DNA polymerase (2.5 U ml^{-1}).

This was then subjected to the same reaction temperature cycle indicated above and the resulting product was gel purified and extracted from agarose in the same manner and prepared for cloning, see below. Primer 1 and primer 2 contained the recognition sequences for *Ava*I and *Eco*RI respectively.

2.3 Ligation of Products from PCR Site Directed Mutagenisis

After the final stage of mutagenisis (using fusion PCR), an aliquot of product was run on a 1% agarose gel containing 10 µg ml^{-1} ethidium bromide with Bioline Hyper ladder 100bp size marker, which contains known quantities of DNA per band. From this it was possible to obtain a rough estimate of the amount of DNA product present in the PCR reaction. The remaining gel purified DNA was then digested with the restriction enzymes *Eco*RI and *Ava*I according to the manufactures instructions.

Each digestion was carried out for 2hrs 30min at 37°C. Restriction enzymes were then heat-inactivated at 65°C for 15 mins.

The rough estimate of PCR product, obtained earlier, was used in the following equation to calculate the approximate amount of insert DNA required for ligation:

ng insert = (ng vector x kbp size insert/kbp size vector) x molar ratio insert/vector

The standard molar ratio used was 3:1

The ligation reaction was then set-up in the following manner:

X µl insert sticky ends
200 ng pUC19 vector
2ul 10x Promega ligase buffer
1 µl BSA (10mg ml^{-1} stock)
2 µl T4 DNA Ligase

Temperature Cycle Ligation, as described by Anders *et al.* 1996, was then carried out overnight. Ligated DNA was then used to transform JM109 competent cells.

Although the first mutated sequences were obtained by fusion PCR, this was later replaced by the Stratagene QuikChange method, since this was quicker, more reliable and efficient.

2.4 Stratagene QuikChange® Site Directed Mutagenisis

The tem construct was obtained from plasmid miniprep, see below, and was used as a template in the first mutagenisis reactions. Constructs containing multiple drug binding sites were prepared using other mutants as templates. The principle of this method is explained in fig 2.4. The QuikChange® reaction was set up according to Stratagene's guidelines:

5 µl of 10× reaction buffer (100 mM KCl, 100 mM $(NH_4)_2$ SO_4, 200 mM Tris-HCl (pH 8.8), 20 mM $MgSO_4$, 1% Triton® X-100, 1 mg ml^{-1} nuclease-free bovine serum albumin (BSA))
X µl (5–50 ng) of dsDNA template (0.2-0.5 ml of plasmid miniprep was generally used)
X µl (125 ng) of oligonucleotide primer 1 (Forward primer)
X µl (125 ng) of oligonucleotide primer 2 (Reverse primer)

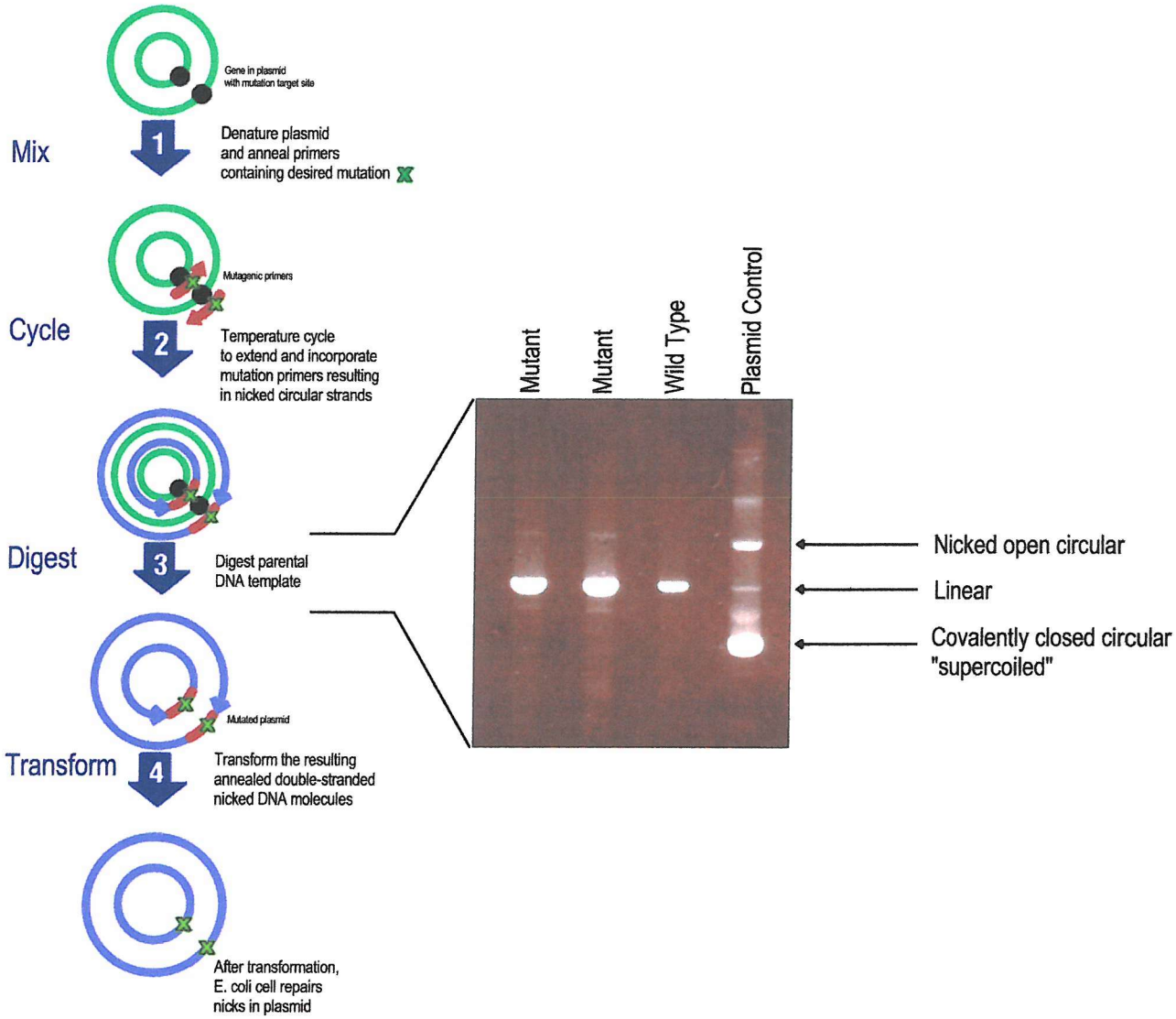

Fig 2.4, diagram of Stratagene QuikChange site-directed mutagenesis. The desired mutation is inserted during the cycle phase which produces nicked circular strands. *Dpn*I digests remaining parental DNA leaving the mutated DNA intact. This is then transformed into E. *coli*. An agarose gel is included to show example results produced by this method. Successful reactions contain a faint band corresponding to the nicked mutant DNA after enzyme digestion. Smeared products and linear DNA correspond to cleaved parental DNA.

1 µl of dNTP mix (10mM each of dATP, dTTP, dCTP and dGTP)
sterile H_2O to a final volume of 50 µl

Then add:

1 µl of *Pfu* Turbo™ DNA polymerase (2.5 U/µl)

This was then subjected to the following in a Techne GeneAmp 2000 thermal cycler:

Segment	*Cycles*	*Description*	*Temperature*	*Time*
1	1	denaturation	95°C	30 s
2	25	denaturation	95°C	30 s
		primer annealing	55°C	1 min
		polymerisation	68°C	6 mins

To check the outcome of the initial reaction, a 10ul aliquot was run on a 1% agarose gel containing 10ug ml^{-1} ethidium bromide. The above mixture should now contain nicked circular strands containing the original tem construct with the required mutation. However, much of the mixture contains unmodified tem parental DNA. Parental DNA is dam methylated and is thus susceptible to the restriction enzyme *Dpn*I while mutated products are not. 1ul of *Dpn*I was added to each reaction mixture and left in the thermal cycler at 37°C for at least 3 hrs. After this time, the enzyme was heat inactivated at 65°C for 15 mins. At this stage a 5 µl aliquot was run on a 1% agarose gel containing 10 µg ml^{-1} ethidium bromide to check for *Dpn*I digestion and the presence of mutated products. Mutated products are visible as a faint band corresponding to open circular nicked DNA, fig 2.4. If all was successful, 1 µl from the resulting mixture was then used to transform competent *E. coli* JM109 by electroporation, see below.

2.5 Preparation of Chemical- Competent Cells

5ml of 2xTY (16g tryptone, 10g yeast extract, 5g NaCl $1L^{-1}$) media was inoculated with 80 µl of JM109 glycerol stock and grown overnight in an orbital shaker (New Brunswick Scientific Co. Inc, Edison N.J., USA) at 37°C. 500 µl of this was then used to inoculate 50ml 2xYT cell culture and was grown until the O.D. at 600nm reached ca. 0.4-0.6. The cells were then spun-down in a Beckman JA-20 rotor at 5000rpm for 5 mins at 2-4°C. All tips and microtubes were pre-chilled to ca. 2°C before use. The supernatant was discarded and the pellet was gently resuspended in 25ml of transformation buffer (50 mM $CaCl_2$, 10 mM Tris-HCl, pH 7.4). Cells were then left on ice for 30 mins. After this time, the cells were centrifuged again at 5000rpm at 2-4°C and resuspended in 5ml of transformation buffer. Competent cells were stored at 4°C until use and are viable for approximately 5-7 days. Due to the lower yields of DNA obtained from the QuikChange assay and superior efficiencies of transformation, the use of competent cells prepared in this manner was superseded by electroporation.

2.6 Preparation Electro-Competent Cells

5ml of 2xTY (16g tryptone, 10g yeast extract, 5g NaCl $1L^{-1}$) media was inoculated with 80 µl of JM109 glycerol stock and grown overnight in an orbital shaker (New Brunswick Scientific Co. Inc, Edison N.J., USA) at 37°C. 500 µl of this was then used to inoculate 1L 2xTY cell culture and was grown until the O.D. at 600nm reached ca. 0.5-1.0. Cells were then centrifuged in Beckman JA-20 rotor at 3000 rpm at 4°C for 15 min. The pellet was then resuspended in 1L sterile cold water and centrifuged again with the same conditions. Resuspension and centrifugation was carried out twice as above but with 500ml sterile cold water then once with 20ml sterile cold water. After the final centrifugation step, cells were resuspended in 2-3ml sterile cold 10% glycerol (0.2µm filter sterilised). 40 :l aliquots were frozen down on dry ice and stored at –70°C. Competent cells, made by this procedure are viable for 3-4 months.

2.7 Chemical Transformation

10 µl of ligation mixture was added to pre-chilled microtubes and 100-200 µl of competent cells. This was left on ice for 30 mins. After this time, cells were heat shocked at 42°C for 1 min and immediately replaced on ice for 2 mins. 400 ml of ice-cold 2xTY media, supplemented with 80 mM glucose, was added and cells were allowed to recover for 40 mins in an orbital shaker at 37°C (200rpm). After this time, cells were then transferred to agar plates containing 100 mg ml^{-1} carbenicillin, 0.5 mM 5-bromo-4-chloro-3-indolyl B-galactosidase (X-gal), 0.5 mM isopropyl B-D-thioglactopyranoside (IPTG) and incubated overnight at 37°C. Clones were selected by blue/white screening and successful colonies were removed with a platinum inoculation loop and grown 5ml 2xTY media overnight, containing 100 mg ml^{-1} carbenicillin and prepared for T7 sequencing.

2.8 Electroporation

Electro-competent cells were removed from –70°C and thawed on ice. 1ul of ligation or QuikChange® mix was then added and the cell suspension and left on ice for 5 mins. After this time, the cells were transferred to a BTX disposable electroporation cuvette, pre-chilled to ca. 2°C. The cuvette was flicked to mix and settle the cell mixture (the cell suspension must be in contact with both sides of the cuvette) and left on ice for a further 1 min. Electroporation was carried out on a Biorad Pulse Controller and Gene Pulsar machines with the following settings:

Resistance:	200 Ohms
Capacitance:	25 µFD
Voltage:	1.2 Kv
Pulse length:	4.5 ms

Immediately after pulsing, 1ml of 2xTY media, supplemented with 80 mM glucose, was added and the mixture was transferred to a polypropylene tube and left to recover for 1 hr in an orbital shaker at 37°C (200 rpm). After this time, cells were

transferred to agar plates containing 100 mg ml^{-1} carbenicillin, 0.5 mM 5-bromo-4-chloro-3-indolyl ß-galactosidase (X-gal), 0.5 mM isopropyl B-D-thioglactopyranoside (IPTG) and incubated overnight at 37°C. Clones were selected by blue/white screening and successful colonies were removed with a platinum inoculation loop and grown 5ml 2xTY media overnight, containing 100 µg ml-1 carbenicillin and prepared for T7 sequencing.

2.9 Plasmid Miniprep

5ml of 2xTY (16g tryptone, 10g yeast extract, 5g NaCl $1L^{-1}$) media was inoculated with 80 µl of a construct glycerol stock and grown overnight in an orbital shaker (New Brunswick Scientific Co. Inc, Edison N.J., USA) at 37°C. For sequencing, positive clones were isolated with a sterile inoculation loop and used to inoculate 5ml 2xTY media. This culture was then minipreped using Promega Plasmid Miniprep or Qiagen QIAprep Spin Miniprep kits. Protocols were carried out according to manufactures instructions. The QIA Spin Miniprep kit was found to be more reliable as judged by $\forall$-^{32}P labelling.

2.10 T7 DNA Polymerase Sequencing

Positive clones were subjected to plasmid miniprep and eluted in 50 µl of sterile water. 10 µl of this was stored at -20°C as a first generation DNA stock. The remaining 40 µl was denatured by the addition of 10 µl 2M NaOH. This was left at ambient temperature for 10 mins. The DNA was then precipitated with 1/3 volume ethanol and 1/9 volume 3M Na-acetate (pH 4.8). After precipitation the DNA was washed with 70% ethanol and dried under vacum in Savant SpeedVac Concentrator (Stratech Scientific London) for 5 mins. The sequencing protocol was then carried out, according to manufactures instructions, using an Amersham Pharmacia Biotech T7 SequencingTM Kit.

2.11 DNA Precipitation

DNA samples were precipitated with the addition of 1/9 volume 3M sodium acetate and 1/3 volume absolute ethanol relative to the starting total volume of the solution.

This was left in dry ice for 10 mins and then subjected to centrifugation at 14000 rpm for 10 mins in a bench top centrifuge. Since the DNA in use was usually radioactive, precipitation could be checked by comparing the cps in the pellet, which is not usually visible, and the supernatant. If the required, more ethanol was added and the procedure repeated. Samples were then washed with 120 µl 70% ethanol and finally dried under vacum in Savant SpeedVac Concentrator (Stratech Scientific London) for 5 mins.

2.12 Radiolabelling

To the entire plasmid miniprep, prepared as described, 20 µl of 5x AMV Reverse Transcriptase buffer was added and the volume adjusted to 100 µl. This was restricted with 2µl of *Eco*RI and *Aval* for 2 hrs at 37°C. After cleavage, the DNA fragment was labelled by the addition of 0.5 µl AMV Reverse Transcriptase in the presence of [∀-^{32}]dATP. This fills in part of the "sticky end" at the 3'-end of the *Eco*RI restriction site. The 150bp DNA fragment was then purified by running on non-denaturing 8% PAGE run at 27.5V cm^{-1} for 50 mins. The DNA was identified by exposure to X-ray film, excised from the gel and eluted overnight in 400 µl 10mM Tris-HCl, pH 7.5 containing 0.1 mM EDTA. Usually, 200 µl of this was for preparing reconstituted nucleosome cores and the remaining 100 µl was precipitated and resuspended in TE buffer to a concentration of 10 cps µl^{-1} using a hand-held Geiger counter; and used for experiments with free DNA.

2.13 Preparation of H1-Stripped Chromatin

Nucleosomes were purified from chicken erythrocytes in a method modified from (Lutter 1978, Drew and Travers 1985, Drew and Calladine 1987, Brown and Fox 1997). 250ml of fresh chicken blood was collected from the local abattoir and was collected in flasks containing 1/7 volume 84 mM sodium citrate, pH 7.0. 50ml of blood was used for each purification and the remaining 200ml was stored at 4°C in case it was required.

50ml of blood was diluted to 1L by the addition of 15 mM sodium cacodylate, 60

mM KCl, 15 mM NaCl, 0.5 mM spermidine, 0.15 mM spermine, 0.34 M sucrose, 0.2 mM PMSF, 1 mM benzamidine and 15 mM ∃-mercaptoethanol, pH 6.0 (solution 1). This was then centrifuged in a Beckman JA21 centrifuge, with a prechilled JA-20 rotor at 4°C, for 8 mins at 2000 rpm. The pellet was then resuspended in 500ml of solution 1 and the above steps were repeated three times. Solution 1 was then adjusted to pH 7.5 using Tris base and 0.1% (v/v) Nonidet P40. The erythrocyte pellet was then resuspended in 500ml of this solution, which causes the cells to lyse releasing the nuclei. This was then centrifuged at 3000rpm for 3 mins and the supernatant discarded. This was repeated three times. After the final wash, the pellet was resuspended in 15 mM sodium cacodylate, 60 mM KCl, 15 mM NaCl, 0.5 mM spermidine, 0.15 mM spermine, 0.34 M sucrose, 0.2 mM PMSF, 1 mM benzamidine and 15 mM β-mercaptoethanol, pH 6.0 (solution 2) and centrifuged again at 3000rpm for 10 mins. Solution 2 was adjusted to pH 7.5 using Tris base and the pellet was resuspended in 100ml of this. At this point the absorbance at 260nm was measured in 0.1 M NaOH. Before proceeding to the next step the absorbance should read ca. 50U ml^{-1} of nuclei and the nuclei suspension should be adjusted to this value if necessary. It was generally found, that for fresh chicken blood, this was rarely necessary.

The next stage of the purification is to release the DNA from the nuclear cell wall so that when the nuclei are lysed the chromatin can be separated from the nuclear envelope. Before carrying this out on the whole nuclei solution a trial digest was preformed to determine the correct digestion time.

1ml of the nuclei solution was adjusted to 1 mM $CaCl_2$ and incubated in a water bath at 37°C for 3 mins. MNase was then added to a concentration of 40U ml^{-1} (expressed as units of absorbance released) and the reaction was incubated at 37°C. 333 µl samples were removed after 5 mins, 10 mins and 20 mins. Digestion was stopped by adjusting the solution to 2 mM EDTA. Samples were then centrifuged at 5000rpm for 10 mins and the pellet was resuspended in 1ml 10 mM Tris-HCl, pH 8.0, 0.2 mM EDTA and 0.2 mM PMSF (solution 3). This was then kept on ice for 30 mins with

occasional inversion to ensure that the chromatin remained in solution. The low salt in this solution osmotically lyses the nuclear membrane releasing the digested DNA chromatin into solution. The A_{260}, in 0.1 M NaOH, was determined and the samples were centrifuged for a further 10 mins at 5000 rpm. With the correct level of digestion, ca. 70-80% of the measured absorbance is released into the supernatant. In general a digestion time of 20 mins was required to achieve these parameters. With the digestion time calibrated, the above was preformed on the whole nuclei suspension. After centrifugation, samples were resuspended in 100ml of solution 3.

The total volume of the supernatant was then accurately measured and transferred to a 250ml conical flask at 4°C. 4 M NaCl was then added drop-wise while stirring so as to obtain a final concentration of 0.65 M. This step releases H1 and H5 from the chromatin. This was then transferred to a column of 4B-CL Sepharose previously equilibrated with 20mM sodium cacodylate, pH 6.0, 0.63 M NaCl, 0.2 mM PMSF and 1 mM EDTA and run for 6-8 hrs. The absorbance of all column fractions was then measured at 260nm in 0.1 M NaOH and a graph plotted. This usually gave two peaks. The first peak corresponds to H1-stripped chromatin, followed by H1/H5. SDS-PAGE was used to analyse selected fractions and check for the appearance of histone H1/H5, fig 2.5. Fractions high in nucleosomes, usually 1-1.5 mg ml^{-1} and free of H1/H5 were concentrated to 2.5-3.0 mg ml^{-1} using Sartorius 100kda cut-off spin filters and stored at 4°C until use. Nucleosomes stored in this manner showed signs of degradation after 3-4 months at which a point a new purification had to be carried out.

2.14 Protein Gels and Coomassie Staining

2 µl of column fraction was mixed with 2 µl SDS-loading buffer and boiled for 3 mins. Samples were then loaded onto a 15% SDS-Polyacrylamide gel (5% Stacking gel: 330 µl 30% acrylamide mix, 250 µl 1M Tris (pH 6.8), 20 µl 10% SDS, 20 µl 10% ammonium persulfate, 20 µl TEMED, 1.4µl H_2O. Resolving gel: 2.5ml 30% acrylamide mix, 1.3ml 1.5 M Tris (pH 8.8), 50 µl 10% SDS, 50 µl 10% ammonium persulfate). The gel was run at 8V cm^{-1} until the samples cleared the stacking gel at

which time the voltage was increased to 11.5V cm^{-1} and the gel run until the dye front reached the bottom.

For staining, 0.25g of Coomassie Brilliant Blue R250 was dissolved in 90ml of methanol:H_2O (1:1 v/v) and 10ml of glacial acetic acid. The solution was then filtered though Whatmann No. 3 chromatography paper to remove any undissolved matter. The gel was then stained in this solution for 4-5 hours. After this time, the gel was immersed in destain (in 90ml of methanol:H_2O (1:1 v/v) and 10ml of glacial acetic acid) for 4-5 hours; the solution was changed 5-7 times over this period. The gel was then dried between two sheets of Promega Gel Drying Film for 1 hr at 50°C. The purity and amount, from selected column fractions, of the purified proteins could then be observed, fig 2.5a.

2.15 Reconstitution of Histones with Radiolabelled Constructs

Radiolabelled constructs were reconstituted by the salt exchange method as previously described (Drew and Travers 1985, Ramsey 1986, Brown and Fox 1997). Precipitated DNA, ca. 2000cps as measured by a hand-held Geiger Counter, was dissolved in 12 µl of 20 mM Tris-HCl, pH 7.4, containing 0.1 mM EDTA (DNA buffer). This was then transferred to a fresh microtube.

60 µl of 30mM Tris-HCl, pH 8.0, 4.5M NaCl and 1mM EDTA (High Salt Buffer) was mixed with 15ul 5mM PMSF, dissolved in 100% propanol. 8 µl of this solution was mixed with the radiolabelled construct. 18 µl of H1-stripped chromatin, 2.5-3mg ml^{-1} (corresponding to approximately 50ug of nucleosome cores), was then added and the mixture was incubated at 37°C for 25 mins. The high ionic strength in this solution causes nucleosome disruption and incorporation of the radiolabelled construct, fig 2.5b. Since there is a vast excess of chromatin relative to the construct almost all labelled DNA is incorporated.

After incubation, the salt concentration of the solution was slowly lowered to exactly 100mM. This was carried out by the stepwise addition of 5mM Tris-HCl, pH 8.0,

A.

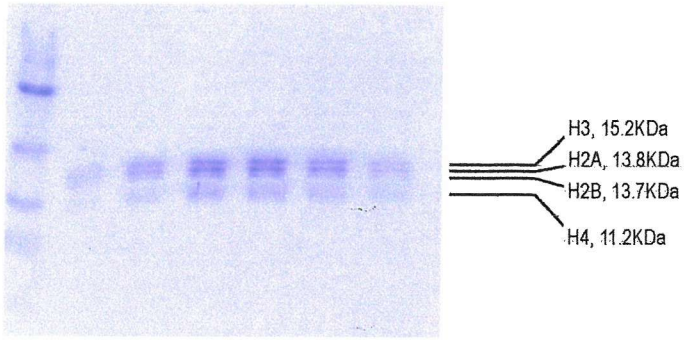

B.

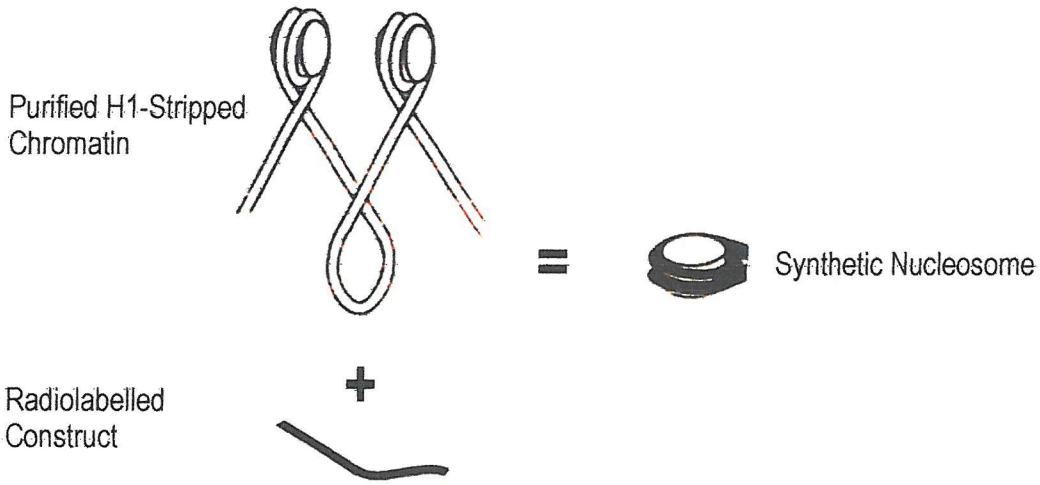

C.

Figure 2.5. A, Coomassie stained protein gel showing all four histones purified from various fractions. B, the process of histone reconstitution with radio-labelled constructs. C, a standard histone gel-shift showing retardation of reconstituted construct.

1mM EDTA and 0.1% Nonidet P40 (Low Salt Buffer) at ambient temperature. Four additions of 10ul were made followed by eleven additions of 20 µl leaving 5 mins between each addition.

The integrity of the synthetic nucleosomes was then checked by non-denaturing PAGE. Histone bound DNA gel-shifts and usually 85-95% was associated with the retarded species, fig 2.5c. It should be noted that the actual reconstitution may be better than that measured by PAGE since the conditions of gel-electrophoresis may disrupt the complex.

The reconstituted nucleosome core particles were stored at 4°C until use.

2.16 Reconstitution of Histones with Radiolabelled Constructs in the Presence of Ligand

Precipitated DNA was dissolved in 72 µl of DNA buffer for Hoechst 33258 constructs and 84 µl for echinomycin constructs. These DNA solutions were then split into six 12 µl aliquots for Hoechst and seven 12 µl aliquots for echinomycin experiments. High Salt Buffer/PMSF mix and 18 µl of purified H1-Stripped nucleosome cores was added as described above to each aliquot and the mixture incubated at 37°C for 25 mins. For each reaction the following concentrations of ligand were dissolved in Low Salt Buffer, these were higher than required to account for the 40 µl of solution present before the addition of Low Salt Buffer. This gives the same concentration range used in footprinting assays, for both ligands.

After reconstitution samples were prepared for gel electrophoresis, see below.

2.17 DNaseI Footprinting

For digestions with free DNA, approximately 2 µl of construct (roughly 50cps on a hand held Geiger counter) was mixed with 2 µl of ligand, dissolved in 10 mM Tris-HCl, pH 7.5, at the appropriate concentration. This halves the added ligand concentration. Ligand-DNA mixtures were allowed to equilibrate for 10 mins at

ambient temperature.

After equilibration, 2 µl of DNaseI was added at a concentration of 0.072 units ml^{-1} and digestion was allowed to proceed for 1 min (Mg^{2+} was added to the DNaseI dilution buffer previously). This was stopped by the addition of 5 µl 80% Formamide, 10 mM EDTA, 1 mM NaOH and 0.1% bromophenol blue (STOP buffer). Samples were concentrated in a Speed Vac for 5 mins and prepared for gel electrophoresis. Additional NaCl was not added to free DNA digests.

For digestions with histone reconstituted DNA, approximately 10 µl of construct (roughly 50cps on a hand held Geiger counter) was mixed with 10 µl of ligand, dissolved in 10 mM Tris-HCl, pH 7.5 and 100 mM NaCl, at the appropriate concentration. This halves the added ligand concentration. More ligand is required for these experiments since the concentration of unlabelled genomic DNA, present in the histone purification, is higher. Ligand-nucleosome mixtures were left to equilibrate for 10mins at ambient temperature.

After equilibration, 4 µl of DNaseI was added at a concentration of 14 units ml^{-1} and digestion was allowed to proceed for 1 min. This was stopped by the addition of 100 µl of buffered phenol, pH 8.0. 100 µl of sterile water was also added to increase the volume of the aqueous phase. Samples were then centrifuged at 14000rpm for 5 mins on a bench-top centrifuge. The aqueous layer was then isolated. This was carried out twice followed by two extractions with 100 µl ether. Trace amounts of ether were then evaporated at 50°C for three minutes with caps left open. The DNA was then precipitated and dried as described, resuspended in STOP buffer and prepared for gel electrophoresis.

2.18 Hydroxyl Radical Footprinting

For digestions with free DNA, approximately 2 µl of construct (roughly 50cps on a hand held Geiger counter) was mixed with 10 µl of ligand, dissolved in 10 mM Tris-HCl, pH 7.5, at the appropriate concentration. Ligand-DNA mixtures were left to

equilibrate for 10 mins at ambient temperature.

For hydroxyl radical footprinting, fresh solutions of the following were prepared:

A 0.2 mM ferrous ammonium sulphate
B 0.4 mM EDTA
C 10 mM L-ascorbic acid
D 0.1% hydrogen peroxide

These were prepared in 1ml sterile water for digestions using free DNA or 100 mM NaCl for digestions using reconstituted nucleosomes. Reactants were then mixed in a micro tube in a ratio of 1:1:2:2 (A:B:C:D) and used immediately.

Digestion of free DNA

10µl of freshly prepared hydroxyl radical mix was added to the drug-DNA mixture and digestion was allowed to proceed for 10-15 min at ambient temperature. This was stopped by the addition of 100 µl ethanol and 10 µl 3M-sodium acetate. Samples were then precipitated and prepared for gel electrophoresis.

Digestion of reconstituted nucleosomal DNA

For digestions with histone reconstituted DNA, approximately 10ul of construct (roughly 50cps on a hand held Geiger counter) was mixed with 10ul of ligand, dissolved in 10mM Tris-HCl, pH 7.5 and 100mM NaCl, at the appropriate concentration. This halves the added ligand concentration. Samples were allowed to equilibrate for 10 mins. After equilibration, of the drug and nucleosome, 40 µl of freshly prepared hydroxyl radical mix was added and digestion was allowed to proceed for 10-15 min. This was stopped by the addition of 100 µl of buffered phenol, pH 8.0. 100 µl of sterile water was also added to increase the volume of the aqueous phase. Samples were then centrifuged at 14000rpm for 5 mins on a bench-top centrifuge. The aqueous layer was then isolated. This was carried out twice followed by two extractions with 100 µl ether. Trace amounts of ether were

evaporated at 50oC for three minutes with caps left open. The DNA was then precipitated and dried as described, resuspended in STOP buffer and prepared for gel electrophoresis.

2.19 Gel Electrophoresis

For sequencing gels, DNA samples were heated to 100°C for three minutes before loading on to 5% denaturing polyacrylamide gels containing 8M Urea (17 ml National Diagnostic Sequagel, 5ml 10x TBE-Urea buffer (216g Tris, 110g boric acid, 18.8g EDTA, 1 Kg urea in 2L H_2O), 28ml 50% 8M Urea, 200 µl 20% Ammonium Persulfate and 40 µl TEMED). Gels were 0.3mm thick, 40cm long and were run at 1500V, 42W until the dye front reached the end of the gel, usually 2 hrs.

For histone gel-shifts, a 4 µl aliquot from the reconstitution mixture was mixed with 3 µl ficol loading buffer and loaded onto 5% non-denaturing polyacrylamide gels (6ml National Diagnostic Protogel (33% solution), 5ml 5x TBE buffer, 39ml water, 200 µl 20% Ammonium Persulfate and 40 µl TEMED). Gels were 0.3mm thick, 20cm long and were run at 200V, 8W until the dye front was approximately 3/4 down the gel.

After electrophoresis, all gels were fixed in 10% (v/v) acetic acid for 10 mins. After this time, gels were then transferred to Whatmann 3MM chromatography paper, covered with Saran wrap and dried under vacum at 80°C for 1hr. They were then either exposed to X-ray film or to a Kodak phosphor imager plate overnight, which was scanned the following morning on Molecular Dynamics STORM 860 phosphor imager.

3 The Interaction of Ligands with Target Sites Located on the Outer Surface of the DNA Superhelix.

Introduction

In the late 80's, Waring and co-workers postulated that changes in digestion patterns of histone-bound DNA in the presence of ligands were due to rotation of the DNA on the protein surface. They suggested that this was driven by the binding of drugs to the outer surface of the DNA superhelix followed by their movement through 180° so that they then faced in towards the protein. This was thought to optimise the interaction of the ligand with the walls of the minor groove via an increase in non-bonded interactions between the drug and the DNA. However, as described in chapter 1, Hoechst 33258 causes little structural distortion in the DNA helix upon binding to its recognition sequence. Hence, the number of ligand molecules, which were calculated to produce this rotation, is very imprecise. However, for echinomycin the analysis was more acceptable since this ligand unwinds the DNA by approximately 48° per bound ligand and hence alters the surface helical repeat (h_s), which could be detected.

We therefore decided to assess the interaction of single ligand molecules with unique binding sites, which face away from the histone core octamer. It should then be possible to ascertain what contribution, if any, a single molecule would have on the repositioning of the superhelix, *in vitro*. This could then be compared to results for the binding of drug molecules to two outward facing sites. In addition, by using such a minimalist system other possible modes of interaction as yet unobserved, between the ligand and the nucleosome, may yet be highlighted. Five constructs, derived from fragment *tem*, were made for this purpose: *35h, 46h, 3546h, 44e and 74e.*

Results

The interaction of ligands with the *tem* sequence

DNA fragment *tem*, fig 3.1, was designed by taking the *tyrT* DNA sequence, for which its rotational position with nucleosome core particles has been well described (Drew, 1985) and removing all CpG and $(A/T)_4$ sites, while retaining the order of pyrimidine and purine bases. Therefore all known targets for echinomycin and Hoechst 33258 were removed from the sequence. This fragment would then be able to act as a template for introducing unique ligand binding sites at desired locations. Before studying the effects of ligands on these single sites it is first necessary to demonstrate that:

1. *The tem sequence adopts a unique rotational position when reconstituted as nucleosome core particles.*
2. *Ligands do not produce any footprints on this fragment, as is expected.*

DNaseI footprinting gels showing the interaction of Hoechst and echinomycin with *tem* free DNA are presented in fig 3.2 a and b. It can been seen that there is no significant interaction of each ligand with *tem*.

Rotational positioning

The rotational positioning of the *tem* construct, when complexed as a nucleosome, was determined by examining by its cleavage by hydroxyl radicals and is shown in fig 3.3. Hydroxyl radical cleavage reveals the expected phasing pattern, with maximal cleavage at positions 37, 47, 57 and 67. This is most clearly seen from the differential cleavage plot along side the gel. In comparison, digestion of uncomplexed free DNA produces a relatively even pattern of cleavage products with occasional differences which, are probably due to sequence-specific conformational changes in DNA structure. We can therefore conclude that this fragment does adopt a unique orientation when bound to the histone octamer. The exact translational position of these nucleosomes was not determined experimentally. This figure also

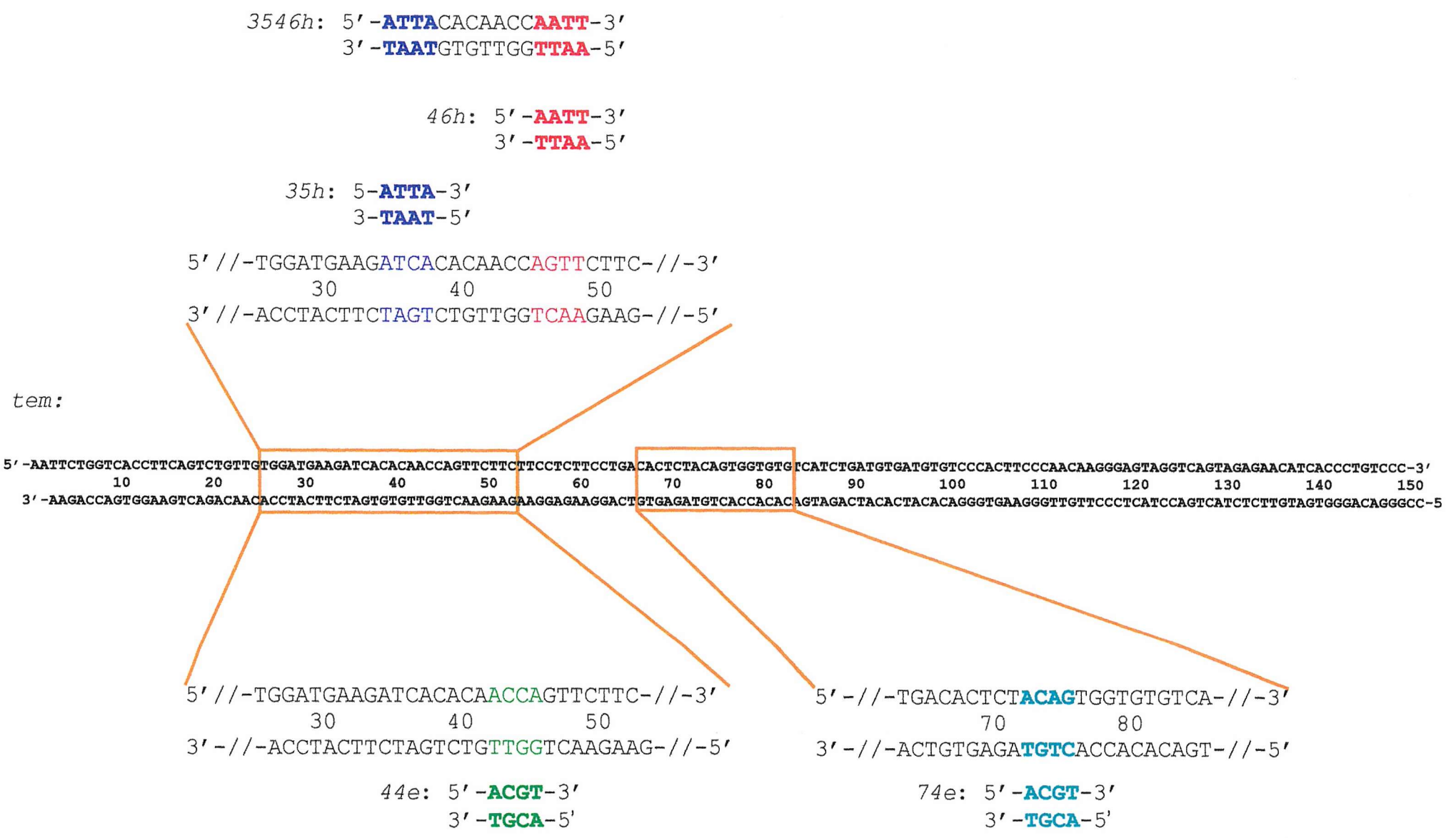

Fig 3.1 sequences of constructs *35h*, *46h*, *3546h*, *73h*, *74e* and *44e*. The *tem* construct is shown in the center. Expanded regions show where each mutation was introduced and the target sequence of each construct is indicated. These coloured targets are the only difference between the ligand construct and the parent sequence *tem*.

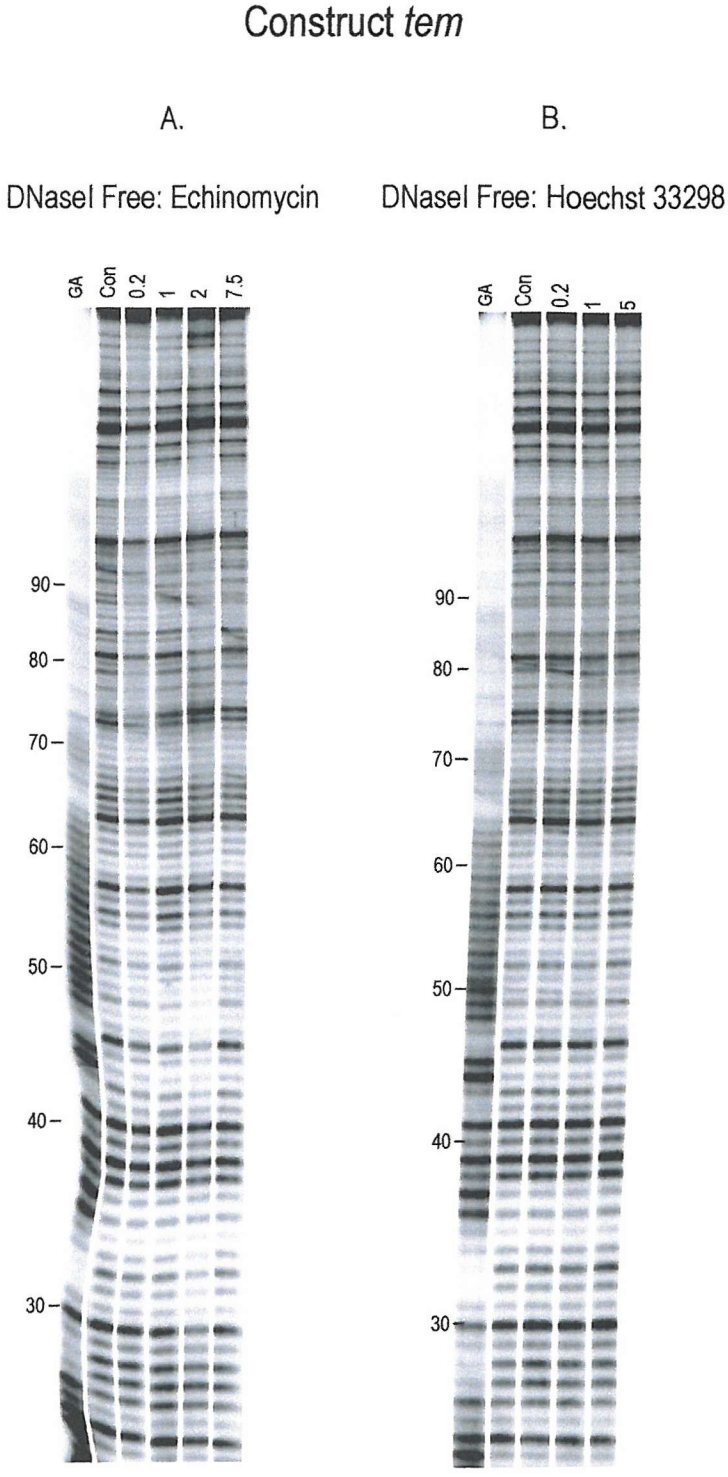

Fig 3.2 DNaseI digestion data on the interaction between Hoechst 33258 and echinomycin with construct *tem*. The ligand concentration is shown at the top of each lane and is expressed in μM. "Con" indicates the ligand free control digestion and "GA" are Maxam-Gilbert sequencing lanes specific for guanine and adenine. Black bars indicate the ligand target site and numbers while numbers correspond to the sequence.

The Hydroxyl Phasing Pattern of Construct *tem*

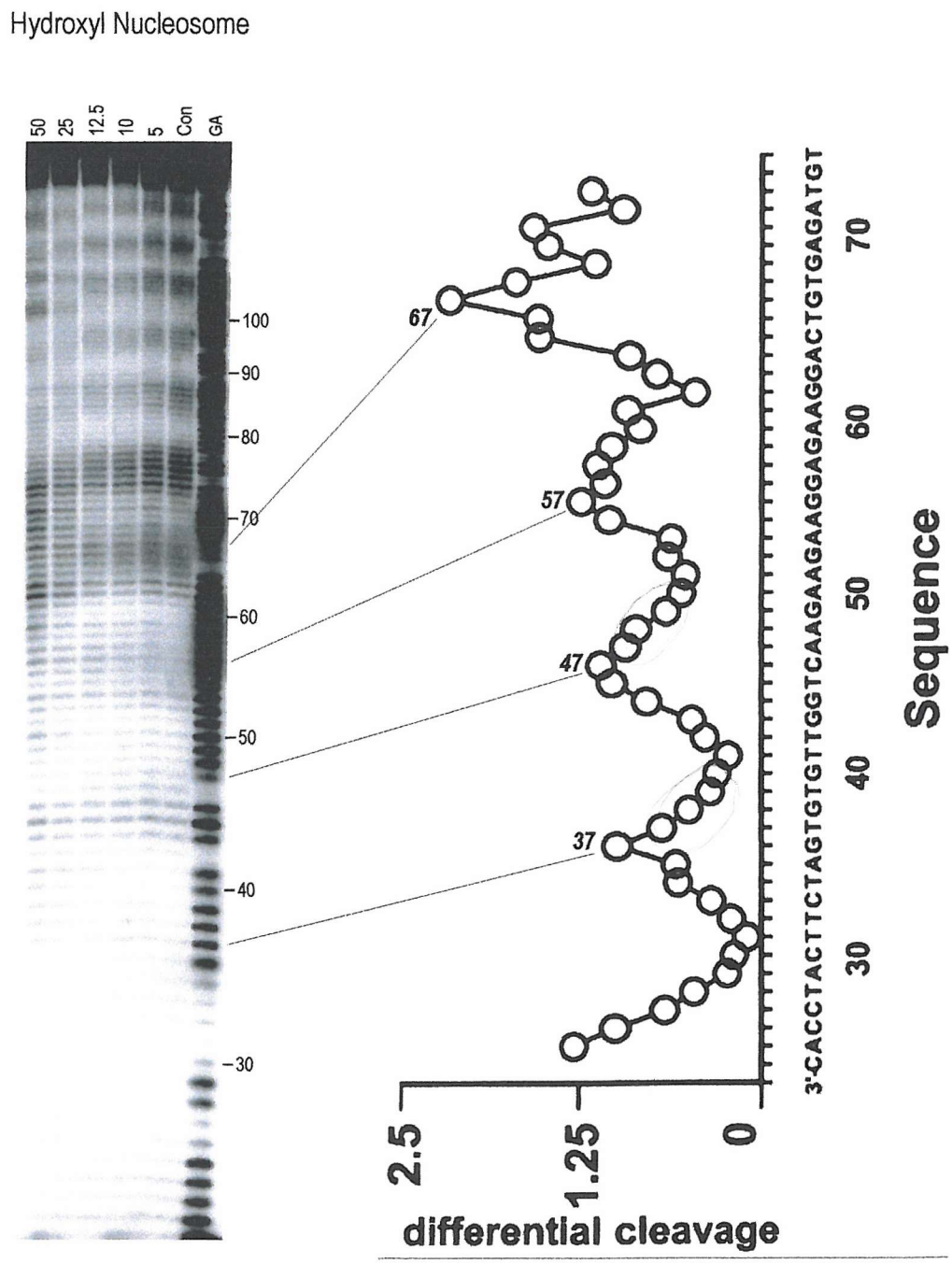

Fig 3.3 hydroxyl radical digestion of construct *tem* in the presence of Hoechst . The ligand concentration is shown at the top of each lane and is expressed in μM. "Con" indicates the ligand free control digestion and "GA"are Maxam-Gilbert sequencing lanes specific for guanine and adenine. Numbers correspond to the sequence. On the right is presented a differential cleavage plot of the hydroxyl phasing pattern from the control lane. Each band was divided by the corresponding band in free DNA (data not shown). Points of maxima represent minor grooves facing solution, while minima represent minor grooves facing the histone protein complex. The DNA sequence shown is the negative strand. Numbers at the top of each cleavage maxima indicate its position in the DNA sequence.

shows that high concentrations of Hoechst 33258 (>12.5μM) disrupt the phased cleavage pattern. This is probably due to non-specific interactions between the ligand and the DNA, which affect its interaction with the protein surface. On the basis of these results, further fragments were designed with unique drug binding sites positioned so as to face towards or away from the protein core.

Construct *46h* (fig 3.1) was prepared, containing a single 5'-AATT-3' target site, positioned so as to lie with its minor groove facing away from the protein. This allowed observations of the binding of Hoechst 33258 to a single strong recognition sequence. The construct *35h* contained the target 5'-ATTA-3' so as to study the binding to a weak site on the outer surface of the nucleosome. Construct *3546h* was a hybrid of *35h* and *46h*. It was then possible to ascertain the interaction of Hoechst 33285 with two ligand sites on the outer surface and compare this to the single site data. Any change associated with the binding of one extra drug molecule could then be determined. Construct *44e* contained a good echinomycin binding site ACGT and allowed the interaction of a single echinomycin molecule with an outer facing site on the nucleosome to be studied. Target sites *35h*, *46h*, *3546h* and *44e* were created by fusion PCR site-directed mutagenesis while *74e* was created using QickChange.

It is possible, although unlikely, that the rotational positioning of the DNA superhelix could be altered relative to the parent construct *tem* when the sequence is changed by mutagenisis. However, previous work carried out by Brown 1997 (PhD Thesis) demonstrated that varying the DNA sequence by as much as 14bp did not alter the rotational positioning of the fragments under study. All of the constructs made in this present series of studies involve the change of only 1-4bp and hence it seems unlikely that the rotational positioning on these DNA fragments will be altered. However, this was evaluated by carrying out DNaseI and hydroxyl radical digestion of nucleosome DNA. Although slight differences in cleavage maxima were evident between constructs, these probably result from minor differences in structure, rather than alterations in rotational positioning.

In general each DNA construct was considered to lie in essentially the same rotational position when reconstituted as nucleosome cores. Fragments containing echinomycin target sites could not be assayed by hydroxyl radicals in the presence of the drug due to the addition of DMSO and the rotational position was determined by DNaseI digestion.

All the target sites presented in this thesis were designed with reference to this cleavage pattern and by making use of the crystal structure of the nucleosome (Luger *et al.* 1997). For simplicity, we assumed that the histone octamer would position across the majority of the 150bp of the labelled DNA fragment since this would afford the largest number of DNA-protein contacts. From the hydroxyl cleavage pattern of tem there is a clear cleavage maximum across position 67bp in the construct. This represents an outer facing minor groove and is roughly half-way along the construct's length. From this, we concluded that the approximate dyad position would be here (making the assumption that the histone octamer would bind the longest possible length of DNA). However, slight differences in the assigned cleavage maxima between constructs may be due to small differences in the positioning of each fragment. Although differences in positioning are unlikely to be a result of the base sequence changes. The approximate location of the target sites mapped in the crystal structure provided additional information concerning the environment surrounding the binding sites. For example, does the ligand approach the site from the top of the nucleosome or does it have to manoeuvre through the superhelix gyres? Will positioning the target site near a tail region or other structures influence ligand binding? Making use of the crystal structure in this manner provided a clearer picture of the mechanism and action of these interactions. A molecular representation of all six target sites is presented in figures 3.4, 3.10 and 3.14.

Construct *35h*

Construct *46h*

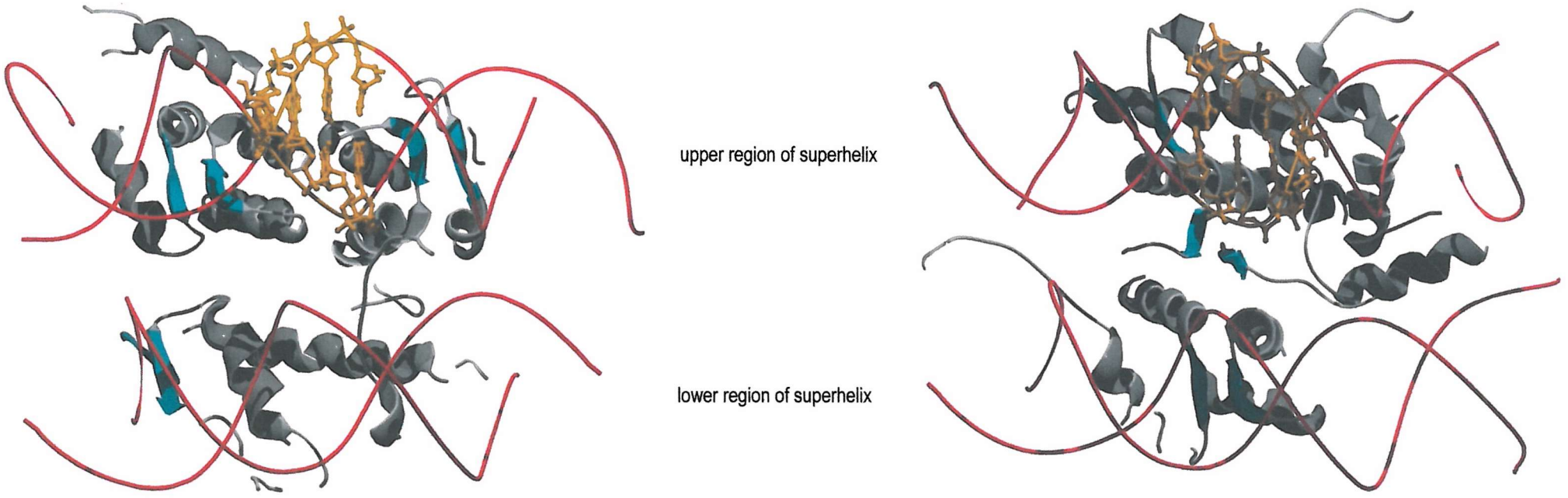

Figure 3.4 Molecular graphics of the *35h* and *46h* target sites. Each image shows a small portion of the nucleosome core particle. DNA strands are shown as red ribbons, the target sites are coloured orange and are presented as ribbon-ball and stick structures. A portion of the histone octamer is shown as grey ribbons. Since only a small region of the complex is presented, there appears to be two DNA helices. These actually correspond to the one helix which is wraps around the protein complex. The upper and lower portions of the DNA superhelix are indicated. The view is looking towards the nuclesome perpendicular to the superhelix axis. Images were created in Swiss-Pdb viewer, from the pdb file submitted by Luger *et al.* 1997, and rendered in Pov-ray for Windows.

Hoechst 33258

46h

The sequence of *46h* is shown in fig 3.1 and was created so that ligand recognition sequence would lie approximately half way between one end of the fragment and the nucleosome dyad.

The AATT target site is located at base pairs 46-49 and judging from hydroxyl radical cleavage of the parent construct *tem*, fig 3.3, it should lie with its minor groove on the outer surface of the DNA superhelix. DNaseI footprinting experiments with the *46h* construct are presented in fig 3.5a, which shows cleavage of *46h* free DNA and confirms the binding of Hoechst 33258 to the target site. Differential cleavage plots derived from data are shown in fig 3.6a, from a region around the target site and show that this is fully saturated at 0.2μM ligand with a significant reduction in cleavage with 0.05μM ligand. The signal for this type of analysis was obtained from phosphor imager data. The relative amount of radioactivity from each band, between positions 30-80bp of the construct, was quantified from phosphor imager scans using ImageQuant software. This was then divided by the sum total of all counts across the measured region so as to normalise the data. For free DNA plots the amount of radioactivity in each band, in a lane where drug was added to free DNA, was divided by the corresponding band from the ligand free control, from free DNA. For nucleosome plots, the amount of radioactivity in each band, in a lane where drug was added to nucleosome DNA, was divided by the corresponding band from the ligand free control, from free DNA. In both cases normalised data was used so as to account for factors such as unequal gel loading.

Due to the nature of the DNaseI cleavage, the digestion pattern is uneven, reflecting the dependence of enzyme on the local conformation of the DNA. The footprint covers 7bp, and it should be noted that, as expected, this is the only drug binding site on this fragment.

Construct *46h*

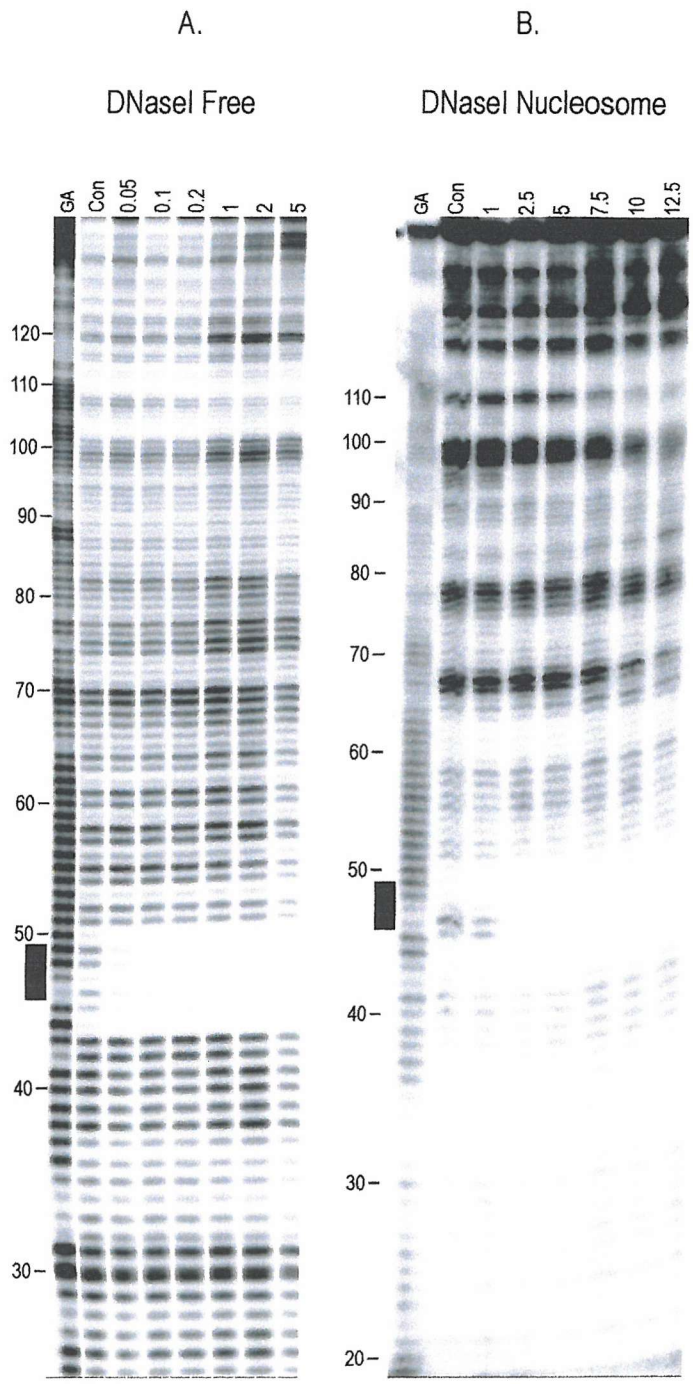

Figure 3.5 DNaseI digestion data on the interaction between Hoechst 33258 and construct *46h*. The ligand concentration is shown at the top of each lane and is expressed in μM. "Con" indicates the ligand free control digestion and "GA" are Maxam-Gilbert sequencing lanes specific for guanine and adenine. Black bars indicate the ligand target site while numbers correspond to the sequence.

Differential Cleavage of Free and Histone-Bound *46h* in the Presence of Hoechst 33258 (DNaseI)

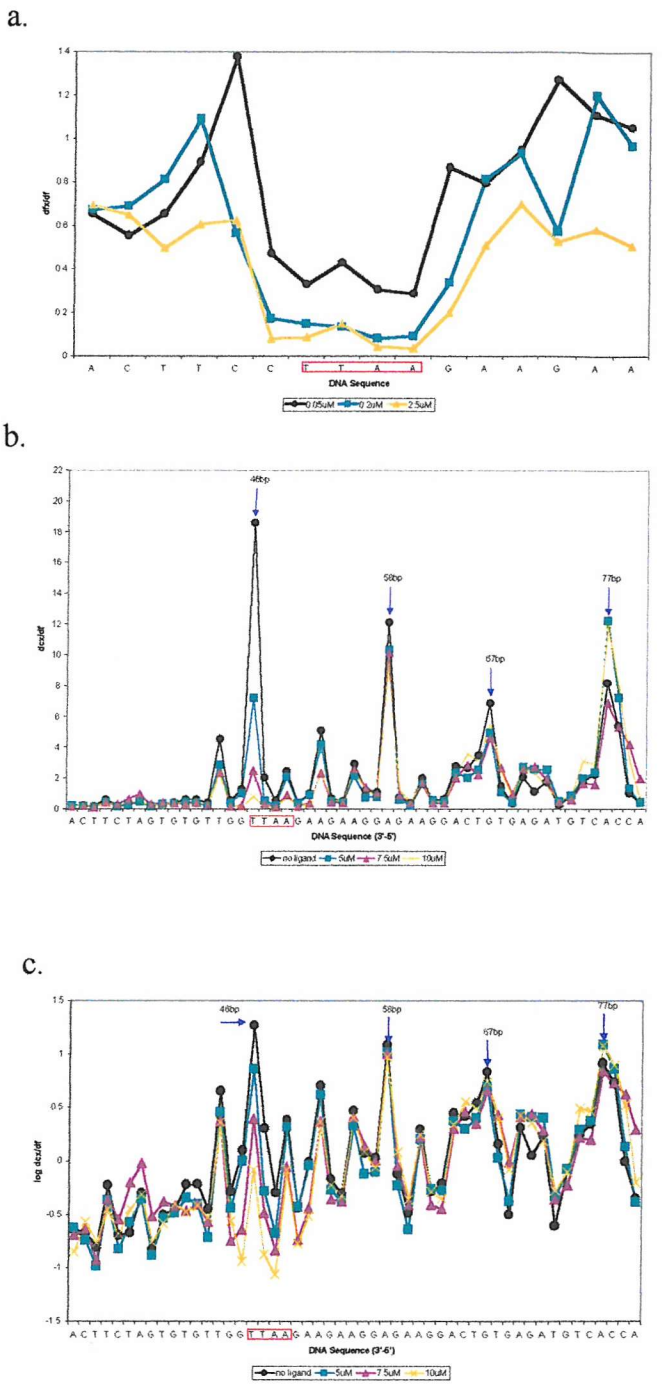

Fig 3.6 Differential cleavage across the 5'-AATT-3' target site for *46h* free (a) and histone-bound (b and c) DNA in the presence of Hoechst 33258 as determined by DNaseI. The DNA sequence is shown in the 3'-5' direction and the target site is indicated by a red box. (a), the y-axis shows the value obtained for the division of each band, from a lane where Hoechst has been added (dfx), by the exact corresponding band in the ligand free control (df). (b), the y-axis shows the value obtained for the division of each band in the histone-bound sample (dcx) by the corresponding band in the free DNA (df). (c), data from (b) presented on a logarithmic scale. Arrows indicate resolved cleavage maxima where the minor groove faces away from the histone core. For clarity, only three concentrations of ligand are presented in each chart.

Fig 3.5b shows DNaseI cleavage of histone-bound the *46h* in the presence of varying concentrations of Hoechst 33258. The histone-phasing pattern is clear with cleavage maxima separated by ca. 10bp as the minor groove alternates from facing the protein core and facing the solvent. This pattern is weaker towards the 3'-end of the fragment and a clear phasing pattern was rarely obtained before 40bp on any of the constructs studied. Analysis of these results allows an accurate determination of cleavage maxima, i.e. regions where the minor groove faces away from the protein surface as shown in fig 3.6a. Regions of maximal cleavage are found at positions 46, 58, 67 and 77bp, in similar locations to the parent construct *tem*. The remaining cleavage maxima could not be accurately defined from the gels since these bands become too closely packed to resolve. However, visual inspection indicates further maxima at approximately ca. 97 and 106-108bp. The expected maxima at ca. 85-87bp, is in a region where the DNA is cut poorly by the enzyme on both free and histone-bound DNA. This makes it difficult to resolve and demonstrates the importance of using more than one footprinting probe. For these practical reasons data analysis was generally carried out between positions 30-80bp of each construct. Since the nucleosome is by its nature symmetrical, obtaining accurate data analysis for positions beyond the dyad was not considered crucial in determining whether the DNA superhelix had rotated or undergone some other form of conformational change in the presence of ligands.

DNaseI digestion of this construct indicates that the minor groove of the AATT target site lies in a region on the outer facing surface as judged by its position relative to cleavage maxima in the control. Position 46 lies directly on the maximum point of cleavage, which would place thymine 49 just on the inward/outward boundary of the DNA superhelix. Based on its position in the crystal structure this site, although accessible, is facing the lower portion of the DNA superhelix and thus the drug must partially approach its target between the superhelical gyres. As the concentration of Hoechst is increased, cleavage across the target site becomes attenuated in a manner consistent with the drug binding. This is the first report of a drug-induced footprint on nucleosomal DNA and protection is obvious both visually in each gel and in the

analysis. Most of the other bands in the digestion are not affected by addition of the ligand. The exact size of the Hoechst 33258 footprint is difficult to estimate since enzyme cleavage is reduced at both sides of the target site as the minor groove turns towards the protein surface. However, this attenuation covers at least 5bp and is located directly across the target site. There is no evidence for a change in the rotational setting of the DNA superhelix with increased ligand concentration. It should be noted that higher concentrations of ligand are always required in nucleosome experiments, relative to those with free DNA, due to the presence of large quantities of chicken DNA.

At concentrations of 5μM and below the only changes in the cleavage pattern are around the desired binding site. At higher Hoechst 33258 concentrations, there are other regions where the cleavage is altered. Attenuations are evident at positions 66-68 and 76-77bp while enhancements are observed at positions 63-64, 74-75 and 82bp. Visual inspection of the gel indicates that there are further reductions in cleavage at the two maxima around positions 100 and 110bp. The majority of these altered cleavage patterns occur between 7.5-10μM ligand concentration. Since these altered cleavage patterns occur at relatively high ligand concentrations it may be that they correspond to non-specific binding of the drug, probably involving interactions between the positively charged piperazine group and the sugar phosphate backbone of the DNA helix. Since some of these changes are associated with regions where the DNA should be inaccessible these changes may indicate wholesale displacement of the DNA from the protein as observed by Waring and co-workers with high concentrations of Hoechst (Portugal and Waring 1986; Portugal and Waring 1997a; Portugal and Waring 1997b).

35h

It appears that Hoechst can produce footprints at a single outward facing AATT sites on nucleosomal DNA. Since AATT is the best minor groove binding site, we also assessed the interaction of this ligand with a weaker target site (ATTA) on the outer surface of the nucleosome. To this end, construct *35h* was designed, fig 3.1. The

construct contains the target 5'-ATTA-3' across base pairs 35-38 and sits in a rotational position similar to that of the sequence *46h* as judged by the cleavage profiles.

The results for DNaseI cleavage of *35h* are presented in fig 3.7. The first panel shows binding of the ligand to free *35h* DNA and confirms its interaction with the proposed binding site. By comparison with fig 3.5a, it is clear that the interaction of Hoechst 33258 with this target is weaker than that observed with AATT in construct *46h*. Since higher ligand concentrations are required to produce a footprint. In addition, it is interesting to note that the free DNaseI cleavage patterns between these two constructs (*46h* and *35h*) appear different. This is difficult to explain since the only differences between each DNA fragment are in the targets sites and all construct sequences were confirmed with T7 DNA polymerase sequencing. It may be that slightly different concentrations of DNaseI were used in each experiment resulting in an altered cleavage pattern or fluctuations in the ambient temperature during each digest may have brought about a similar result. Fig 3.8a shows differential cleavage plots for the region around this binding site and it can be seen that there are few changes at low Hoechst concentrations, but that a complete footprint extending over 6bp is evident with 2:M. It should be noted that no other drug footprints are found in this fragment. In comparison, full saturation of the *46h* AATT target was found at a concentration of 0.2μM Hoechst making the *35h* ATTA site approximately an order of magnitude weaker. It is interesting to note that the footprint is again displaced in the 3' direction; the upper (5') edge of the footprint corresponds to the beginning of the binding site, while the footprint continues for several bases beyond the lower (3') end.

Figure 3.7b shows the results obtained for the interaction of H33258 with *35h* nucleosomal DNA. Upon visual inspection of the gel a footprint is clearly visible across the target site. However, as shown in the differential cleavage plot in fig 3.8b, the phasing pattern is not accurately resolved across this region, and clear phasing was only observed after 40bp in many of the constructs studied. The interaction is

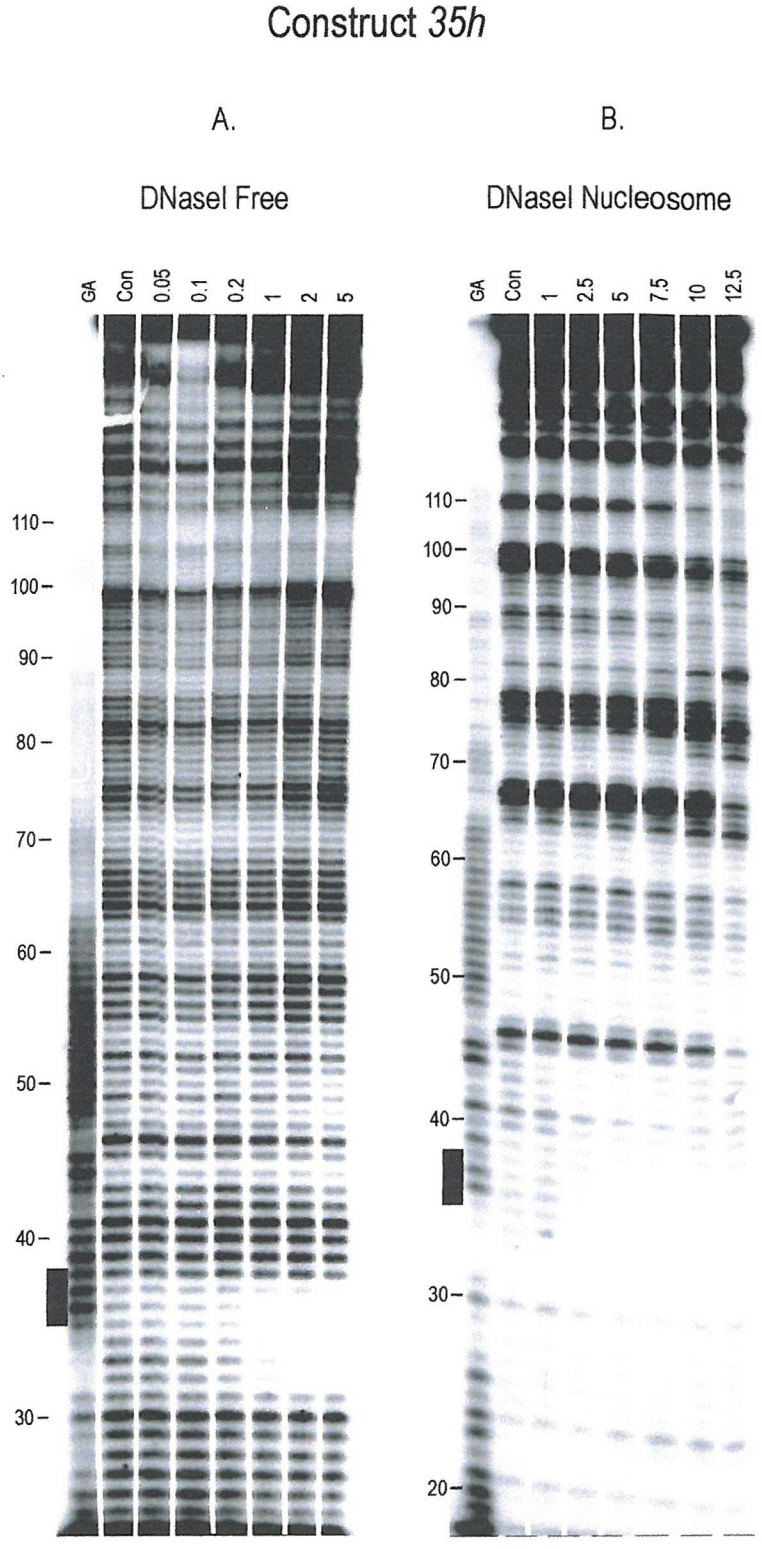

Figure 3.7 DNaseI digestion data on the interaction between Hoechst 33258 and construct 35*h*. The ligand concentration is shown at the top of each lane and is expressed in μM. "Con" indicates the ligand free control digestion and "GA" are Maxam-Gilbert sequencing lanes specific for guanine and adenine. Black bars indicate the ligand target site while numbers correspond to the sequence.

Differential Cleavage of Free and Histone-Bound *35h* in the Presence of Hoechst 33258 (DNaseI)

a.

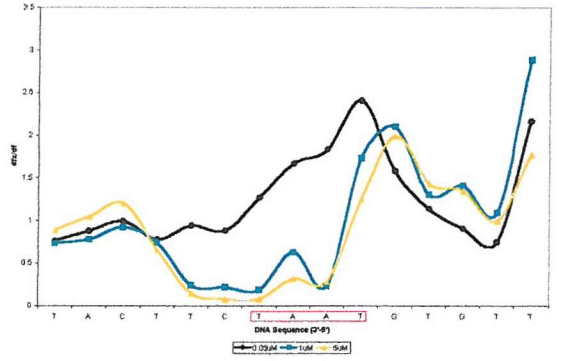

b.

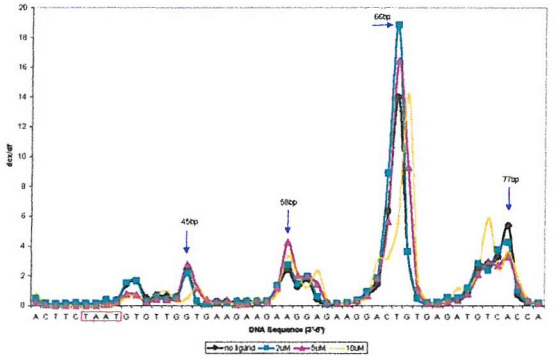

c.

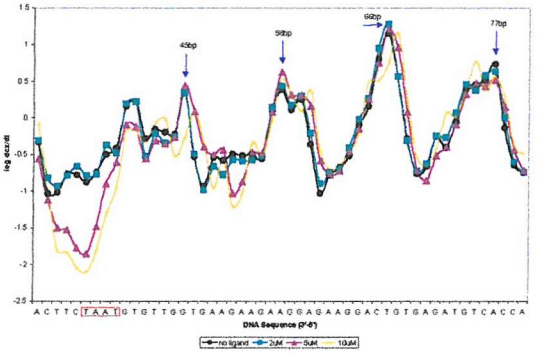

Fig 3.8 Differential cleavage across the 5'-TAAT-3' target site for *35h* free (a) and histone-bound (b and c) DNA in the presence of Hoechst 33258 as determined by DNaseI. The DNA sequence is shown in the 3'-5' direction and the target site is indicated by a red box. (a), the y-axis shows the value obtained for the division of each band, from a lane where Hoechst has been added (dfx), by the exact corresponding band in the ligand free control (df). (b), the y-axis shows the value obtained for the division of each band in the histone-bound sample (dcx) by the corresponding band in the free DNA (df). (c), data from (b) presented on a logarithmic scale. Arrows indicate resolved cleavage maxima where the minor groove faces away from the histone core. For clarity, only three concentrations of ligand are presented in each chart.

more easily visualised in fig 3.8c and from this type of analysis the interaction of Hoechst with the target on histone-bound DNA can be clearly seen. It may be significant that the 3'-shift in the footprint appears to be less than that observed in the free DNA suggesting a change in the local conformation of the DNA when bound to the histone octamer. It is also interesting to note that the ligand concentration required to produce a footprint at the *35h* target site is very similar to that found with *46h* despite that fact that the ATTA target is a much weaker. This is largely explained by the different total DNA concentration in the experiments with free and nucleosomal DNA. The higher DNA concentration used in core experiments (ca. 1.6μg of carrier chromatin per experimental sample) mean that the concentration dependence of the footprint is no longer dictated by the ligand dissociation constant but by stoichiometry.

In addition to the footprint, further attenuated cleavage and band enhancements are evident at high ligand concentration in a similar manner to that found in construct *46h*. Attenuations in cleavage are found at positions 45-47, 66-68, 76-77bp and 87-90bp while enhancements are noticeable at positions 63-64, 72-75 and 82bp. Visual inspection of the gel reveals that these altered cleavage products are repeated beyond the dyad region of the nucleosome. As with construct *46h*, this is thought to correspond to type II non-specific binding of the ligand to the superhelix at high concentration, which may potentially displace the DNA from the protein surface.

3546h

Based on the results with *46h* and *35h* it was decided to study the simultaneous binding of two Hoechst molecules to a fragment containing both sites on the outer facing surface of the nucleosome. This was done with construct *3546h*, the sequence of which is shown in figure 3.1. The weak ATTA site is located across base pairs 35-38 and is followed by the strong AATT target covering base pairs 46-49. Thus the separation between each target site is 8bp across a region where the minor groove turns towards the histone core. A molecular graphic of this is presented in fig 3.10.

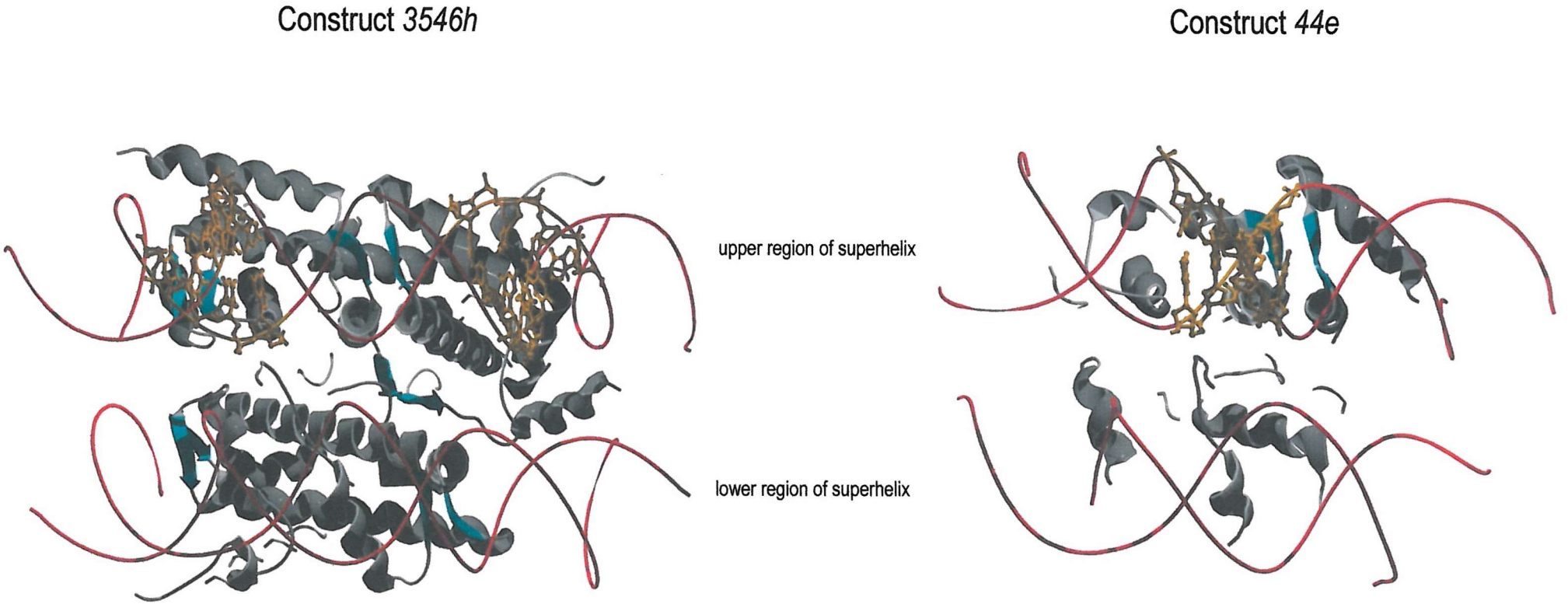

Figure 3.10 Molecular graphics of the *3546h* and *44e* target sites. Each image shows a small portion of the nucleosome core particle. DNA strands are shown as red ribbons, the target sites are coloured orange and are presented as ribbon-ball and stick structures. A portion of the histone octamer is shown as grey ribbons. Since only a small region of the complex is presented, there appears to be two DNA helices. These actually correspond to the one helix which is wraps around the protein complex. The upper and lower portions of the DNA superhelix are indicated. The view is looking towards the nucleosome perpendicular to the superhelix axis. Images were created in Swiss-PdB Viewer, from the pdb file submitted by Luger *et al.* 1997, and rendered in Pov-Ray for Windows.

The interaction of Hoechst 33258 with free *3546h*, as judged by DNaseI, is presented in fig 3.11a. It is clearly evident that the drug binds to the AATT site at a lower concentration than to ATTA, demonstrating its greater affinity. Interaction with AATT is apparent at the lowest ligand concentration (0.05μM) and the site is fully saturated at a concentration of 0.2μM. The differential cleavage plot in fig 3.12a confirms that the size of the footprint is 7bp. In contrast, there is a weak attenuation of cleavage at ATTA with and a full footprint is not observed until 2μM. These results confirm that AATT is a much stronger binding site for Hoechst than ATTA.

Fig 3.11b shows DNaseI cleavage of with histone-bound *3546h* DNA in the presence of Hoechst 33258. The nucleosome-phasing pattern is clear and like all other constructs, is weaker near the 3' (lower) end of the sequence although in this instance a weak cleavage maxima can be identified at position 36bp. Analysis of these results identifies cleavage maxima at positions 36, 45, 55, 67 and 76 (fig 3.12b). Further visual inspection indicates other maxima around positions 95, 107 and 118bp. Therefore these nucleosomes are positioned in an identical manner to all the other constructs and the parental sequence *tem*. Hence both target sites lie in the same orientation as found in constructs *35h* and *46h*, figs (3.4 and 3.10), and should therefore be accessible to the ligand.

Visual inspection of the gel shows clear footprints across each target site. This is also evident in the differential plot shown in fig 3.12b. Binding to AATT is distinct at 5μM and is fully saturated by 10μM Hoechst. However, despite the ligands weaker interaction with ATTA, a similar binding profile is evident across this target site. Hence both sites are saturated at a concentration of 10μM drug and it appears as though Hoechst is interacting with these sequences as if they were equivalent. The size of each footprint is ca. 6bp, but this is difficult to accurately measure since digestion is attenuated on each side of the target sites as the minor groove turns towards the histone core.

The results of hydroxyl radical digestion of histone-bound *3546h* in the presence of

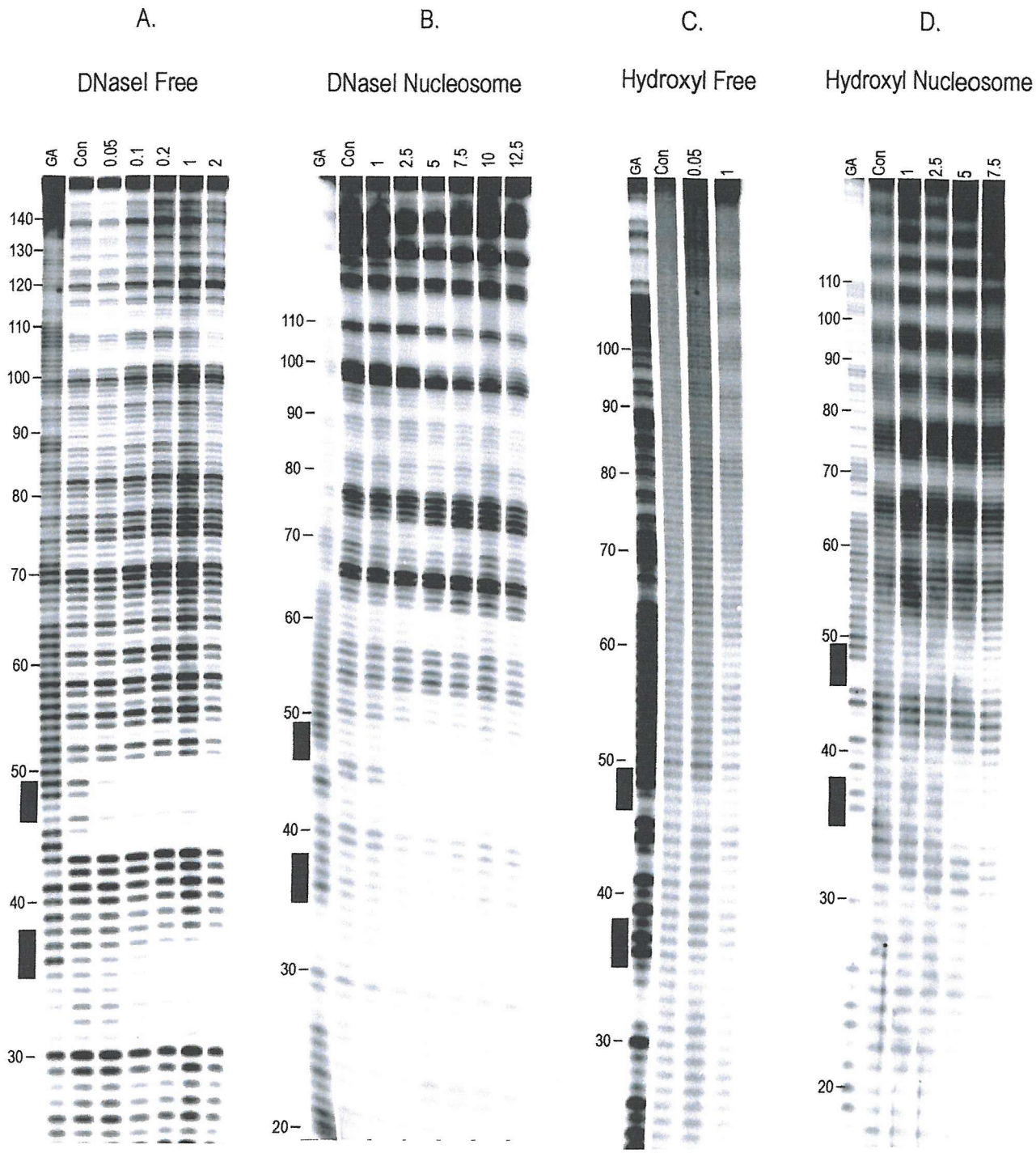

Figure 3.11 DNaseI and hydroxyl radical digestion data on the interaction between Hoechst 33258 and construct *3546h*. The ligand concentration is shown at the top of each lane and is expressed in μM. "Con" indicates the ligand free control digestion and "GA" are Maxam-Gilbert sequencing lanes specific for guanine and adenine. Black bars indicate the ligand target sites while numbers correspond to the sequence.

Differential Cleavage of Free and Histone-Bound *3546h* in the Presence of Hoechst 33258 (DNaseI)

a.

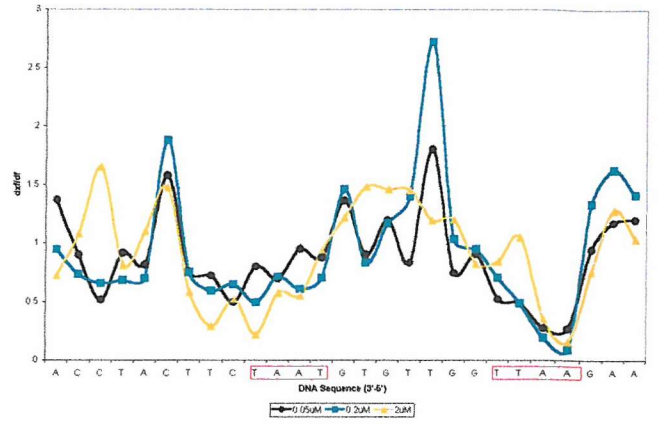

b.

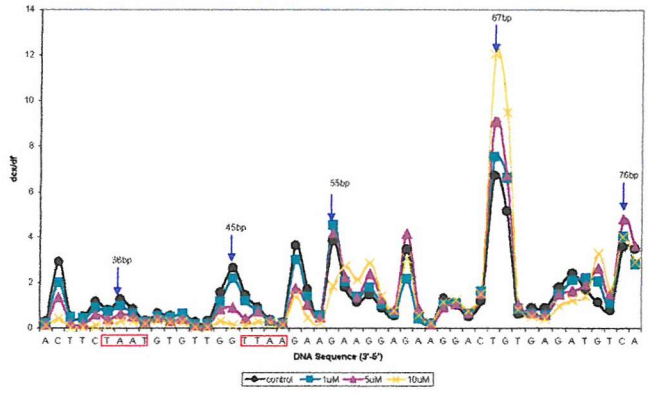

c.

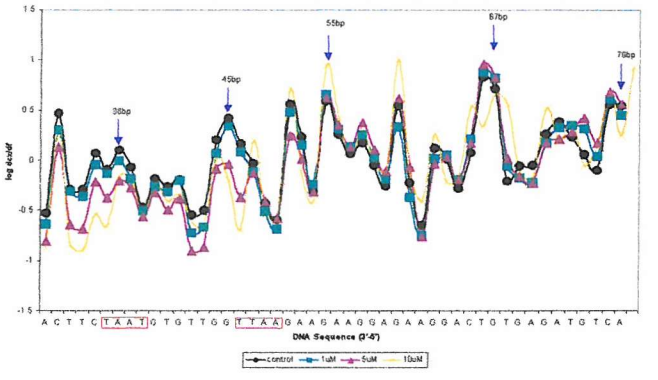

Fig 3.12 Differential cleavage across the 5'-ATTA-3' and 5'-AATT-3' target sites for *3546h* free (a) and histone-bound (b and c) DNA in the presence of Hoechst 33258 as determined by DNaseI. The DNA sequence is shown in the 3'-5' direction and the target site is indicated by a red box. (a), the y-axis shows the value obtained for the division of each band, from a lane where Hoechst has been added (dfx), by the exact corresponding band in the ligand free control (df). (b), the y-axis shows the value obtained for the division of each band in the histone-bound sample (dcx) by the corresponding band in the free DNA (df). (c), data from (b) presented on a logarithmic scale. Arrows indicate resolved cleavage maxima where the minor groove faces away from the histone core. For clarity, only three concentrations of ligand are presented in each chart.

Differential Cleavage of Free and Histone-Bound *3546h* in the Presence of Hoechst 33258 (Hydroxyl)

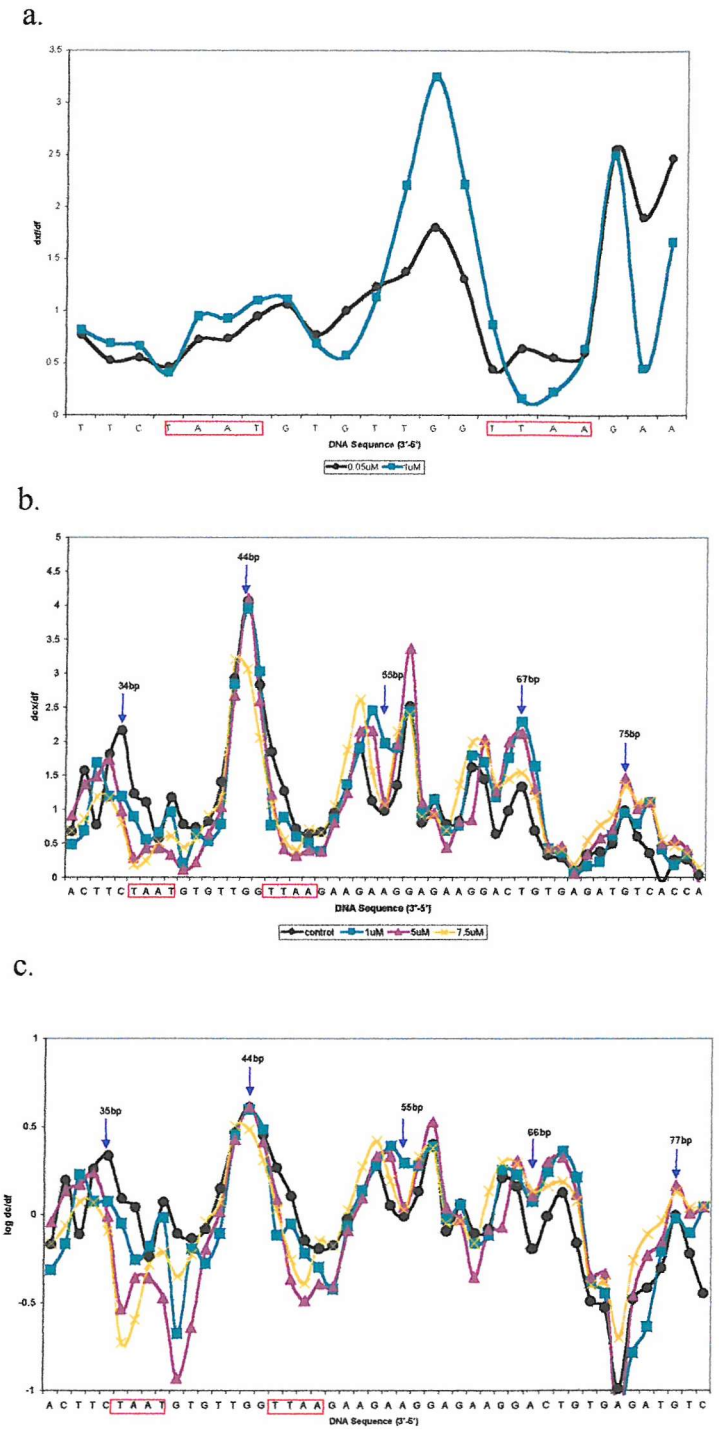

Fig 3.13 Differential cleavage across the 5'-ATTA-3' and 5'-AATT-3' target sites for *3546h* free (a) and histone-bound (b and c) DNA in the presence of Hoechst 33258 as determined by hydroxyl radicals. The DNA sequence is shown in the 3'-5' direction and the target site is indicated by a red box. (a), the y-axis shows the value obtained for the division of each band, from a lane where Hoechst has been added (dfx), by the exact corresponding band in the ligand free control (df). (b), the y-axis shows the value obtained for the division of each band in the histone-bound sample (dcx) by the corresponding band in the free DNA (df). (c), data from (b) presented on a logarithmic scale. Arrows indicate resolved cleavage maxima where the minor groove faces away from the histone core. For clarity, only three concentrations of ligand are presented in each chart.

Hoechst 33258 are presented in figure 3.11c-d. Binding to the target sites in free DNA, 3.11c, is confirmed although, as with all other Hoechst constructs, only weak footprints are observed. Analysis of these data, fig 3.13a, highlights these interactions more clearly. Each footprint is approximately 4bp in size as measured with this probe and gives a more accurate measure of the binding site than that obtained using DNaseI, where footprints tend to be over-estimated.

The interaction of Hoechst with histone-bound *3546h* is presented in fig 3.11d. The cleavage maxima in the drug free core bound DNA are located at positions 34, 44, 55, 67 and 75bp, (fig 3.13b). Further maxima can be seen around positions 86, 96 and 107bp, demonstrating that the rotational position of these nucleosomes is essentially identical to that of *tem* and other constructs. Addition of Hoechst indicates footprints at both sites, which can be seen in the differential cleavage plots, fig 3.13b. However it is interesting to note that binding to ATTA appears to be stronger than binding to AATT. The footprint is 4bp in size across ATTA and 5bp across the AATT target site. These data may indicate that the ligand has a greater affinity for the ATTA site than AATT when complexed as a nucleosome and assayed by hydroxyl radicals.

In addition to binding to the target sites subtle changes in hydroxyl radical cleavage are also apparent at other locations in the construct. Slight enhancements in differential cleavage are observed at positions. Unlike the DNaseI results, no additional regions of attenuation are evident. Most importantly, the rotational position of this construct is not affected by the binding of two Hoechst 33258 molecules to the outer surface of the nucleosome, and the phased cleavage pattern is still evident at all Hoechst concentrations.

Echinomycin

44e

Similar experiments were performed with DNA constructs containing outward facing echinomycin sites. The sequence of *44e* is shown in fig 3.1. It contains a single good echinomycin site (5'-ACGT-3') site beginning at position 44 with the central CG step covering base pairs 45 and 46. Based upon hydroxyl cleavage of *tem* and analysis of the crystal structure the minor groove of the target should be accessible on the outward facing surface of the nucleosome, and this is represented in fig 3.10.

The results with DNaseI are presented in fig 3.14. 3.14a shows the interaction of the ligand with free *44e* DNA and confirms that echinomycin interacts with the expected target site. Analysis of these results shows that the footprint is complete by 2μM ligand. This is shown in the differential cleavage plot, which also reveals enhanced cleavage at guanine 39 (in the 3'-lower side of the target sequence), which presumably reflects changes in the local conformation of the DNA as the drug interacts with its target (fig 3.15a). The greater amount of echinomycin required to produce this footprint relative to those obtained from Hoechst 33258 demonstrates the lower affinity of the drug for DNA.

3.14b shows the results obtained for the interaction of echinomycin with histone-bound *44e*. The gel shows a strong phasing pattern characteristic of nucleosome DNA and the differential cleavage plots (fig 3.15b) identify cleavage maxima at positions 45, 58, 67 and 76bp.

Visual inspection of this gel suggests that echinomycin does not produce a footprint at this histone-bound target site, even at concentrations as high as 50μM. Quantitive analysis of these data (fig 3.15b) suggest that there may be a small reduction in the 3' vicinity of the binding site, consistent with weak drug binding. However, a weak footprint of this magnitude might also be a consequence of the ligand interacting

Construct *44e*

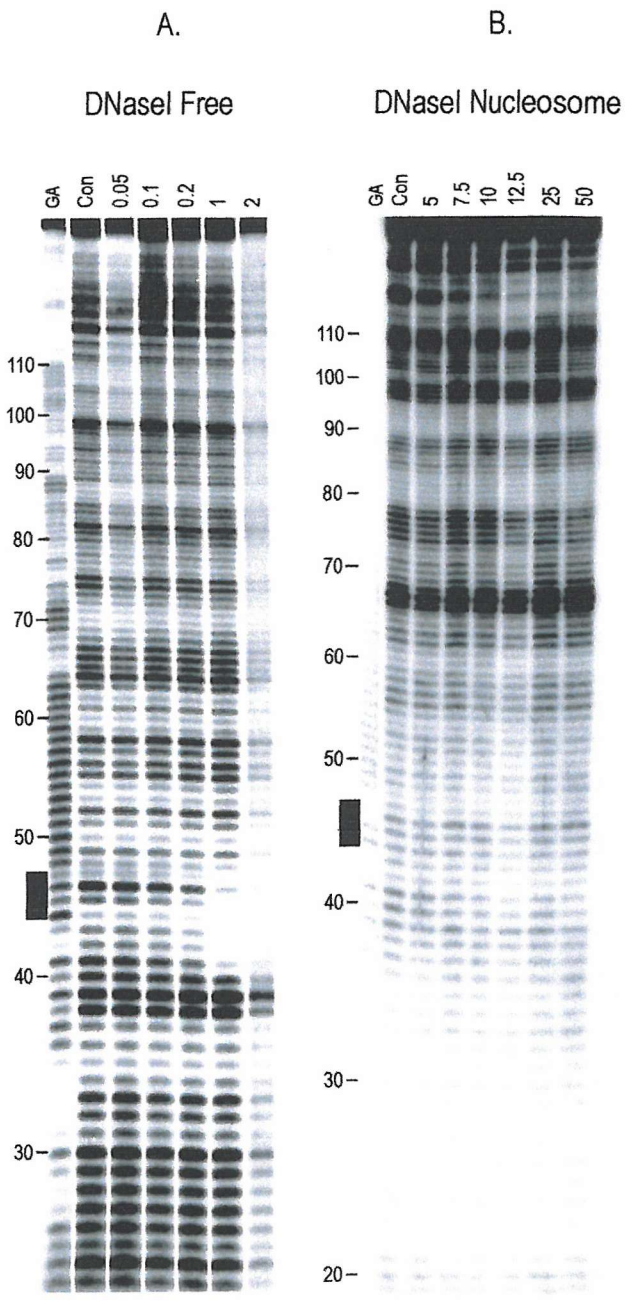

Fig 3.14 DNaseI digestion data on the interaction between echinomycin and constructs *44e*. The ligand concentration is shown at the top of each lane and is expressed in μM. "Con" indicates the ligand free control digestion and "GA" are Maxam-Gilbert sequencing lanes specific for guanine and adenine. Black bars indicate the ligand target site and numbers correspond to the sequence.

Differential Cleavage of Free and Histone-Bound *44e* in the Presence of Echinomycin (DNaseI)

a.

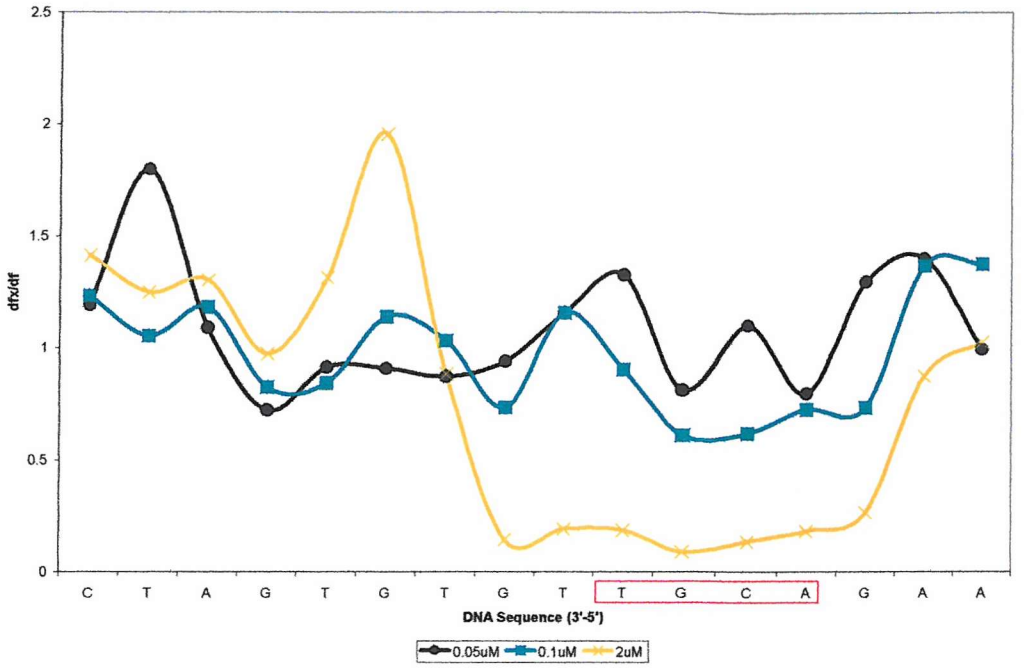

b.

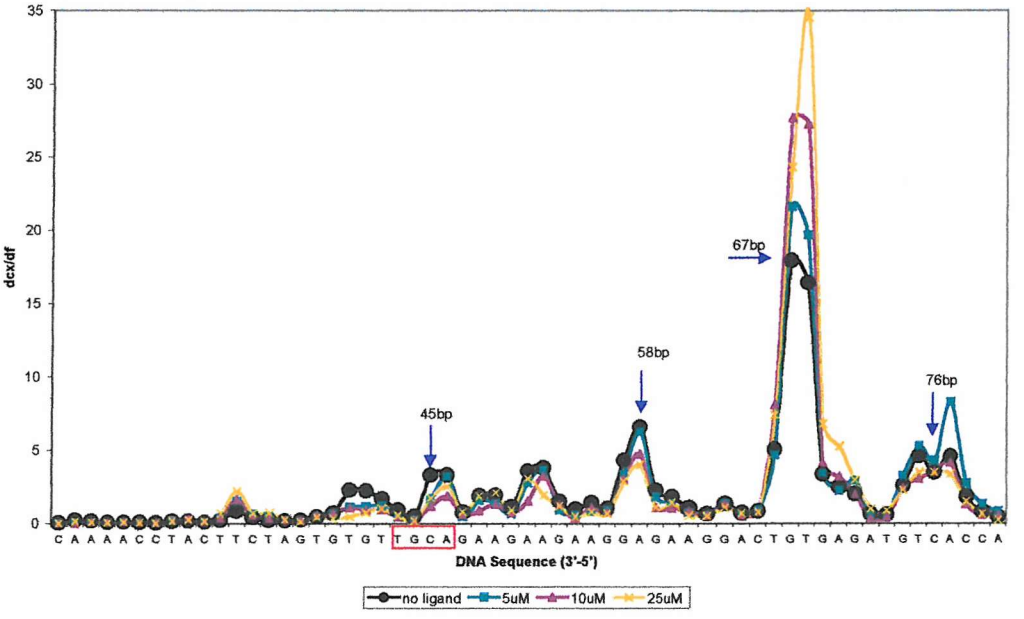

Fig 3.15 Differential cleavage across the 5'-ACGT-3' target site for *44e* free (b) and histone-bound (b) DNA in the presence of Echinomycin as determined by DNaseI. The DNA sequence is shown in the 3'-5' direction and the target site is indicated by a red box. (a), the y-axis shows the value obtained for the division of each band, from a lane where Hoechst has been added (dfx), by the exact corresponding band in the ligand free control (df). (b), the y-axis shows the value obtained for the division of each band in the histone-bound sample (dcx) by the corresponding band in the free DNA (df). Arrows indicate resolved cleavage maxima where the minor groove faces away from the histone core. For clarity, only three concentrations of ligand are presented in each chart.

with the small proportion of contaminating free DNA. We therefore conclude that echinomycin does not interact with this site on histone-bound DNA.

Some other minor changes in the cleavage pattern are evident in other regions remote from the drug binding site. In particular there appears to be a region of protection around position 130. Other subtle changes in relative cleavage intensity can be seen at the cleavage maxima around positions 66-68, 75-79, and 87-89bp. We suggest that these are caused by other weak non-specific interactions between the drug and the DNA.

74e

The results with Hoechst demonstrate that the position of an outer facing target site affects a ligand's ability to bind to the sequence. The results for construct *44e* demonstrate that echinomycin does not interact with this outer facing target site. Based on this it was considered important to examine the effect of positioning an echinomycin binding site across the nucleosome dyad since the binding of Hoechst to this region appears to have a strong destabilising effect upon the structure of the nucleosome.

Construct *74e* contains one strong echinomycin target site (5'-ACGT-3') with the CG step across positions 74 and 75, fig 3.16.

DNaseI results for this construct are presented in fig 3.17. 3.17a demonstrates that the ligand binds to the target site on free DNA and reveals that the site is fully saturated by 5μM ligand (there was very little difference between 2 and 5μM). The differential cleavage plot suggests that the footprint covers 6bp (3.18a). However, DNaseI cleavage is very weak across this region of the fragment and binding to the target is mainly characterised by the loss of the strong band at position 74. The footprint at this site is accompanied by the appearance of an enhancement across positions 68-69. These are presumed to reflect changes in the local conformation of

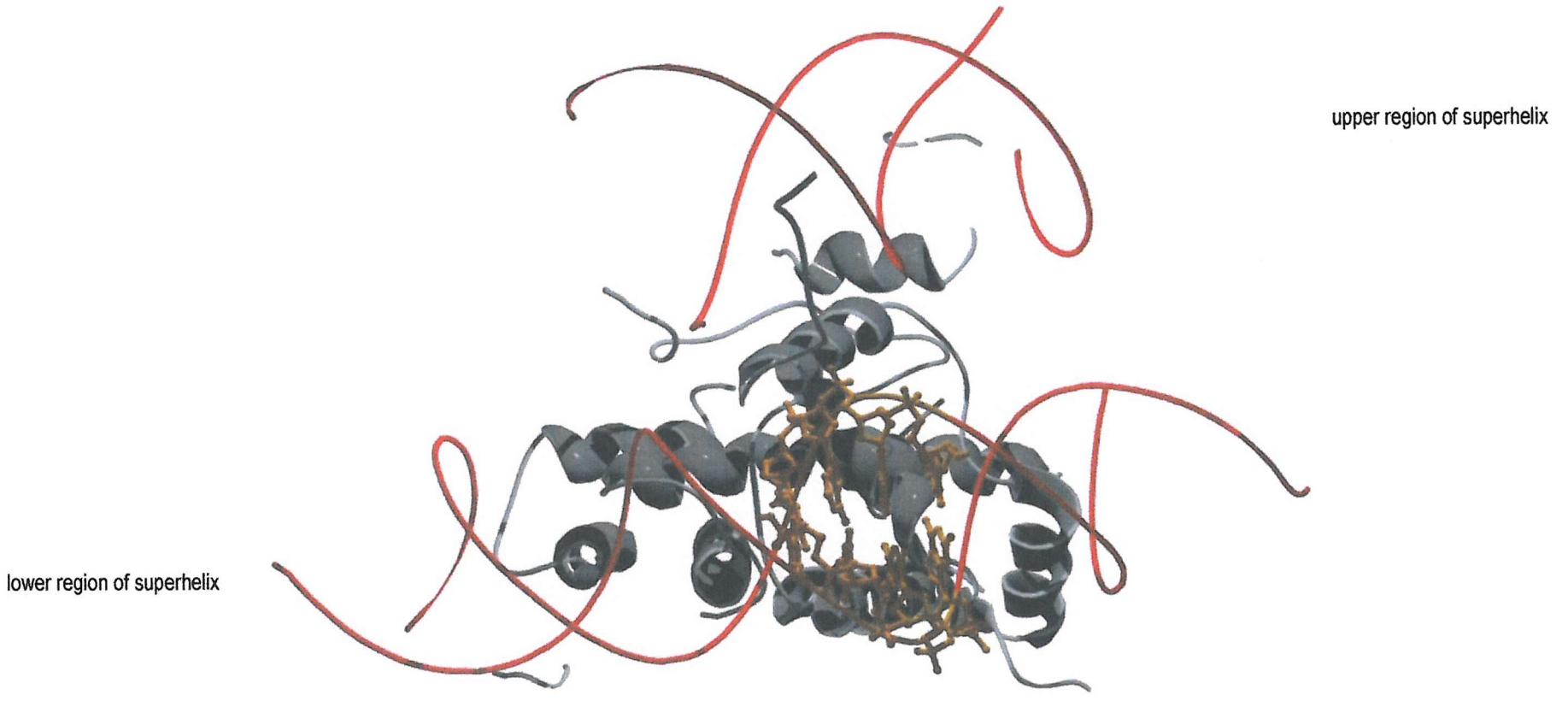

Figure 3.16 Molecular graphics of the *73h* and 74*e* target sites. Each image shows a small portion of the nucleosome core particle. DNA strands are shown as red ribbons, the target sites are coloured orange and are presented as ribbon-ball and stick structures. A portion of the histone octamer is shown as grey ribbons. Since only a small region of the complex is presented, there appears to be two DNA helices. These actually correspond to the one helix which is wraps around the protein complex. The upper and lower portions of the DNA superhelix are indicated. The view is looking towards the nuclesome perpendicular to the superhelix axis. Images were created in Swiss-Pdb viewer, from the pdb file submitted by Luger *et al.* 1997, and rendered in Pov-ray for Windows.

Construct *74e*

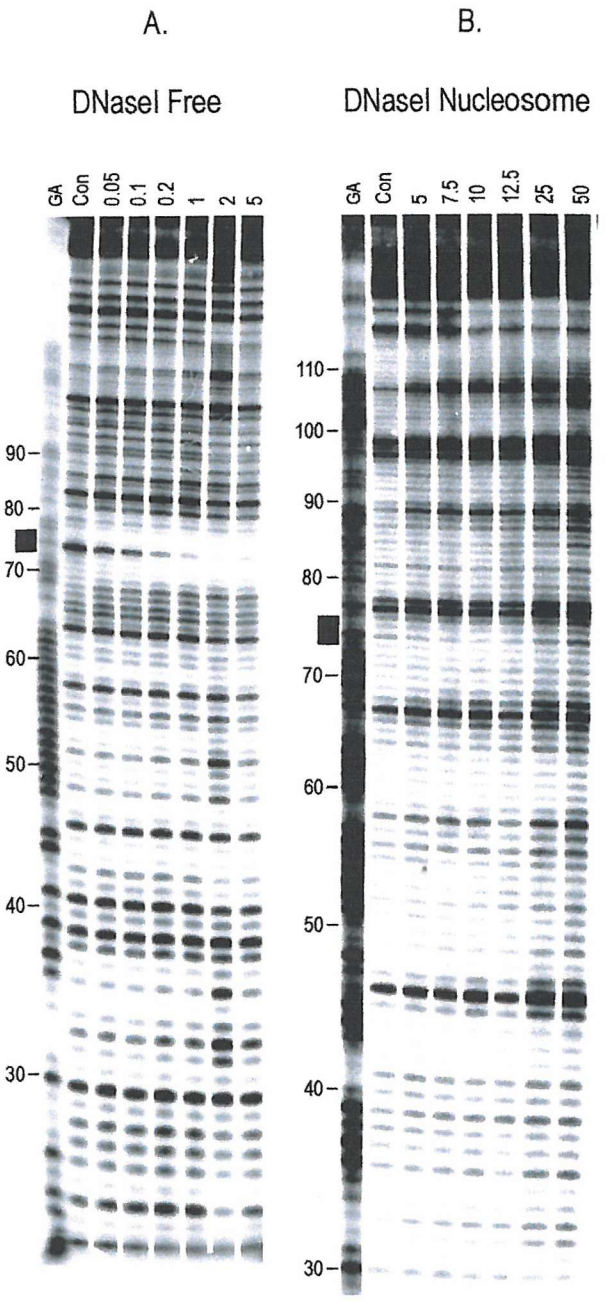

Fig 3.17 DNaseI digestion data on the interaction between echinomycin and constructs *74e*. The ligand concentration is shown at the top of each lane and is expressed in μM. "Con" indicates the ligand free control digestion and "GA" are Maxam-Gilbert sequencing lanes specific for guanine and adenine. Black bars indicate the ligand target site and numbers correspond to the sequence.

Differential Cleavage of Free and Histone-Bound *74e* in the Presence of Echinomycin (DNaseI)

I.

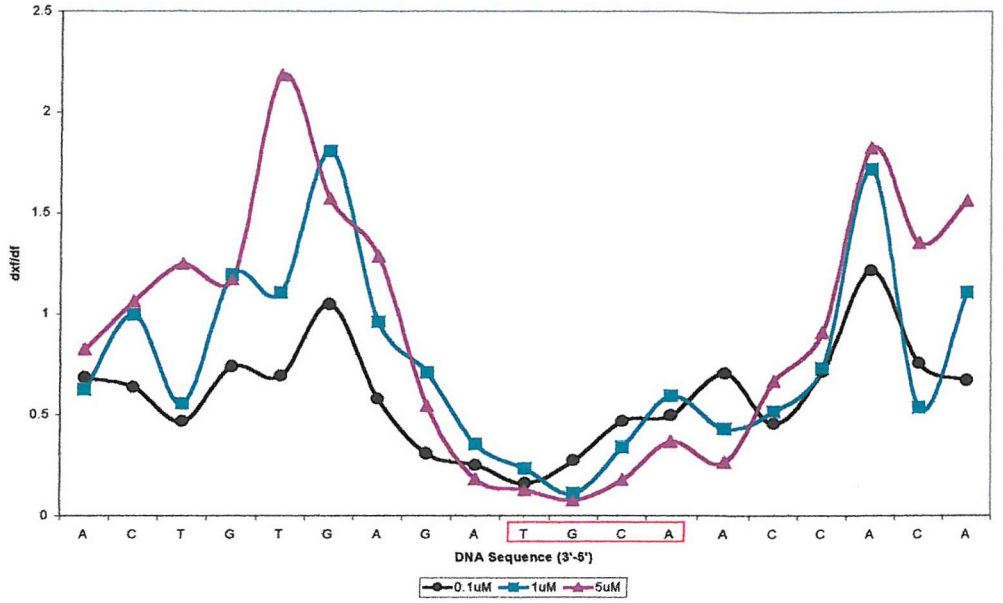

II.

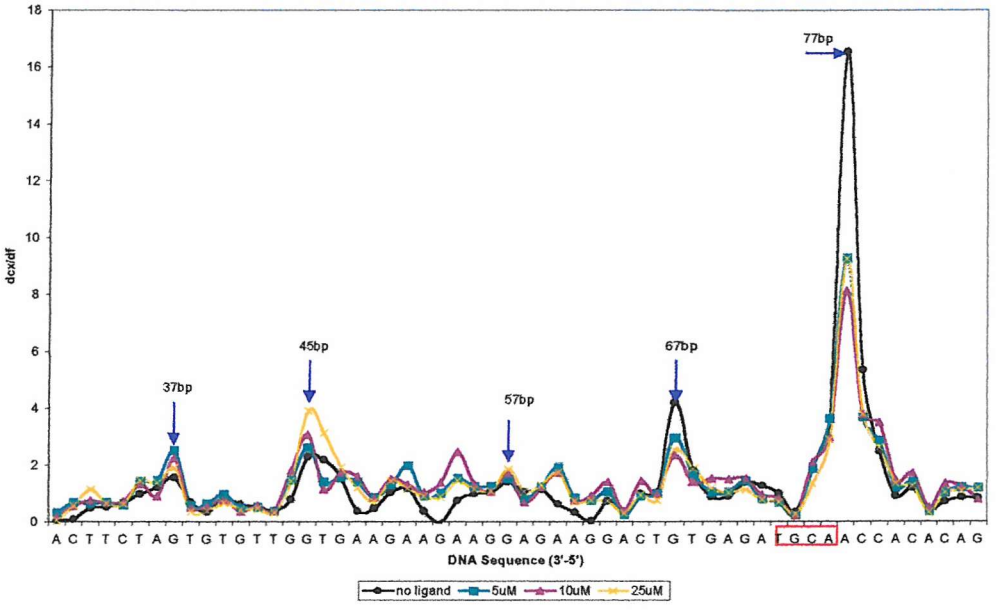

Fig 3.18 Differential cleavage across the 5'-ACGT-3' target site for *74e* free (panel I) and histone-bound (panel II) DNA in the presence of Echinomycin as determined by DNaseI. The DNA sequence is shown in the 3'-5' direction and the target site is indicated by a red box. Panel I, the y-axis shows the value obtained for the division of each band, from a lane where Hoechst has been added (dfx), by the exact corresponding band in the ligand free control (df). Panel II, the y-axis shows the value obtained for the division of each band in the histone-bound sample (dcx) by the corresponding band in the free DNA (df). Arrows indicate resolved cleavage maxima where the minor groove faces away from the histone core. For clarity, only three concentrations of ligand are presented in each chart.

the DNA helix as the drug intercalates into the helix.

The interaction of echinomycin with *74e* histone-bound DNA, as probed by DNaseI, is presented in 3.17b. The cleavage maxima of the drug-free histone-bound DNA are found at similar positions as in all constructs and are indicated in the differential cleavage plot shown in fig 3.18b. In this instance it can be seen that echinomycin has no effect on the cleavage pattern. These results suggest that echinomycin is not able to bind to outward facing target sites on the nucleosome. However, it should be noted that the exact orientation of this site appears to be just on the outer surface. Although the DNaseI data suggests that the first two nucleotides in the target are buried the final two are not suggesting that this site is an intermediate between inner and outer facing orientations.

Discussion

The results presented in this chapter show that one or two Hoechst 335258 molecules can bind to target sites that are located on the outward facing surface of histone-bound DNA. This binding occurs without causing a change in the rotational positioning of the DNA superhelix. This is the first direct observation of ligand molecules interacting with nucleosome core particles in such a manner. Although previous studies of drug-nucleosome interactions showed evidence of drug binding they failed to show a discrete footprint. However, these results do not agree with the theory proposed by Waring and co-workers where it was suggested that the binding of Hoechst molecules to the outer surface causes the bound nucleosomal DNA to rotate through 180° leaving the drugs located on the inner surface of the superhelix. In addition, it appears that single echinomycin molecules can not bind to the outward facing DNA.

The binding of Hoechst to the outer surface of the nucleosome

DNaseI footprinting results on free DNA show that the binding of Hoechst to the AATT target in construct *46h* is stronger than the binding to the ATTA target from

construct *35h*. However, on the nucleosome DNaseI cleavage indicates that the drug binds both sites in an almost identical manner and hydroxyl radical digestion suggests that binding to the ATTA site is stronger despite the fact that this is the weaker of the two sites. It should be noted that the footprinting probes used in these studies give an overall statistical picture of the entire population of molecules in the experiment. Therefore DNaseI may indicate that, on average, both sites are occupied while hydroxyl radicals show that the ATTA site is occupied more often than the AATT site. These differences are a property of the probe used. It may be that DNaseI is more effective at capturing a "snap-shot" of a system, which is in rapid exchange and hence shows both sites occupied by the ligand. Hydroxyl radicals, due to their smaller size, may be more sensitive to rapid changes and hence indicate that exchange across the AATT is faster than that of the ATTA site where the drug might have a longer residency time. In addition, differences in the local conformation and accessibility of the DNA at each site cannot be ruled out.

Besides the footprints, altered cleavage patterns are observed in constructs *35h* and *46h* when complexed as nucleosome core particles. These changes in digestion, observed mainly in the DNaseI results, are almost identical between DNA fragments suggesting a common factor. These cleavage patterns do not appear to represent type I specific minor groove binding of the drug since the regions of attenuation are too small to account for this. However, given that they are present at higher drug concentrations, above those required for binding to the primary target site, it is proposed that these altered cleavage patterns represent type II non-specific binding of Hoechst to exposed regions of the nucleosomal DNA.

Is there a role for echinomycin on the outer surface?

The observation that even a single echinomycin molecule fails to interact with target sites located on the outer surface of the nucleosome may lie in the structure of the DNA superhelix itself. Figure 3.19a shows a cartoon for the binding of echinomycin to free DNA. The two intercalating chromophores bracket the 5'-CG-3' base step making primary contacts between alanine and the N2-amino group of guanine.

Figure 3.19b, illustrates the possible problems encountered for echinomycin when attempting to bind in the same way to a fragment of curved DNA. Lines 1 and 1' represent the direction each chromophore must take to intercalate into a free double helix and are shown as a reference. On the section of curved DNA lines 2 and 2' represent the new direction of intercalation. This is perhaps the first problem encountered by the drug when it attempts to bind to DNA in this conformation. In order to achieve intercalation at the new angles of lines 2 and 2', the quinoxaline chromophores must move towards the peptide ring by an angle equal to that between paths 1 and 2. Steric clash with the octa-peptide ring may prevent this to any great degree. Intercalation of the chromophore rings stabilises the drug-DNA complex to a great extent. Due to the fixed length of the peptide ring, it is impossible for the drug to fully intercalate if the DNA duplex remains curved. Since the length across the CG step is increased on the outside of the curve. This implies that if echinomycin is going to bind to the outer surface of the nucleosome then regions where the DNA path is straighter, for example across the dyad region, would possibly be preferred although this was not seen in the results.

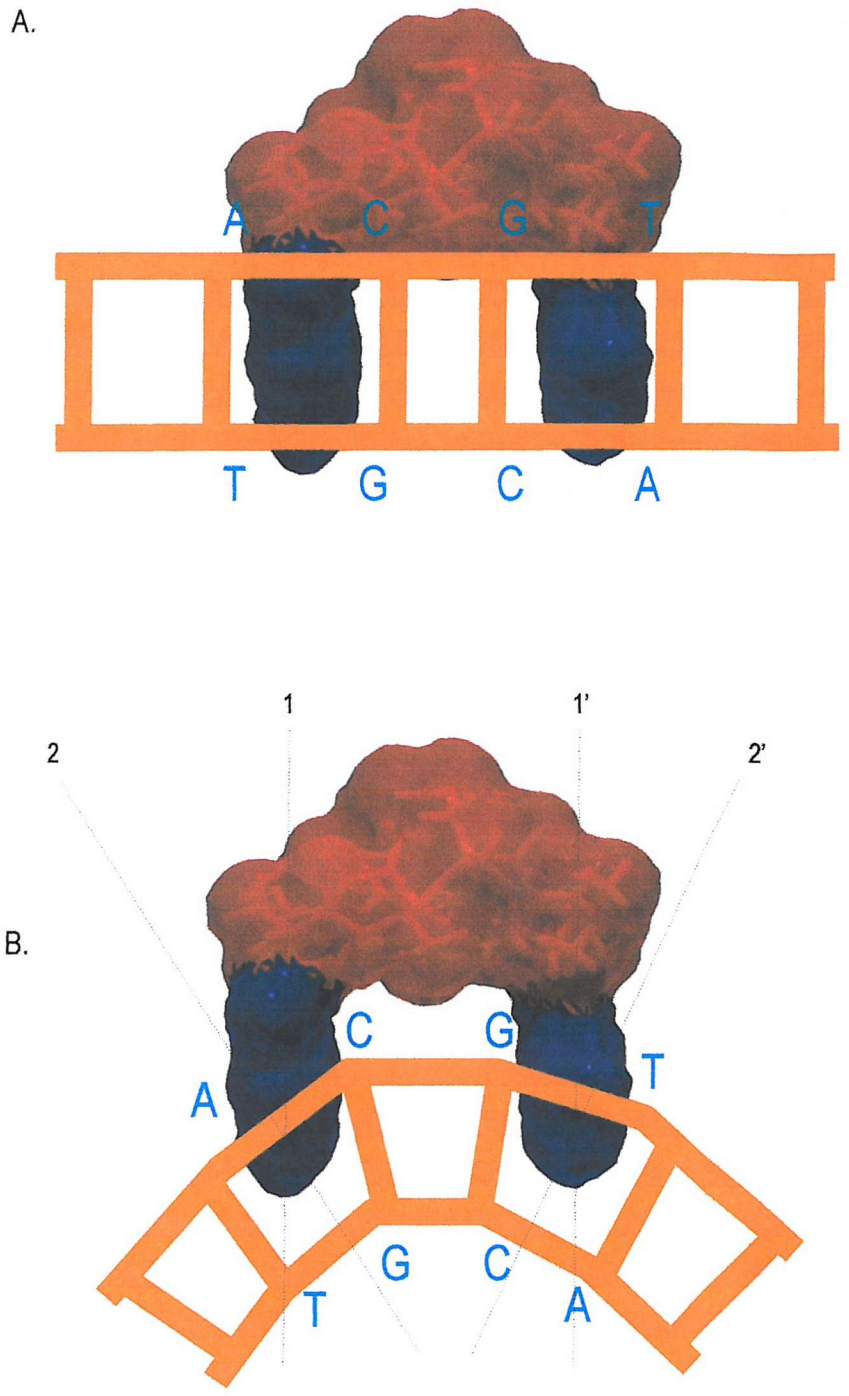

Fig 3.19 A comparison between the binding of echinomycin to free DNA (A) and to a segment of curved DNA(B). Each carboxylic acid chromophore is shown in blue and a cartoon of the DNA duplex is shown in orange. In (B), lines 1 and 1' represent the direction of intercalation in free DNA. Lines 2 and 2' indicate the direction of intercalation in the curved segment. See text for details.

4 The Interaction of Hoechst 33258 and Echinomycin with Single Target Sites Located on the Inner Surface of the DNA Superhelix

Introduction

The results presented in chapter 3 demonstrate that Hoechst can bind to some single sites located on the outer surface of the DNA superhelix without altering the conformation or orientation of the DNA on the protein surface. In contrast echinomycin showed little interaction with histone-bound DNA. The binding of ligands across the dyad caused some changes in nucleosome structure consistent with disruption of the protein-DNA interaction, but in all these constructs no change in the rotational position of the DNA superhelix was detected. Based on these results, it was considered important to study the interaction of ligands with single sites, which face towards the inner surface of the superhelix since binding of ligands to these locations could disrupt histone-DNA contacts, which may in turn be the driving force for rotation of the DNA superhelix. Since the major interaction between the octamer and the DNA occurs at every inward facing minor groove it seems unlikely that binding of ligands to outward facing sites should affect the DNA-protein contacts. However, the protein will mask these sites, which face towards the core, and interactions with them should be energetically less favourable. This chapter considers the interaction of Hoechst and echinomycin with single inward facing target sites. To this end the following constructs were made: *39e, 50e, 100e, 58h, 3558h* and *73h.*

Results

The sequences of the constructs used in this chapter are shown in fig 4.1. Construct *58h* contains one good Hoechst binding site (AATT) covering positions 58-61bp. This target should lie on the inner surface of the superhelix and should not be easily accessible to the ligand. *3558h* was a hybrid of constructs *35h* and *58h.* This

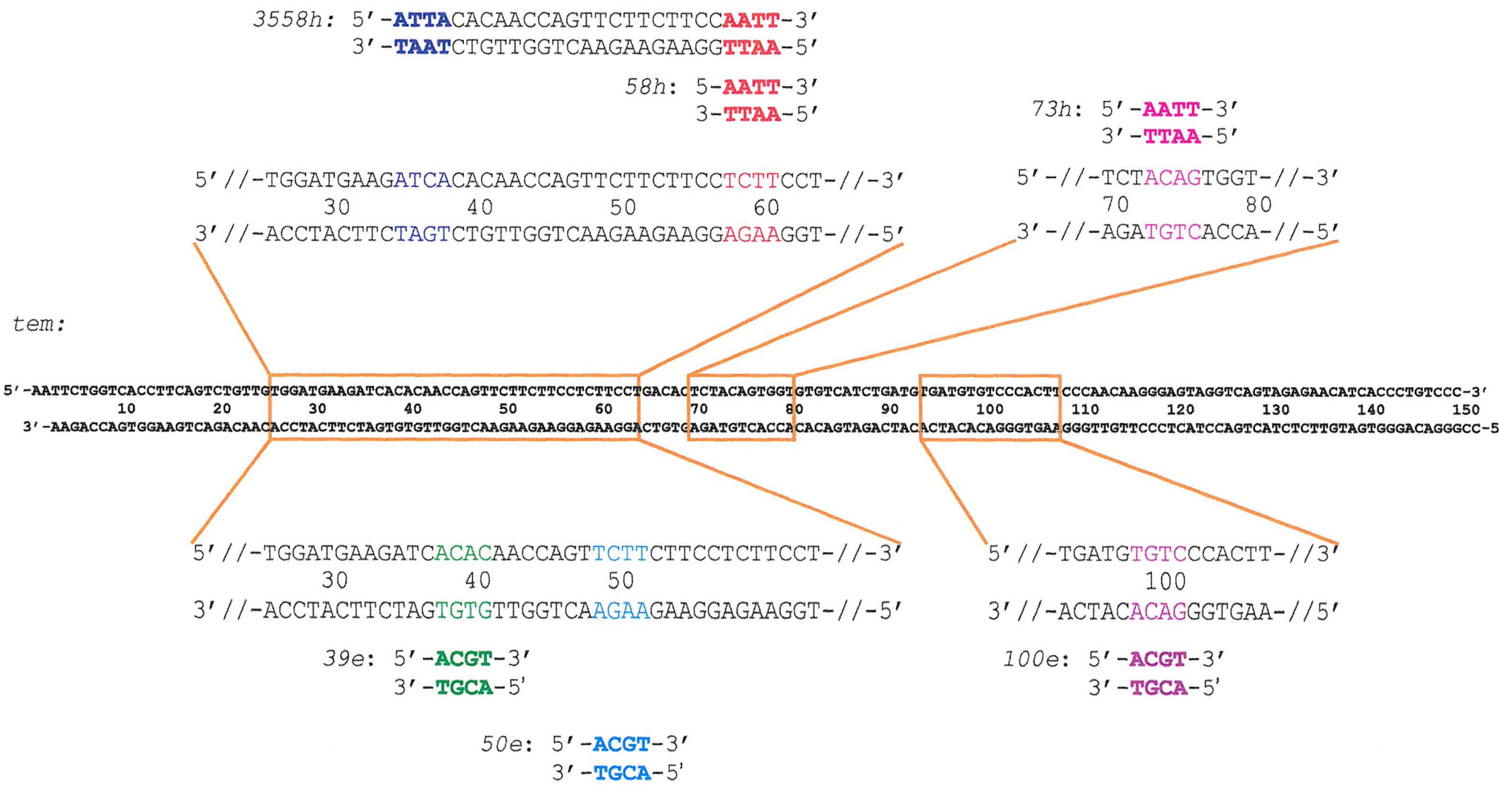

Fig 4.1 sequences of constructs *58h, 3558h, 73h, 39e, 50e* and *100e*. The *tem* construct is shown in the center. Expanded regions show where each mutation was introduced and the target sequence of each construct is indicated. These coloured targets are the only difference between the ligand construct and the parent sequence *tem*.

construct allows us to compare the interaction with a strong site (AATT) facing towards the protein core with a weaker site (ATTA) facing away from the histone surface. Construct *73h* contained one good AATT site across positions 73-76bp and should be relatively inaccessible.

Constructs *39e, 50e* and *100e* all contained one good echinomycin binding site (ACGT). The binding site in *39e* covers positions 38-41, with the CpG step at positions 39 and 40, in *50e* the target covers base pairs 49-52, with the CpG step at positions 50 and 51, while for *100e* the site is found across positions 99-102, with the CpG step at positions 100 and 101. All these sites were engineered in positions for which the minor groove faces the inner surface of the DNA superhelix.

Echinomycin

39e

In this fragment the echinomycin ACGT site is located on the inner surface of the superhelix and should not be accessible to the ligand. A graphic of the target site is presented in fig 4.2 and demonstrates that the CG step should face towards the histone core. The rotational position was confirmed in the same manner as used for all other constructs by DNaseI digestion studies. As previously noted, hydroxyl radicals can not be used to confirm the rotational setting in the presence of echinomycin since the DMSO used to dissolve this ligand strongly inhibits the reaction. Nevertheless, since the DNaseI cleavage patterns for echinomycin constructs are similar to those obtained with the Hoechst constructs it is reasonable to propose that they adopt the same rotational position.

A DNaseI footprint showing the interaction of echinomycin with *39e* free DNA is presented in figure 4.3a and confirms binding to the target site. The footprint is about 8bp in size and as can be seen from the differential cleavage plot presented in fig 4.4a it can be seen that the site is fully saturated at a concentration of 7.5μM ligand. In addition to this footprint there is an enhancement around positions 31-

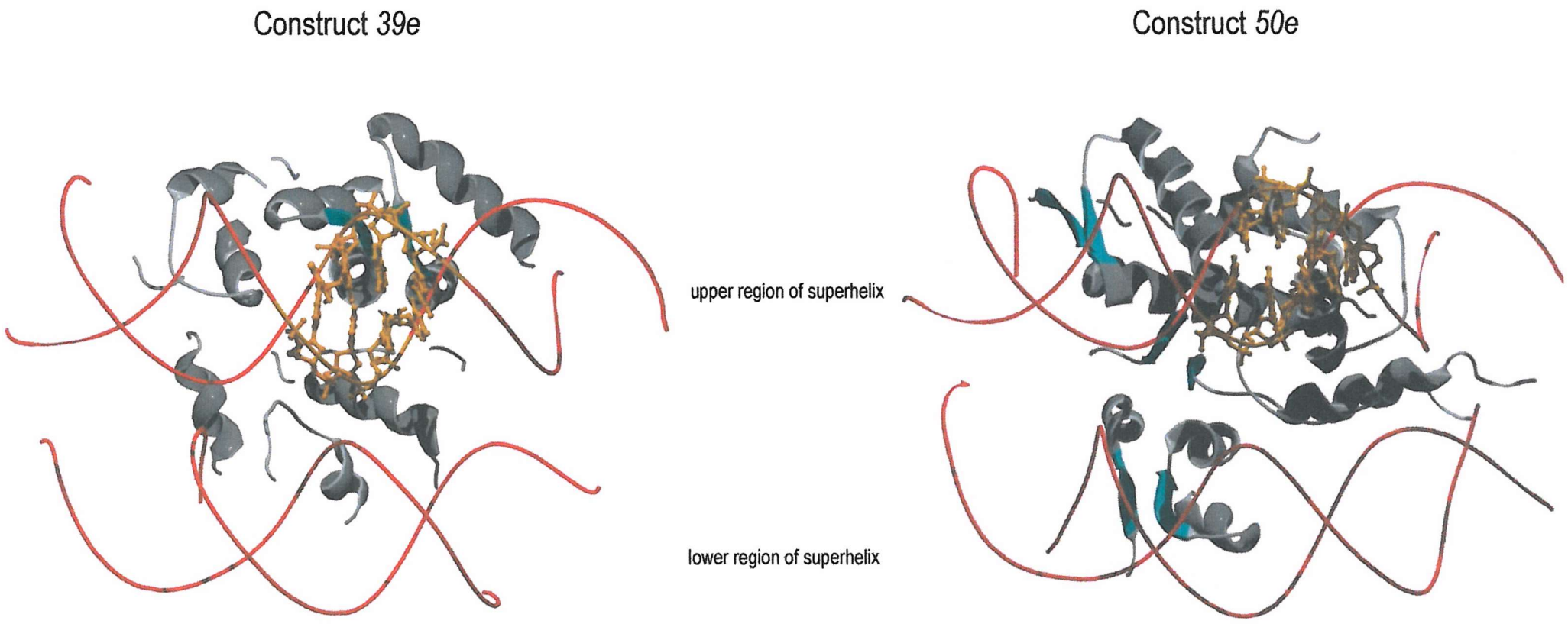

Figure 4.2 Molecular graphics of the *39e* and *50e* target sites. Each image shows a small portion of the nucleosomecore particle. DNA strands are shown as red ribbons, the target sites are coloured orange and are presented as ribbon-ball and stick structures. A portion of the histone octamer is shown as grey ribbons for helices and strands while sheets are coloured teal. Since only a small region of the complex is presented, there appears to be two DNA helices. These actually correspond to the one helix which is wrapped around the protein complex. The upper and lower portions of the DNA superhelix are indicated. The view is looking towards the nucleosome perpendicular to the superhelix axis. Images were created in Swiss-PdB Viewer (v3.7b), from the pdb file submitted by Luger *et al.* 1997 (1aoi.pdb), and rendered in Pov-Ray for Windows 98 .

Construct *39e*

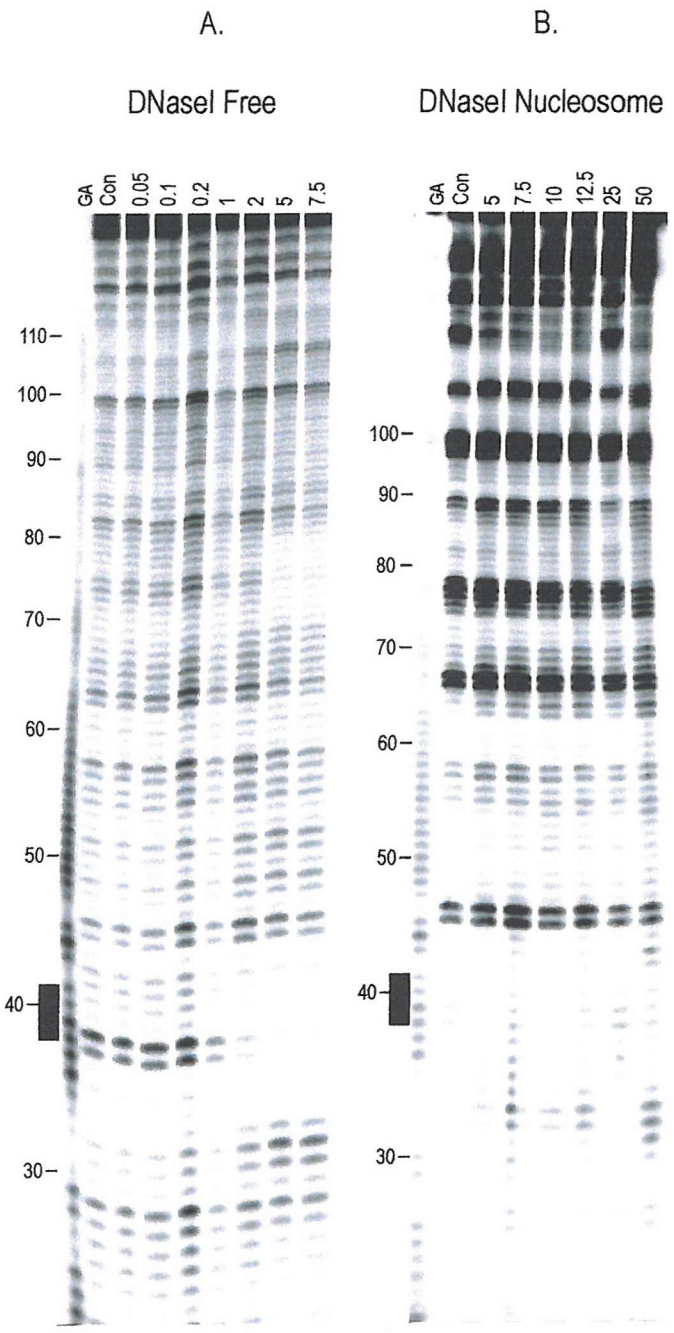

Fig 4.3 DNaseI digestion data on the interaction between echinomycin and constructs *39e*.The ligand concentration is shown at the top of each lane and is expressed in μM. "Con" indicates the ligand free control digestion and "GA" are Maxam-Gilbert sequencing lanes specific for guanine and adenine. Black bars indicate the ligand target site and numbers correspond to the sequence.

Differential Cleavage of Free and Histone-Bound *39e* in the Presence of Echinomycin (DNaseI)

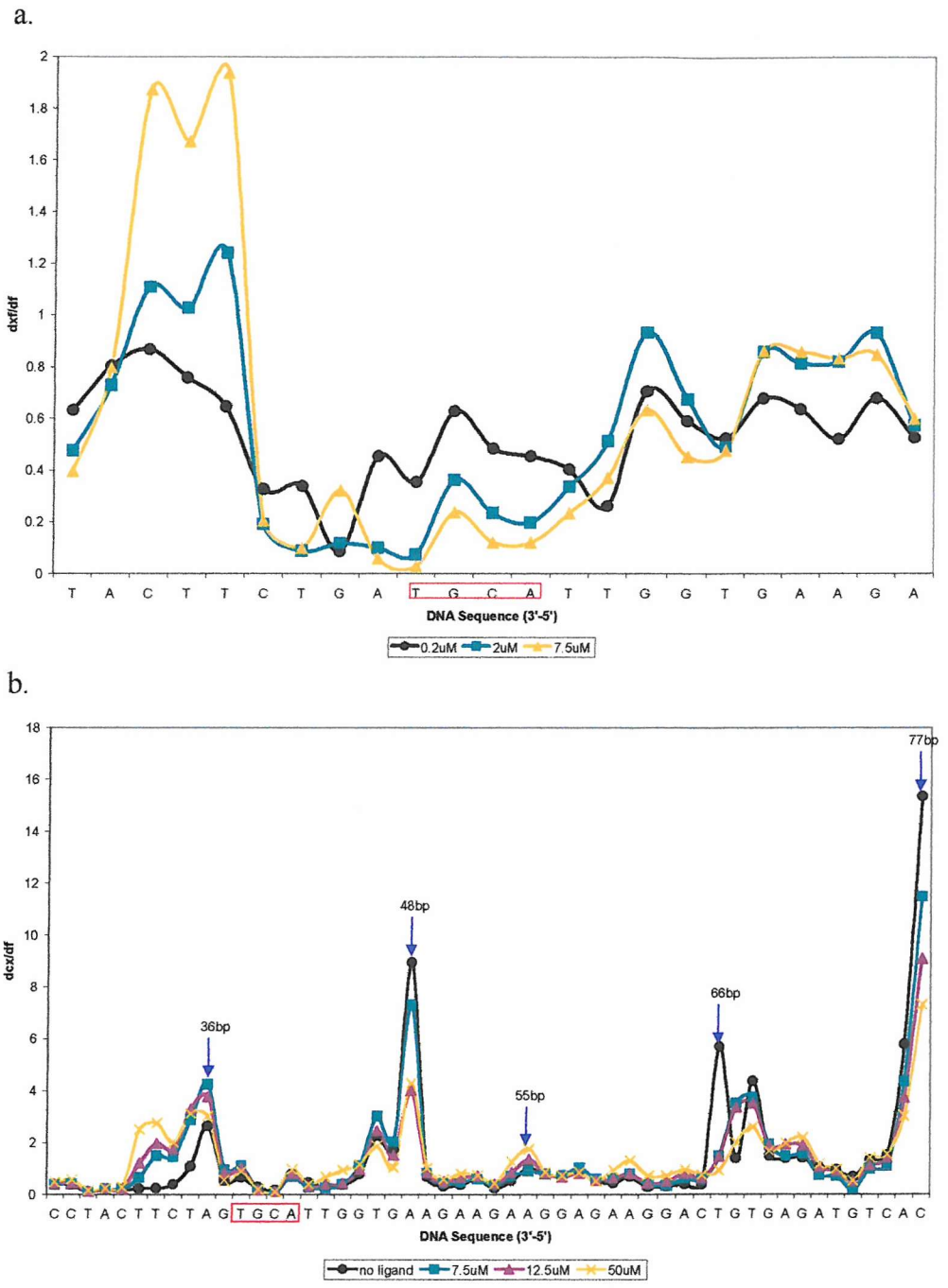

Fig 4.4 Differential cleavage across the 5'-ACGT-3' target site for *39e* free (a) and histone-bound (b) DNA in the presence of Echinomycin as determined by DNaseI. The DNA sequence is shown in the 3'-5' direction and the target site is indicated by a red box. (a), the y-axis shows the value obtained for the division of each band, from a lane where Hoechst has been added (dfx), by the exact corresponding band in the ligand free control (df). (b), the y-axis shows the value obtained for the division of each band in the histone-bound sample (dcx) by the corresponding band in the free DNA (df). Arrows indicate resolved cleavage maxima where the minor groove faces away from the histone core. For clarity, only three concentrations of ligand are presented in each chart.

34bp on the 3'-side of the drug binding site, which is thought to reflect distortions in the local conformation of the helix, caused by drug binding.

Fig 4.3b shows the interaction of echinomycin with histone-bound *39e*. The 10 base pair phasing pattern seen in the control lane confirms the expected rotational position of this target site. Maxima are identified at positions 36, 48, 55, 66 and 77bp. As expected the ligand binding site is in a region of poor DNaseI cleavage (facing towards the protein) and visual inspection of the gel indicates little evidence for a footprint. Analysis of these results, fig 4.4b, does not show any significant interaction across the target site. However, visual inspection of the gel shows that there is some enhancement across positions 31-33bp with increasing drug concentration as seen with free DNA in the presence of echinomycin and this is also indicated in figure 4.4b. In addition there are some subtle increases in DNaseI cleavage across other regions of the construct. This is better seen by presenting differential cleavage plots of drug-bound core samples divided by drug-free core samples (instead of by drug-free free DNA); this is presented in fig 4.5. This analysis reveals further subtle alterations in the cleavage pattern. The very strong enhancement can be seen across positions 31-34bp, and it appears that DNaseI cleavage across all inward-facing regions has been increased by about 2-fold except where the sequence approaches the dyad. On close inspection, this can be seen on the gel, fig 4.3b, where it appears as though there is a general increase in background cleavage. However, it is still clear that, for the most part, the nucleosome-phasing pattern is maintained.

Therefore, although no footprint is observed across the ligand target site, the enhancement across bases 31-34, which is also seen in the free DNA, and additional changes in the core cleavage pattern suggest that some form of interaction between the ligand and the histone-DNA complex has occurred. However, drug binding to a small fraction of unbound DNA could explain this. Most importantly the rotational position of these nucleosomes has not changed in the presence of echinomycin and the phasing pattern has been conserved even in the presence of high concentrations

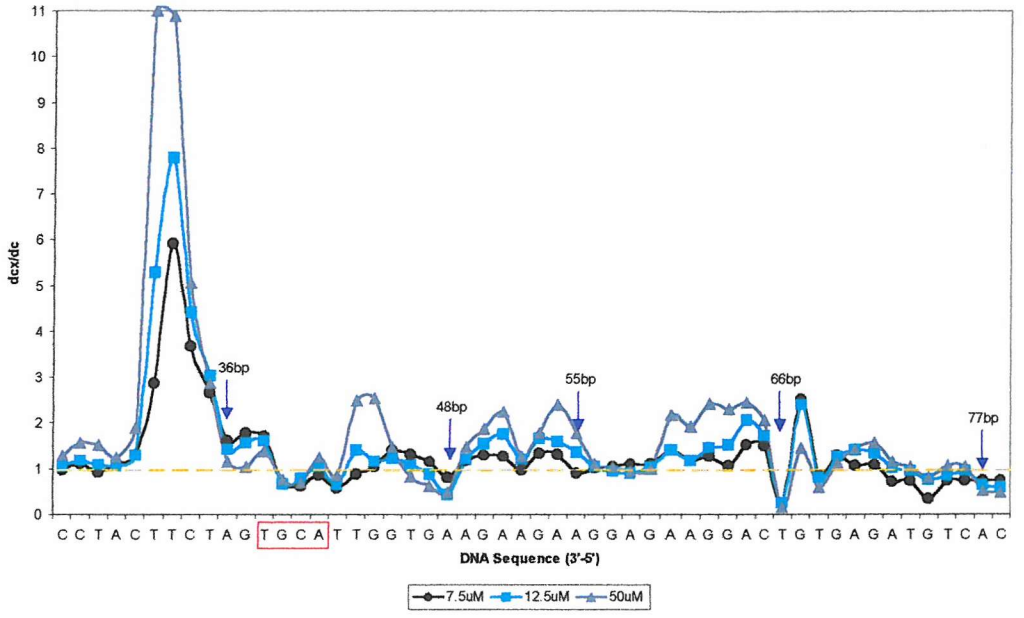

Fig 4.5 Differential cleavage across the 5'-ACGT-3' target site for *39e* histone-bound DNA in the presence of Echinomycin as determined by DNaseI. The DNA sequence is shown in the 3'-5' direction and the target site is indicated by a red box. The y-axis shows the value obtained for the division of each band in the histone-bound sample where Hoechst was added (dcx) by the corresponding band in the histone control (dc). For clarity, only three concentrations of ligand are presented in each chart. Blue arrows indicate the position of identified maxima identified from figure 4.4b.

of this ligand.

50e

The *50e* construct contains an inner facing echinomycin ACGT target, at positions 49-52. It was engineered so that the start of the target sequence is 11bp downstream from the start of the *39e* site. Based on the results of *39e* it was considered important to evaluate the binding of echinomycin to an equivalent site, which was closer to the nucleosome dyad where the DNA should be even less accessible. A representation of this site is presented in figure 4.2.

The DNaseI cleavage patterns for the binding of echinomycin to free *50e* DNA are presented in fig 4.6a. A clear footprint is evident where positions 47-53bp are protected from enzyme cleavage and the differential cleavage plots are shown in fig 4.7a. The footprint is not complete until 7.5μM. Unlike the *39e* site there are no 3' enhancements on the 3' side of this site though there is a small enhancement directly 5' to ACGT with the highest drug concentration. Since these are identical target sequences these differences must reflect the different DNA sequences surrounding the site. In *39e* the target has AG rich sequences on the 3'-side while in *50e* these sequences are more mixed sequence. Polypurine sites tend to be cut less well by DNaseI than mixed sequence DNA, presumably due to their unusual structure, and may therefore be more susceptible to distortion by drug binding. Regions that are cut efficiently by the enzyme will not be able to show enhanced cleavage on drug binding as they are already in an optimal conformation.

Fig 4.6b shows the results obtained for the binding of echinomycin to histone-bound *50e*. The 10bp-phasing pattern is clear in the drug-free controls and analysis, fig 4.7b, confirms that the target site is in the correct orientation, and faces towards the nucleosome core. A graphic of this is presented in fig 4.2. On addition of

Construct 50e

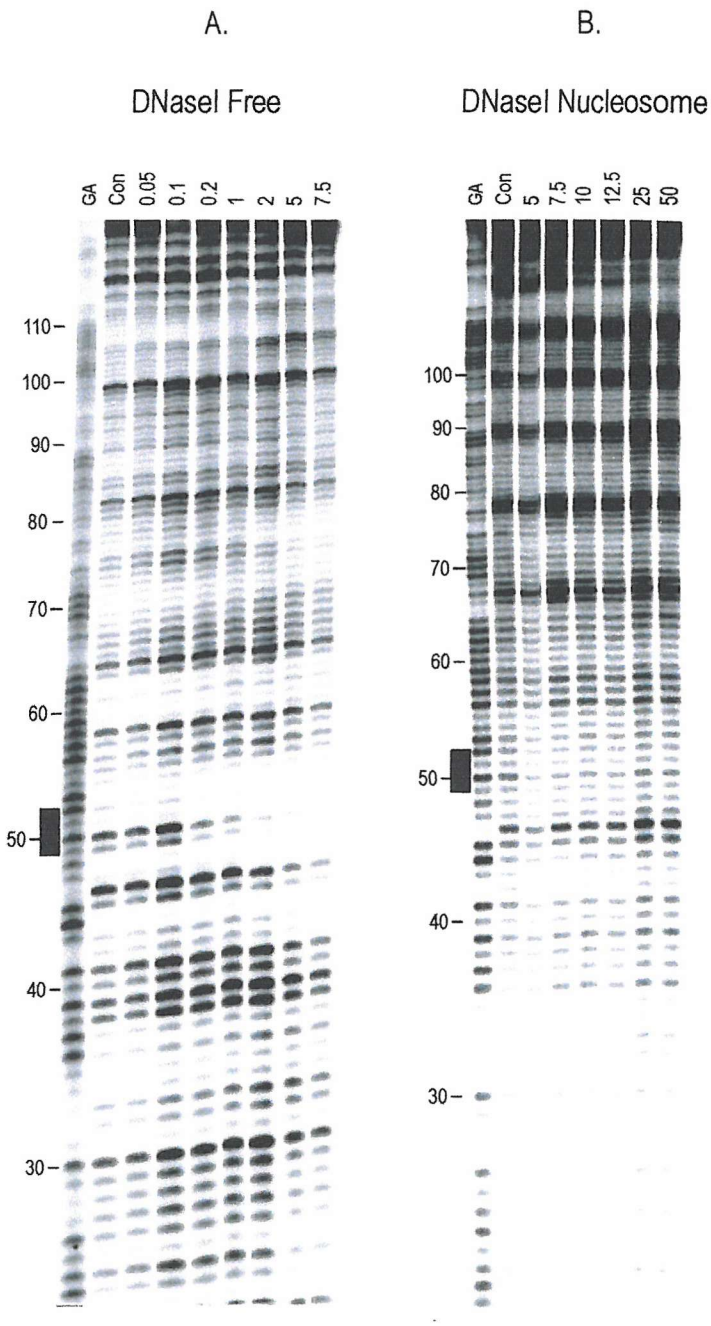

Fig 4.6 DNaseI digestion data on the interaction between echinomycin and constructs *50e*.The ligand concentration is shown at the top of each lane and is expressed in μM. "Con" indicates the ligand free control digestion and "GA" are Maxam-Gilbert sequencing lanes specific for guanine and adenine. Black bars indicate the ligand target site and numbers correspond to the sequence.

Differential Cleavage of Free and Histone-Bound *50e* in the Presence of Echinomycin (DNaseI)

a.

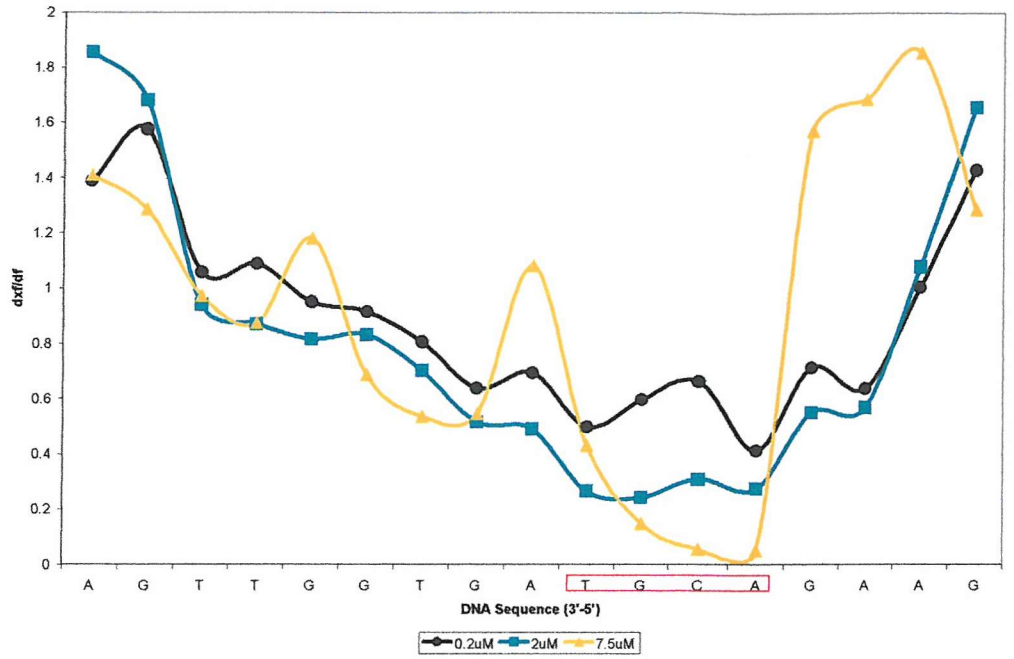

b.

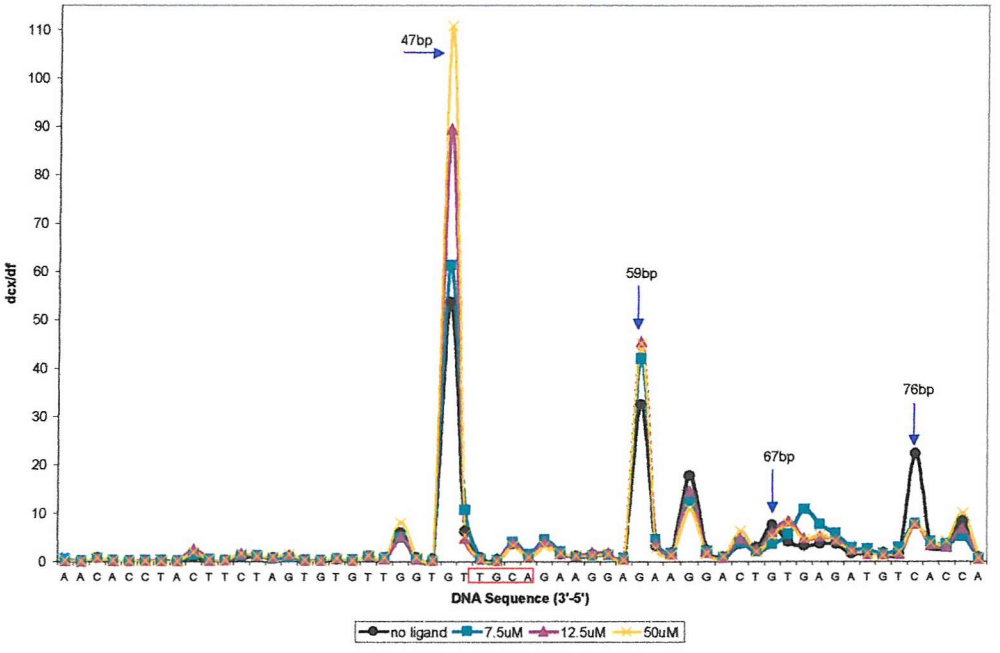

Fig 4.7 Differential cleavage across the 5'-ACGT-3' target site for *50e* free (a) and histone-bound (b) DNA in the presence of Echinomycin as determined by DNaseI. The DNA sequence is shown in the 3'-5' direction and the target site is indicated by a red box. (a), the y-axis shows the value obtained for the division of each band, from a lane where Hoechst has been added (dfx), by the exact corresponding band in the ligand free control (df). (b), the y-axis shows the value obtained for the division of each band in the histone-bound sample (dcx) by the corresponding band in the free DNA (df). Arrows indicate resolved cleavage maxima where the minor groove faces away from the histone core. For clarity, only three concentrations of ligand are presented in each chart.

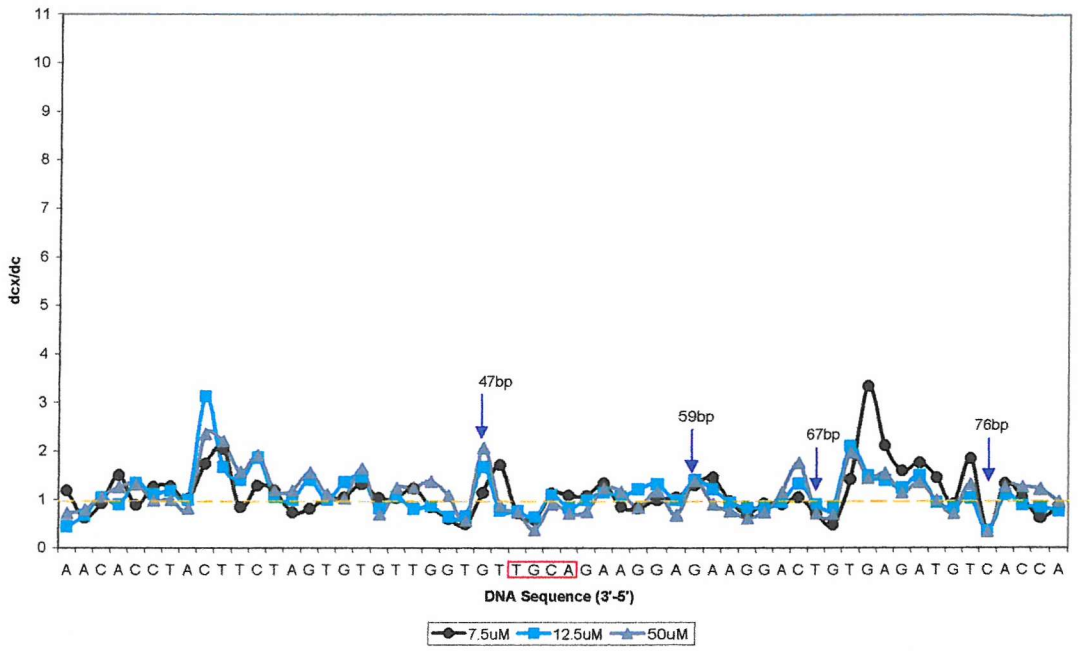

Fig 4.8 Differential cleavage across the 5'-ACGT-3' target site for *50e* histone-bound DNA in the presence of Echinomycin as determined by DNaseI. The DNA sequence is shown in the 3'-5' direction and the target site is indicated by a red box. The y-axis shows the value obtained for the division of each band in the histone-bound sample where Hoechst was added (dcx) by the corresponding band in the histone control (dc). For clarity, only three concentrations of ligand are presented in each chart. Blue arrows indicate the position of identified maxima identified from figure 4.4b.

echinomycin there are no significant changes in the digestion pattern across the ligand target site. In addition, differential cleavage plot shown in fig 4.8, (of the core a samples only) indicates that there is little change in the digestion pattern. From these data there is little evidence to support the binding of the drug to the ACGT target site in *50e.* In addition, there is no change in the rotational position of these fragments or a loss in the nucleosome-phasing pattern despite high concentrations of ligand present in the reaction mixture.

100e

This construct was designed so that the target site is located at an equivalent distance from the nucleosome dyad as found in *50e* and should confirm the results seen with this fragment. The site is presented graphically in fig 4.9. Fig 4.10a shows the binding of echinomycin to free *100e* DNA as assayed by DNaseI digestion and a clear footprint can be seen at the target site. Differential cleavage plots of these results are presented in fig 4.11a and show a clear attenuation across the target site, with saturation at 5:M echinomycin. The footprint is 6-7bp in size and is the only identified binding site in the fragment.

The interaction of echinomycin with nucleosome-bound *100e* is presented in fig 4.10b and analysis is presented in fig 4.11b. Outer facing minor grooves are identified at positions 46, 57, 68, 78, 87, 97 and 108bp and therefore the target site lies in a region of minimum cleavage. Most importantly, this site is exactly the same distance for the dyad as the target in construct *50e.* It can be seen that there is no clear interaction of the ligand with the target site and there is no footprint. It therefore appears that, as expected, echinomycin cannot bind to this target site and that there is no change in the rotational setting of this construct These results are very similar to that obtained with construct *50e.*

Construct *100e*

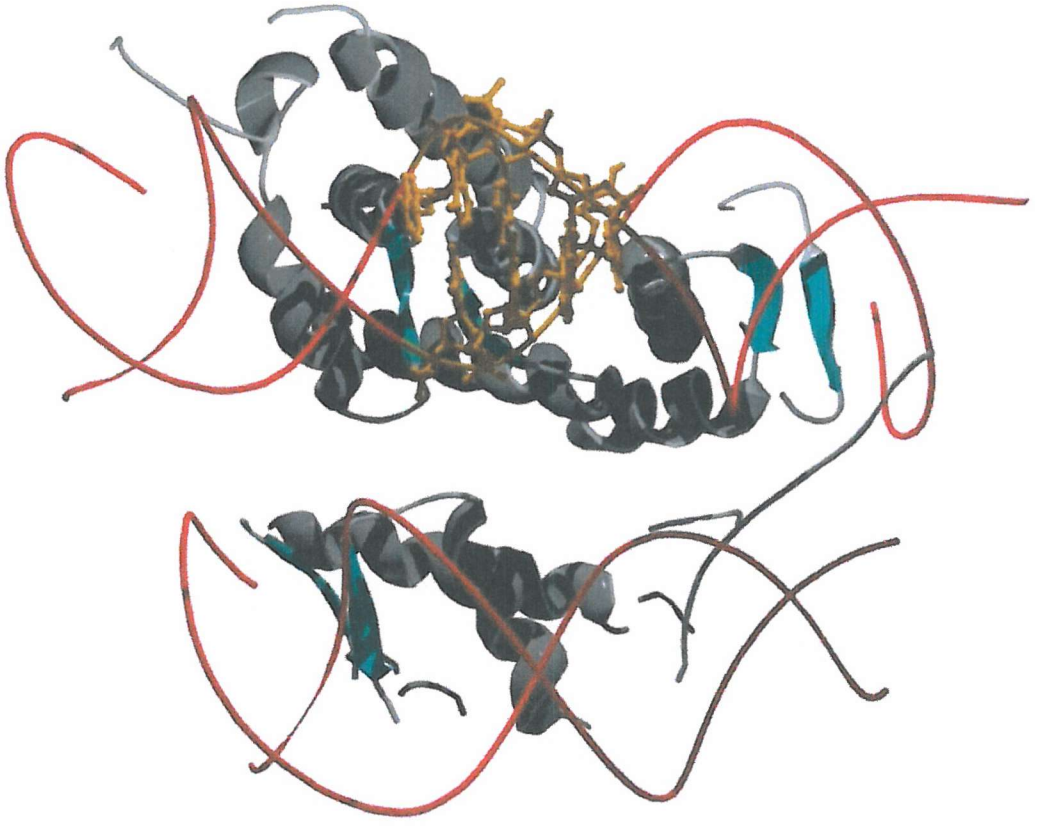

upper region of superhelix

lower region of superhelix

Figure 4.9 Molecular graphics of the *100e* target site. Each image shows a small portion of the nucleosome core particle. DNA strands are shown as red ribbons, the target sites are coloured orange and are presented as ribbon-ball and stick structures. A portion of the histone octamer is shown as grey ribbons. Since only a small region of the complex is presented, there appears to be two DNA helices. These actually correspond to the one helix which is wraps around the protein complex. The upper and lower portions of the DNA superhelix are indicated. The view is looking towards the nuclesome perpendicular to the superhelix axis. Images were created in Swiss-Pdb viewer, from the pdb file submitted by Luger *et al.* 1997, and rendered in Pov-ray for Windows.

Construct *100e*

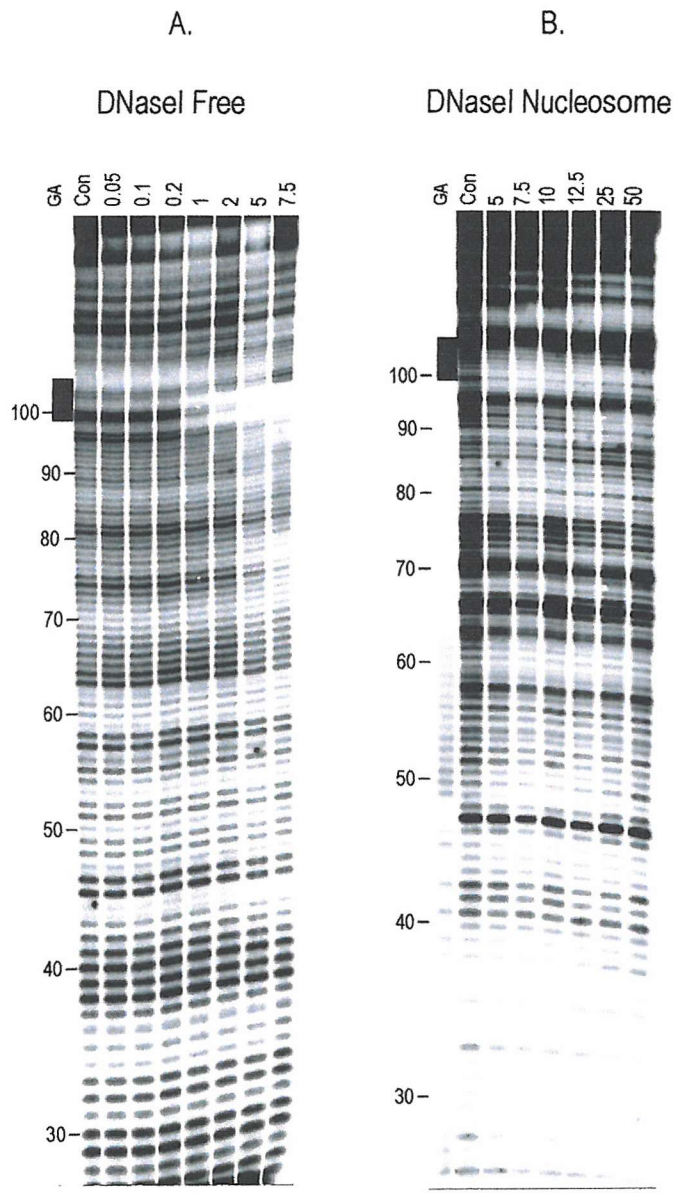

Fig 4.10 DNaseI digestion data on the interaction between echinomycin and constructs *100e*.The ligand concentration is shown at the top of each lane and is expressed in μM. "Con" indicates the ligand free control digestion and "GA" are Maxam-Gilbert sequencing lanes specific for guanine and adenine. Black bars indicate the ligand target site and numbers correspond to the sequence.

Differential Cleavage of Free and Histone-Bound *100e* in the Presence of Echinomycin (DNaseI)

a.

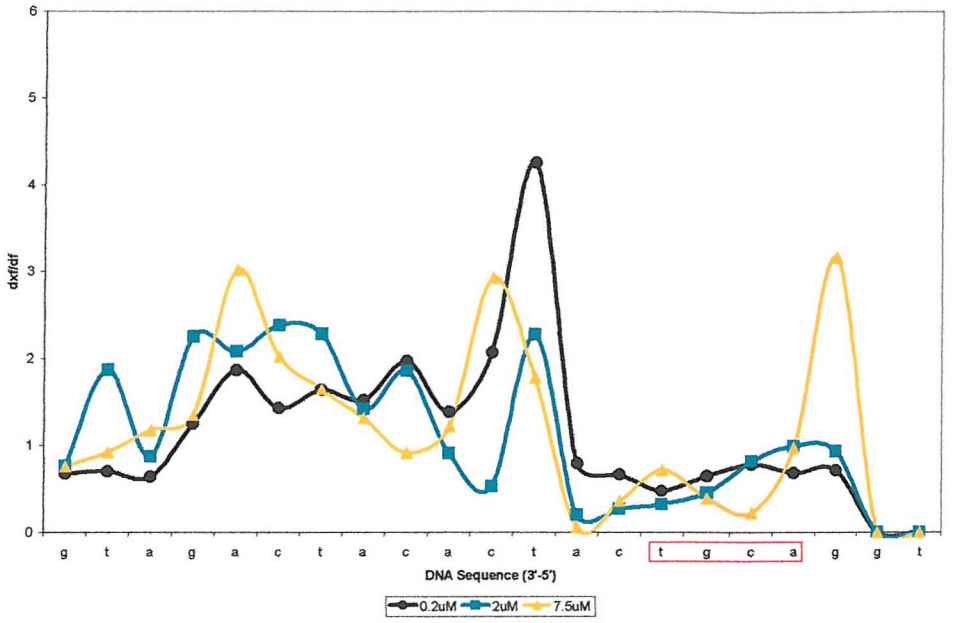

b.

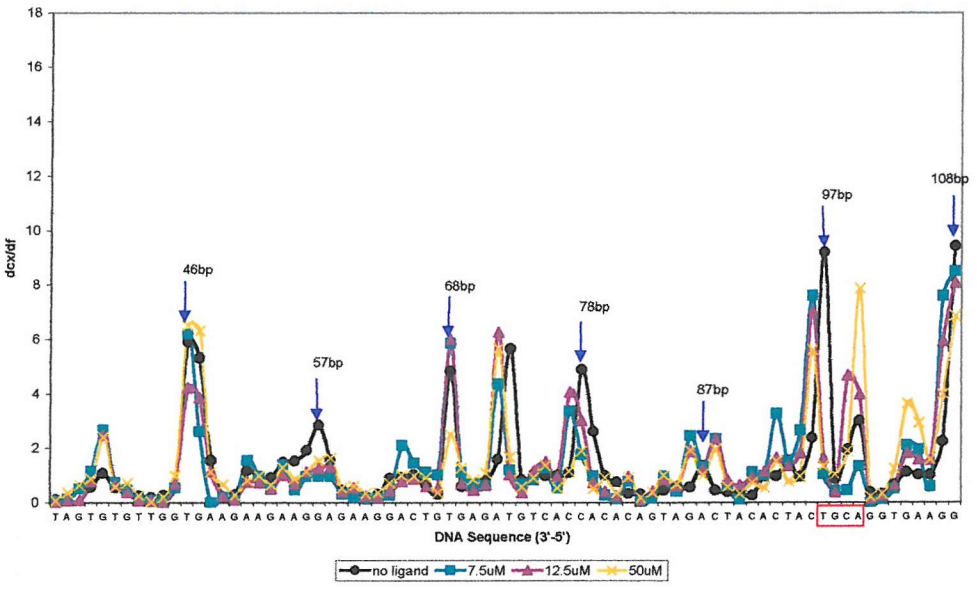

Fig 4.11 Differential cleavage across the 5'-ACGT-3' target site for *100e* free (a) and histone-bound (b) DNA in the presence of Echinomycin as determined by DNaseI. The DNA sequence is shown in the 3'-5' direction and the target site is indicated by a red box. (a), the y-axis shows the value obtained for the division of each band, from a lane where Hoechst has been added (dfx), by the exact corresponding band in the ligand free control (df). (b), the y-axis shows the value obtained for the division of each band in the histone-bound sample (dcx) by the corresponding band in the free DNA (df). Arrows indicate resolved cleavage maxima where the minor groove faces away from the histone core. For clarity, only three concentrations of ligand are presented in each chart.

Hoechst 33258

58h

In the previous chapter it was demonstrated that Hoechst 33258 can bind to the outer surface of the histone-bound DNA superhelix. Since the binding of two molecules has little affect on the rotational position of the superhelix, it was decided to study the interaction of the drug with inward facing targets. Construct *58h* contains an AATT across positions 58-61bp and should be inaccessible to the drug when bound to the histone octamer, fig 4.12.

The binding of Hoechst to *58h* free DNA is presented in fig 4.13a. It can be seen that the drug protects positions 54-60bp from DNaseI cleavage and binds to the AATT target site as expected. Interaction with the DNA is observed at 0.05μM ligand and the target is completely saturated at 0.2μM. The differential cleavage plot in figure 4.14 confirms this.

The Interaction of Hoechst 33258 with *58h* nucleosomes as assayed by DNaseI is presented in fig 4.13b and differential cleavage analysis is shown on fig 4.14b. The 10bp/turn phasing pattern is clear and maxima are identified at 45, 58, 66 and 75bp. The rotational position of the sequence in the ligand-free control is identical to the *tem* construct and as expected, the target is found in a region of attenuated DNaseI cleavage therefore representing a minor groove, which faces the protein core. There is little evidence for binding of the drug across the target site, although the maxima at position 58bp does appear to be reduced with increasing drug concentration. However, with high concentrations of Hoechst, the maxima are disrupted in other regions in the construct and this presumably reflects Type II non-specific binding of the drug as was observed in the previous chapter. Therefore it is difficult to evaluate whether the loss of this peak (58) is due to a specific drug interaction across the target site or whether it is caused by disruption in the phasing pattern due to the intermediate binding of many drug molecules. Most importantly, there is no detected change in the rotational position in the presence of the drug.

Construct *58h*

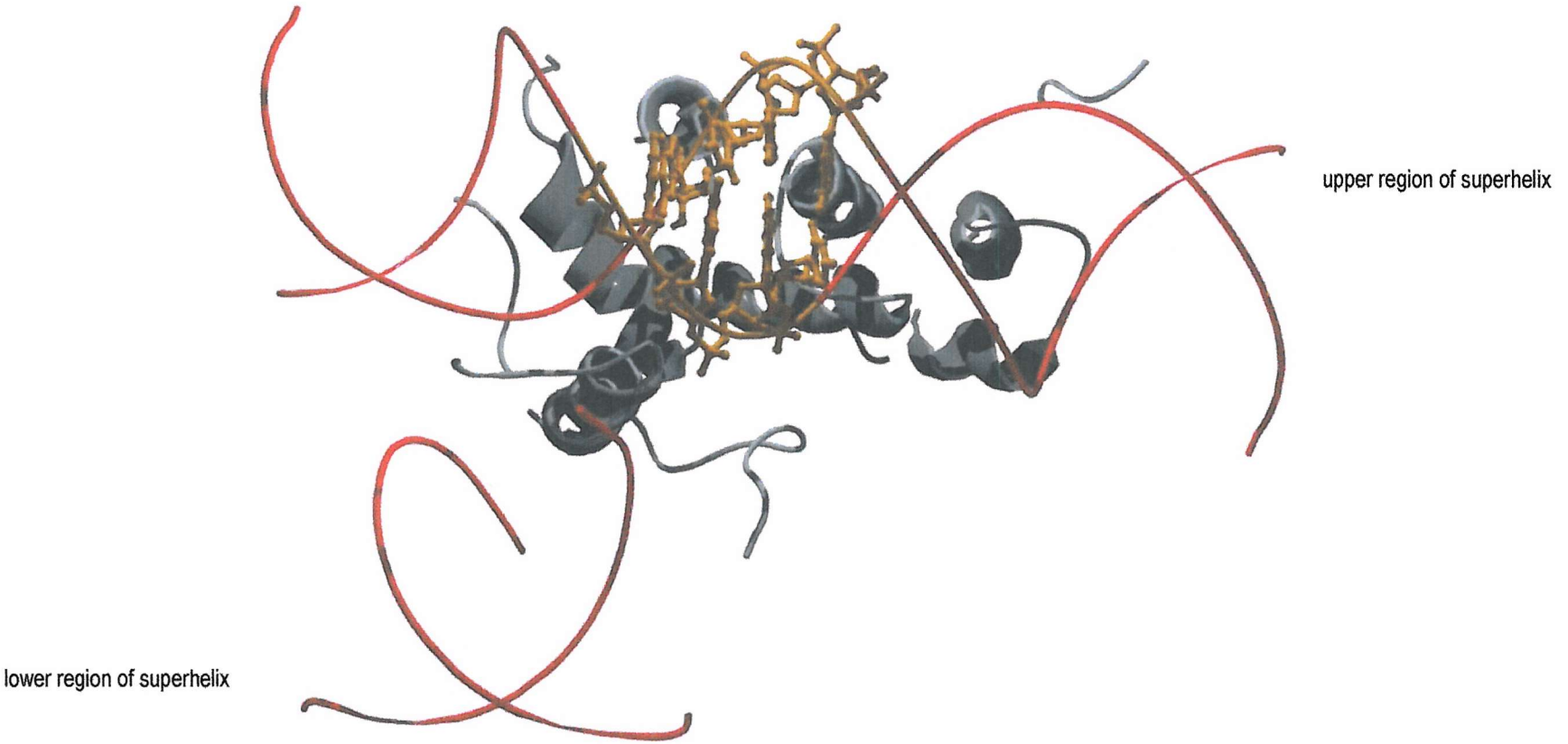

Figure 4.12 Molecular graphics of the *58h* target site. Each image shows a small portion of the nucleosome core particle. DNA strands are shown as red ribbons, the target sites are coloured orange and are presented as ribbon-ball and stick structures. A portion of the histone octamer is shown as grey ribbons for helices and strands while sheets are coloured teal. Since only a small region of the complex is presented, there appears to be two DNA helices. These actually correspond to the one helix which is wrapped around the protein complex. The upper and lower portions of the DNA superhelix are indicated. The view is looking towards the nucleosome perpendicular to the superhelix axis. Images were created in Swiss-Pdb viewer, from the pdb file submitted by Luger *et al.* 1997, and rendered in Pov-ray for Windows.

Construct *58h*

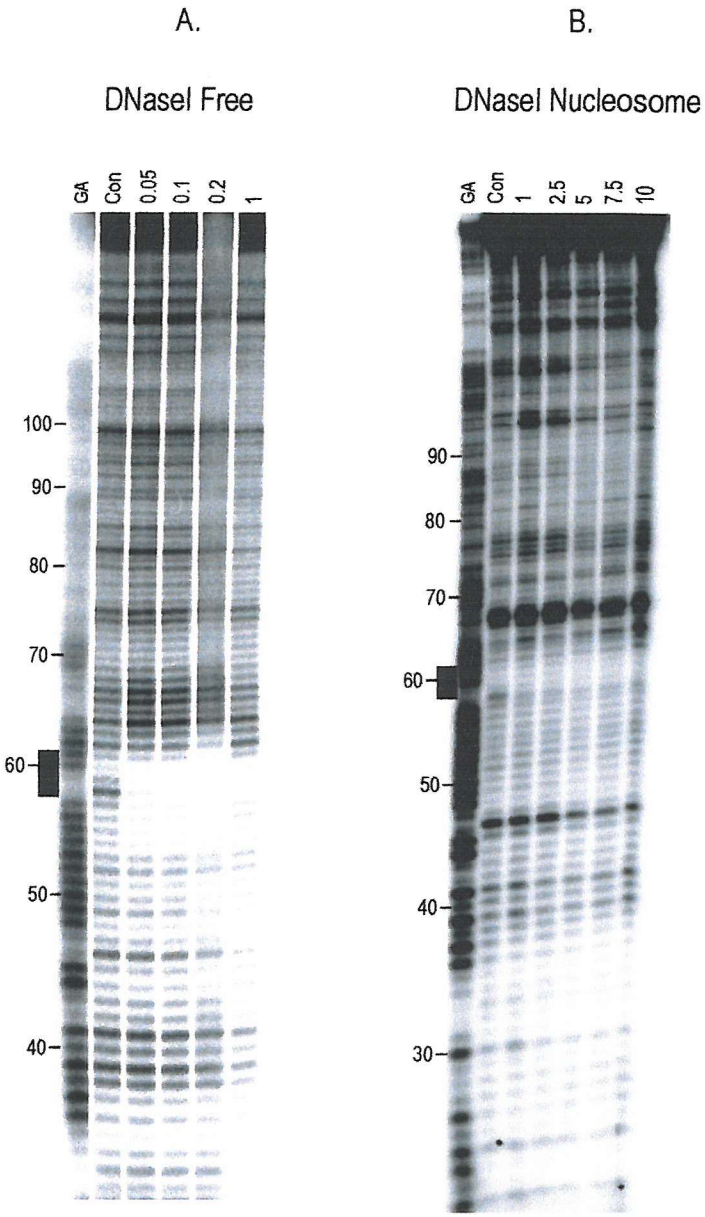

Fig 4.13 DNaseI digestion data on the interaction between echinomycin and constructs 58h .The ligand concentration is shown at the top of each lane and is expressed in μM. "Con" indicates the ligand free control digestion and "GA" are Maxam-Gilbert sequencing lanes specific for guanine and adenine. Black bars indicate the ligand target site and numbers correspond to the sequence.

Differential Cleavage of Free and Histone-Bound *58h* in the Presence of Hoechst 33258 (DNaseI)

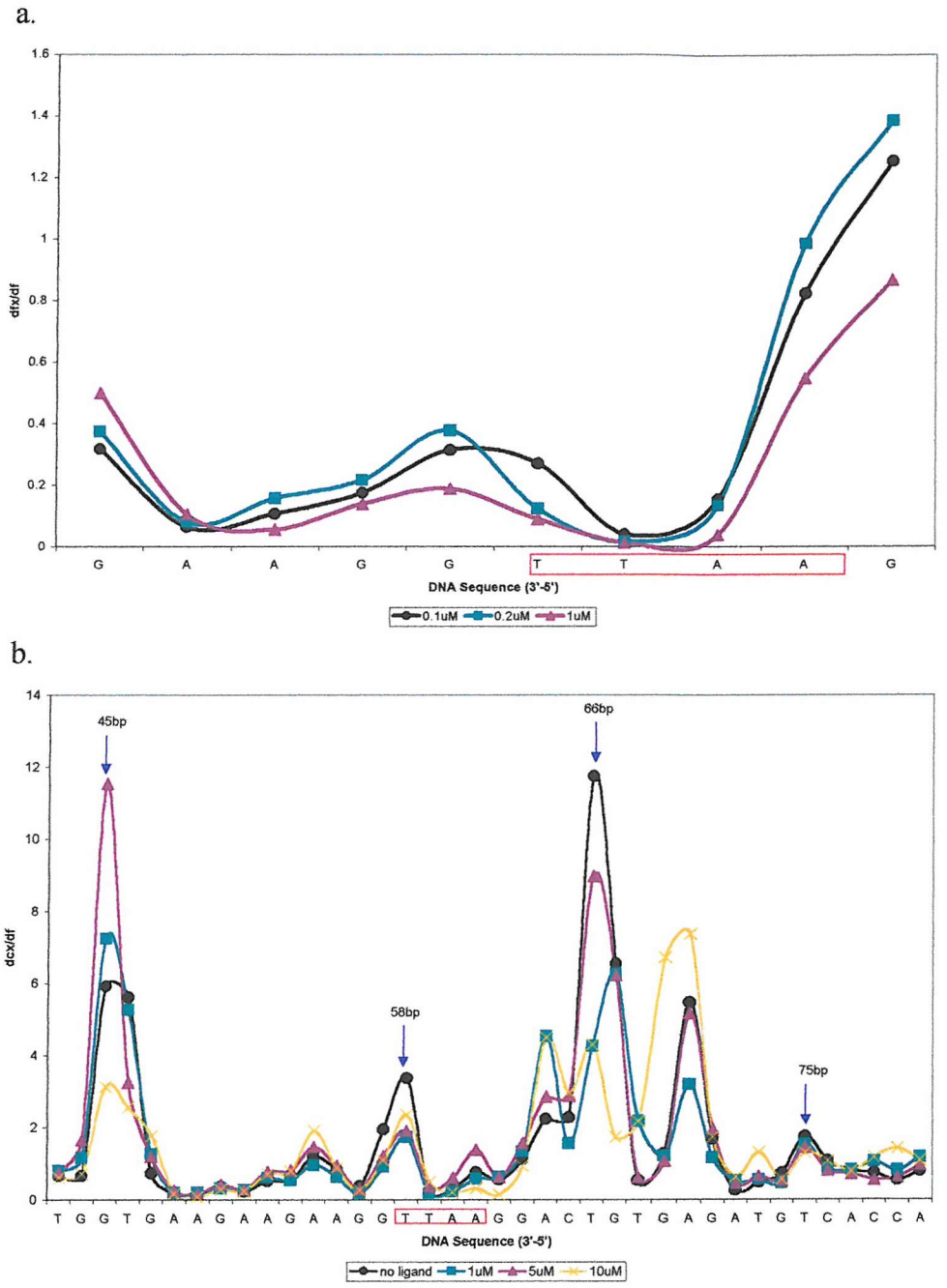

Fig 4.14 Differential cleavage across the 5'-AATT-3' target site for *58h* free (a) and histone-bound (b) DNA in the presence of Hoechst 33258 as determined by DNaseI. The DNA sequence is shown in the 3'-5' direction and the target site is indicated by a red box. Panel I, the y-axis shows the value obtained for the division of each band, from a lane where Hoechst has been added (dfx), by the exact corresponding band in the ligand free control (df). Panel II, the y-axis shows the value obtained for the division of each band in the histone-bound sample (dcx) by the corresponding band in the free DNA (df). Arrows indicate resolved cleavage maxima where the minor groove faces away from the histone core. For clarity, only three concentrations of ligand are presented in each chart.

3558h

This construct was designed to compare the interaction of Hoechst with a good site (AATT) with the minor groove facing towards the protein core, with a poorer site (TAAT) with the minor groove facing away from the protein core. This fragment is a hybrid of sites 35h and 58h. With free DNA, the drug should preferentially bind to the AATT site at position 58bp rather than the weaker ATTA at positions 35-38bp. However, the stronger site should be occluded where as the weaker site should face away from the protein. A molecular representation of this construct when bound to the histone octamer is presented in figure 4.15.

Fig 4.16a shows DNaseI digestion patterns for the binding of Hoechst to free *3558h* DNA. It can be seen that the drug interacts at the AATT site with a greater affinity than found at ATTA. Each footprint is ca.7bp in size and the differential cleavage plots confirm the binding to the correct point on the DNA sequence (fig 4.17a).

Fig 4.16b shows the interaction of Hoechst 33258 with *3558h* nucleosomes as assessed by DNaseI and a differential cleavage plot is shown in fig 4.17b. Protection from cleavage is evident across the lower site at positions 32-38bp (ATTA) with saturation observed at about 5mM ligand. Besides this, there is little difference between these results and those obtained for construct *58h*. There is no evidence for a change in the rotational position of the DNA with increasing ligand concentration. Binding to the upper target site at 58-61bp (AATT) is difficult to assess since this is in a region of poor DNaseI cleavage on account of the inward facing minor groove. However, as seen with fragment *58h* the band at position 58bp is attenuated in a manner suggesting some form of interaction. No other significant changes in the phasing-pattern are evident, even at the highest ligand concentration.

These results are confirmed by the data obtained for hydroxyl radical digestion, which are presented in fig 4.16c and d. Hydroxyl radical cleavage of free DNA also shows binding to the target sites and as can be seen binding is stronger to the upper

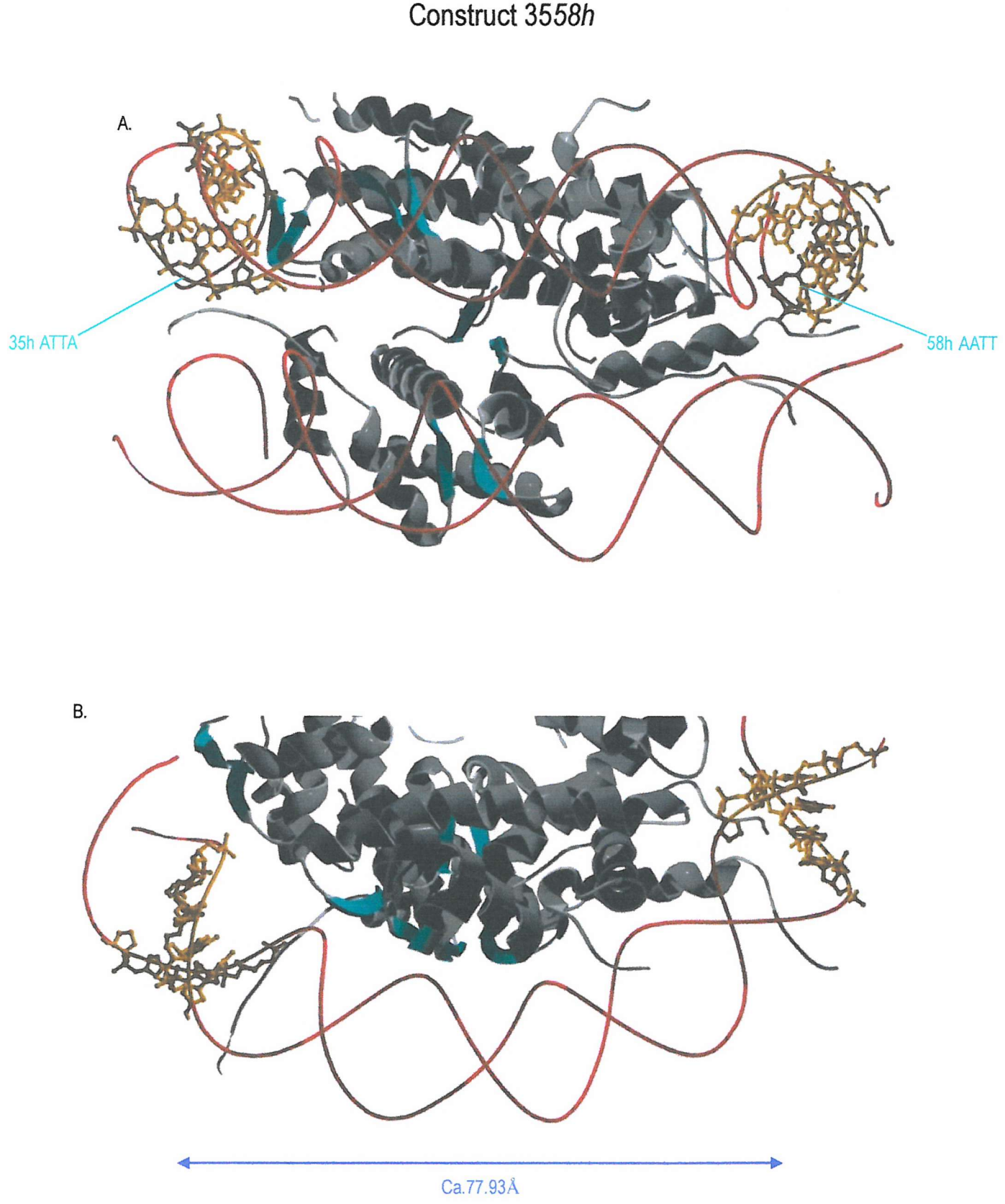

Figure 4.15 Molecular graphics of the 3558*h* target sites. Each image shows a small portion of the nucleosome core particle. DNA strands are shown as red ribbons, the target sites are coloured orange and are presented as ribbon-ball and stick structures. A portion of the histone octamer is shown as grey ribbons for helices and strands while sheets are coloured teal. Since only a small region of the complex is presented, there appears to be two DNA helices. These actually correspond to the one helix which is wrapped around the protein complex. The upper and lower portions of the DNA superhelix are indicated. (a)The view is looking towards the nucleosome perpendicular to the superhelix axis, (b) view looking along the superhelix axis from above. The lower portion of the superhelix has been omitted for clarity. Images were created in Swiss-Pdb viewer, from the pdb file submitted by Luger *et al.* 1997, and rendered in Po-ray for Windows.

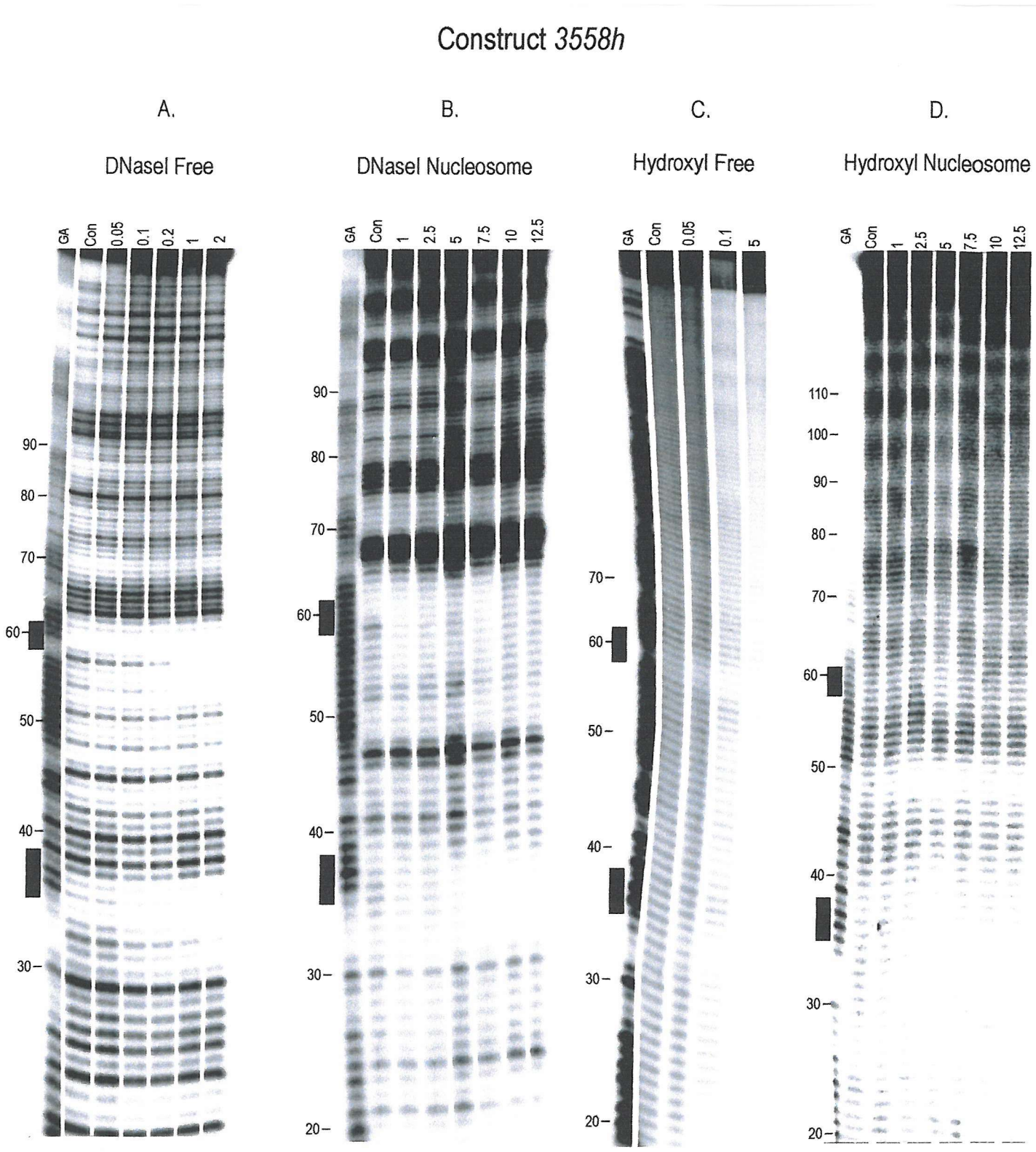

Fig 4.16 DNaseI and hydroxyl radical digestion data on the interaction between Hoechst 33258 and construct 3558*h*. The ligand concentration is shown at the top of each lane and is expressed in μM. "Con" indicates the ligand free control digestion and "GA" are Maxam-Gilbert sequencing lanes specific for guanine and adenine. Black bars indicate the ligand target site and numbers while numbers correspond to the sequence.

Differential Cleavage of Free and Histone-Bound 3558*h* in the Presence of Hoechst 33258 (DNaseI)

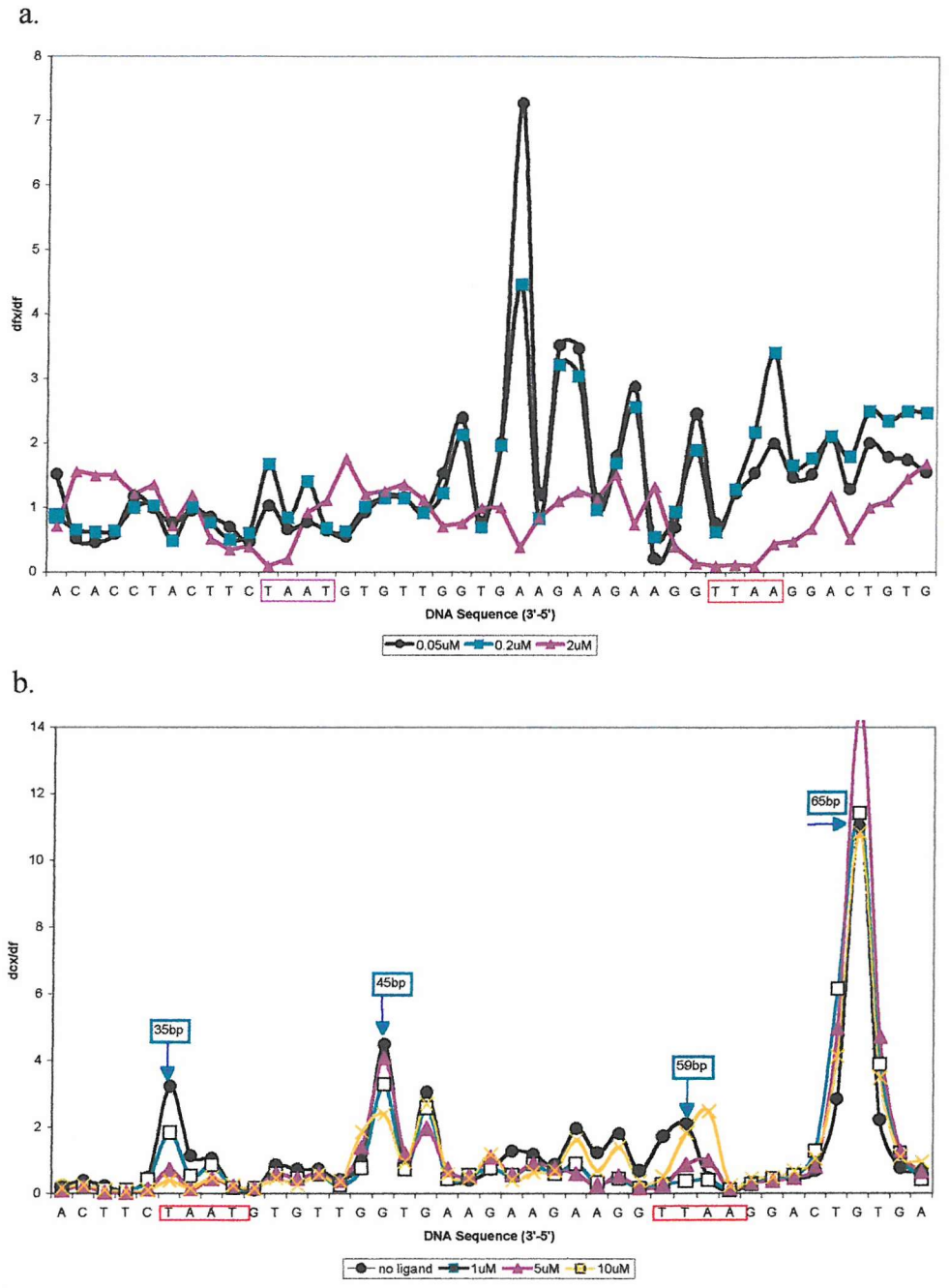

Fig 4.17 Differential cleavage across the TAAT and AATT target sites for 3558*h* free (a) and histone-bound (b) DNA in the presence of Hoechst 33258 as determined by DNaseI. The DNA sequence is shown in the 3'-5' direction and the target site is indicated by a red box. (a), the y-axis shows the value obtained for the division of each band, from a lane where Hoechst has been added (dfx), by the exact corresponding band in the ligand free control (df). (b), the y-axis shows the value obtained for the division of each band in the histone-bound sample (dcx) by the corresponding band in the free DNA (df). Arrows indicate resolved cleavage maxima where the minor groove faces away from the histone core. For clarity, only three concentrations of ligand are presented in each chart.

Differential Cleavage of Free and Histone-Bound *3558h* in the Presence of Hoechst 33258 (hydroxyl radicals)

a.

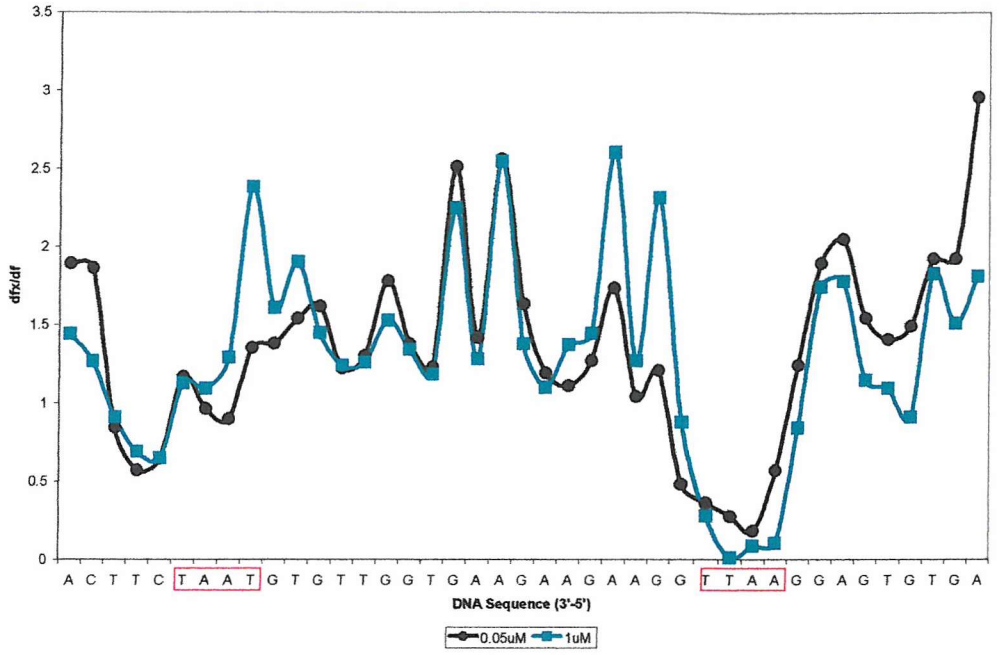

b.

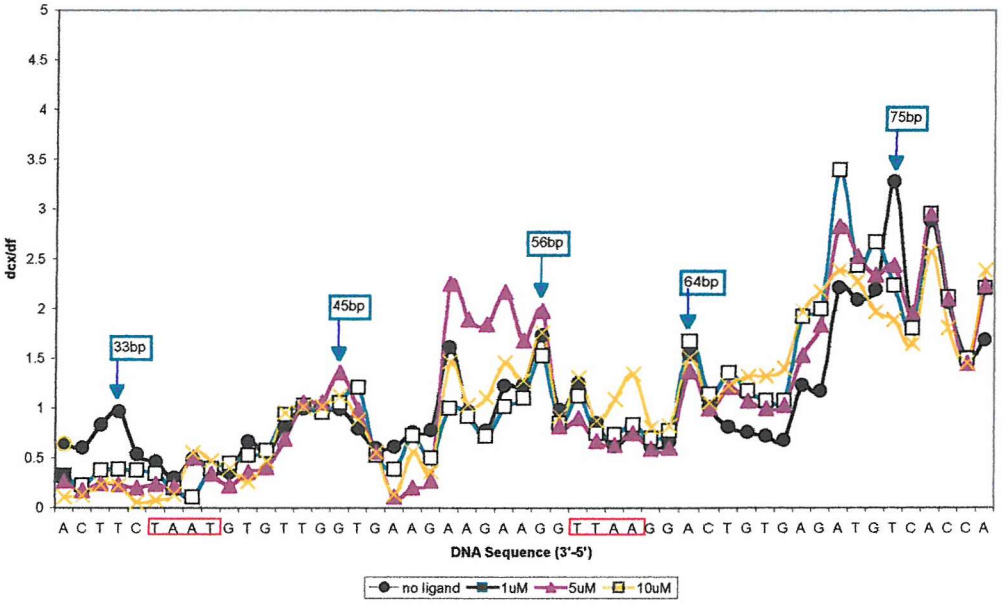

Fig 4.18 Differential cleavage across the ATTA and AATT target sites for *3558h* free (a) and histone-bound (b) DNA in the presence of Hoechst 33258 as determined by hydroxyl radicals. The DNA sequence is shown in the 3'-5' direction and the target site is indicated by a red box. (a), the y-axis shows the value obtained for the division of each band, from a lane where Hoechst has been added (dfx), by the exact corresponding band in the ligand free control (df). (b), the y-axis shows the value obtained for the division of each band in the histone-bound sample (dcx) by the corresponding band in the free DNA (df). Arrows indicate resolved cleavage maxima where the minor groove faces away from the histone core. For clarity, only three concentrations of ligand are presented in each chart.

AATT site than the lower affinity ATTA site. Differential cleavage plots show that each site is saturated by 1:M ligand, with this probe, and each footprint is roughly 4-5bp is size (fig 4.18a).

From the hydroxyl digested core DNA cleavage maxima are identified at positions 33, 45, 56, 64 and 75bp which confirms the rotational setting of each target and can be seen in the differential cleavage plot in figure 4.18d. The weaker site (ATTA) is found on the outer surface while the stronger site (AATT) is found facing the histone octamer. With increasing drug concentration there is a clear interaction across the lower target site. There is no evidence for binding across the AATT step at positions 58-61bp and with 10:M Hoechst there is some degradation in the phasing pattern, which is probably due to non-specific binding of the drug to the DNA superhelix. Most importantly, as with the DNaseI results, there is no change in the rotational position of the DNA superhelix with increasing ligand concentration. These results suggest that Hoechst binds much better to the outward facing ATTA than the inward facing AATT.

73h

Construct *73h* was designed so that a site would be placed at an inward facing minor groove close to the dyad. The sequence of *73h* is shown in fig 4.1 and contains a good Hoechst, AATT, at positions 73-76bp. This site is also flanked by one adenine on each side, generating the site TAATTT. Therefore there is a weak ATTA site covering positions 72-75bp and a TAAA site at positions 74-77bp. Based on previous studies the order of binding is expected to be AATT>TAAA>ATTA. A molecular representation of the site is presented in figure 4.19 and shows that the target is expected to face towards the histone core.

The DNaseI results for this construct are presented in fig 4.20. 4.20a, which shows binding to free DNA confirms the interaction of Hoechst with this target site and shows that the footprint is complete. The differential cleavage plots show that with

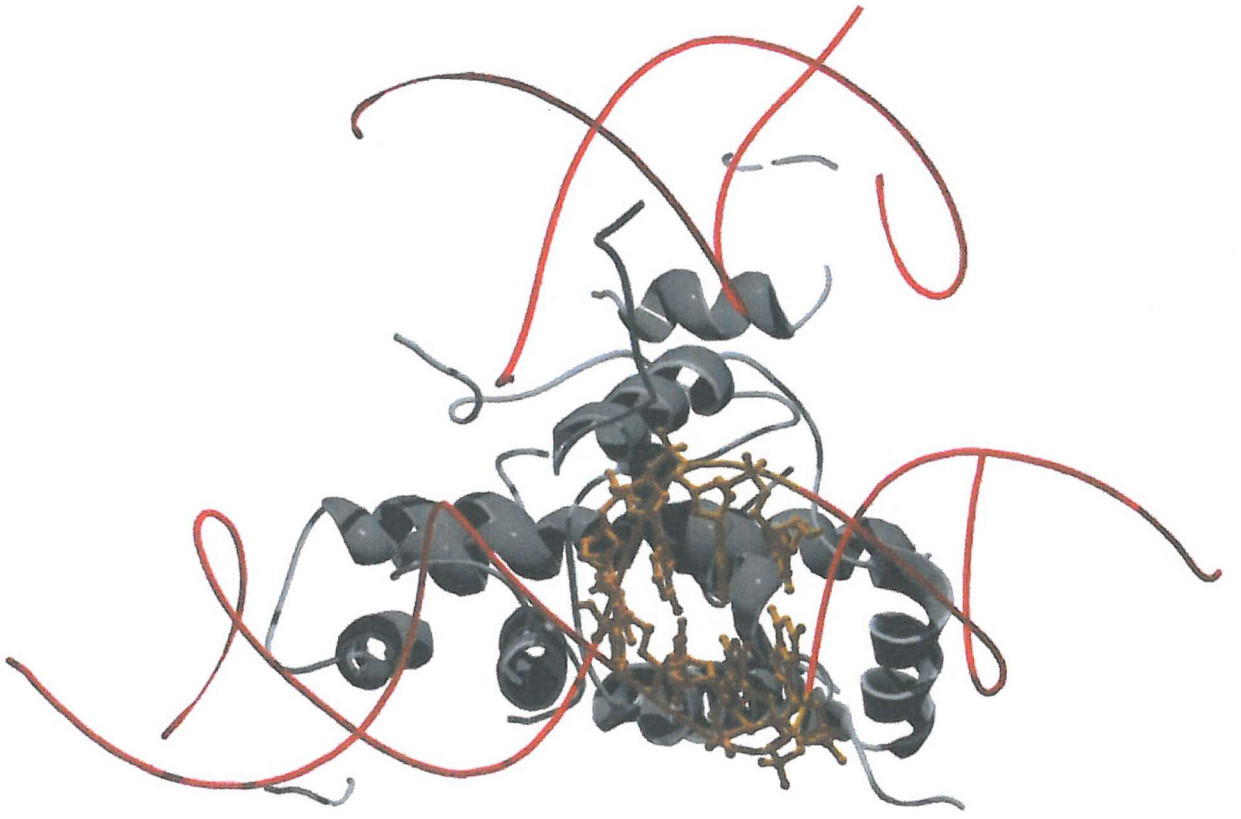

Figure 4.19 Molecular graphics of the *73h* and 74*e* target sites. Each image shows a small portion of the nucleosome core particle. DNA strands are shown as red ribbons, the target sites are coloured orange and are presented as ribbon-ball and stick structures. A portion of the histone octamer is shown as grey ribbons. Since only a small region of the complex is presented, there appears to be two DNA helices. These actually correspond to the one helix which is wraps around the protein complex. The upper and lower portions of the DNA superhelix are indicated. The view is looking towards the nuclesome perpendicular to the superhelix axis. Images were created in Swiss-Pdb viewer, from the pdb file submitted by Luger *et al.* 1997, and rendered in Pov-ray for Windows.

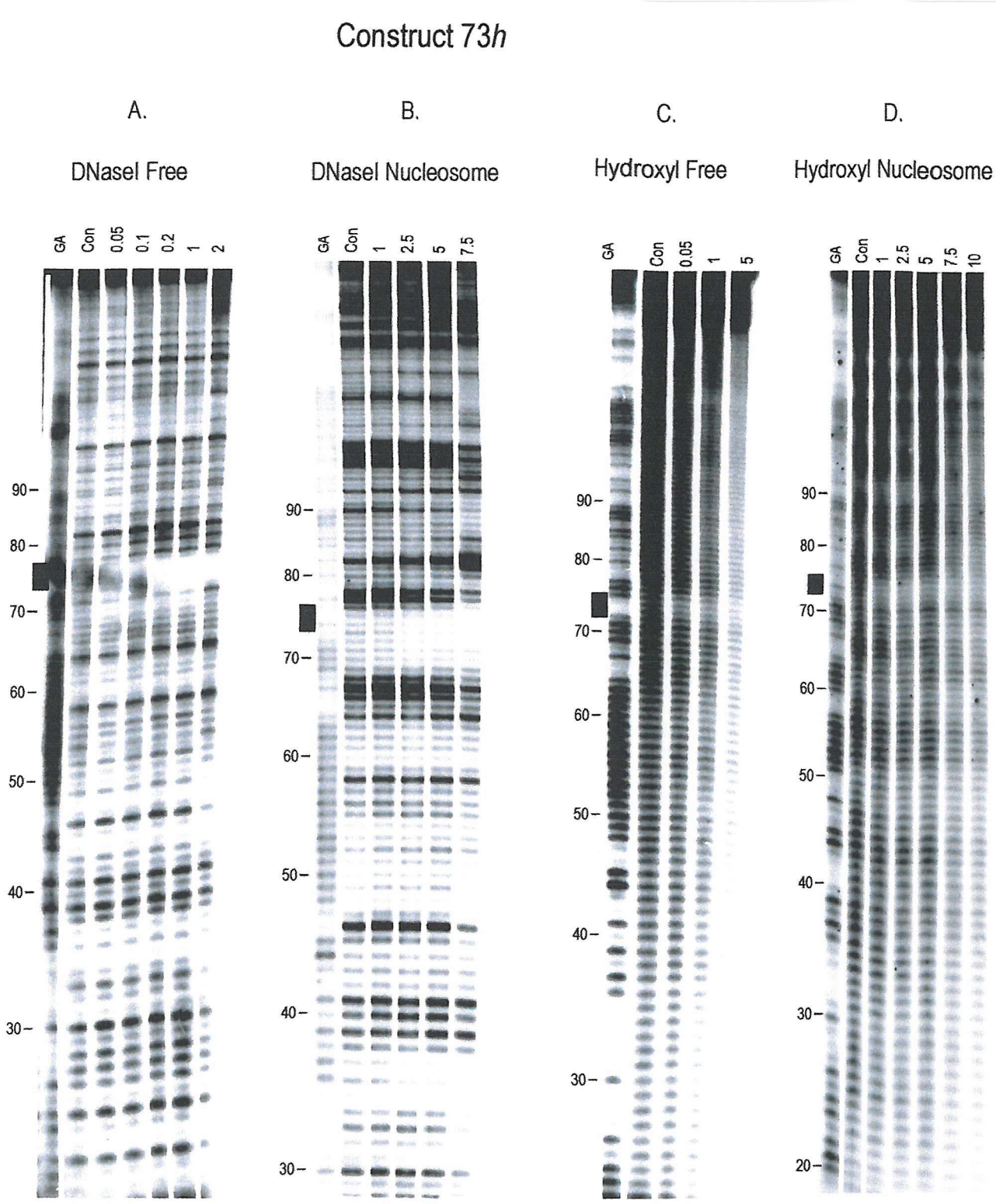

Figure 4.20 DNaseI and hydroxyl radical digestion data on the interaction between Hoechst 33258 and construct 73*h*. The ligand concentration is shown at the top of each lane and is expressed in μM. "Con" indicates the ligand free control digestion and "GA" are Maxam-Gilbert sequencing lanes specific for guanine and adenine. Black bars indicate the ligand target sites while numbers correspond to the sequence.

Differential Cleavage of Free and Histone-Bound *73h* in the Presence of Hoechst 33258 (DNaseI)

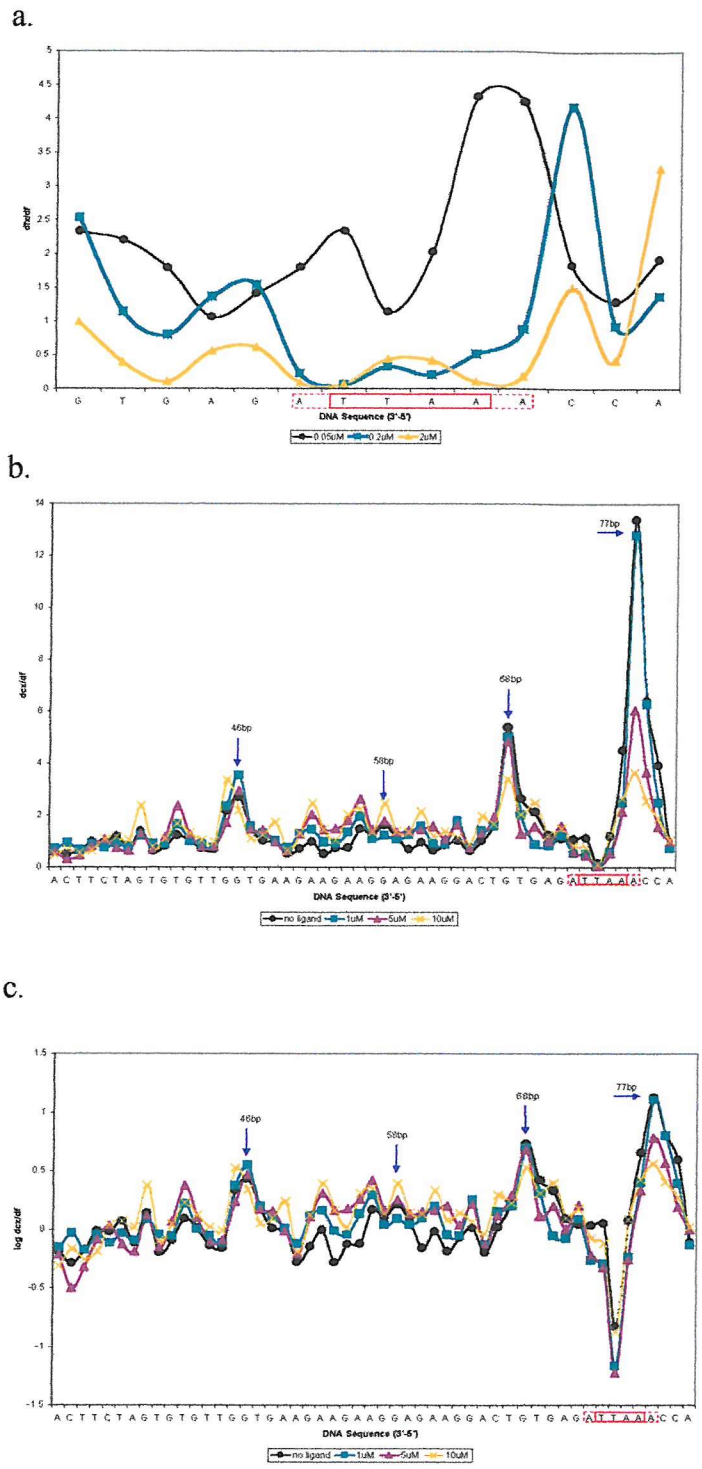

Fig 4.21 Differential cleavage across the 5'-AATT-3' target site for *73h* free (a) and histone-bound (b and c) DNA in the presence of Hoechst 33258 as determined by DNaseI. The DNA sequence is shown in the 3'-5' direction and the target site is indicated by a red box. (a), the y-axis shows the value obtained for the division of each band, from a lane where Hoechst has been added (dfx), by the exact corresponding band in the ligand free control (df). (b), the y-axis shows the value obtained for the division of each band in the histone-bound sample (dcx) by the corresponding band in the free DNA (df). (c), data from (b) presented on a logarithmic scale. Arrows indicate resolved cleavage maxima where the minor groove faces away from the histone core. For clarity, only three concentrations of ligand are presented in each chart.

Differential Cleavage of Free and Histone-Bound *73h* in the Presence of Hoechst 33258 (hydroxyls)

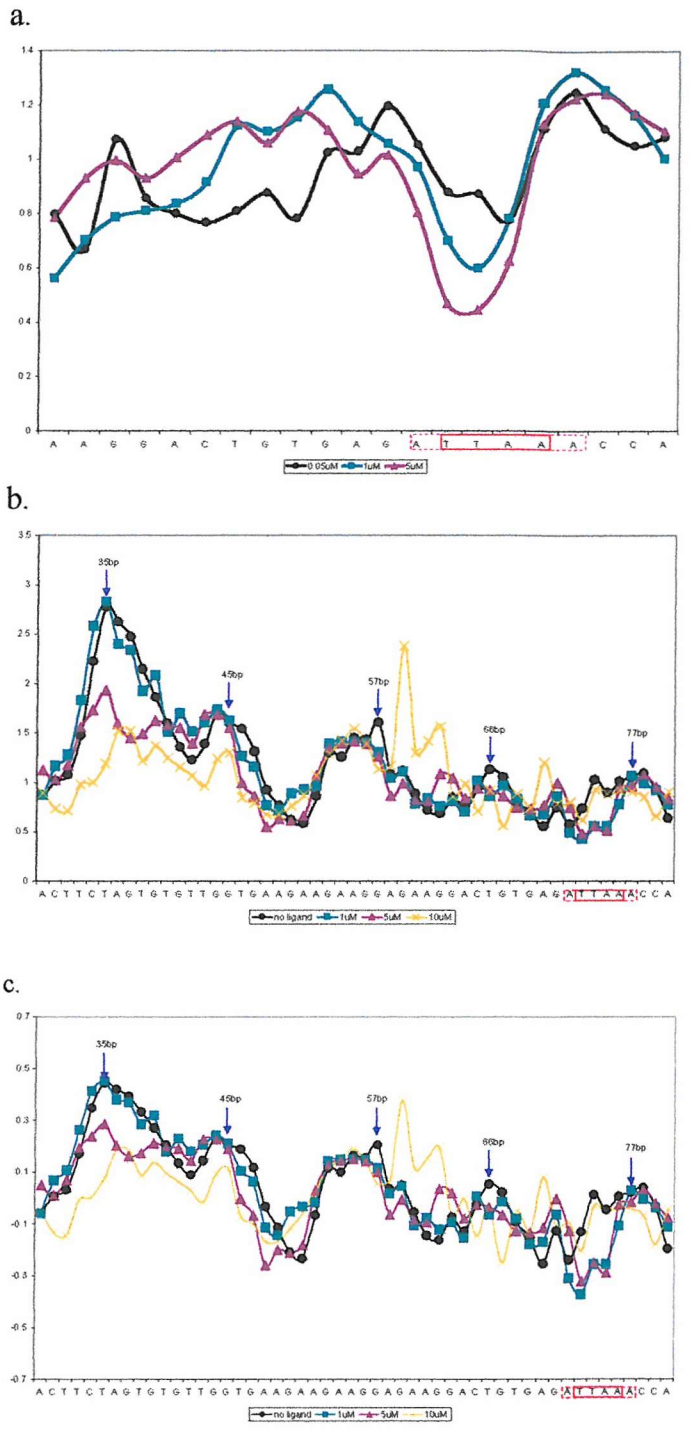

Fig 4.22 Differential cleavage across the 5'-AATT-3' target site for *73h* free (a) and histone-bound (b and c) DNA in the presence of Hoechst 33258 as determined by hydroxyl radicals. The DNA sequence is shown in the 3'-5' direction and the target site is indicated by a red box. (a), the y-axis shows the value obtained for the division of each band, from a lane where Hoechst has been added (dfx), by the exact corresponding band in the ligand free control (df). (b), the y-axis shows the value obtained for the division of each band in the histone-bound sample (dcx) by the corresponding band in the free DNA (df). (c), data from (b) presented as on a logarithmic scale. Arrows indicate resolved cleavage maxima where the minor groove faces away from the histone core. For clarity, only three concentrations of ligand are presented in each chart.

0.2μM ligand, the footprint covers 6bp and corresponds to interaction with AATT (fig 4.21). With 2μM Hoechst attenuated cleavage extends into sequences flanking the AATT site and presumably reflects secondary binding of the molecule to ATTA and AAAT.

DNaseI footprints for assessing the interaction of Hoechst with histone-bound *73h* are presented in 4.20b and analysis of these results in fig 4.21b. Identified cleavage maxima for the histone-bound DNA are found at positions 46, 58, 67 and 77bp. The gel shows a clear footprint across the target site and this is confirmed in the analysis. Binding is apparent at 5μM as judged by attenuation in the cleavage maxima at position 77bp. From these data, it appears that Hoechst binds to the target site although it is noted that part of this binding site may be exposed. However, unlike the other constructs presented so far, it is clear that there are many other substantial changes in the cleavage pattern in the presence of ligand. Further attenuation in DNaseI cleavage is found at positions 46-47, 67-68, 90, and 97-100bp while enhancements are observed at positions 81-83, 95 and 106bp. In fact, at this concentration it appears that there is a removal of the nucleosome-phasing pattern. Since this was not observed with any of the other constructs it is unlikely to be a result of type II non-specific binding of the ligand, and must be a direct result of the interaction of the ligand with this binding site.

Results of hydroxyl radical digestion of free *73h* in the presence of Hoechst 33258 are presented in fig 4.20c. A clear footprint can be seen at the ligand target site and binding is confirmed in the data analysis, fig 4.22a. It should also be noted that this region shows attenuated cleavage compared to the remainder of the fragment in the drug-free control. This region corresponds to 6bp of A/T DNA and this attenuation most probably reflects a reduction in minor groove width. Addition of Hoechst further reduces the cleavage in this region. However, these results confirm the binding of Hoechst to the target and the location of the footprint suggests that the AATT step is the preferred site over the other potential binding sites.

The results for the interaction of the ligand with histone-bound *73h* are presented in fig 4.20d. From the gel it is difficult to see any clear interaction across the target site. However, with increasing Hoechst concentration there is a dramatic loss in the nucleosome-phasing pattern, which is more pronounced that seen in the DNaseI results. Differential cleavage plots of these results are presented, fig 4.22b-c and confirm the loss of phasing. Cleavage maxima in the absence of ligand are the same as those obtained for all other constructs and are found at positions 35, 45, 57, 66 and 77bp.

The data suggest the presence of a footprint across the AATT site up to 5μM though this is complicated by the observation that the drug binding site coincides with a region of attenuated cleavage However, even by this concentration the phased cleavage pattern is lessened, especially towards the ends of the fragment. When the concentration is raised to 10μM the pattern becomes much less clear and the footprint across the target site is lost. It therefore appears that the interaction of Hoechst with this binding site, close to the dyad, causes a disruption of the nucleosome structure.

Discussion

The results presented in this chapter show little interaction of echinomycin and Hoechst with nucleosomes containing unique single target sites which face towards the protein core. A few very small changes in DNaseI digestion, in the presence of echinomycin ligand concentrations, are observed.

The interaction of echinomycin with the inner surface of the DNA superhelix

From the results presented in this chapter it appears that single molecules of echinomycin do not alter the rotational position of the DNA superhelix of the nucleosome-bound DNA. Some minor changes in cleavage are observed, for

example with construct 39e across positions 31-34bp, which is also present in the free DNA and is a drug specific enhancement, and therefore represents an alteration in the structure of the DNA when the ligand binds. It is suggested that these enhancements represent background binding to free DNA, which is present as a small proportion in the nucleosome samples. Since there is no obvious alteration in the nucleosome phasing pattern we assume that in the most part, echinomycin has not bound to the target sites in this series of experiments. Most importantly, there is no change in the rotational setting of these samples.

The role of Hoechst on the inner surface

The results indicate that there is no significant interaction of a single Hoechst molecule with the inner surface of the DNA superhelix with constructs *3558h* and *58h* where little interaction was observed across the 58-61bp AATT site. The fact that a footprint is observed across the 35-38bp ATTA site confirms that the rotational position of these nucleosomes has not changed. Since both DNaseI and hydroxyl radical cleavage data show no obvious changes in the DNA structure of the superhelix, it is concluded that the drug simply does not bind to the inner facing target site. However, the loss of the band at position 58 could indicate some kind of weak interaction between the drug and the DNA.

With construct *73h* there were significant changes in the cleavage patterns with both DNaseI and hydroxyl radicals. These data suggest that binding near to the nucleosome dyad has profound consequences up on the structure of the particle. It appears that binding to this region causes a loss in phasing pattern, which is ultimately translated as a displacement of the DNA superhelix from the histone octamer. This suggests that this region of the DNA superhelix is extremely sensitive to ligand binding. In addition, as demonstrated in chapter 6, ligand binding to this region also disrupts nucleosome formation. Since this site is inner facing we might expect some unfavourable interactions to occur between the bound drug and the surface of the histone octamer. In addition, it is surprising that the binding of a single Hoechst molecule, at this position, has such profound consequences upon the

conformation of the core particle. In relation to the site exposure model (Polach and Widom 1995; Polach and Widom 1996; Widom 1998; Anderson and Widom 2000; Polach *et al* 2000) we would expect this area of the superhelix to be exposed much less often and therefore the ligand occupancy at this position should be low, further demonstrating the sensitivity of this region. However, the hydroxyl radical and DNaseI data suggest that the last A-T step (position 76) in the target is exposed and that an additional A-T step (position 77) from the parent fragment is located right on the point of cleavage maxima. Alternatively, may be that the ligand, in addition to binding the TTAA site with low occupancy, is also binding the overlapping 3'-TAAA-5' across positions 74-77bp which may now become more favourable. Since this is still very close to the interface between the DNA and protein, unfavourable interactions between the ligand and histone octamer may still occur leading to disruption in the complex. Such a mechanism would provide a route to drug binding across this region of the DNA superhelix without having to wait on full site exposure.

5 The Interaction of Hoechst and Echinomycin with more than One Target Site on the Inner Surface of the Nucleosome Core Particle

Introduction

The results presented in chapter 4 demonstrate that Hoechst and echinomycin do not bind to single inward facing targets and that they have little effect on the conformation and orientation of DNA on the protein surface. This chapter considers the interaction of these ligands with two and three closely spaced inward facing sites.

The results presented in chapter 3 showed that Hoechst can bind to the outer surface of the nucleosome without affecting the rotational position of the DNA, while little interaction is observed between echinomycin and single outward facing sites. However, it has been suggested that superhelix rotation may occur upon the binding of two or more ligand molecules on the outer DNA surface (Portugal & Waring, 1986). The action of two and three ligands on the inner surface of the superhelix was therefore explored. Six constructs were made for this purpose: *4958h* was used to study the binding of two Hoechst molecules and H3 was used to study the interaction with three Hoechst molecules. *2030e*, *3950e*, and *7080e* were used to study the binding of two molecules of echinomycin while E3 was utilised to study the interaction of three echinomycin molecules with the inner surface of the DNA superhelix.

Results

The sequences of the constructs used in this chapter are shown in fig 5.1. Construct *4958h* contains two good Hoechst binding sites (5'-AATT-3'). There are 5 base pairs between the end of one site and the beginning of the second and over this region the minor groove turns away from the protein core towards solution. The first target site

Fig 5.1 sequences of constructs *4958h, H3, 2030e, 3950e, 7080e* and *E3*. The *tem* construct is shown in the center. Expanded regions show where each mutation was introduced and the target sequence of each construct is indicated. These coloured targets are the only difference between the ligand construct and the parent sequence *tem*.

covers positions 49-52bp and the second target covers positions 58-61bp therefore both of these targets should also lie on the inner surface of the superhelix and should not be easily accessible to the ligand. Construct H3 contains the same binding sites as found in *4958h* with an additional 5'-AAAA-3' site across positions 40-43bp where the minor groove faces the protein core.

Construct *2030e* contains two 5'-ACGT-3' targets. The first one covers base pairs 19-22, with the CG step at 20 and 21bp, while the second target covers base pairs 29-32, with the CG step at 30 and 31bp. Therefore the separation between each drug site is 6bp. This fragment allows us to assess the binding of two echinomycin molecules, to inward facing target sites, close to the end of the superhelix. The next construct *3950e* was a hybrid of sequences *39e* and *50e*. This provided two inward facing 5'-ACGT-3' target sites located at the approximate centre of the bound DNA on one symmetrical face of the nucleosome. The first sites covers base pairs 38-41 and the second site is across base pairs 49-52. The CG steps are at positions 39-40 and 50-51 base pairs respectively. These sites are separated by 8bp. Construct *7080e* was designed so as to study the interaction across the inner facing minor grooves close to the nucleosomal dyad axis. This also contains two 5'-ACGT-3' target sites covering positions 69-72 and 79-82bp with CpG steps at positions 70-71 and 80-81bp. These sites are separated by 6bp where the minor groove turns out to face solution. The final construct, E3 contained the same ACGT sites as found in *3950e* with an additional site across positions 58-61bp, so that the CG step covers positions 59 and 60bp.

Hoechst 33258

4958h

A visual representation of each target in this construct as it is orientated on the core particle is presented in fig 5.2 and, as can be seen, each site should be positioned in a region where the minor groove faces the protein core and the spatial separation between the centre of each target is approximately 37Δ across the curve of the DNA

Construct *4958h*

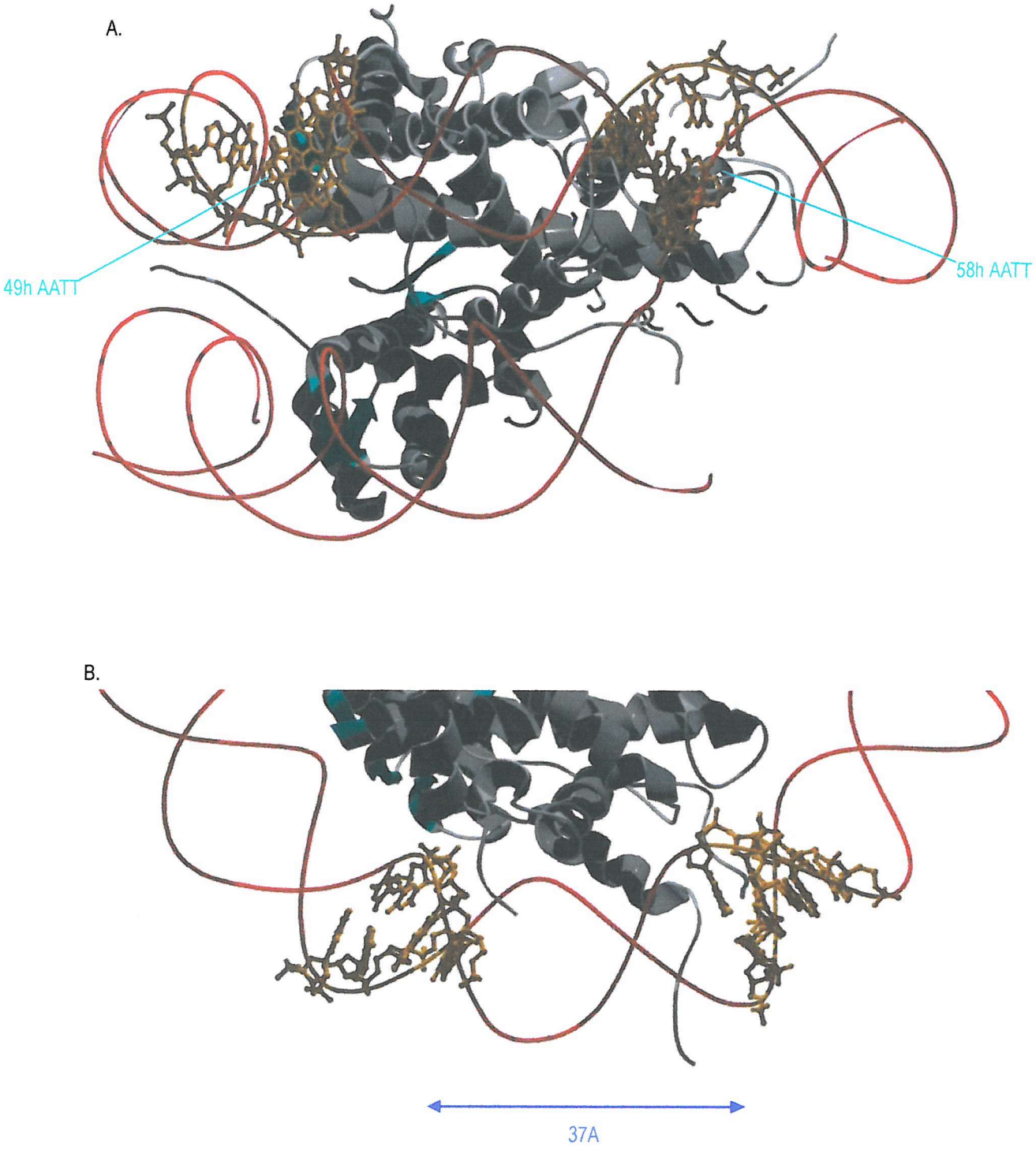

Figure 5.2 Molecular graphics of the 4958h target sites. Each image shows a small portion of the nucleosome core particle. DNA strands are shown as red ribbons, the target sites are coloured orange and are presented as ribbon-ball and stick structures. A portion of the histone octamer is shown as grey ribbons for helices and strands while sheets are coloured teal. Since only a small region of the complex is presented, there appears to be two DNA helices. These actually correspond to the one helix which is wrapped around the protein complex. (a)The view is looking towards the nucleosome perpendicular to the superhelix axis, (b) view looking along the superhelix axis from above. The lower portion of the superhelix has been omitted for clarity. Images were created in Swiss-Pdb viewer, from the pdb file submitted by Luger *et al.* 1997, and rendered in Po-ray for Windows.

superhelix.

DNaseI footprinting results for the interaction of Hoechst 33258 with free *4958h* DNA are presented in fig 5.3a and analysis are shown in fig 5.4a. This confirms binding of the ligand to the engineered target sites. Interaction with each site is clearly observed at 0.2μM. As a consequence of the size of DNaseI the two footprints almost coalesce into a single footprint, and are separated by a single (weak) cleavage product at position 53. At the high concentration of 5μM there is further attenuation of DNaseI cleavage products throughout the construct sequence, which is attributed to type II binding of the ligand.

The results of DNaseI cleavage for the interaction of Hoechst 33258 with histone-bound *4958h* are presented in fig 5.3b and data analysis is shown in fig 5.4b. Cleavage maxima in the ligand free control are found at 37, 46, 56, 67, 76 and visual inspection of the gel indicates further maxima around positions 87, 97-99 and 108bp. This is the same rotational position, which is observed for other constructs and is identical to the parent sequence *tem*. This confirms that the intended target sites are positioned on the inner side of the superhelix. Notice that the target sites therefore lie in a region where the DNA is cut poorly, corresponding to a region where the minor groove is facing the protein core.

As the concentration of Hoechst is increased towards 10μM there are some clear changes in the cleavage pattern throughout the sequence. DNaseI cleavage products are attenuated at positions 25, 36-39 49-52, 57-60, 78, 87-89, 97-99, and 108bp which correspond to the cleavage maxima in the ligand free control while other regions of enhanced cleavage are observed at positions 102-105, 92-94, 84, 74, 63, 53 43-44 and 28. These changes in digestion products cannot be directly attributed to drug binding and so must represent changes in the interaction of the DNA with the protein surface. These points of enhancement lie almost halfway between the original nucleosome peaks and are observed at 7.5-10μM ligand concentration. The attenuations at positions 49-52 and 57-60bp may correspond to ligand footprints and

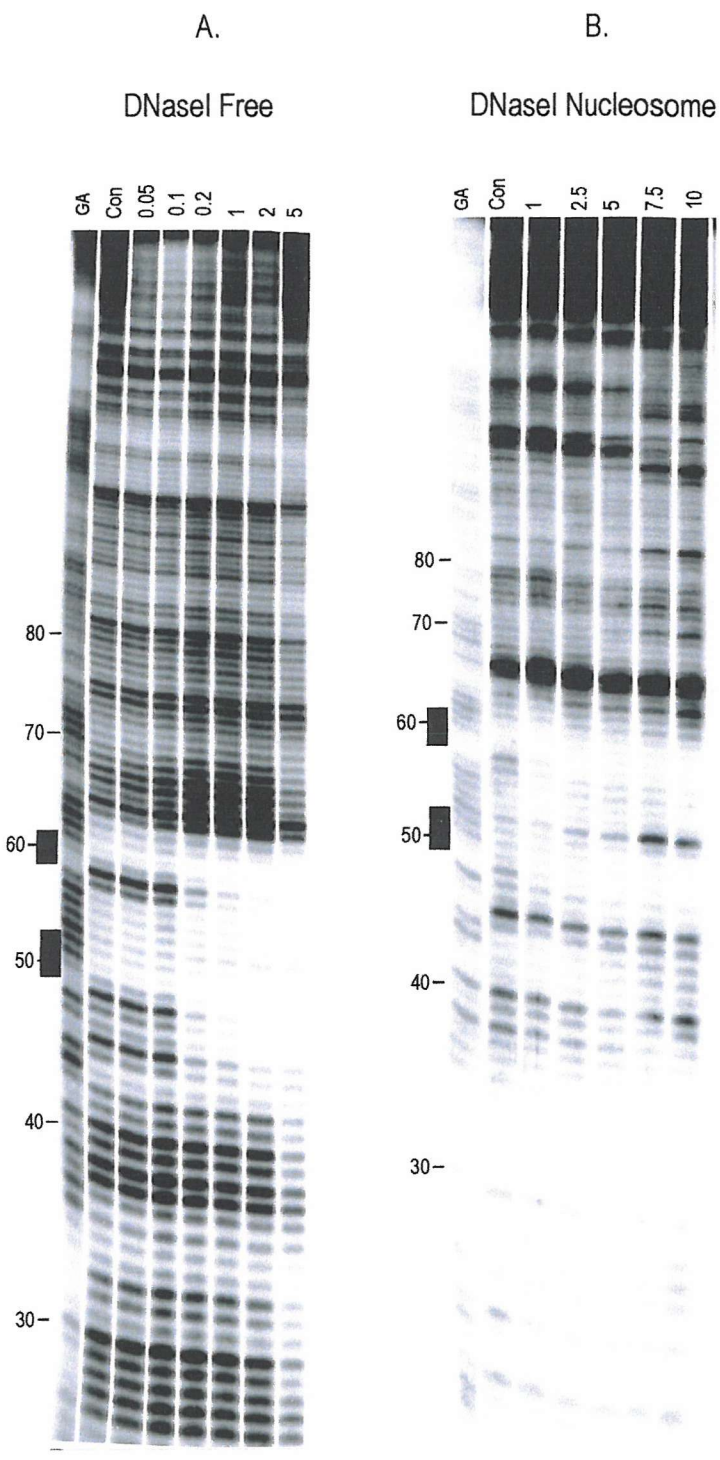

Fig 5.3 DNaseI and hydroxyl radical digestion data on the interaction between Hoechst 33258 and construct 4958*h*. The ligand concentration is shown at the top of each lane and is expressed in μM. "Con" indicates the ligand free control digestion and "GA" are Maxam-Gilbert sequencing lanes specific for guanine and adenine. Black bars indicate the ligand target site and numbers while numbers correspond to the sequence.

Differential Cleavage of Free and Histone-Bound 4958*h* in the Presence of Hoechst 33258 (DNaseI)

a.

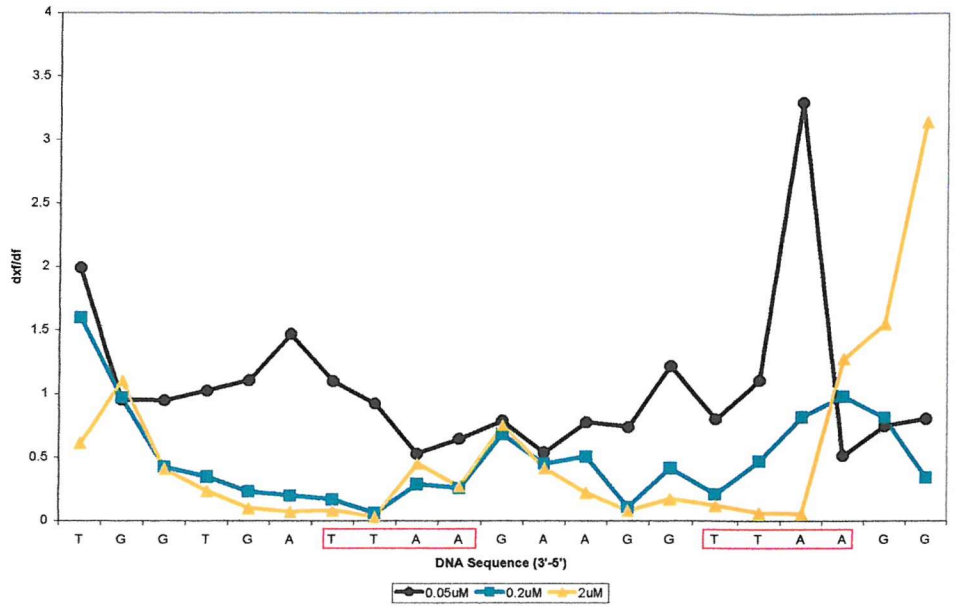

b.

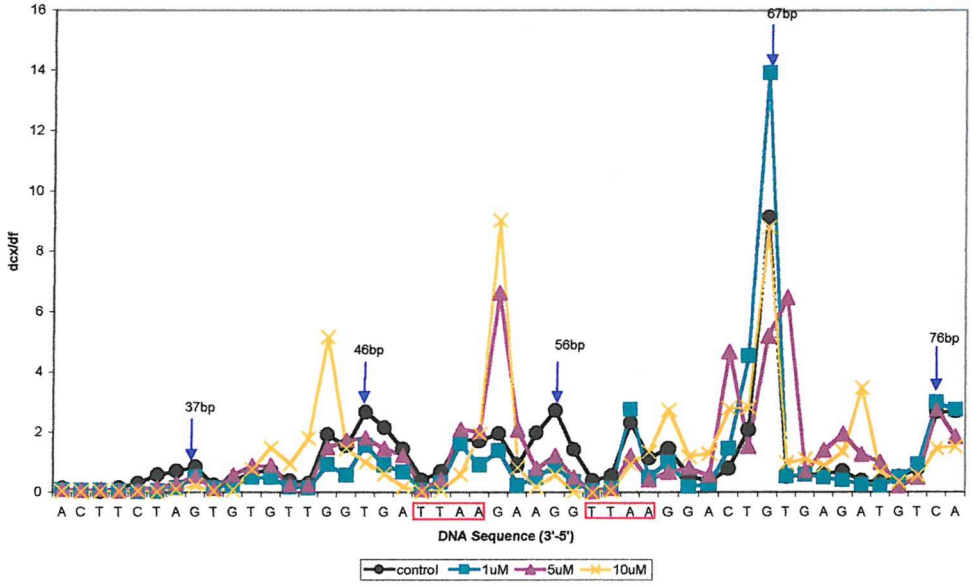

Fig 5.4 Differential cleavage across the AATT target sites for *4958h* free (a) and histone-bound (b) DNA in the presence of Hoechst 33258 as determined by DNaseI. The DNA sequence is shown in the 3'-5' direction and the target site is indicated by a red box. (a), the y-axis shows the value obtained for the division of each band, from a lane where Hoechst has been added (dfx), by the exact corresponding band in the ligand free control (df). (b), the y-axis shows the value obtained for the division of each band in the histone-bound sample (dcx) by the corresponding band in the free DNA (df). Arrows indicate resolved cleavage maxima where the minor groove faces away from the histone core. For clarity, only three concentrations of ligand are presented in each chart.

a strong enhancement is also found between the target sites at position 53.

Quantitive analysis of the histone-bound cleavage patterns is presented in fig 5.4b confirming the new peaks in the ligand treated samples. Overall there is an average movement of cleavage maxima by approximately 3.5bp deduced from the data between positions 30-80bp of the fragment. For example, the original peak at position 46 appears to have "moved" to position 44 with 10:M ligand, this is clearly indicated in fig 5.4b. The next outer facing minor groove was identified at position 56bp, but with the addition of Hoechst this also appears to have moved, this time to position 53bp. In both cases there is a corresponding attenuation across the region originally identified as a cleavage maxima in the ligand free control. However, this pattern is not repeated, to the same extent, at the next two outer facing minor grooves. In this case, there is the appearance of a new peak positions 62bp and 72bp but the original peaks at positions 67bp and 76bp are maintained. From the results of *4958h* it appears that, on average, there has been a shift in cleavage maxima by 3.5bp, the implications of which are discussed at the end of the chapter.

H3

The next step in this series of experiments was to add an additional Hoechst site to see whether this would alter the digestion pattern observed in *4958h* any further. This was carried out with construct H3 where the additional site is located across positions 40-43bp and is in the form AAAA. A representation of this construct bound as a nucleosome core particle is presented in fig 5.5. The spatial separation between each site is 31Δ between AAAA (40-43bp) and AATT (49-52bp) and 37Δ between AATT (49-52bp) and AATT (58-61bp).

DNaseI footprinting results for the interaction of Hoechst 33258 with free *H3* DNA are presented in fig 5.6a and analysis is shown in fig 5.7a. Binding of the ligand to the engineered target sites is confirmed although the interaction with AAAA appears weaker than with AATT. Complete saturation of all sites is evident at 2:M Hoechst.

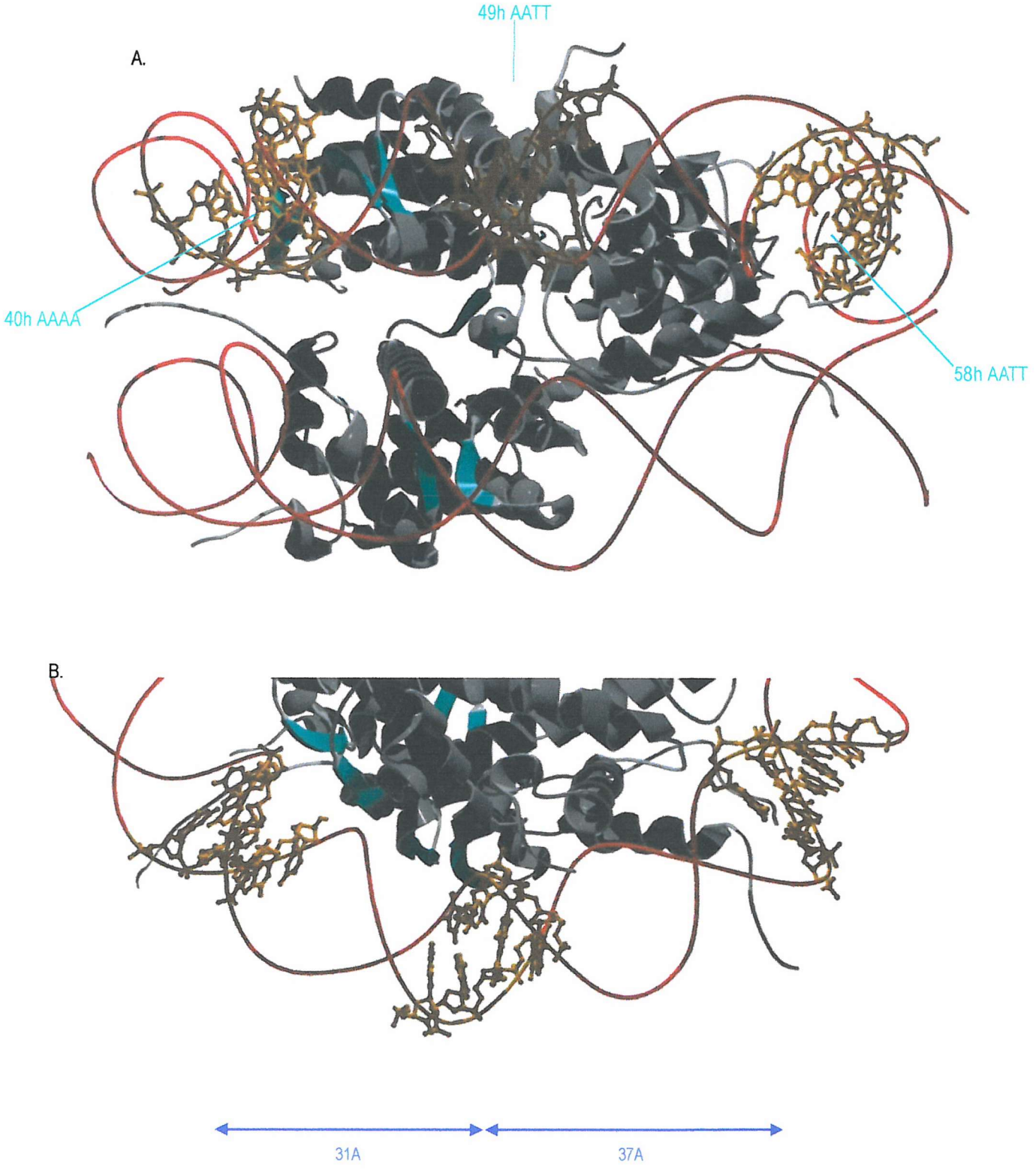

Figure 5.5 Molecular graphics of the *H3* target sites. Each image shows a small portion of the nucleosome core particle. DNA strands are shown as red ribbons, the target sites are coloured orange and are presented as ribbon-ball and stick structures. A portion of the histone octamer is shown as grey ribbons for helices and strands while sheets are coloured teal. Since only a small region of the complex is presented, there appears to be two DNA helices. These actually correspond to the one helix which is wrapped around the protein complex. (a)The view is looking towards the nucleosome perpendicular to the superhelix axis, (b) view looking along the superhelix axis from above. The lower portion of the superhelix has been omitted for clarity. Images were created in Swiss-Pdb viewer, from the pdb file submitted by Luger *et al.* 1997, and rendered in Po-ray for Windows.

As with *4958h* the footprints almost coalesce into a single footprint, and are separated by (weak) cleavage products at positions 44 and 53bp.

The results of DNaseI cleavage for the interaction of Hoechst 33258 with histone-bound *H3* are presented in fig 5.6b and data analysis is shown in fig 5.7b. Cleavage maxima in the ligand free control are found at 45-46, 56-57, 67, 77 and further maxima are evident around positions 86, 96 and 107bp. Therefore, as in the previous construct, the target sites are located in a region where the minor groove faces the protein core.

With increasing drug concentration similar changes are observed in DNaseI cleavage as seen with to *4958h* and it appears that the control cleavage maxima have moved from their original positions. With the highest drug concentration the maxima located at 35, 46, 56, 67, 76, 86, 96 and 107bp are all attenuated. In addition there are regions of attenuated cleavage across 35-43, 47-51 and 55-59bp, which are located across each of the target sites and may therefore correspond to ligand footprints. In addition to these attenuations in cleavage, regions of enhancement are observed at positions 63, 72-73, 82, 92-94, and 103bp. Below 63bp it is difficult to see regions of enhanced cleavage but the data analysis presented in fig 5.7b highlights the appearance of the peaks at 63 and 72bp with 10:M Hoechst. It is interesting to note that although the maximum at position 46bp is strongly attenuated, the peak expected around position 42 is not evident hence supporting the idea that attenuations across the target sites are due to binding of the ligand with the DNA superhelix. In comparison a movement of this peak was observed with construct *4958h*, which doesn't contain a drug binding site across this region.

From these results, it again appears that the rotational position of the DNA superhelix has altered in the presence of Hoechst. However, there is one important difference between these results and those of *4958h*. In *4958h* average peak shift was approximately 3.5bp. Inspection of fig 5.7b indicates that the average peak movement between positions 30-80bp of the construct has increased to 4.6bp. A

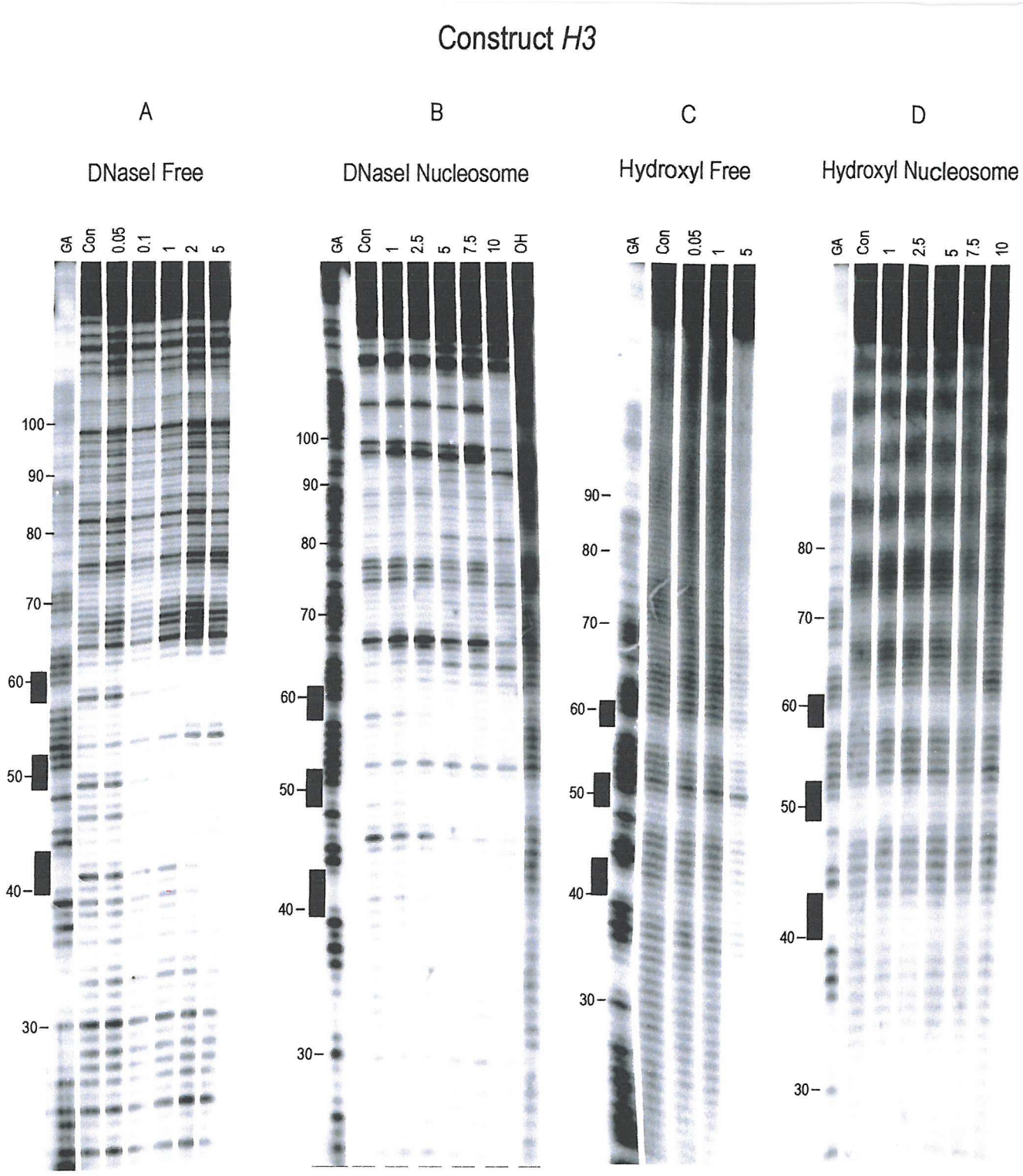

Figure 5.6 DNaseI and hydroxyl radical digestion data on the interaction between Hoechst 33258 and construct *H3*. The ligand concentration is shown at the top of each lane and is expressed in μM. "Con" indicates the ligand free control digestion and "GA" are Maxam-Gilbert sequencing lanes specific for guanine and adenine. Black bars indicate the ligand target sites while numbers correspond to the sequence The additional "OH" lane in (b) is hydroxyl cleavage preformed in the absence of ligand.

Differential Cleavage of Free and Histone-Bound *H3* in the Presence of Hoechst 33258 (DNaseI)

a.

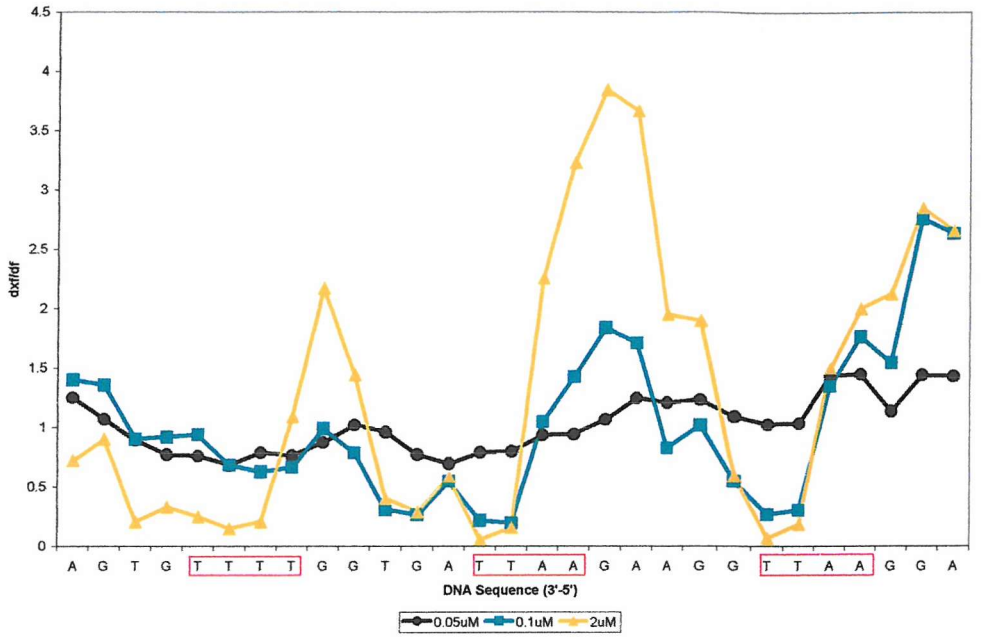

b.

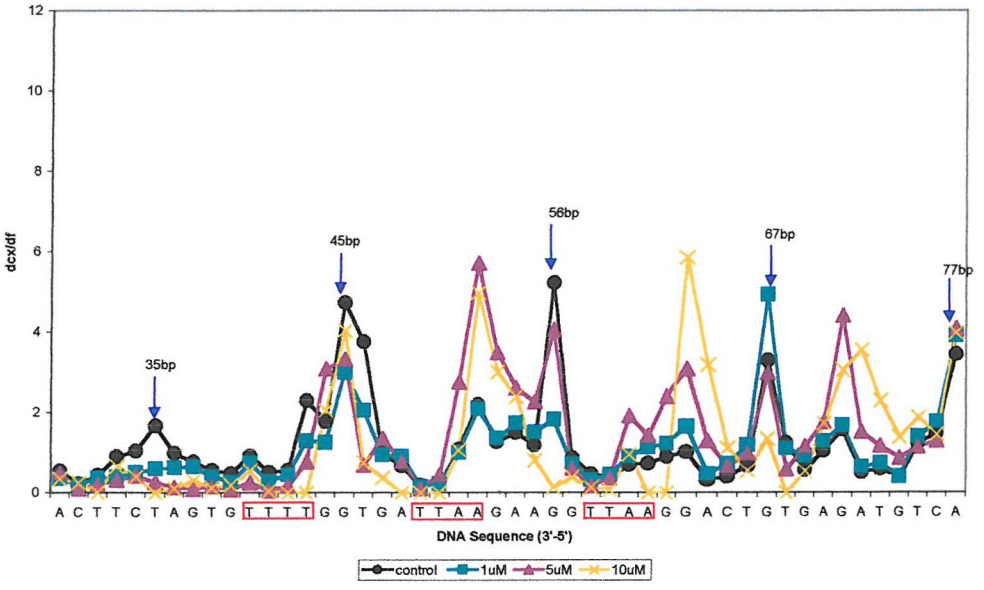

Fig 5.7 Differential cleavage across the AAA and AATT target sites for *H3* free (a) and histone-bound (b) DNA in the presence of Hoechst 33258 as determined by DNaseI. The DNA sequence is shown in the 3'-5' direction and the target site is indicated by a red box. (a), the y-axis shows the value obtained for the division of each band, from a lane where Hoechst has been added (dfx), by the exact corresponding band in the ligand free control (df). (b), the y-axis shows the value obtained for the division of each band in the histone-bound sample (dcx) by the corresponding band in the free DNA (df). Arrows indicate resolved cleavage maxima where the minor groove faces away from the histone core. For clarity, only three concentrations of ligand are presented in each chart.

Differential Cleavage of Free and Histone-Bound *H3* in the Presence of Hoechst 33258 (Hydroxyl Radicals)

a.

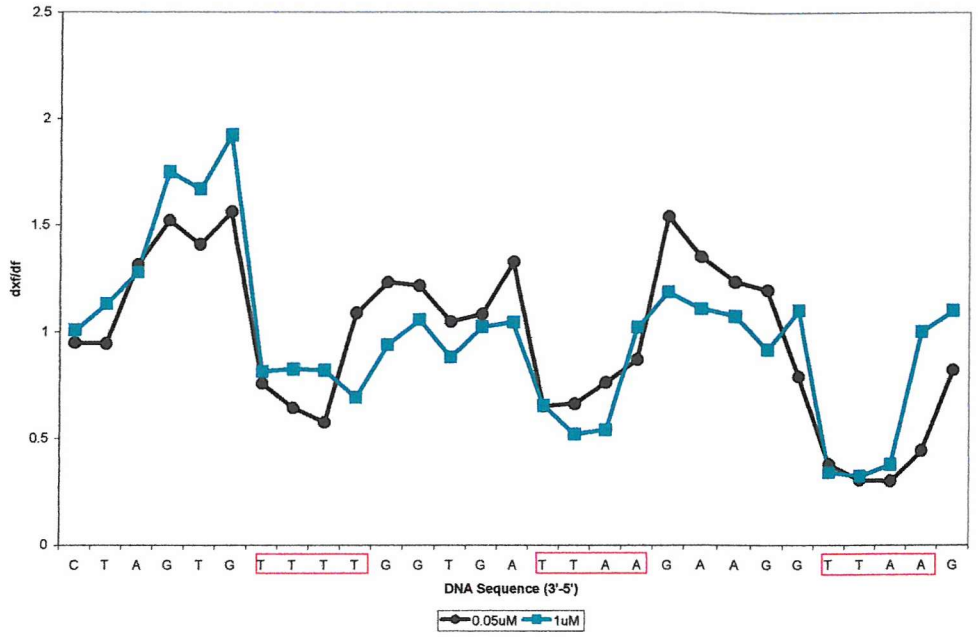

b.

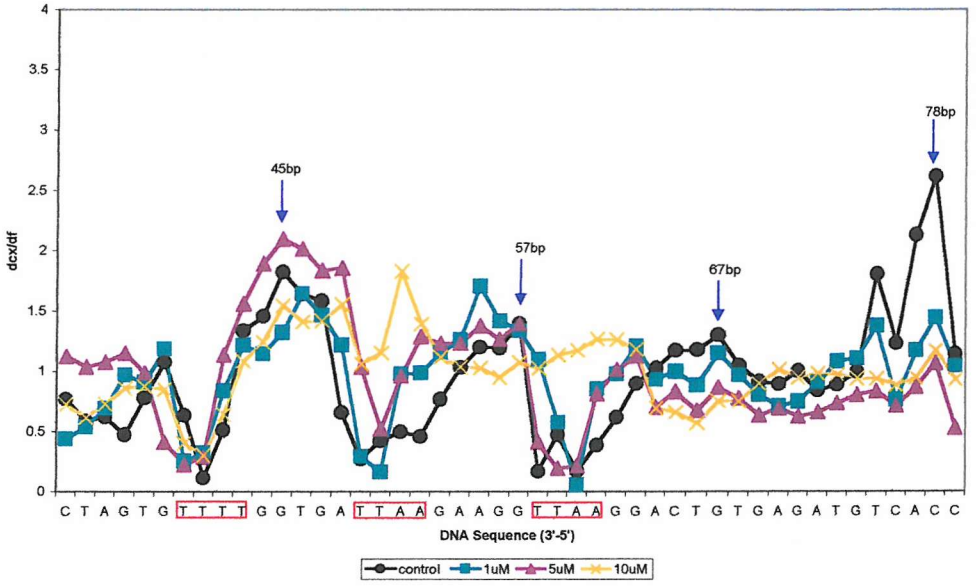

Fig 5.8 Differential cleavage across the AAA and AATT target sites for *H3* free (a) and histone-bound (b) DNA in the presence of Hoechst 33258 as determined by hydroxyl radicals. The DNA sequence is shown in the 3'-5' direction and the target site is indicated by a red box. (a), the y-axis shows the value obtained for the division of each band, from a lane where Hoechst has been added (dfx), by the exact corresponding band in the ligand free control (df). (b), the y-axis shows the value obtained for the division of each band in the histone-bound sample (dcx) by the corresponding band in the free DNA (df). Arrows indicate resolved cleavage maxima where the minor groove faces away from the histone core. For clarity, only three concentrations of ligand are presented in each chart.

further difference between these results and construct *4958h* lies across the region surrounding position 67bp. Although a new maximum appears at position 62bp in *4958h*, the original maximum is still maintained, but with H3 this maxima is very much reduced. It is tempting to speculate that this reflects a greater number of molecules, which have experienced a change in the rotational position of the DNA superhelix with *H3* compared to *4958h*.

Hydroxyl radical footprinting results for the interaction of Hoechst 33258 with free *H3* DNA are presented in fig 5.6c and differential cleavage analysis is shown in fig 5.8a. Binding of the ligand to each of the expected targets is confirmed by the presence of footprints. The interaction of the ligand with histone-bound *H3* was also assessed by hydroxyl radical footprinting and the results are presented in fig 5.6d. Differential cleavage analysis of these data between positions 30-80bp is shown in fig 5.8b. It can be seen, that as expected, each target site is positioned in a region where the minor groove turns to face the histone core as indicated by the regions of attenuated cleavage. As the concentration of drug is increased there is a change in the nucleosome-phasing pattern. Although there appears to be a deterioration in the pattern between positions 49-80bp, regions of enhanced cleavage are observed at 49-52 and 58-61bp. Attenuation in cleavage is also apparent across positions 64-68 and 75-78bp and further inspection of the gel indicates new cleavage maxima between those present in the drug-free control, between positions 77-87, 87-98, and 98-106bp. Therefore it appears that a change in the rotational position is also observed with hydroxyl radicals and construct H3.

Echinomycin

2030e

Since two inward facing Hoechst sites appear to affect the conformation of the nucleosome we next examined whether echinomycin would have a similar affect using fragment *2030e*. A molecular representation of the position of these target sites in the nucleosome are presented in fig 5.9 and a detailed view of *2030e* is presented

The Position of the *2030e, 3950e* and *7080e* Target Sites on the Histone Core

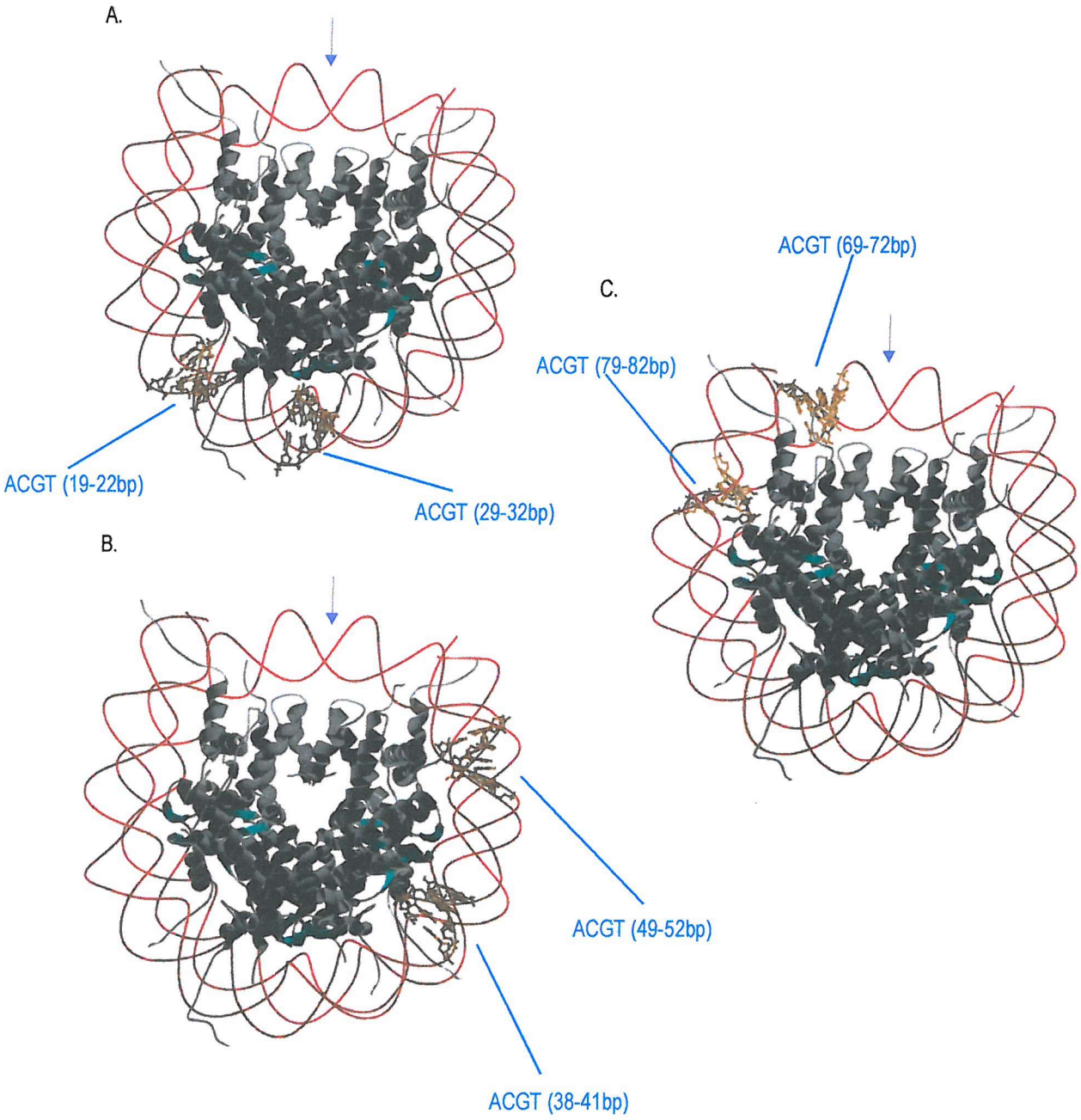

Fig 5.9, The translational position of the target sites in *2030e* (A), *3950e* (B) and *7080e* (C) are presented. DNA strands are shown as red ribbons, the target sites are coloured yellow and are presented as ribbon-ball and stick structures. A portion of the histone octamer is shown as grey ribbons for helices and strands while sheets are coloured teal For clarity only the first 74bp of the DNA superhelix are presented (except in the case of *7080e* where 80bp 82bp are shown. In each image, the position of the dyad is marked by a small purple arrow. Images were created in Swiss-Pdb viewer, from the pdb file submitted by Luger *et al.* 1997, and rendered in Po-ray for Windows.

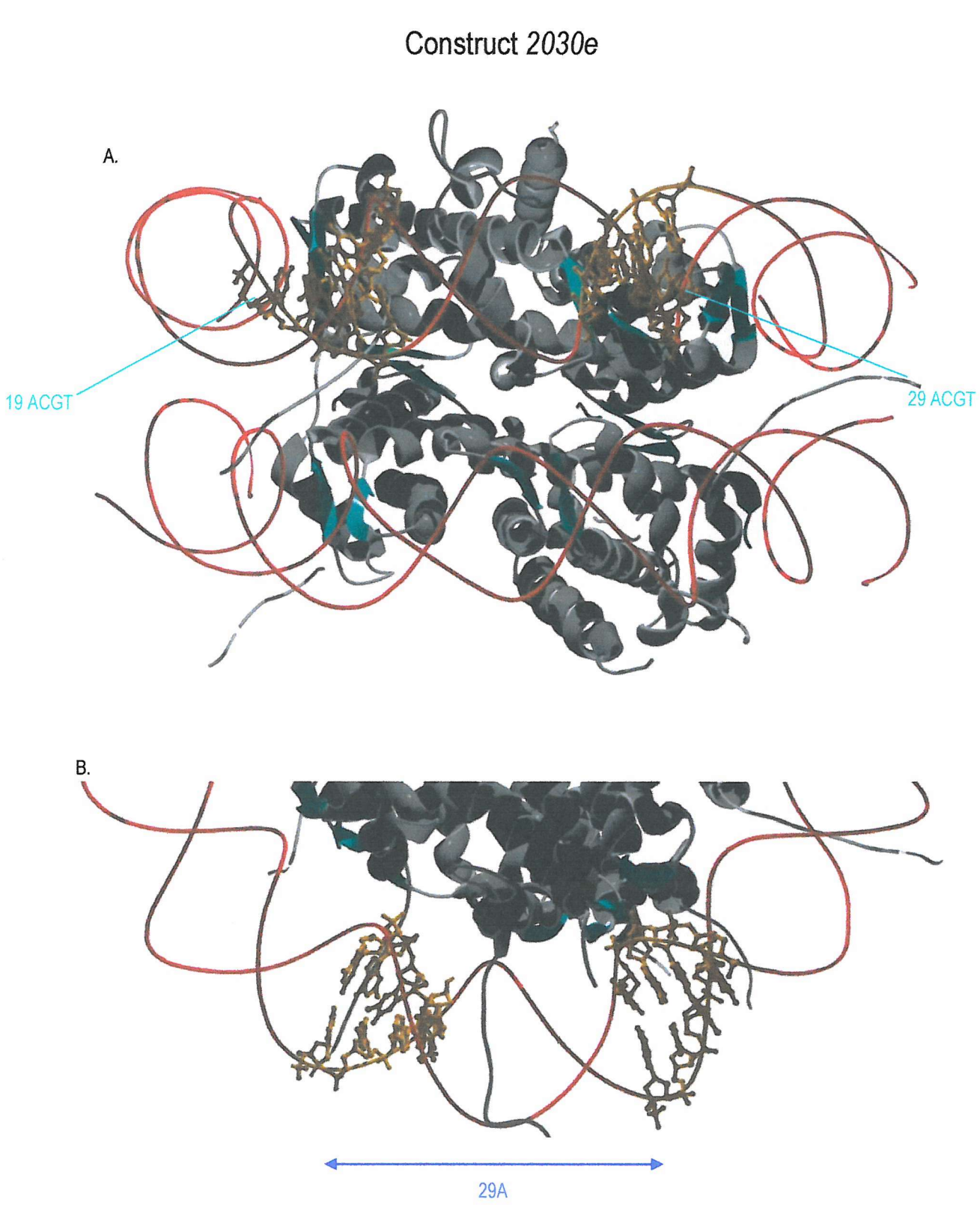

Figure 5.10 Molecular graphics of the *2030e* target sites. Each image shows a small portion of the nucleosome core particle. DNA strands are shown as red ribbons, the target sites are coloured orange and are presented as ribbon-ball and stick structures. A portion of the histone octamer is shown as grey ribbons for helices and strands while sheets are coloured teal. Since only a small region of the complex is presented, there appears to be two DNA helices. These actually correspond to the one helix which is wrapped around the protein complex. (a)The view is looking towards the nucleosome perpendicular to the superhelix axis, (b) view looking along the superhelix axis from above. The lower portion of the superhelix has been omitted for clarity. Images were created in Swiss-Pdb viewer, from the pdb file submitted by Luger *et al.* 1997, and rendered in Po-ray for Windows.

Construct *2030e*

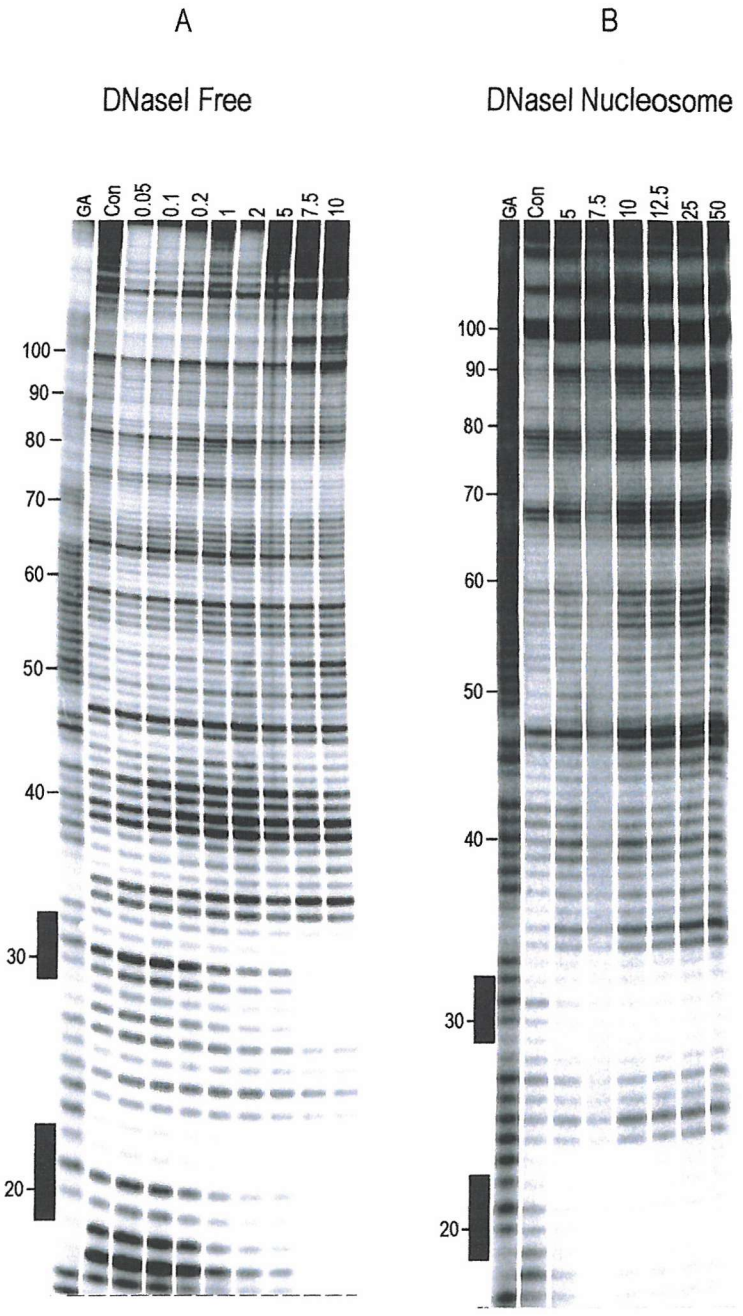

Fig 5.11 DNaseI digestion data on the interaction between echinomycin and construct *2030e*. The ligand concentration is shown at the top of each lane and is expressed in μM. "Con" indicates the ligand free control digestion and "GA" are Maxam-Gilbert sequencing lanes specific for guanine and adenine. Black bars indicate the ligand target site and numbers correspond to the sequence.

Differential Cleavage of Free and Histone-Bound *2030e* in the Presence of Echinomycin (DNaseI)

a.

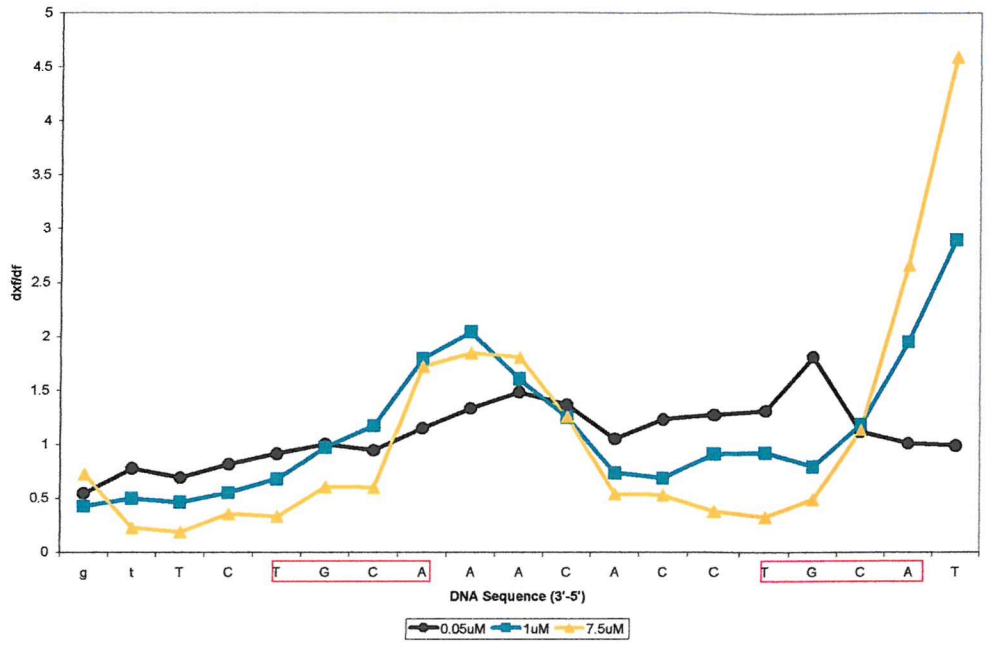

b.

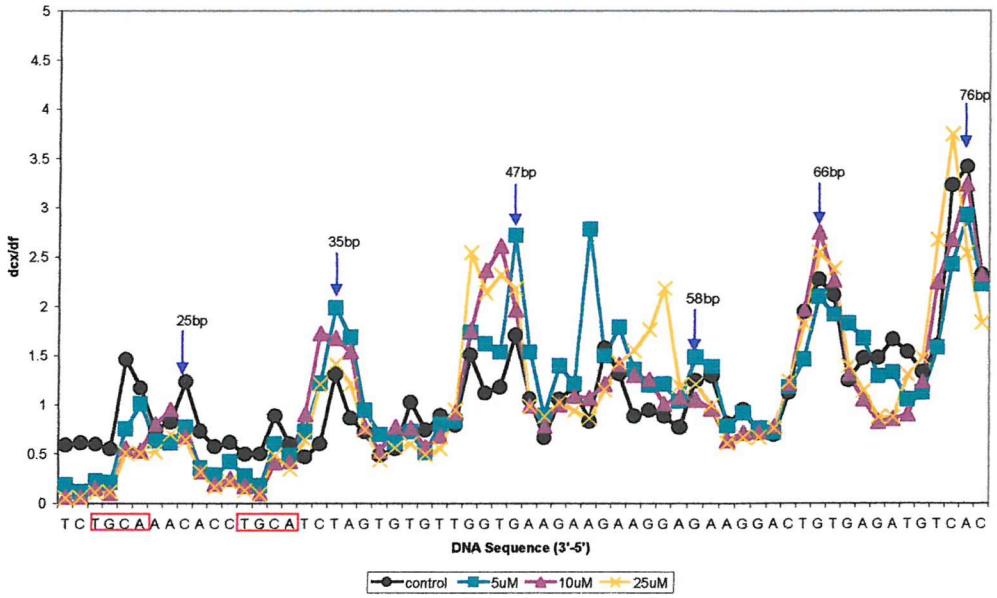

Fig 5.12 Differential cleavage across the 5'-ACGT-3' target sites for *2030e* free (a) and histone-bound (b) DNA in the presence of Echinomycin as determined by DNaseI. The DNA sequence is shown in the 3'-5' direction and the target site is indicated by a red box. (a), the y-axis shows the value obtained for the division of each band, from a lane where Hoechst has been added (dfx), by the exact corresponding band in the ligand free control (df). (b), the y-axis shows the value obtained for the division of each band in the histone-bound sample (dcx) by the corresponding band in the free DNA (df). Arrows indicate resolved cleavage maxima where the minor groove faces away from the histone core. For clarity, only three concentrations of ligand are presented in each chart.

in fig 5.10. As can be seen the targets are close to one end of the DNA superhelix facing towards the histone core with the sites separated by approximately 29Å.

DNaseI footprints for the interaction of echinomycin with free *2030e* DNA are presented fig 5.11a and differential cleavage analysis is presented in fig 5.12a. Both of the expected sites show complete footprints by 7.5μM. The size of the footprint is about 6-7bp at each site. As expected the ligand does not significantly affect DNaseI cleavage in the remainder of the fragment, though some bands are attenuated around positions 73-76bp.

The interaction of echinomycin with histone-bound *2030e* is presented in fig 5.11b and the corresponding analysis is presented in fig 5.12b. As expected, each target lies in a region of poor DNaseI cleavage where the minor groove faces the protein core. Echinomycin produces two distinct DNaseI footprints in the vicinity of these histone-bound ACGT target sites. It appears that the drug is still able to bind to the sites on the nucleosome DNA despite the fact that they were designed so as to face the protein core. This is the first example of clear DNaseI footprints with echinomycin on histone-bound DNA. In the remainder of the sequence there is a general increase in cleavage at almost all positions, which is especially pronounced at minor grooves facing away from the protein core. The cleavage maxima are still located at positions 25, 35, 47, 57, 66, 76 and 96bp and there is therefore no change in the rotational position of the DNA. It appears that two echinomycin molecules can bind to these target sites close to the end of the superhelix without significantly altering the structure of the nucleosome. It should also be noted that although these sites appear to face the histone octamer it may be that this portion of the DNA superhelix is outside the nucleosome position. Under these circumstances echinomycin would have full access to each target site.

3950e

We next moved the two inward facing ACGT target sites further towards the dyad, away from the ends of the nucleosomal DNA. This was done using construct *3950e,*

for which molecular graphics representations are shown in fig 5.9. A more detailed view of these sites is presented in fig 5.13 revealing that the sites are separated by about 40Δ.

DNaseI footprints showing the interaction of echinomycin with free *3950e* DNA are shown in fig 5.14a and differential cleavage analysis of these data are presented in fig 5.15a. It can be seen that echinomycin produces clear footprints at each site which are evident at 7.5μM. As seen with *39e* there is a drug-induced enhancement at positions 34-36bp below the lower ACGT target. Similar enhancements are not seen below the upper site.

Fig 5.14b shows DNaseI cleavage patterns for the interaction of echinomycin with histone-bound *3950e*. The digestion pattern of the drug-free DNA confirms that this adopts the same rotational position as the other fragments and *tem*. The digestion products confirm that each site is found in a region where the minor groove is not easily accessible and hence must face the histone octamer. Direct binding to the targets, is therefore not easily detected, however footprints are apparent at both target sites, as indicated by the reduced cleavage of the bands at positions 39 and 50. These footprints are accompanied by some examples of enhanced DNaseI cleavage; the most prominent of these is found at positions 31-33 in the same region as the drug-induced enhancements seen with free DNA. These enhancements may indicate the binding of echinomycin to this nucleosomal DNA, though they could arise from interactions of the drug with the small amount of contaminating free DNA. Further, less prominent, enhancements are evident at positions 63, 64, 68, 74, 86, 87, and ca. 108bp. Other regions of attenuated cleavage are also observed. Bands at positions 23-28 are lost at 10μM ligand. Further regions of reduced DNaseI cleavage with increasing echinomycin concentration are observed at positions 76 and 78 and 95bp. In addition, the cleavage maxima at positions ca. 120 and 130bp are also attenuated in the presence of the drug. This pattern of band enhancement and attenuation, remote from the drug binding sites, is similar to that observed for the interaction of Hoechst with constructs *4958h* and *H3*. These changes cannot represent a change in

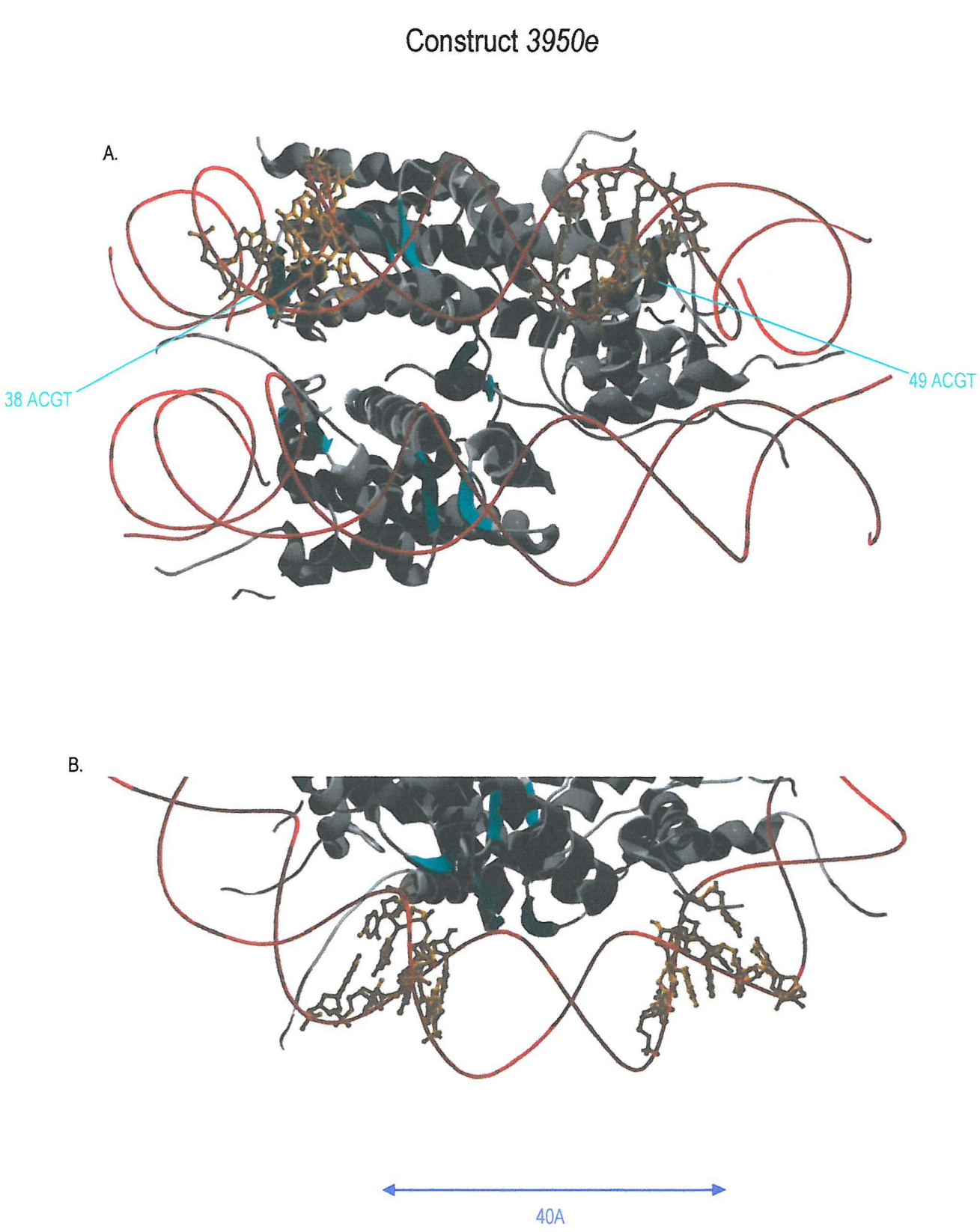

Figure 5.13 Molecular graphics of the *3950e* target sites. Each image shows a small portion of the nucleosome core particle. DNA strands are shown as red ribbons, the target sites are coloured orange and are presented as ribbon-ball and stick structures. A portion of the histone octamer is shown as grey ribbons for helices and strands while sheets are coloured teal. Since only a small region of the complex is presented, there appears to be two DNA helices. These actually correspond to the one helix which is wrapped around the protein complex. (a)The view is looking towards the nucleosome perpendicular to the superhelix axis, (b) view looking along the superhelix axis from above. The lower portion of the superhelix has been omitted for clarity. Images were created in Swiss-Pdb viewer, from the pdb file submitted by Luger *et al.* 1997, and rendered in Po-ray for Windows.

Construct *3950e*

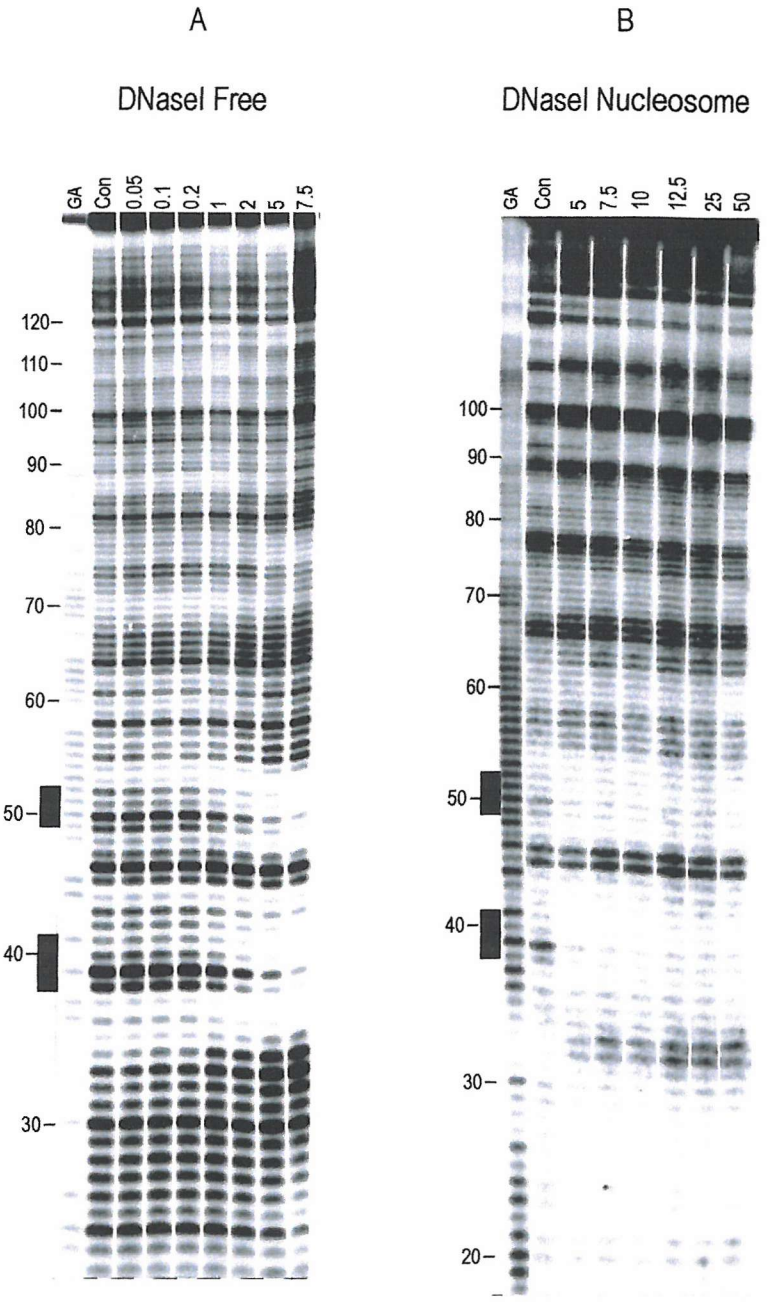

Fig 5.14 DNaseI digestion data on the interaction between echinomycin and construct *3950e*. The ligand concentration is shown at the top of each lane and is expressed in μM. "Con" indicates the ligand free control digestion and "GA" are Maxam-Gilbert sequencing lanes specific for guanine and adenine. Black bars indicate the ligand target site and numbers correspond to the sequence.

Differential Cleavage of Free and Histone-Bound *3950e* in the Presence of Echinomycin (DNaseI)

a.

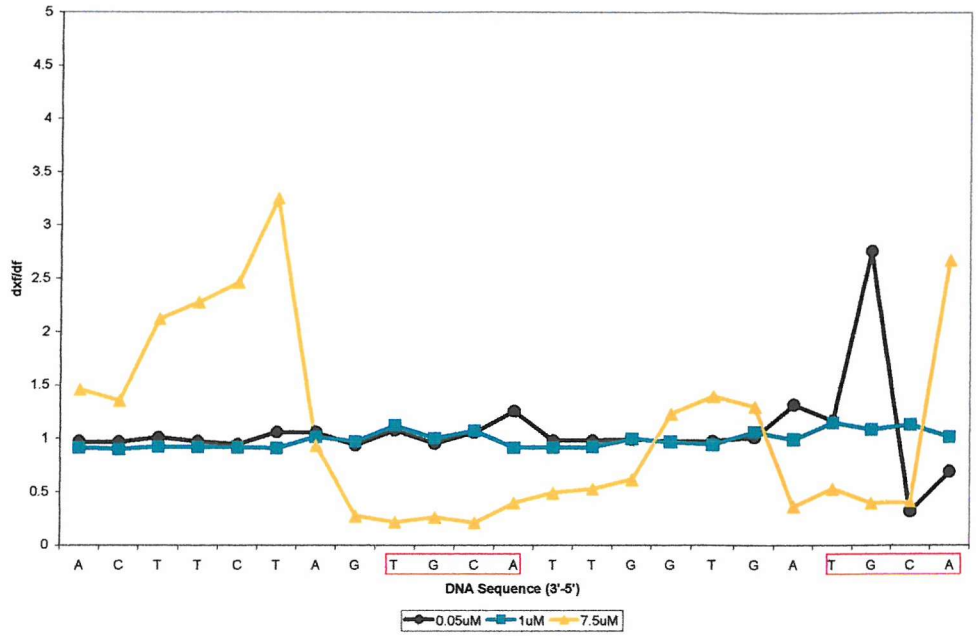

b.

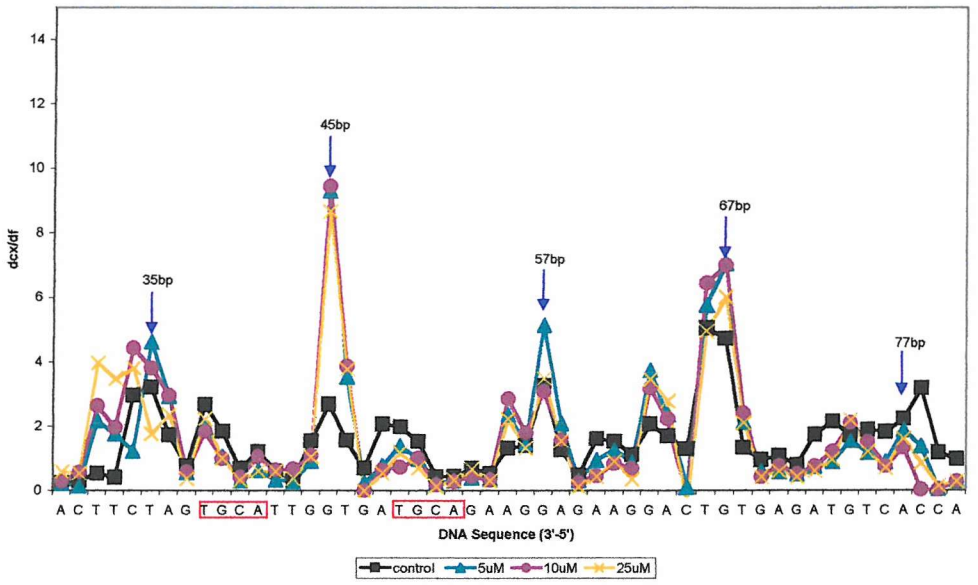

Fig 5.15 Differential cleavage across the 5'-ACGT-3' target sites for *3950e* free (a) and histone-bound (b) DNA in the presence of Echinomycin as determined by DNaseI. The DNA sequence is shown in the 3'-5' direction and the target site is indicated by a red box. (a), the y-axis shows the value obtained for the division of each band, from a lane where echinomycin has been added (dfx), by the exact corresponding band in the ligand free control (df). (b), the y-axis shows the value obtained for the division of each band in the histone-bound sample (dcx) by the corresponding band in the free DNA (df). Arrows indicate resolved cleavage maxima where the minor groove faces away from the histone core. For clarity, only three concentrations of ligand are presented in each chart.

the rotational position of the superhelix for all the DNA molecules since the original cleavage maxima are evident, but these may suggest that a portion of the histone-bound DNA fragments have adopted a different configuration. Positions 120 and 130bp appear far removed from the target sites. However, when the DNA is bound to the histone octamer these positions would be close to each target site but would be located on the lower portion of the superhelix. Since these regions are attenuated as the concentration of ligand is increased, this suggests that some interaction may occur between echinomycin and the DNA in these experiments. Under these circumstances the presence of these drugs may inhibit DNaseI cleavage across a small portion of the superhelix below each target site.

7080e

For the final set of experiments in this series, the inward facing echinomycin sites were moved so that they were close to the dyad. Molecular graphics of the histone-bound sites are presented in figs 5.9 and 5.16. Based on the previous results it was expected that interaction of the ligand with these sites on the nucleosome would cause little, if any, change in DNaseI digestion. DNaseI footprinting results for the interaction of echinomycin with free *7080e* DNA are presented in fig 5.17a and differential cleavage analysis of these data are presented in fig 5.18a. The ligand interacts with both target sites and a footprint is evident across base pairs 68-74bp for the first site and 79-85bp for the second site. Both saturate at 7.5μM echinomycin. There are no enhancements flanking either site. Although there are no clear footprints with this fragment, the strong bands at positions 70 and 81, within each of the intended target sites, are attenuated on addition of the ligand.

Figs 5.17b and 5.18b show the interaction of echinomycin with histone-bound *7080e*. Overall, the interaction of echinomycin with these nucleosomes has not altered the rotational position of the core particle since cleavage maxima at the highest drug concentration remain in the same positions as found in the control. These results are similar to those obtained in the previous chapter for single inward facing echinomycin target sites. If binding did occur, we might expect to see a greater

Construct *7080e*

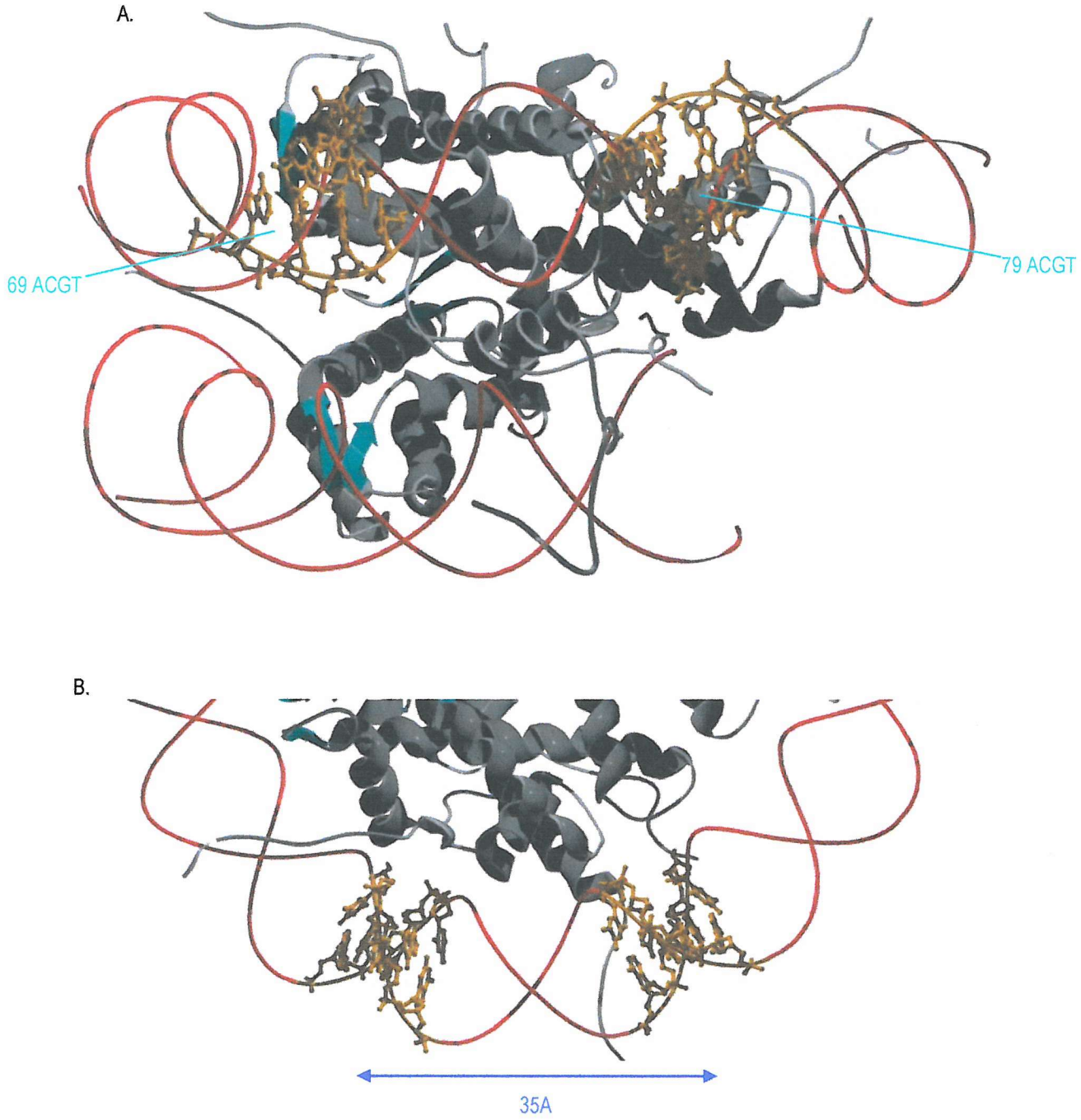

Figure 5.16 Molecular graphics of the *7080e* target sites. Each image shows a small portion of the nucleosome core particle. DNA strands are shown as red ribbons, the target sites are coloured orange and are presented as ribbon-ball and stick structures. A portion of the histone octamer is shown as grey ribbons for helices and strands while sheets are coloured teal. Since only a small region of the complex is presented, there appears to be two DNA helices. These actually correspond to the one helix which is wrapped around the protein complex. (a)The view is looking towards the nucleosome perpendicular to the superhelix axis, (b) view looking along the superhelix axis from above. The lower portion of the superhelix has been omitted for clarity. Images were created in Swiss-Pdb viewer, from the pdb file submitted by Luger *et al.* 1997, and rendered in Po-ray for Windows.

Construct *7080e*

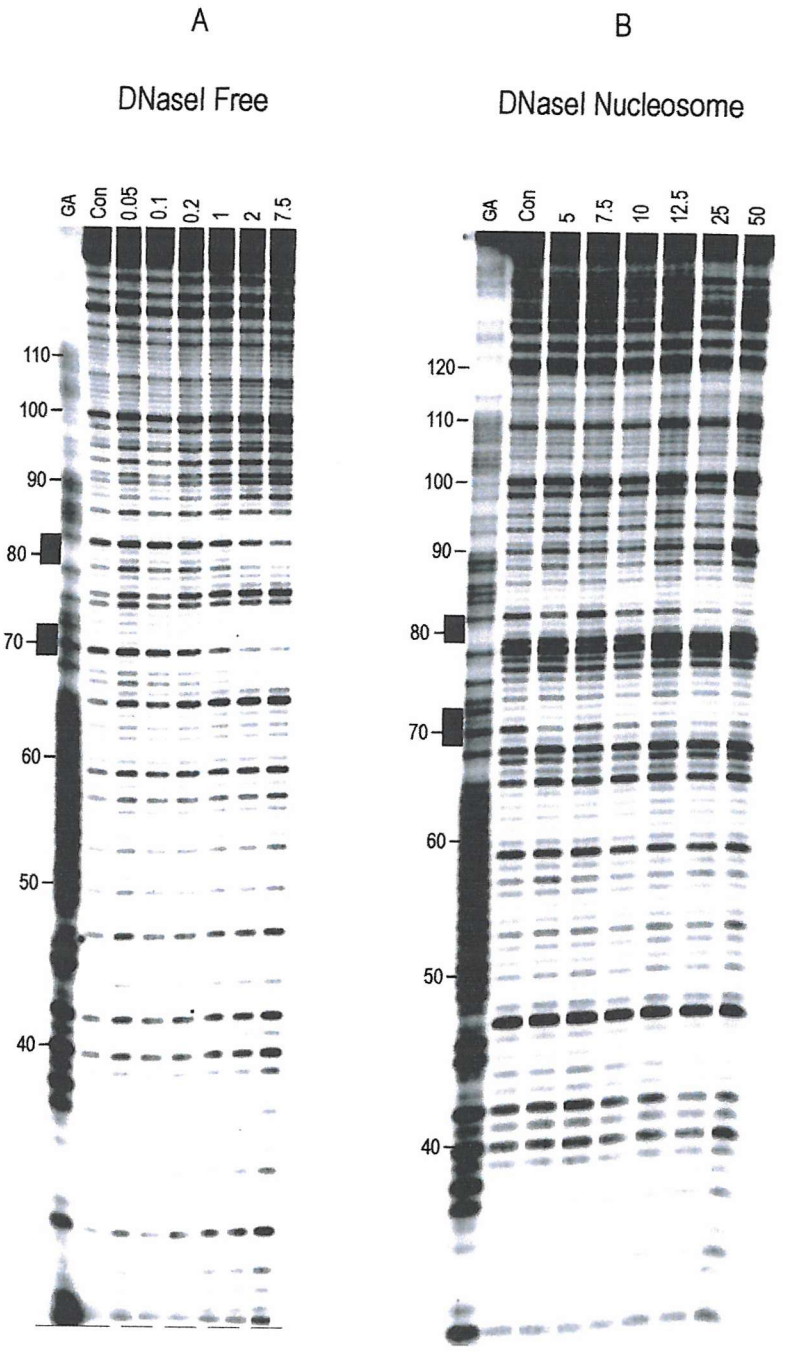

Fig 5.17 DNaseI digestion data on the interaction between echinomycin and construct *7080e*. The ligand concentration is shown at the top of each lane and is expressed in μM. "Con" indicates the ligand free control digestion and "GA" are Maxam-Gilbert sequencing lanes specific for guanine and adenine. Black bars indicate the ligand target site and numbers correspond to the sequence.

Differential Cleavage of Free and Histone-Bound *7080e* in the Presence of Echinomycin (DNaseI)

a.

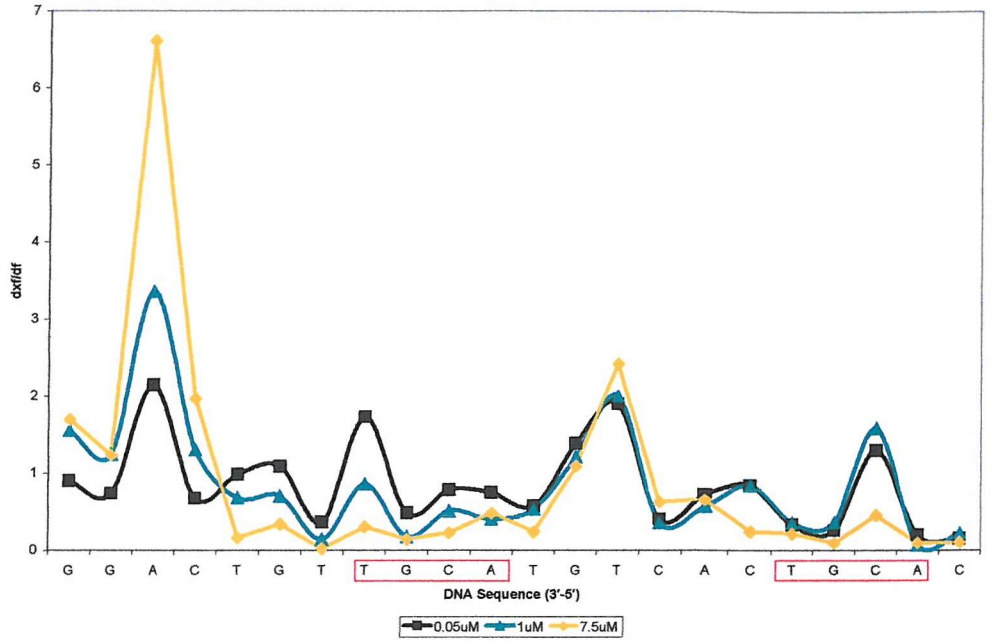

b.

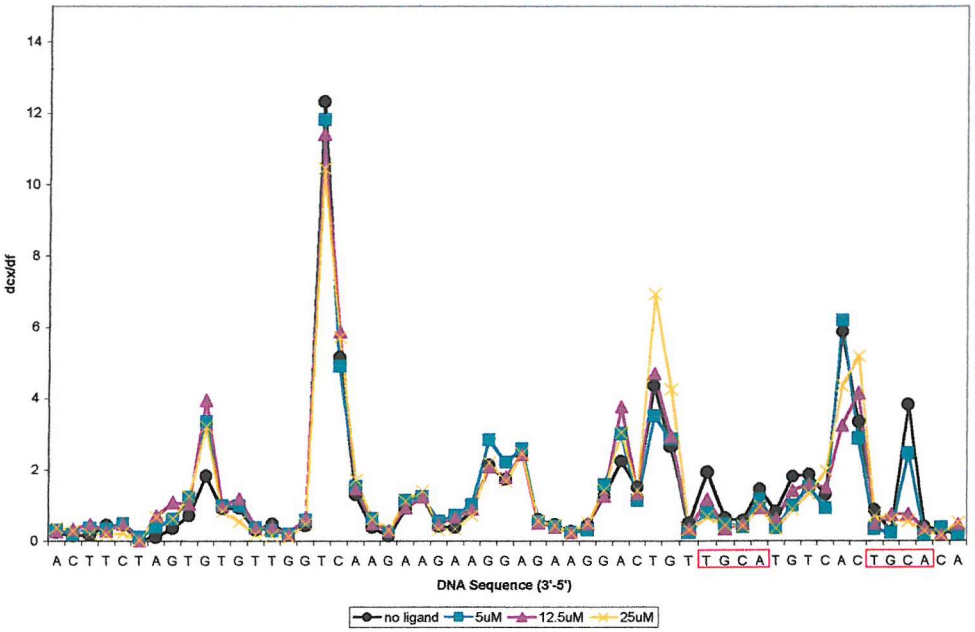

Fig 5.18 Differential cleavage across the 5'-ACGT-3' target sites for *7080e* free (a) and histone-bound (b) DNA in the presence of Echinomycin as determined by DNaseI. The DNA sequence is shown in the 3'-5' direction and the target site is indicated by a red box. (a), the y-axis shows the value obtained for the division of each band, from a lane where echinomycin has been added (dfx), by the exact corresponding band in the ligand free control (df). (b), the y-axis shows the value obtained for the division of each band in the histone-bound sample (dcx) by the corresponding band in the free DNA (df). Arrows indicate resolved cleavage maxima where the minor groove faces away from the histone core. For clarity, only three concentrations of ligand are presented in each chart.

alteration in the nucleosome phasing pattern, which is not observed. In addition, based upon the model by Widom and co-workers, site exposure across these target sites should be a rare event, which further reduces the chances of a ligand molecule interacting with the target sequences.

E3

From the results presented so far it appears that echinomycin constructs containing two inward facing target sites do not undergo a significant change in their position relative to the histone core in the presence of ligand. Therefore we decided to add an additional target site to ascertain whether this would alter the conformation of these particles in a similar manner to that observed for *4958h* and *H3*. Construct E3 contains the two targets found in *3950e* with the additional ACGT site located across positions 58-61bp. A molecular representation of these histone-bound sites is presented in fig 5.19.

DNaseI cleavage showing the interaction of echinomycin with free *E3* DNA is shown in fig 5.20a from where it can be seen that full binding across each of the target sites occurs at 7.5:M ligand. Differential cleavage plots derived from these data are presented in fig 5.21a. As was observed with constructs *39e* and *3950e* there is a drug-induced enhancement across positions 32-34bp below the lower ACGT target. Other 3' enhancements are not detected with the remaining two sites.

Figs 5.20b and 5.21b show DNaseI footprints for the interaction of echinomycin with histone-bound *E3*. The digestion pattern of the drug-free DNA is identical to that observed for all other constructs confirming that each site is found in a region where the minor groove is not easily accessible and hence must face the histone octamer. Examination of the digestion pattern suggests that, even with three inward facing sites, this construct has not under gone a change in the rotational position of the superhelix. Although there are a few drug-induced changes in the cleavage pattern these are much less pronounced than that seen with constructs *4959h* and *H3*. Most

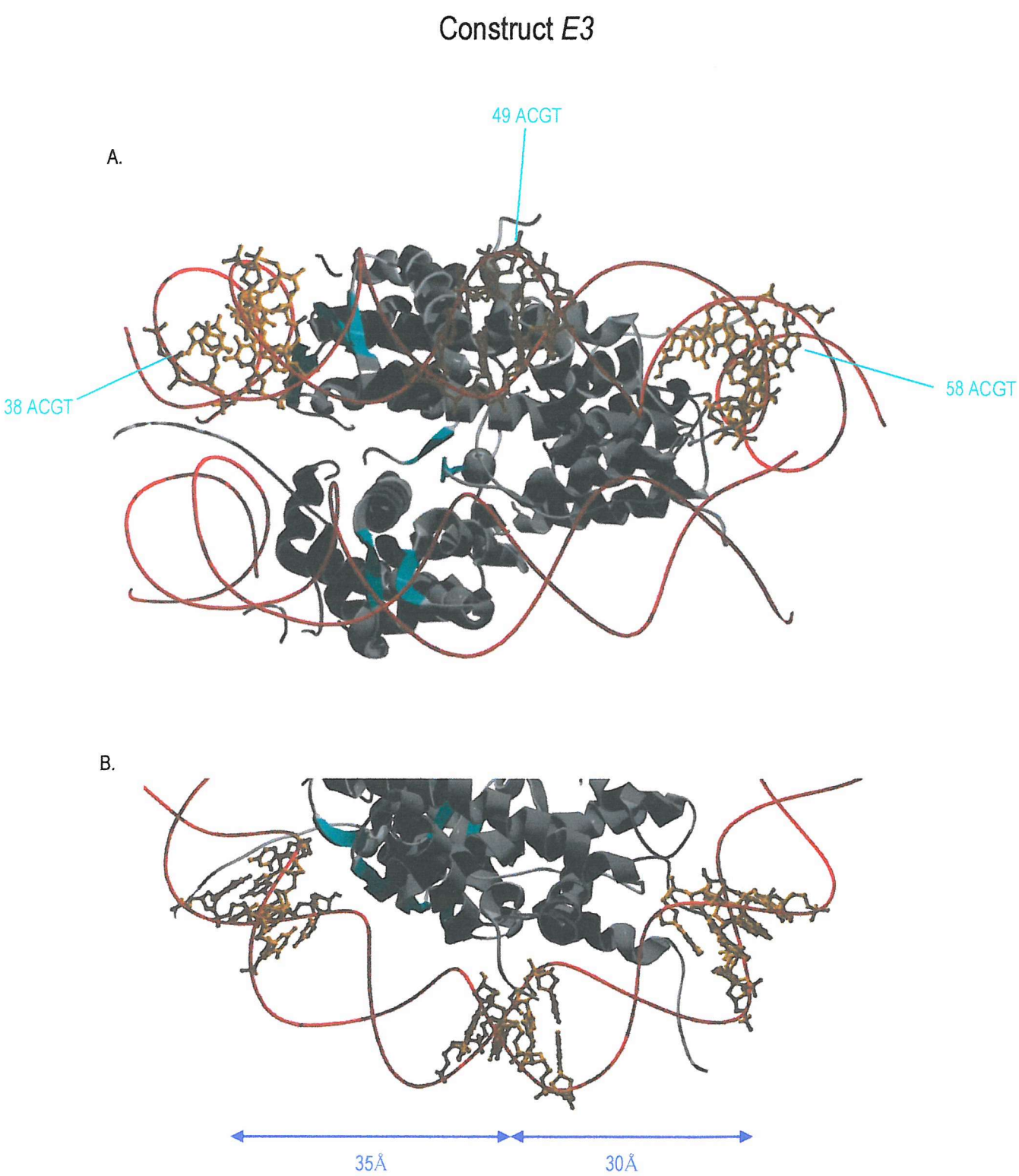

Figure 5.19 Molecular graphics of the *E3* target sites. Each image shows a small portion of the nucleosome core particle. DNA strands are shown as red ribbons, the target sites are coloured yellow and are presented as ribbon-ball and stick structures. A portion of the histone octamer is shown as grey ribbons for helices and strands while sheets are coloured teal. Since only a small region of the complex is presented, there appears to be two DNA helices. These actually correspond to the one helix which is wrapped around the protein complex. (a)The view is looking towards the nucleosome perpendicular to the superhelix axis, (b) view looking along the superhelix axis from above. The lower portion of the superhelix has been omitted for clarity. Images were created in Swiss-Pdb viewer, from the pdb file submitted by Luger *et al.* 1997, and rendered in Po-ray for Windows.

Construct *E3*

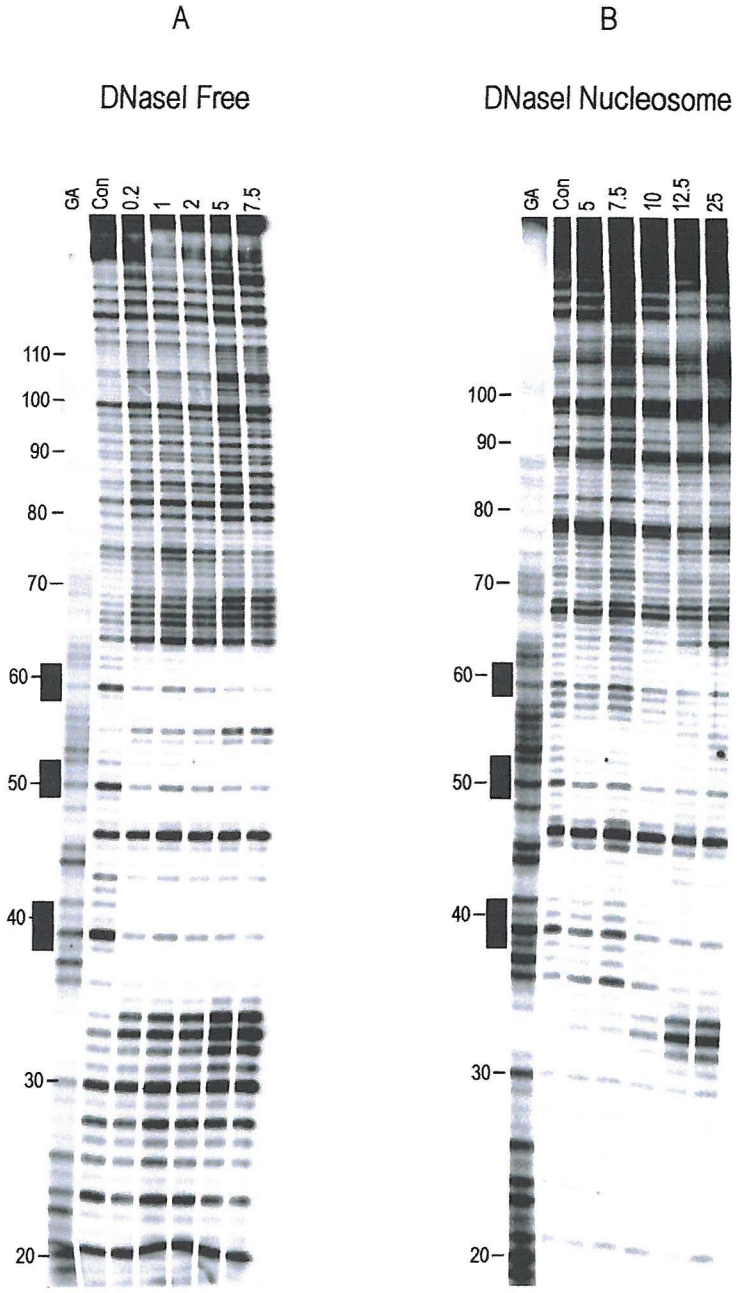

Fig 5.20 DNaseI digestion data on the interaction between echinomycin and construct *E3*. The ligand concentration is shown at the top of each lane and is expressed in μM. "Con" indicates the ligand free control digestion and "GA"are Maxam-Gilbert sequencing lanes specific for guanine and adenine. Black bars indicate the ligand target site and numbers correspond to the sequence.

Differential Cleavage of Free and Histone-Bound *E3* in the Presence of Echinomycin (DNaseI)

a.

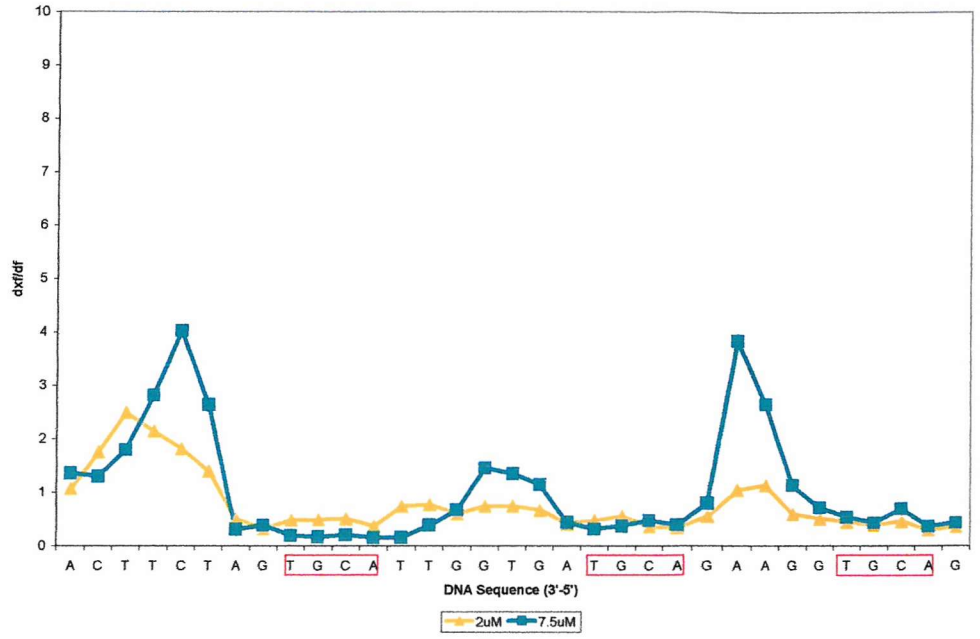

b.

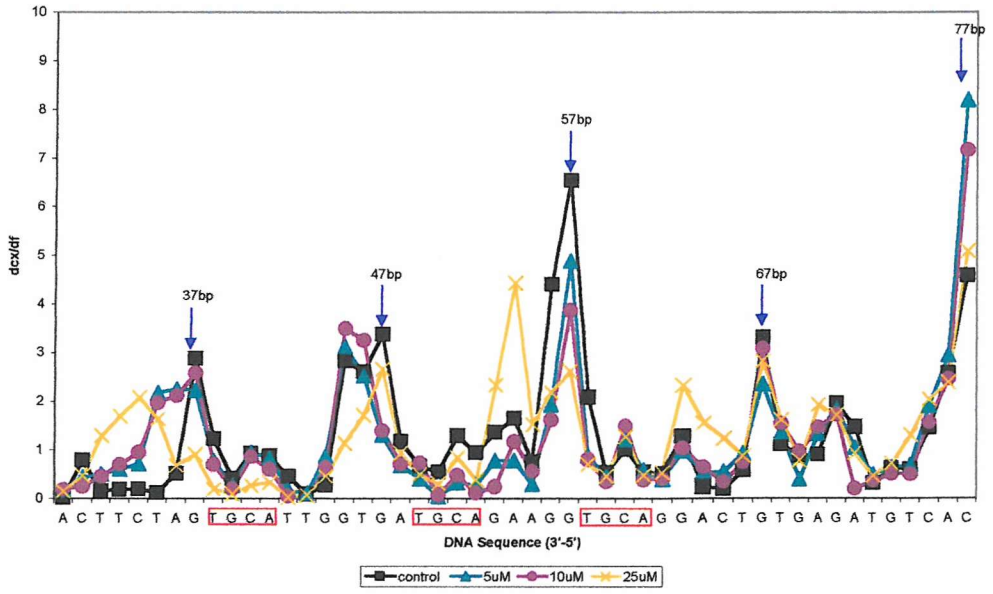

Fig 5.21 Differential cleavage across the 5'-ACGT-3' target sites for *E3* free (a) and histone-bound (b) DNA in the presence of Echinomycin as determined by DNaseI. The DNA sequence is shown in the 3'-5' direction and the target site is indicated by a red box. (a), the y-axis shows the value obtained for the division of each band, from a lane where echinomycin has been added (dfx), by the exact corresponding band in the ligand free control (df). (b), the y-axis shows the value obtained for the division of each band in the histone-bound sample (dcx) by the corresponding band in the free DNA (df). Arrows indicate resolved cleavage maxima where the minor groove faces away from the histone core. For clarity, only three concentrations of ligand are presented in each chart.

obvious changes in the digestion pattern are the enhancements across positions 32-34bp, which are also present in the drug-bound free DNA. These enhancements were also seen with *3950e*. Above this point attenuation in DNaseI cleavage is observed across positions 36-41bp directly across one of the target sites. Weaker attenuation is also observed across the remaining two target sites. As with other constructs these changes in cleavage may be the result of drug binding to the histone-bound DNA or it may be the result of binding to background free DNA in the sample. Additional changes indicate enhancements at of positions 64 and 75. In general these changes do not appear to represent a change in the rotational position of the DNA superhelix and are very similar to that observed with construct *3950e*.

Discussion

The results presented in this chapter suggest that the binding of more than one ligand molecule to the inner surface of the DNA superhelix can cause changes in the conformation of the nucleosome. This observation is different for the two drugs and sheds some light on the possible mechanisms for the conformational changes that occur on binding. The two ligands have very different properties. Hoechst is smaller than echinomycin and does not distort the DNA helix. In addition it has one formal positive charge on the piperazine ring, while echinomycin is composed primarily of neutral amino acids. In this chapter, a minimum number of targets were engineered into the DNA sequence *tem*. It was considered more valuable to obtain data on the events leading up to superhelix rotation rather than to obtain a DNA fragment, which immediately exhibited this phenomenon.

The binding of Hoechst: superhelix re-positioning?

The results obtained for the interaction of Hoechst 33258 with *4958h* and *H3* nucleosomes show that at 7.5μM the ligand generates new bands in the DNaseI digests, which are approximately half way between the cleavage maxima in the drug-free control. In addition, there is a corresponding attenuation of many but not all the original peaks. Distinct footprints are observed at each target site demonstrating that despite the occlusion of each target by the histone octamer, these have been bound by

the ligand. By comparison with the early results of Waring and co-workers, we might propose that the binding of two Hoechst 33258 molecules to the target sites on *4958h* and three to the target sites on *H3* nucleosomes causes a change in the rotational position of the DNA superhelix (Portugal and Waring 1986; Portugal and Waring 1987a; Portugal and Waring 1987b).

If we consider that the average helical repeat of nucleosome DNA is 10.1bp/turn then a change in the rotational position of the DNA by 1bp would represent a rotational movement of 35.46° (360)10.1) between the DNA helix and the surface of the histone octamer. From the results of *4958h* it appears that, on average, there has been a shift in cleavage maxima by 3.5bp. It therefore follows that this may represent a change in the rotational position of this DNA by 124.75° (35.46° x 3.5) with respect to the histone core with addition of Hoechst 33258. It should be noted that this calculation only takes into account the changes observed in the analysed data between base pairs 30-80 of the construct and does not take into account further changes beyond these points.

This is slightly different to earlier results obtained by Waring and co-workers, where the DNA superhelix was thought to have moved through a full 180° with respect to the histone core upon the addition of ligands. However, the tyrT fragment used in the original studies contained many more ligand binding sites than either of these fragments. With construct H3, the average peak shift across positions 30-80bp was 4.6bp. By using the same calculation, this would correspond to a change in the rotational position by approximately 166.77° with respect to the protein core and presumably the greater extent of this change reflects the additional ligand target site.

Although the final conclusions are similar, these results are not the same as those originally observed (Portugal & Waring, 1986; Portugal & Waring, 1987a; Portugal & Waring, 1987b). Based on the DNaseI results, it seems that the binding of Hoechst to the *inner surface* of the DNA brings, about repositioning of the superhelix. This is in contrast to the previous work, which suggested that changes in phasing were

caused by the binding to *outward facing* sites. In light of the structure of the nucleosome it seems unlikely that the DNA superhelix would rotate on the surface of the histone core since this would be energetically unfavourable. Rather, it seems more likely that the DNA becomes transiently exposed, in a manner similar to that described by Widom and co-workers (Polach *et al.*, 2000; Polach & Widom, 1995; Polach & Widom, 1996; Widom, 1998). During this transient exposure, Hoechst would have access to the target sites as they dissociate from the protein core; when the ligand-bound DNA associates with the histone core it adopts a new position. Although site exposure suggests a cooperative interaction between the two sites (see section 1.18) it is not clear whether this is occurring with constructs *4958h* and *H3*. The model proposes that successful binding to the site closest to the edge of the DNA superhelix will increase the binding of a Hoechst molecule to the next site.

The results obtained with hydroxyl radical cleavage provided a less clear picture for the change in the rotational position of the DNA superhelix, than that observed with DNaseI. Since the phasing pattern appears broadened, with high concentrations of drug, could the superhelix be caught between two states, i.e. the original rotational setting and the new rotational setting? Given the different actions of the two cleavage probes it may be that DNaseI more effectively freezes out a dominant conformation which is more difficult to detect with the much smaller hydroxyl radical.

The interaction of echinomycin at the inner surface

The results for echinomycin are in contrast to those obtained with Hoechst. However, by using the three double site constructs, with the targets at different translational positions, and a fragment containing three targets, some interesting results were generated. The results with construct *2030e* demonstrate that, provided the target sites are located in a region where the DNA helix is fairly mobile (i.e. close to the ends of the nucleosome) echinomycin molecules can bind to the superhelix. This appears to have some effect on the conformation of the nucleosome as judged by the enhanced DNaseI throughout the entire histone-bound DNA sequence. It may be that saturation of these targets makes it more difficult for the superhelix to dock with

protein octamer in these regions and causing the DNA across a large proportion of the nucleosome to become more mobile. Therefore, even though echinomycin is bound at the edge of the superhelix, it is still capable of disrupting interactions between the DNA and the protein octamer across large distances. There is no loss in the nucleosome-phasing pattern with increased drug concentration, although some increases in cleavage across the entire sequence may indicate that a small proportion of DNA molecules have undergone a change. In reference to the literature, this is the first time the binding of echinomycin has been directly observed on nucleosomal DNA since the previous studies revealed changes in cleavage but no drug footprints. It is interesting to note that binding to the site at 19-22bp appears to be more efficient compared to the binding at 29-32bp and this may reflect the differences in site exposure between the two targets.

When the sites are located close to the nucleosome dyad axis, as in construct *7080e*, these alterations in nucleosome structure are not evident and are consistent with the fact that site exposure of these targets will occur much less often. In both constructs, echinomycin has not caused a change in the rotational setting of the superhelix.

Similar results were observed with construct *3950e* with no drug-induced alteration of the rotational setting. However, DNaseI enhancements are more localised and the changes around positions such as 31-33bp indicate that the drug may have access to its target sites. Since this particular enhancement is present in *3950e* free DNA it could arise from a small amount of non-reconstituted material. In addition, attenuations at positions 23-28 and 37-42bp may actually be very weak drug footprints. Since other changes are evident in the DNaseI cleavage products, which appear to coincide with these enhancements, and are nucleosome specific, it could be that these footprints and specific changes in DNaseI digestion found in free DNA might be nucleosome specific. This may actually represent a very weak change in the structure of the nucleosome, which is propagated by the binding of echinomycin to the target sites on construct *3950e*.

Based on these results and the analysis of Waring and co-workers (Portugal & Waring, 1986; Portugal & Waring, 1987a; Portugal & Waring, 1987b) it was hoped that the binding of three echinomycin molecules would bring about a change in the rotational setting of the DNA superhelix. However, as the results indicate with construct *E3* there is again no change in the rotational setting of these fragments and in general, these results were very similar to those obtained for *3950e*.

6 The Effect of Hoechst and Echinomycin on Nucleosome Core Formation

Introduction

The results presented so far in this report indicate that two or more Hoechst molecules can bind to target sites located on the outer surface of the nucleosome without affecting the rotational positioning of the histone-bound DNA. However, the binding of two or more molecules on the inner side of the superhelix is sufficient to bring about a change in rotational positioning. In contrast, echinomycin does not to bind to the outer facing surface of nucleosomal DNA and up to three ligand molecules are insufficient to bring about repositioning of the histone-bound DNA. All the data presented so far suggest that conformational changes in the nucleosome are brought about by the binding of ligands to the inner, and not the outer, surface of the DNA superhelix. The previous chapters have described the interaction of drugs with pre-formed nucleosomes, in which the target sites are already occluded by interaction of the protein.

Based upon this, we decided to study the effects of ligands on nucleosome reconstitution. This provides information on how nucleosome formation is affected by the presence of a drug which is already bound to its target sequence. This will presumably mimic the process of transcription in which the DNA is transiently dissociated from the histone octamer in contrast to the previous results which model the effect of the drug on reconstituted DNA. We can envisage several different scenarios:

1. *the drug has no effect on reconstitution*
2. *the drug prevents reconstitution*
3. *the drug alters the location of the DNA on the histone octamer*

Results

All constructs used in this series of experiments were the same as those described in chapters 3-5. Reconstitution was carried out in exactly the same manner, as previously described, except that drugs were added to free DNA and maintained at a constant concentration during reconstitution at this stage rather than after nucleosome formation (see chapter 2, section 2.16). The data are presented as band-shifts. Hence a positive shift (retarded DNA fragment) indicates that nucleosome formation is not affected while no or attenuated shift shows that it is disrupted.

In the following band-shift experiments reconstitution efficiencies typically varied by as much as 5-10% when the same set of samples is run on different gels. This indicates that the gel conditions may affect nucleosome formation. This decreases the resolution of this assay since any ligand-induced effect must be greater than ca. 5-10% to be significant. As a result weak changes in nucleosome formation, resulting from drug binding, will not be detected.

The Interaction of Ligands with the *tem* Sequence During Nucleosome Formation

Before examining the effect of ligands on the reconstitution of various constructs their effect upon reconstitution with the template sequence, *tem*, was studied. The results are presented in fig 6.1 where Hoechst and echinomycin have been added to the reconstitution mixture, before running on non-denaturing PAGE. Quantitive analysis of these results, showing the relative amount of histone-bound and free DNA is presented in fig 6.2. As can be seen there is no change in the level of *tem* nucleosome formation. However, in the presence of 25 and 50:M of echinomycin only 60-50% of the fragment binds to the histone octamer. Since this sequence does not contain any echinomycin sites we presume that this observation is not a result of binding of this ligand to the DNA sequence. In addition some material is retained in the wells at these concentrations which may correspond to drug-induced aggregation

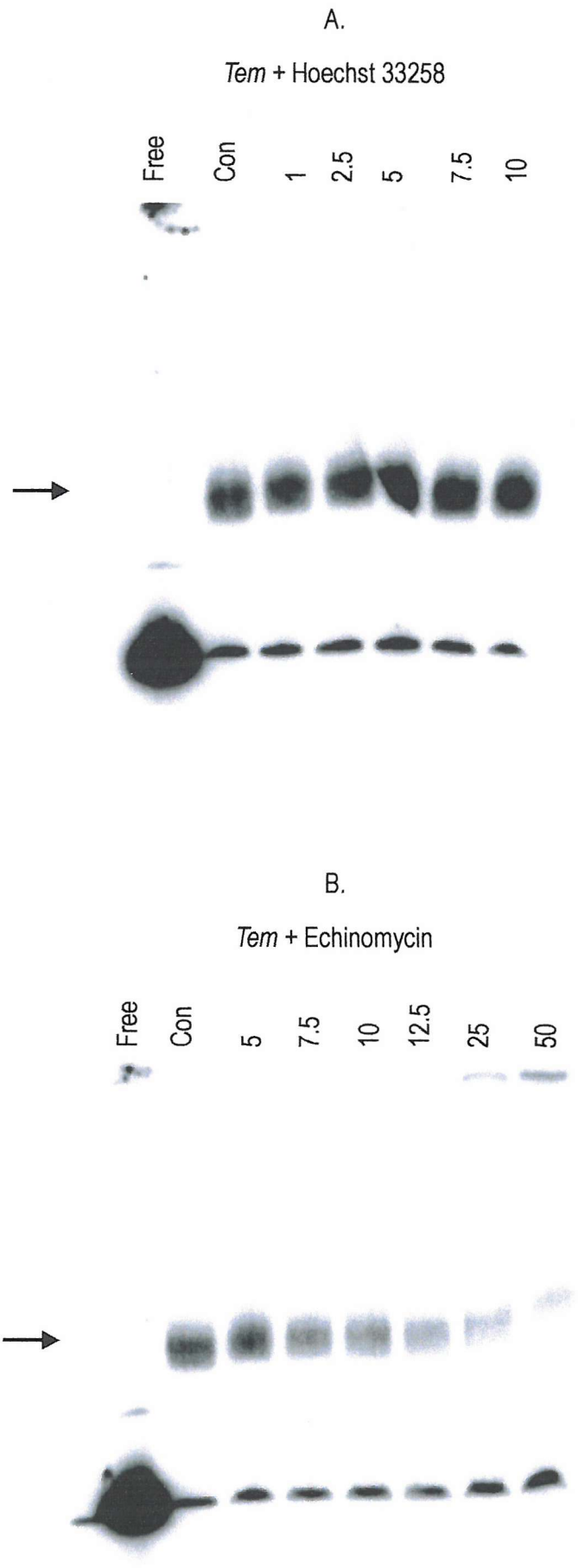

Fig 6.1 Band-shift assays of nucleosome formation in the presence of Hoechst and echinomycin with construct *tem.* The ligand concentration is shown at the top of each lane and is expressed in μM. "Free" indicates unbound DNA and is used as a marker, "Con" is the ligand free control. Bands corresponding to histone-bound DNA are indicated with an arrow.

Nucleosome Formation with Construct *tem* in the Presence of Hoechst and Echinomycin

a.

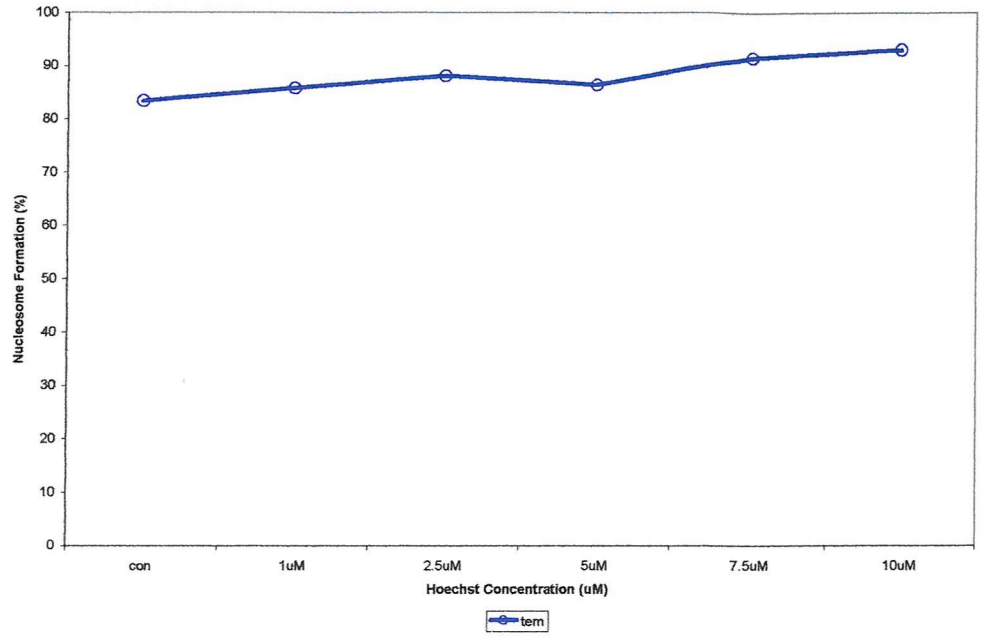

b.

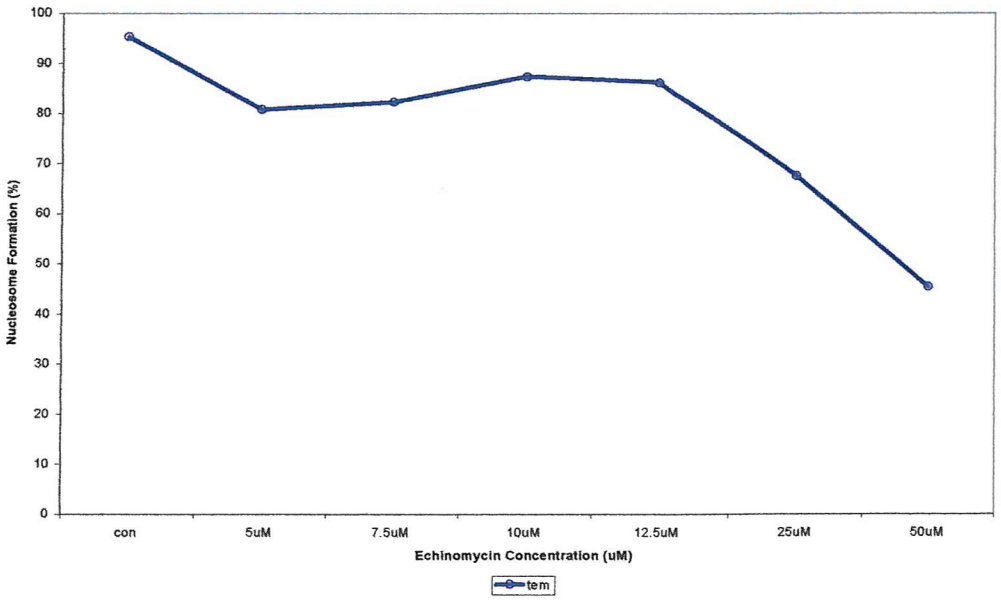

Fig 6.2 Nucleosome formation is expressed as a percentage and is shown in the y-axis. The ligand concentration is shown on the x-axis.

or precipitation.

Nucleosome Formation with Constructs 35h, 46h, 3546h, 44e and 74e

In chapter three, it was demonstrated that Hoechst and echinomycin did not significantly alter the conformation of the nucleosome core particle, which contained their target sites on the outer surface of the DNA superhelix. Band-shift assays for constructs *35h*, *46h* and *3546h* are presented in figs 6.3a-c and quantitive analysis of these data, are shown in fig 6.5a. It can be seen that Hoechst has not affected the efficiency of nucleosome formation, with these fragments.

Similar experiments examining the effect of echinomycin on nucleosome reconstitution with constructs *44e* and *74e* are shown in fig 6.4, with quantitive analysis of these data shown in fig 6.5b. Echinomycin did not interact with pre-formed *44e* and *74e* nucleosomes. With construct *44e*, nucleosome formation decreases to 55% (fig 6.5b) in the presence of 5μM echinomycin and as the concentration of drug is increased the band-shift is steadily abolished so that it represents only 0.3% with 50μM ligand. This effect is clearly much more pronounced than that seen with echinomycin and *tem*. A similar result is obtained with fragment *74e*, though the ligand has less effect at the lower concentrations.

Nucleosome Formation with Constructs 3558h, 73h, 39e, 50e and 100e

Chapter 4 considered the interaction of Hoechst and echinomycin with single inward facing target sites and it was concluded that little change occurred in these nucleosomes with the addition of ligand. The exception to this was *73h* for which the phasing pattern deteriorated at high Hoechst concentrations. Band-shift assays, with construct *3558h* fig 6.6a indicate little change in the efficiency of nucleosome reconstitution, which is clearly indicated in the quantitive analysis, fig 6.8a.

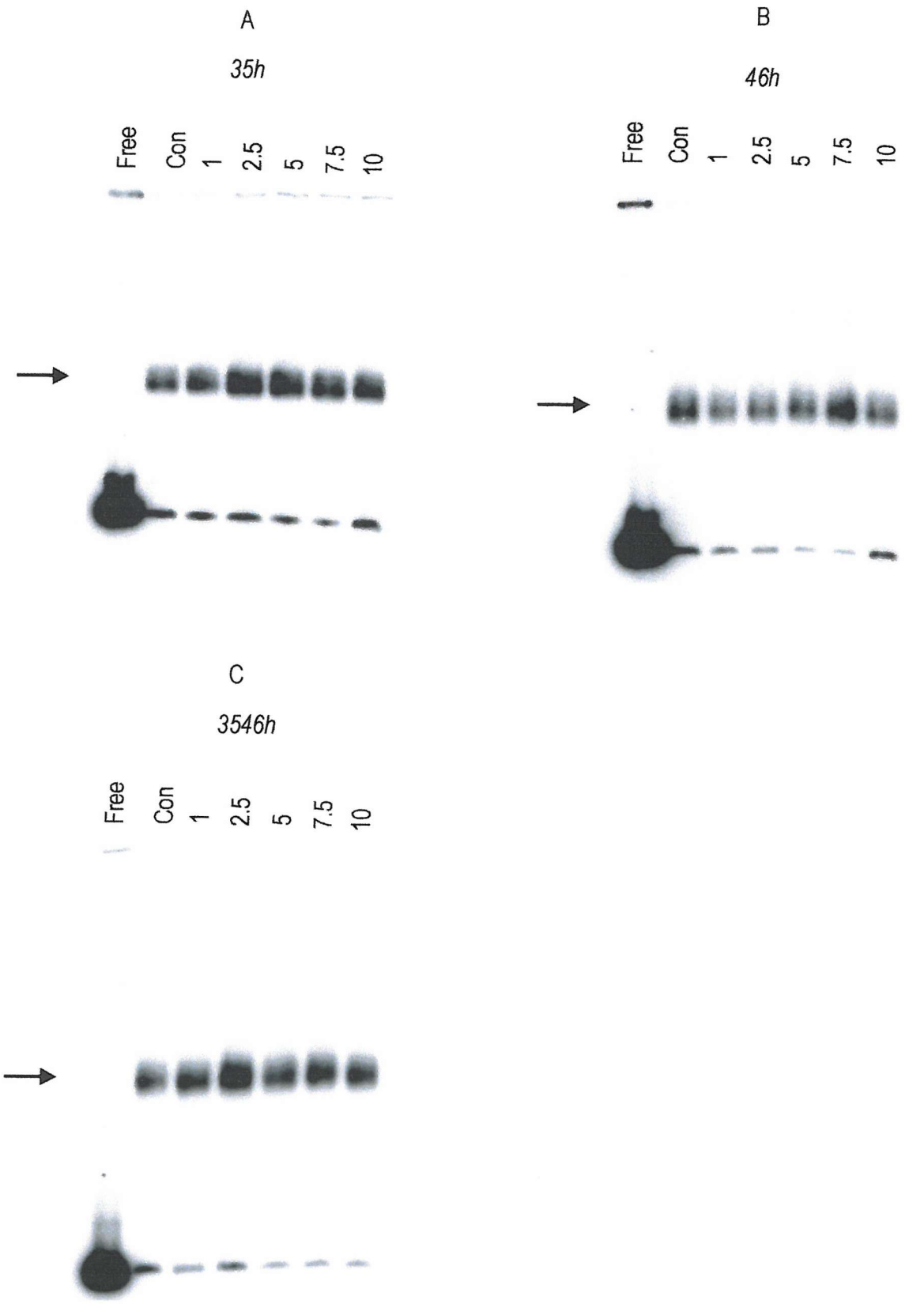

Fig 6.3 Gel shift assays of nucleosome formation in the presence of Hoechst with constructs *35h, 46h and 3546h.*.The ligand concentration is shown at the top of each lane and is expressed in μM. "Free" indicates unbound DNA and is used as a marker, "Con" is the ligand free control. Bans corresponding to histone-bound DNA are indicated with a blue arrow.

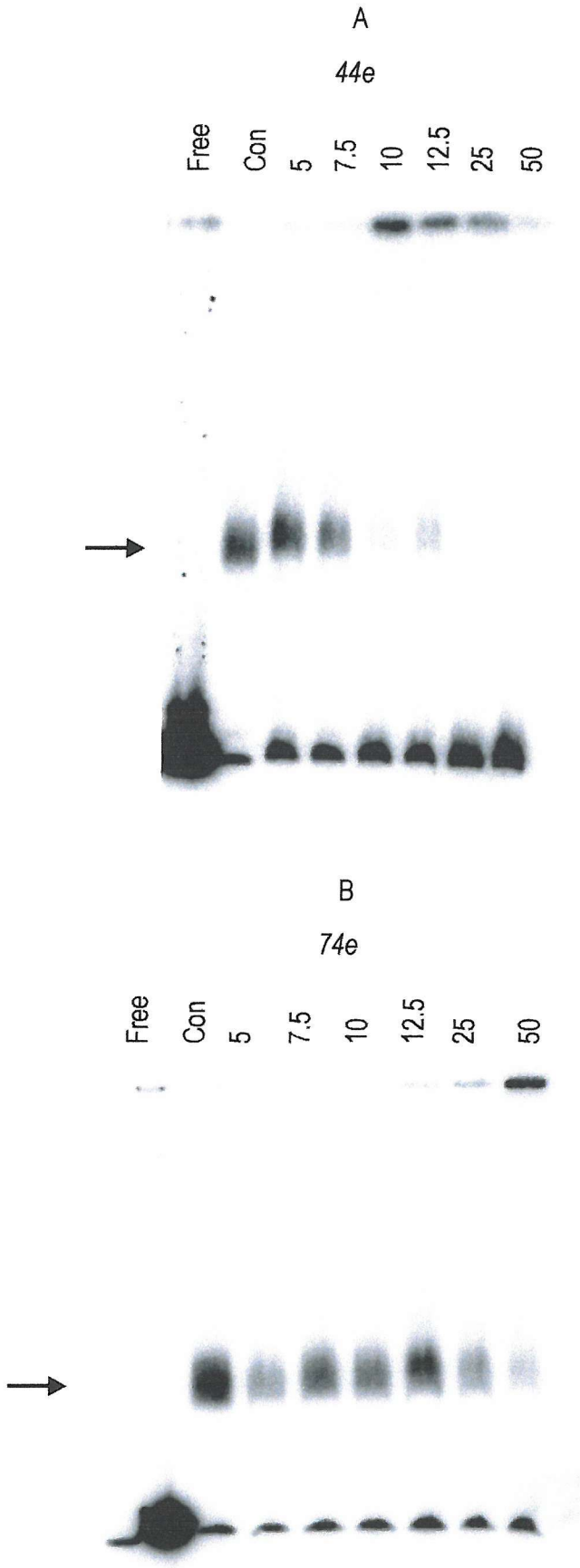

Fig 6.4 Band-shift assays of nucleosome formation in the presence of echinomycin with constructs 44*e* and *74e*. The ligand concentration is shown at the top of each lane and is expressed in μM. "Free" indicates unbound DNA and is used as a marker, "Con" is the ligand free control. Bands corresponding to histone-bound DNA are indicated with an arrow.

Nucleosome Formation with Constructs *35h, 46h, 3546h, 44e* and *74e* in the Presence of Hoechst & Echinomycin

a.

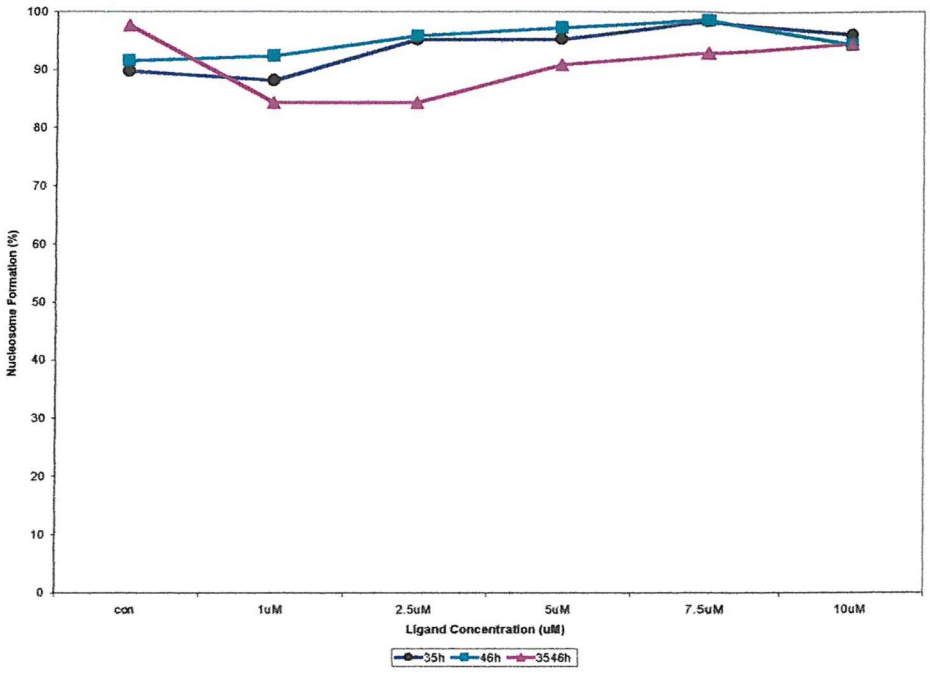

b.

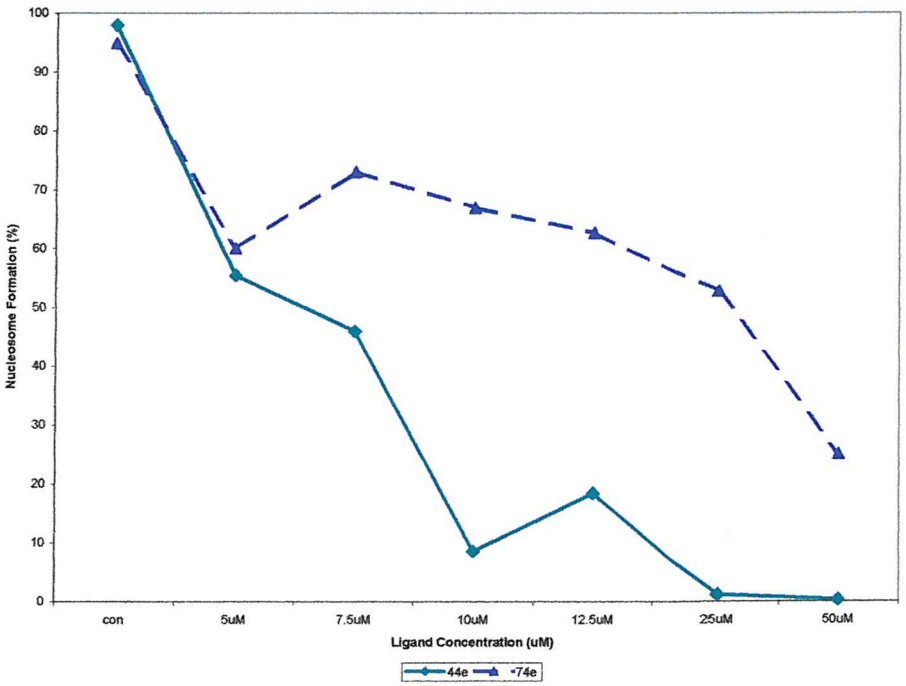

Fig 6.5 Band-shift data for constructs from chapter 3. (a), *35h*, *46h* and *3546h* (b), *44e* and *74e*. Nucleosome formation is expressed as a percentage and is shown in the y-axis. The ligand concentration is shown on the x-axis.

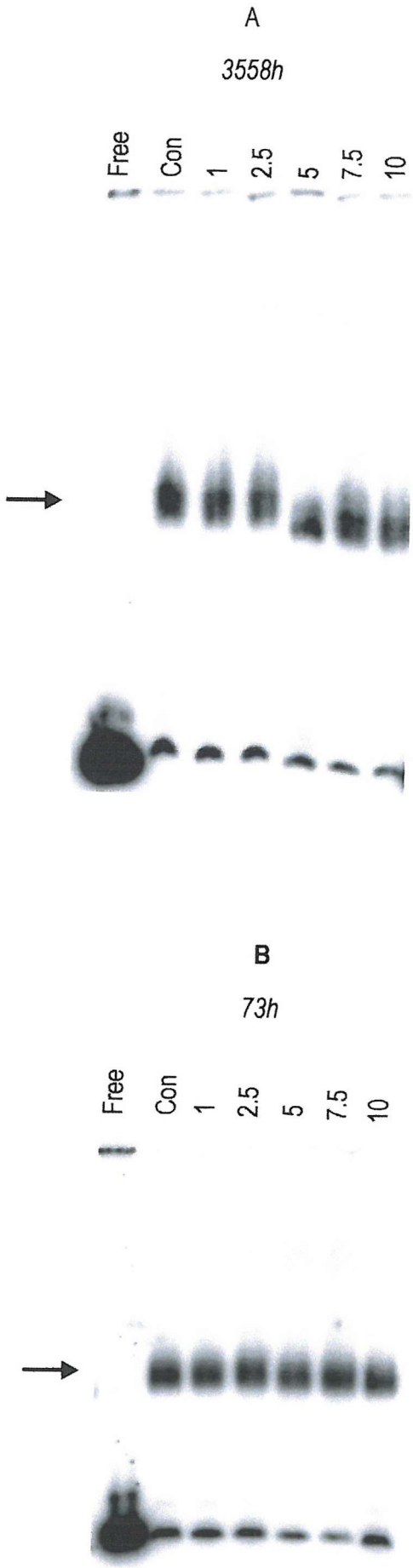

Fig 6.6 Gel shift assays of nucleosome formation in the presence of Hoechst with constructs *3558h* and *73h*. The ligand concentration is shown at the top of each lane and is expressed in μM. "Free" indicates unbound DNA and is used as a marker, "Con" is the ligand free control. Bans corresponding to histone-bound DNA are indicated with a blue arrow.

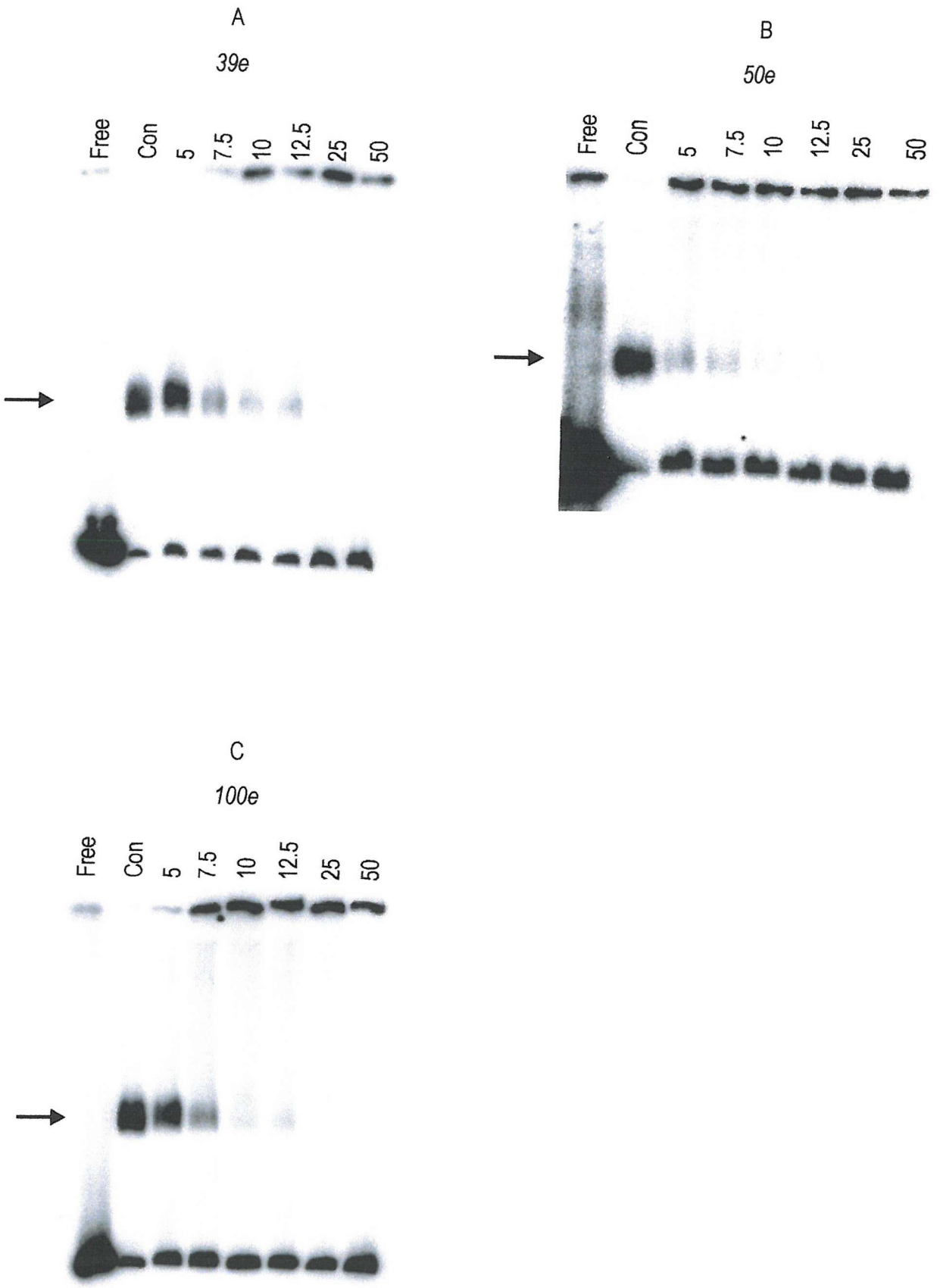

Fig 6.7 Band-shift assays of nucleosome formation in the presence of echinomycin with constructs *39e, 50e* and *100e*. The ligand concentration is shown at the top of each lane and is expressed in μM. "Free" indicates unbound DNA and is used as a marker, "Con" is the ligand free control. Bands corresponding to histone-bound DNA are indicated with an arrow. .

Nucleosome Formation with Constructs *3558h, 73h, 39e, 50e, and 100e* in the Presence of Hoechst & Echinomycin

a.

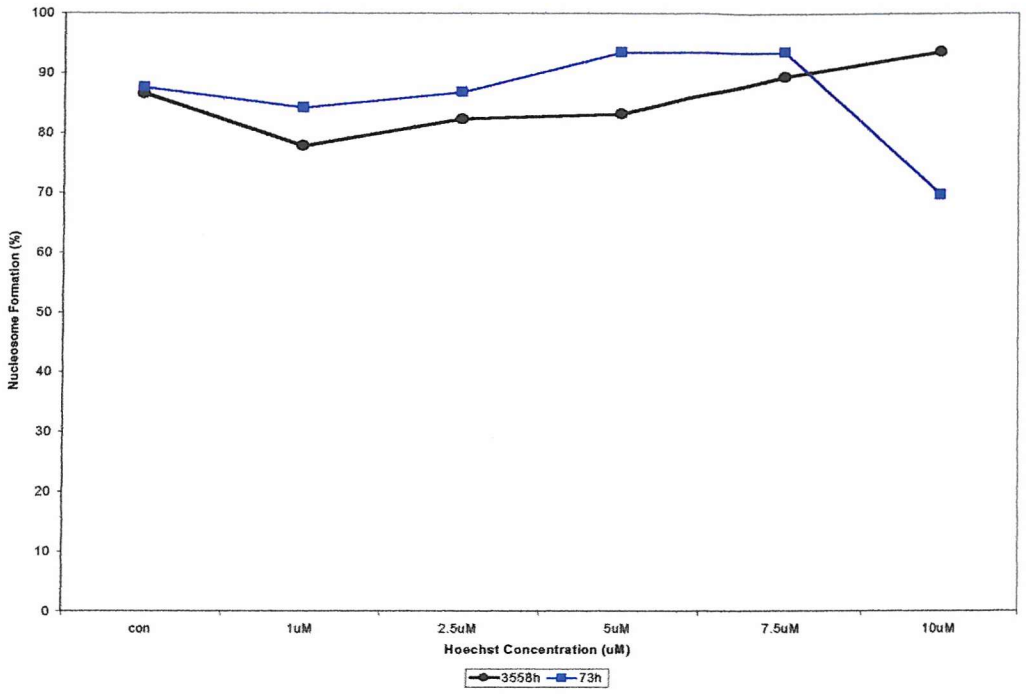

b.

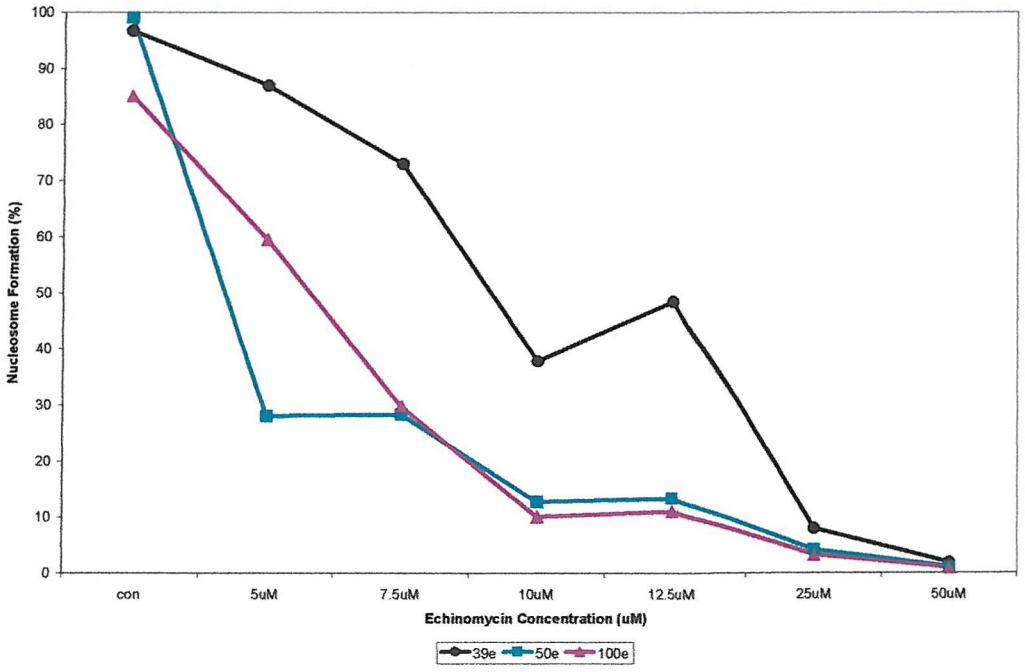

Fig 6.8 Band-shift data for constructs from chapter 4. (a), *3558h* (b), *39e*, *50e*, and *100e* Nucleosome formation is expressed as a percentage and is shown in the y-axis. The ligand concentration is shown on the x-axis.

However, with construct *73h* (fig 6.6b) reconstitution has fallen to 70% with 10μM ligand. In addition, visual inspection of the band-shift for *73h* shows a super-shifted species at concentrations of 2.5, 5 and 7.5:M ligand. The bands in these super-shifts account for less than 1% the total DNA in each sample and most probably represent nucleosomes in which the DNA superhelix is not symmetrically positioned.

In contrast, echinomycin causes a severe disruption in nucleosome formation with constructs *39e*, *50e* and *100e*, fig 6.6a-c. Analysis of these results, fig 6.8b, demonstrates that with *39e* there is a steady fall in histone reconstitution down to less that 2% with the highest ligand concentration. With construct *50e*, where the target site is 11bp closer to the nucleosome dyad, this reduction in nucleosome formation is more rapid and falls to 28% with 5μM echinomycin. This is then followed by a steady reduction and it reaches 1% at the highest ligand concentration. The results obtained for *100e* are very similar except that the initial rate of reduction in reconstitution is slower than observed with *50e*, with 5μM ligand. This is then reduced at approximately the same rate until it reaches 0.91% with 50:M ligand.

Nucleosome Formation with Constructs 4958h, H3, 2030e, 3950e, 7080e and E3

The final series of band-shift experiments involved the constructs from chapter 5, which contain 2-3 ligand target sites located on the inward facing side of the DNA superhelix. The results with pre-formed nucleosomes showed that Hoechst caused extensive conformational change with constructs 4958h and H3. However, the band-shift data with these fragments, shown in figs 6.9 and 6.11a, show that the ligand has very little effect upon the efficiency of nucleosome formation with these constructs, even at the highest concentrations of Hoechst. The band-shift data highlights the fact that, despite having up to three inward facing Hoechst target sites, the integrity of the core particle is maintained in the presence of the ligand. However, it should be remembered that the present data do not distinguish between Hoechst-DNA-Histone

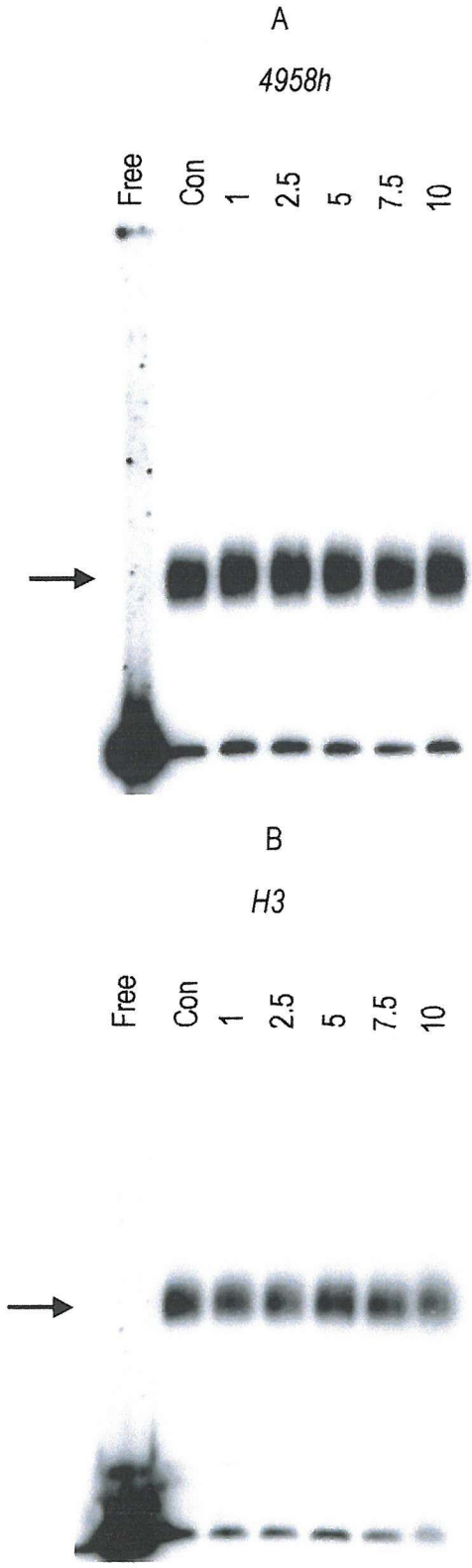

Fig 6.9 Gel shift assays of nucleosome formation in the presence of Hoechst with constructs 4958h and *H3*. The ligand concentration is shown at the top of each lane and is expressed in μM. "Free" indicates unbound DNA and is used as a marker, "Con" is the ligand free control. Bands corresponding to histone-bound DNA are indicated with an arrow.

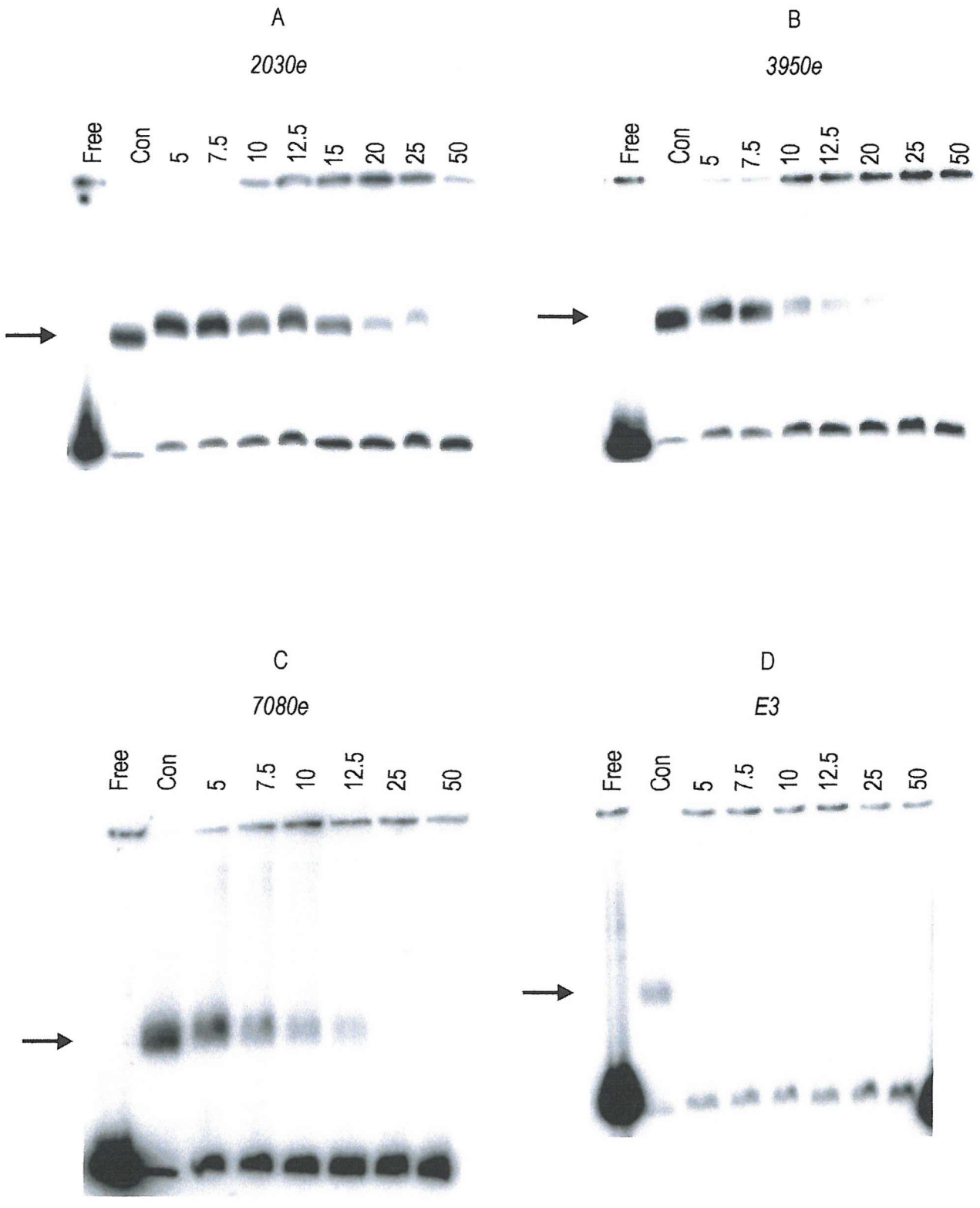

Fig 6.10 Band-shift assays of nucleosome formation in the presence of echinomycin with constructs *2030e, 3950e, 7080e* and *E3*. The ligand concentration is shown at the top of each lane and is expressed in μM. "Free" indicates unbound DNA and is used as a marker, "Con" is the ligand free control. Bands corresponding to histone-bound DNA are indicated with an arrow. .

Nucleosome Formation with Constructs *4958h, H3, 2030e, 3950e, 7080e and E3* in the Presence of Hoechst & Echinomycin

a.

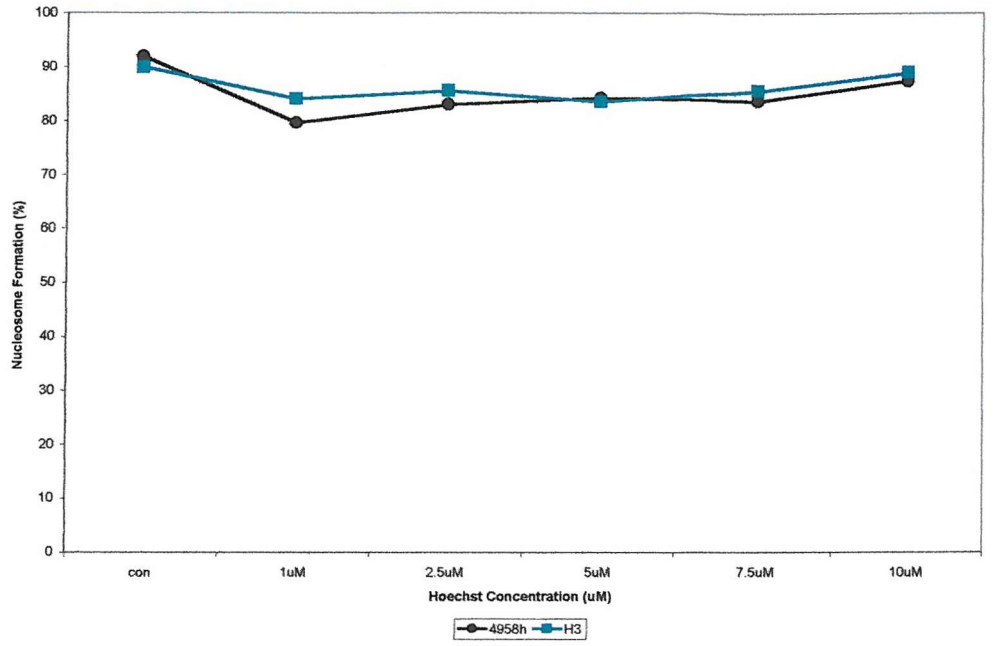

b.

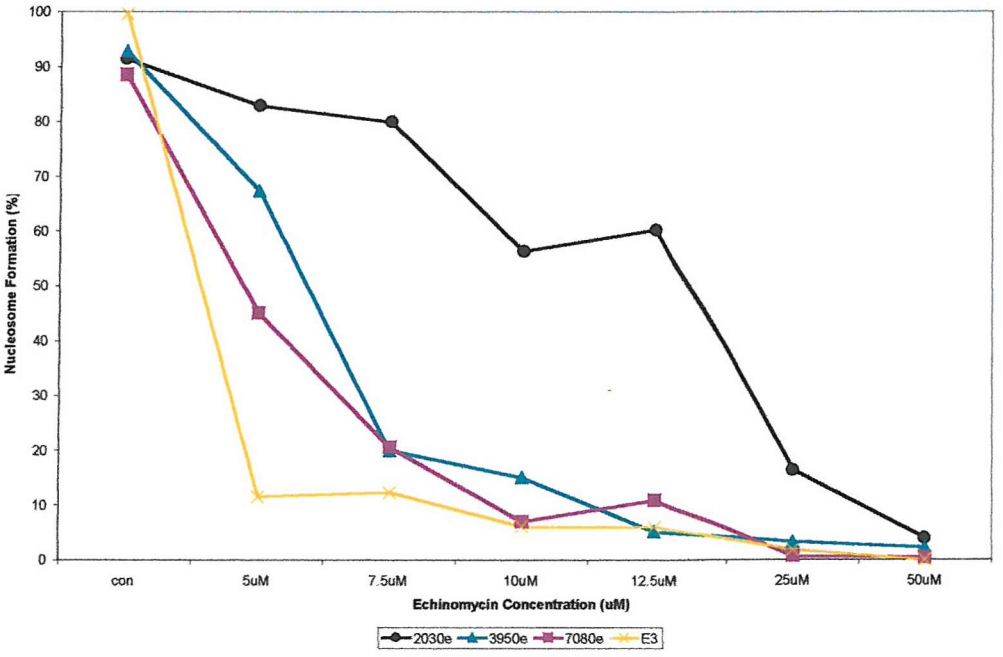

Fig 6.11 Band-shift data for constructs from chapter 5. (a), *4958h* and *H3* (b), *2030e*, *3950e*, *7080e*, and *E3* Nucleosome formation is expressed as a percentage and is shown in the y-axis. The ligand concentration is shown on the x-axis.

formation and exclusion of the ligand during reconstitution.

Once again the results are very different with the echinomycin constructs *2030e*, *3950e*, *7080e* and *E3*. Band-shift assays for these fragments are presented in fig 6.10 and corresponding data analysis is shown in fig 6.11b. As observed with all the echinomycin constructs, in this section, there is a steady decrease in nucleosome formation as the drug concentration is increased. However, the rate of decrease is different for each fragment. With *2030e* reconstitution is reduced to approximately 50% with 10μM ligand. There is then a steady reduction down to 4% with the highest drug concentration. However, with construct *3950e*, 50% nucleosome formation occurs between 5-7.5μM echinomycin, which then falls to 2% with the highest concentration. The results for *7080e* are very similar to *3950e* although the initial rate of inhibition, at 5μM ligand, is 45% for this fragment compared to 67% for *3950e*. With these three constructs, it is also interesting to note the appearance of material retained in the wells, which coincides with the reduction of a histone bound species. As with construct *44e*, this is thought to represent aggregated material, which fails to run into the gel. The final construct, *E3*, shows almost complete inhibition of a histone-bound species with the lowest drug concentration where reconstitution was calculated at only 12% with 5μM echinomycin. With 10μM drug, nucleosome formation was reduced by half to 6%, which is almost identical to *7080e* (7%), and by 50μM there was no detectible signal for a histone-bound species.

Discussion

The results presented in this chapter indicate that Hoechst does not have a significant effect on the formation of nucleosome reconstitution with these fragments, except for construct *73h* where formation was reduced at the highest drug concentration. This is in contrast to the data with echinomycin in which nucleosome formation was severely disrupted in every case. These results shed some light on the action of each ligand molecule and also pose some interesting questions about the process of

nucleosome formation itself.

The interaction of echinomycin with constructs containing previously characterised single outward and inward target sites.

The results obtained from band-shift assays with constructs *44e* and *74e* were unexpected. Since each target site in these DNA fragments lies on the outer surface of the pre-formed nucleosome it was thought that full access of the drug to its target would not inhibit the process of reconstitution. We therefore reasoned that the ligand would simply be displaced from its target site during nucleosome formation. However, the results in this chapter demonstrate, that this is not the case and that the drug prevents nucleosome formation. One plausible explanation for these observations is that echinomycin alters the local DNA conformation on binding to its target sequence. It may be that the histone core can then no longer bind the distorted DNA surface. The average helical repeat of nucleosomal DNA is 10.1 bp/turn. Since echinomycin unwinds the helix by approximately 48° it might be difficult to establish the local histone-DNA contacts present in the crystal structure. This is especially relevant since the emerging rules for nucleosome positioning appear to point to the sequence dependent conformation of DNA. If this is the case, then it might not matter what orientation the drug site is in since all that is required is to alter the DNA conformation to such an extent that it is poorly recognised by the histone octamer. From figs 6.7 and 6.8b it is clear that nucleosome formation is more severely disrupted in constructs *50e* and *100e* relative to construct *39e*. Since the target sites in *50e* and *100e* are both equidistant from the dyad it may be that the severity of disruption is a consequence of the translational position of the target sites. It is also interesting that the results observed with construct *44e* where similar to that obtained for *50e* and *100e* despite the opposite orientation of the target. We therefore conclude that the translational position of the target site in these constructs is more relevant than the rotational setting of the site during histone-DNA reconstitution. Although with construct *74e*, ligand binding had a much lower effect upon formation than with *44e*. This seems to suggest that binding of echinomycin to the outer surface close to

the dyad is better accommodated. However, with constructs containing inner facing target sites, it is plausible that the presence of a bound echinomycin molecule would further disrupt local DNA-histone contacts. Aggregation in core samples was observed in all gel-shift experiments with echinomycin. Since the majority of nucleic acid in the sample is unlabelled chicken genomic DNA it will have many potential echinomycin binding sites. When the ligand is added during these experiments it will also bind to these additional sites, which may inhibit the formation of a large population of potential nucleosomes. We therefore conclude that, in the absence of a bound DNA superhelix, many histone complexes aggregate and may non-specifically bind DNA. These large aggregates may be inhibited from entering the gel matrix and are thus visualised in the wells.

The interaction of echinomycin with constructs containing previously characterised two and three inward facing target sites.

Although two echinomycin molecules bind to construct *2030e*, the level of disruption in nucleosome formation is less than that observed with any other fragment. With construct *3950e*, the results were similar to *50e* and *100e* even though two echinomycin molecules bind to this construct. Finally, when the two sites were placed close to the dyad region there was further disruption in reconstitution.

These data further implicate that the position of the target sites are an important factor during nucleosome formation. However, with construct *E3* nucleosome formation was severely disrupted at low concentrations of echinomycin. We therefore conclude that with construct E3, the disruption in nucleosome formation is a result of binding three echinomycin molecules to the DNA fragment during reconstitution. However, from these data, it is unclear as to what extent the translational position of the sites has on nucleosome formation. We could envisage that a construct containing three targets close to one end of the DNA sequence may require higher ligand concentrations to achieve a similar level of disruption as observed with construct *E3*.

The interaction of Hoechst with constructs during nucleosome formation

The results for constructs *35h*, *46h* and *3546h* indicate that these nucleosomes form with the same rotational position as previously described in chapter 3. Since Hoechst caused little change in the conformation of the nucleosome it was expected that a similar situation would occur during nucleosome formation. Hence after nucleosome formation it is expected that the drug will be bound to the target sites located on the outer surface of the DNA superhelix. However, the result obtained for *73h* suggests that the region close to the dyad is sensitive to drug binding at the inner surface since nucleosome formation was reduced with 10μM Hoechst. Since there was no detectable change in the level of reconstitution with construct *3558h* it is concluded that the drug must be simply displaced or accommodated at the inward facing target (58-61bp). Given that Hoechst contains one formal positive charge and that the surface of the histone octamer is highly basic it would seem reasonable to conclude that the drug is displaced so as to avoid electrostatic repulsion.

With constructs *4958h* and *H3* we conclude that the rotational position of the DNA superhelix has altered in the presence of Hoechst. The ligand should have full access to the target sites during reconstitution. If the DNA superhelix binds to the histone octamer so that the target sites are facing inward, energetically unfavourable clashes between the bound Hoechst molecules and the protein surface may cause the superhelix to lie with a different rotational setting. If rotation did not occur we might expect attenuation in the histone-bound DNA species in the band-shift experiments since presumably the presence of two or more Hoechst molecules would then disrupt nucleosome formation in a manner consistent with that found in constructs containing target sites for echinomycin.

7 General Conclusions

From the results presented in this thesis it is clear that sequence selective DNA binding ligands can interact with nucleosome core particles. However, there are differences in the details of this interaction between the two drugs studied. It was previously suggested by Waring and co-workers (Portugal and Waring 1986; Portugal and Waring 1987a; Portugal and Waring 1987b) that ligands can bind to target sites located on the outer surface of the DNA superhelix, and that this interaction causes the superhelix to rotate through 180° on the surface of the histone core. The driving force for this change in conformation was thought to be an increase in non-bonded interactions between the walls of the minor groove and the bound ligand which would now be located on the histone-facing side of the superhelix and hence on the inner surface of the coil.

In the light of these conclusions, we first decided to assess the interaction of Hoechst and echinomycin with sites located on the outer facing surface of the nucleosome (chapter 3). From these experiments, it was shown that Hoechst could bind to unique target sites with this rotational setting. Binding is also observed with DNA constructs containing two or more outward facing binding sites. These results represent the first direct observation of footprints for the interaction of a ligand with nucleosome-bound DNA.

In contrast, we failed to detect binding of echinomycin to unique outward facing sites, thereby raising some interesting questions. The footprint observed with Hoechst is strongly suggestive that the DNA superhelix has not undergone a change in the rotational position.

It is possible the differences between the present results and those of Waring and co-workers (Portugal and Waring 1986; Portugal and Waring 1987a; Portugal and Waring 1987b) arise from co-operative interactions between two closely spaced echinomycin molecules in the previous studies. The helical repeat of nucleosome

DNA is approximately 10.1bp/turn, hence for two echinomycin molecules to bind in close proximity and remain on the outer surface of the core particle the closest spacing between each target site would be approximately 6bp. Cooperativity has been previously demonstrated for echinomycin binding to two CG sites which are separated by up to 4bp (Bailly *et al.* 1996) but it is presently not clear whether this would extend to 6bp. In addition, the region between each target site, on nucleosome DNA, would have extensive interactions with the histone octamer principally via salt linkages between hydroxyl side-chains and phosphate groups of the helix backbone. If cooperativity, between two CG sites, were mediated through alterations in the conformation of the DNA, then histone-DNA contacts at the inner-facing region between the target sites would presumably inhibit such a mechanism.

Since no significant changes in the rotational position were evident with outer facing Hoechst sites, the next series of experiments evaluated the role of single inward facing sites. The results presented in chapter 4 demonstrated that binding to these did not cause any change in the conformation of the nucleosome, except for construct *73h* where the inner facing site was positioned close to the dyad axis. Waring and co-workers (Portugal and Waring 1986; Portugal and Waring 1987a; Portugal and Waring 1987b) proposed that two or more ligands might be required to bring about a change in the rotational setting of the DNA superhelix. These experiments with single inward facing sites are therefore consistent with this suggestion.

In chapter 5, the studies with 2-3 inner-facing target sites showed that Hoechst 33258 produced clear changes in the digestion pattern of the construct, consistent with a change in the rotational setting of the DNA. These results are in agreement with previous work carried out by Brown and Fox (1996) in which a construct with multiple inward facing Hoechst sites was observed to rotate in the presence of ligand. In contrast, echinomycin failed to alter the rotational position of the DNA superhelix even when three inward facing sites were present.

These different results must reflect differences in the structures and modes of binding

of the two ligands. Hoechst is smaller than echinomycin and causes little change in DNA conformation upon binding. It also carries one formal positive charge. In contrast, echinomycin causes large local distortions in DNA conformation, and is composed primarily of neutral amino acids ordered into a bulky octa-peptide ring.

It has been previously suggested that one contributing factor in the drug-induced rotation of the DNA superhelix might be electrostatic repulsion between a bound ligand and the histone core (Brown and Fox 1996). Under these circumstances, the positively charged piperazine group of Hoechst and the basic surface of the histone octamer may repel each other. Since some rotation is observed with two inward facing Hoechst sites it follows that two positive charges placed consecutively at the inner surface of the superhelix are sufficient to bring about this change in conformation. The presence of a third Hoechst molecule, and hence a third positive charge, increases the number of nucleosomes in the population which undergo this change in the rotational position of the superhelix (observed in the results for construct *H3* relative to *4958h*).

Without formal molecular modelling, it is difficult to envisage exactly what interactions occur between Hoechst and the surface of the histone octamer. However, the nucleosome crystal structure reveals that an arginine side chain penetrates the minor groove every time it faces the protein core (Luger et al. 1997). This side chain is prevented from making hydrogen bond interactions with the surface of exposed DNA bases due to constrains imposed on it by the remainder of the protein. Despite this, it does occlude a significant portion of the minor groove (see fig 7.1). In this figure a section of the histone octamer has been coloured according to electrostatic charge and hence demonstrates the electro-positive nature of the DNA binding surface. What might be the sequence of events, which leads to the observed changes in the rotational position of the DNA superhelix with constructs *4958h* and *H3* in the presence of Hoechst?

In order to interact with nucleosome-bound DNA it seems reasonable to suppose that

A.

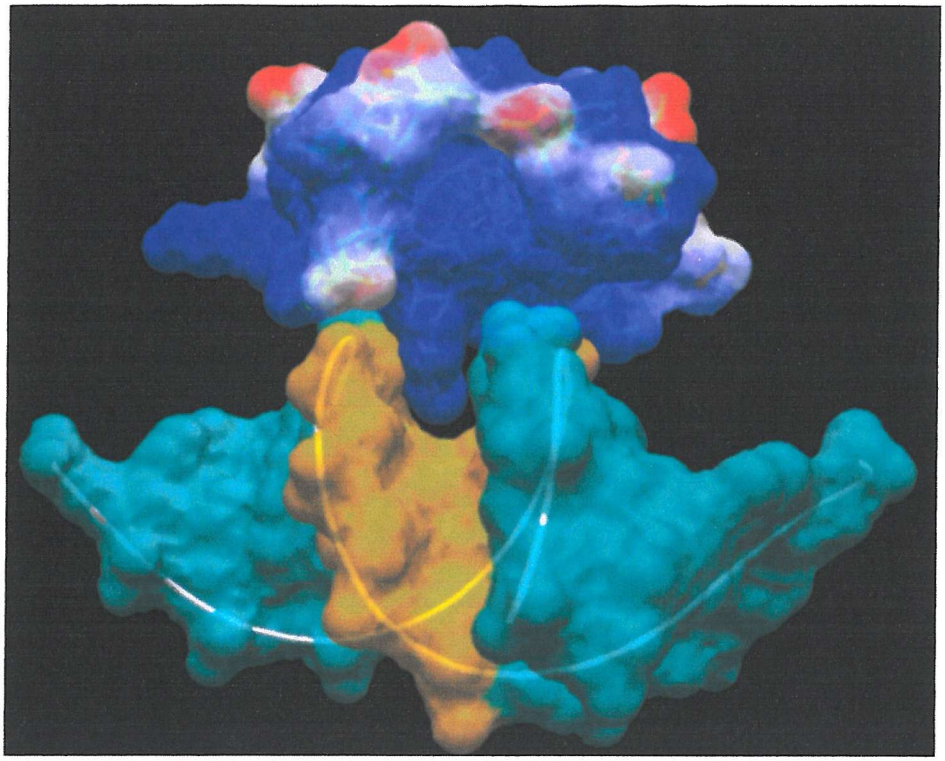

B.

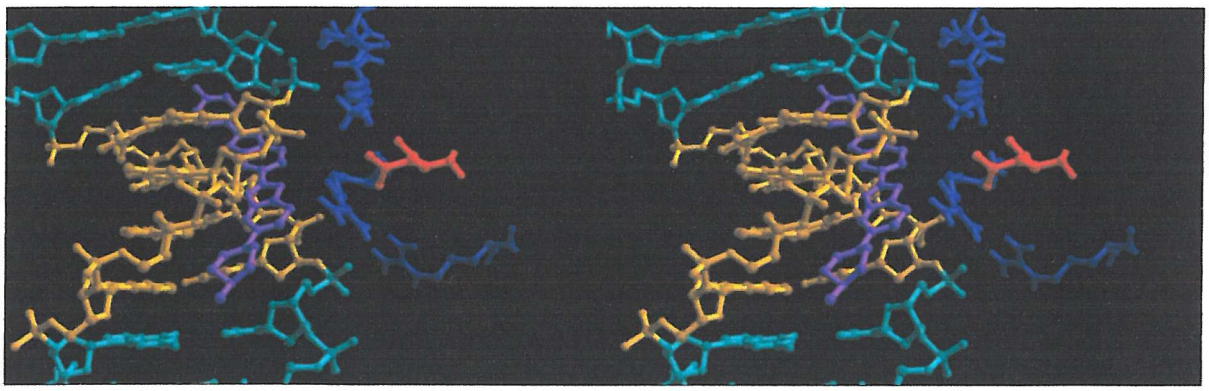

Fig 7.1 Models detailing interactions inside the inner facing minor groove. (A), the electrostatic surface of the histone octamer surrounding the AATT 49-52bp site. Blue indicates regions of positive charge with a potential approaching 1.8 while red indicates regions of negative charge with the potential approaching -1.8. Only a small area of the protein core is shown. The DNA is coloured light green with the AATT target site indicated in orange. This view looks directly into the minor groove from the top of the nucleosome. The presence of arginine is marked in the structure. (B), a stereo view of the interactions between a bound Hoechst molecule and the surface of the histoneoctamer. Acidic amino acids are coloured blue and Arg 83 is coloured red. The DNA is shown in gold with the AATT target site coloured teal. Images were created In Swiss-pdb Viewer, from the submitted file from Luger et al. 1997, and rendered in Pov-Ray for windows 98.

the ligand will have to wait until a target site becomes exposed. According to Widom and co-workers (Polach and Widom 1995), target sites further away from the nucleosome dyad will be exposed more often than those close to the centre. Therefore we might imagine that AAAA across positions 39-42bp (in construct *H3*) is more readily occupied than the AATT sites at positions 49-52 and 58-61bp. This model suggest that binding to AAAA will increase the binding to AATT (49-52bp) which will in turn increase the binding to AATT (58-52bp). These successive interactions will be cooperative. Since rotation is observed with this construct we can assume that non-favourable interactions occur between the ligand and the surface of the histone octamer, and that the binding of one molecule increases the binding of a second Hoechst molecule and so on.

This process of electrostatic repulsion between Hoechst and the surface of the histone core most probably does not occur between the piperazine group and a single histone side-chain (e.g. the minor groove facing arginine). Rather it seems more likely that piperazine interacts with the net positive charge across an area of the core since the situation is made complex by the presence of the DNA backbone and acidic protein side chains (which would neutralize positive charges on the surface of the protein; see Fig 7.1b).

How might the actual process of rotation occur? The information gained from the crystal structure of the nucleosome suggests that the DNA superhelix is unlikely to rotate across the surface of the histone core. Such a process would involve the simultaneous breaking and reforming of many salt linkages and it is unlikely that the binding of Hoechst would provide sufficient energy for this mechanism. It seems more likely that the DNA is transiently displaced from the surface of the protein and re-docks in the new rotational position. It is not clear whether this occurs by wholesale displacement of the DNA or by local displacement and re-docking, which may be subsequently propagated around the structure. However, to maintain the stability of the core, the second scenario appears more favourable.

Although the echinomycin has little effect on the conformation of pre-formed nucleosomes, it causes major disruption when added during the reconstitution process, as assessed by the band-shift experiments. As discussed in chapter 6 it is also interesting to note that inhibition of nucleosome reconstitution appears to be dependent on the translational position of the target sites. The binding of echinomycin to sites, which are expected to be close to the dyad, has a greater effect upon reconstitution than a site placed close to one end of the DNA superhelix. The binding of three ligand molecules, as in construct E3, completely abolishes nucleosome formation. The different results between constructs *44e* and *74e* may be explained by differences in the DNA conformation at each target site when complexed as a nucleosome core particle. Across positions 43-46bp the DNA has smaller helical repeat (10.1bp/turn) than found across the dyad region(10.7bp/turn). Echinomycin unwinds DNA upon binding and requires the path of the helix to be relatively straight. Therefore, it may be that a bound molecule is tolerated near the dyad, during nucleosome formation, since the drug would cause less total conformational deviation in the superhelix from that found in a native nucleosome. In contrast, binding to the site in construct *44e* induces greater conformational differences, in the DNA superhelix, relative to that found in a native nucleosome, i.e. an increased helical repeat from intercalation and less overall curvature in the path of the DNA superhelix.

Although these ligands are not used clinically, the differences in their effects upon the nucleosome may provide some information as to how they might interact with native hetero-chromatin. These results suggest that echinomycin and similar ligands will bind better to transcriptionally active chromatin in which the DNA is more exposed. In contrast minor groove ligands may be better able to bind to chromatin that is not being actively transcribed.

It is not clear whether the Hoechst-induced changes in nucleosome structure will occur in chromatin since the results in this thesis deal with isolated nucleosome core particles. It is interesting to speculate what might happen when a DNA fragment is

bound to more than one histone octamer. Could the ligand still produce a change in the rotational position of the DNA in the nucleosome containing its binding sites? If this does occur would this change in the rotational position be transmitted to other nucleosomes in the chain or would it be localized across one complex? If it were localized these changes may alter the conformation of the linker DNA between nucleosomes. An analogy is twisting an elastic band at its centre when both ends are constrained; the result is a change in structure (writhe) as the energy of twisting is accommodated. It is worth noting that $(A/T)_4$ sites are relatively common (1 in every 16 tetranucleotides – i.e. on average every 64 bases) so that every nucleosome-length fragment will contain at least one, and probably two binding sites.

The work presented in this thesis has attempted to answer some of the questions relating to the interaction of small DNA binding ligands with nucleosome core particles. We now know how many molecules are required to bring about a change in the rotational position of the DNA superhelix. There is strong evidence that the changes in nucleosome positioning are caused by Hoechst binding to the inner and not the outer surface of the nucleosome. In contrast to previous results, these data also demonstrate that echinomycin does not cause a rearrangement of nucleosome-bound DNA. These experiments have provided the first direct observation for ligand binding to the nucleosome, as seen with the clear DNaseI footprints seen with constructs containing outward facing Hoechst sites and an echinomycin construct containing two inner facing sites at the edge of the DNA superhelix. The band-shift studies clearly show that the presence of echinomycin during nucleosome formation inhibits reconstitution in a manner, which is dependent upon the translational position of the target sites. This is in agreement with studies carried out by Widom and co-workers (Polach and Widom 1995; Polach and Widom 1996; Widom 1998; Anderson and Widom 2000; Polach *et al* 2000).

References

Abu-Daya, A., Brown, P. M. & Fox, K. R. (1995). DNA sequence preferences of several AT-selective minor groove binding ligands. *Nucleic Acids Res* **23**(17), 3385-92.

Abu-Daya, A. & Fox, K. R. (1997). Interaction of minor groove binding ligands with long AT tracts. *Nucleic Acids Res* **25**(24), 4962-9.

Addess, K. J. & Feigon, J. (1994a). NMR investigation of Hoogsteen base pairing in quinoxaline antibiotic-- DNA complexes: comparison of 2:1 echinomycin, triostin A and [N- MeCys3,N-MeCys7] TANDEM complexes with DNA oligonucleotides. *Nucleic Acids Res* **22**(24), 5484-91.

Addess, K. J. & Feigon, J. (1994b). Sequence specificity of quinoxaline antibiotics. 1. Solution structure of a 1:1 complex between triostin A and [d(GACGTC)]2 and comparison with the solution structure of the [N-MeCys3,N-MeCys7]TANDEM-[d(GATATC)]2 complex. *Biochemistry* **33**(41), 12386-96.

Addess, K. J. & Feigon, J. (1994c). Sequence specificity of quinoxaline antibiotics. 2. NMR studies of the binding of [N-MeCys3,N-MeCys7]TANDEM and triostin A to DNA containing a CpI step. *Biochemistry* **33**(41), 12397-404.

Addess, K. J., Sinsheimer, J. S. & Feigon, J. (1993). Solution structure of a complex between [N-MeCys3,N-MeCys7]TANDEM and [d(GATATC)]2. *Biochemistry* **32**(10), 2498-508.

Ajiro, K., Yasuda, H. & Tsuji, H. (1996a). Vanadate triggers the transition from chromosome condensation to decondensation in a mitotic mutant (tsTM13) inactivation of p34cdc2/H1 kinase and dephosphorylation of mitosis-specific histone

H3. *Eur J Biochem* **241**(3), 923-30.

Ajiro, K., Yoda, K., Utsumi, K. & Nishikawa, Y. (1996b). Alteration of cell cycle-dependent histone phosphorylations by okadaic acid. Induction of mitosis-specific H3 phosphorylation and chromatin condensation in mammalian interphase cells. *J Biol Chem* **271**(22), 13197-201.

Alffrey, V. G., Faulkner, R. & Mirsky, A. E. (1964). Acetylation and Methylation of Histones and their Possible Role in the Regulation of RNA Synthesis. *Biochemistry* **51**, 786-795.

Alfredson, T. V., Bruins, P. W., Maki, A. H. & Excoffier, J. L. (1994). Conformer interconversion in the LC analysis of triostin A and its under-N-methylated synthetic analogue. *J Chromatogr Sci* **32**(4), 132-8.

Alfredson, T. V. & Maki, A. H. (1990). Phosphorescence and optically detected magnetic resonance studies of echinomycin-DNA complexes. *Biochemistry* **29**(38), 9052-64.

Alfredson, T. V., Maki, A. H. & Waring, M. J. (1991). Optically detected triplet-state magnetic resonance studies of the DNA complexes of the bisquinoline analogue of echinomycin. *Biochemistry* **30**(40), 9665-75.

Althaus, F. R. (1992). Poly ADP-ribosylation: a histone shuttle mechanism in DNA excision repair. *J Cell Sci* **102**(Pt 4), 663-70.

Anderson, J. D. & Widom, J. (2000). Sequence and position-dependence of the equilibrium accessibility of nucleosomal DNA target sites. *J Mol Biol* **296**(4), 979-87.

Anselmi, C., Bocchinfuso, G., De Santis, P., Savino, M. & Scipioni, A. (1999). Dual role of DNA intrinsic curvature and flexibility in determining nucleosome stability. *J Mol Biol* **286**(5), 1293-301.

Ausio, J., Dong, F. & van Holde, K. E. (1989). Use of selectively trypsinized nucleosome core particles to analyze the role of the histone "tails" in the stabilization of the nucleosome. *J Mol Biol* **206**(3), 451-63.

Ausio, J., Seger, D. & Eisenberg, H. (1984). Nucleosome core particle stability and conformational change. Effect of temperature, particle and NaCl concentrations, and crosslinking of histone H3 sulfhydryl groups. *J Mol Biol* **176**(1), 77-104.

Bailly, C., Marchand, C., Waring, M.J.(1993). New Binding Sites for Antitumour Antibiotics Created by Relocating the Purine 2-Amino Group in DNA. *J. Am. Chem. Soc* 115

Bailly, C., Gentle, D., Hamy, F., Purcell, M. & Waring, M. J. (1994). Localized chemical reactivity in DNA associated with the sequence- specific bisintercalation of echinomycin. *Biochem J* **300**(Pt 1), 165-73.

Bailly, C.,Waring, M. J.,Travers, A. A. (1995).Effects of base substitutions on the binding of a DNA-bending protein *J Mol Biol* 253 (1), 1-7

Bailly, C.,Mollegaard, N. E.,Nielsen, P. E.,Waring, M. J. (1995). The influence of the 2-amino group of guanine on DNA conformation. Uranyl and DNase I probing of inosine/diaminopurine substituted DNA. *Embo J* 14(9), 2121-31

Bailly, C.,Waring, M. J. (1995). Transferring the purine 2-amino group from guanines to adenines in DNA changes the sequence-specific binding of antibiotics. *Nucleic Acids Res* 23(6), 885-92

Bailly, C., Hamy, F. & Waring, M. J. (1996). Cooperativity in the binding of echinomycin to DNA fragments containing closely spaced CpG sites. *Biochemistry* **35**(4), 1150-61.

Bailly, C. & Waring, M. J. (1998). DNA recognition by quinoxaline antibiotics: use of base-modified DNA molecules to investigate determinants of sequence-specific binding of triostin A and TANDEM. *Biochem J* **330**(Pt 1), 81-7.

Balasubramanian, B., Pogozelski, W. K. & Tullius, T. D. (1998). DNA strand breaking by the hydroxyl radical is governed by the accessible surface areas of the hydrogen atoms of the DNA backbone. *Proc Natl Acad Sci U S A* **95**(17), 9738-43.

Baldi, P., Brunak, S., Chauvin, Y. & Krogh, A. (1996). Naturally occurring nucleosome positioning signals in human exons and introns. *J Mol Biol* **263**(4), 503-10.

Berman, H. H. & Schneider, B. (1999). Nucleic acid hydration. In *Oxford Handbook of Nuceic Acid Structure* (Neidle, S., ed.), pp. 295-310. Oxford University Press.

Bonvin, A. M., Sunnerhagen, M., Otting, G. & van Gunsteren, W. F. (1998). Water molecules in DNA recognition II: a molecular dynamics view of the structure and hydration of the trp operator. *J Mol Biol* **282**(4), 859-73.

Bostock-Smith, C. E., Laughton, C. A. & Searle, M. S. (1999). Solution structure and dynamics of the A-T tract DNA decamer duplex d(GGTAATTACC)2: implications for recognition by minor groove binding drugs. *Biochem J* **342**(Pt 1), 125-32.

Bostock-Smith, C. E. & Searle, M. S. (1999). DNA minor groove recognition by bis-benzimidazole analogues of Hoechst 33258: insights into structure-DNA affinity

relationships assessed by fluorescence titration measurements. *Nucleic Acids Res* **27**(7), 1619-24.

Boulikas, T. (1990). Poly(ADP-ribosylated) histones in chromatin replication. *J Biol Chem* **265**(24), 14638-47.

Bradbury, E. M. (1992). Reversible histone modifications and the chromosome cell cycle. *Bioessays* **14**(1), 9-16.

Brown, P. M. & Fox, K. R. (1996). Minor groove binding ligands alter the rotational positioning of DNA fragments on nucleosome core particles. *J Mol Biol* **262**(5), 671-85.

Buttinelli, M., Minnock, A., Panetta, G., Waring, M. & Travers, A. (1998). The exocyclic groups of DNA modulate the affinity and positioning of the histone octamer. *Proc Natl Acad Sci U S A* **95**(15), 8544-9.

Buttinelli, M., Negri, R., Di Marcotullio, L. & Di Mauro, E. (1995). Changing nucleosome positions through modification of the DNA rotational information. *Proc Natl Acad Sci U S A* **92**(23), 10747-51.

Cacchione, S., Caneva, R. & Savino, M. (1986). Selective binding of actinomycin D induces a reversible conformational transition of nucleosomes. *Biochim Biophys Acta* **867**(4), 229-33.

Cacchione, S., Cerone, M. A. & Savino, M. (1997). In vitro low propensity to form nucleosomes of four telomeric sequences. *FEBS Lett* **400**(1), 37-41.

Carrondo, M. A., Coll, M., Aymami, J., Wang, A. H., van der Marel, G. A., van Boom, J. H. & Rich, A. (1989). Binding of a Hoechst dye to d(CGCGATATCGCG)

and its influence on the conformation of the DNA fragment. *Biochemistry* **28**(19), 7849-59.

Cera, C., Palu, G., Magno, S. M. & Palumbo, M. (1991). Interaction between second generation anthracyclines and DNA in the nucleosomal structure. *Nucleic Acids Res* **19**(9), 2309-14.

Cera, C. & Palumbo, M. (1991). The peculiar binding properties of 4'-deoxy,4'-iododoxorubicin to isolated DNA and 175 bp nucleosomes. *Nucleic Acids Res* **19**(20), 5707-11.

Chadee, D. N., Hendzel, M. J., Tylipski, C. P., Allis, C. D., Bazett-Jones, D. P., Wright, J. A. & Davie, J. R. (1999). Increased Ser-10 phosphorylation of histone H3 in mitogen-stimulated and oncogene-transformed mouse fibroblasts. *J Biol Chem* **274**(35), 24914-20.

Chaires, J. B., Dattagupta, N. & Crothers, D. M. (1983). Binding of daunomycin to calf thymus nucleosomes. *Biochemistry* **22**(2), 284-92.

Chao, M. V., Gralla, J. & Martinson, H. G. (1979). DNA sequence directs placement of histone cores on restriction fragments during nucleosome formation. *Biochemistry* **18**(6), 1068-74.

Churchill, M. E., Hayes, J. J. & Tullius, T. D. (1990). Detection of drug binding to DNA by hydroxyl radical footprinting. Relationship of distamycin binding sites to DNA structure and positioned nucleosomes on 5S RNA genes of Xenopus. *Biochemistry* **29**(25), 6043-50.

Clarke, M. F., FitzGerald, P. C., Brubaker, J. M. & Simpson, R. T. (1985). Sequence-specific interaction of histones with the simian virus 40 enhancer region in

vitro. *J Biol Chem* **260**(23), 12394-7.

Clements, A., Rojas, J. R., Trievel, R. C., Wang, L., Berger, S. L. & Marmorstein, R. (1999). Crystal structure of the histone acetyltransferase domain of the human PCAF transcriptional regulator bound to coenzyme A. *Embo J* **18**(13), 3521-32.

Cockell, M., Rhodes, D. & Klug, A. (1983). Location of the primary sites of micrococcal nuclease cleavage on the nucleosome core. *J Mol Biol* **170**(2), 423-46.

Cons, B. M. & Fox, K. R. (1989). High resolution hydroxyl radical footprinting of the binding of mithramycin and related antibiotics to DNA. *Nucleic Acids Res* **17**(14), 5447-59.

Costanzo, G., Di Mauro, E., Salina, G. & Negri, R. (1990). Attraction, phasing and neighbour effects of histone octamers on curved DNA. *J Mol Biol* **216**(2), 363-74.

Creighton, T. E. (1992). *Proteins: Structures and Molecular Properties*. 2nd edition edit, W.H. Freeman and Company.

Diaz, B. M. & Walker, I. O. (1983). Trypsin digestion of core chromatin. *Biosci Rep* **3**(3), 283-92.

Dong, F., Hansen, J. C. & van Holde, K. E. (1990a). DNA and protein determinants of nucleosome positioning on sea urchin 5S rRNA gene sequences in vitro. *Proc Natl Acad Sci U S A* **87**(15), 5724-8.

Dong, F., Nelson, C. & Ausio, J. (1990b). Analysis of the changes in the structure and hydration of the nucleosome core particle at moderate ionic strengths. *Biochemistry* **29**(47), 10710-6.

Draganescu, A., Levin, J. R. & Tullius, T. D. (1995). Homeodomain proteins: what governs their ability to recognize specific DNA sequences? *J Mol Biol* **250**(5), 595-608.

Drew, H. R. & Calladine, C. R. (1987). Sequence-specific positioning of core histones on an 860 base-pair DNA. Experiment and theory. *J Mol Biol* **195**(1), 143-73.

Drew, H. R. & Travers, A. A. (1985). DNA bending and its relation to nucleosome positioning. *J Mol Biol* **186**(4), 773-90.

Drew, H. R., Wing, R. M., Takano, T., Broka, C., Tanaka, S., Itakura, K. & Dickerson, R. E. (1981). Structure of a B-DNA dodecamer: conformation and dynamics. *Proc Natl Acad Sci U S A* **78**(4), 2179-83.

Eisfeld, K., Candau, R., Truss, M. & Beato, M. (1997). Binding of NF1 to the MMTV promoter in nucleosomes: influence of rotational phasing, translational positioning and histone H1. *Nucleic Acids Res* **25**(18), 3733-42.

Embrey, K. J., Searle, M. S. & Craik, D. J. (1993). Interaction of Hoechst 33258 with the minor groove of the A + T-rich DNA duplex d(GGTAATTACC)2 studied in solution by NMR spectroscopy. *Eur J Biochem* **211**(3), 437-47.

Fede, A., Labhardt, A., Bannwarth, W. & Leupin, W. (1991). Dynamics and binding mode of Hoechst 33258 to d(GTGGAATTCCAC)2 in the 1:1 solution complex as determined by two-dimensional 1H NMR. *Biochemistry* **30**(48), 11377-88.

Feigon, J., Denny, W. A., Leupin, W. & Kearns, D. R. (1984a). Interactions of antitumor drugs with natural DNA: 1H NMR study of binding mode and kinetics. *J Med Chem* **27**(4), 450-65.

Feigon, J., Wang, A. H., van der Marel, G. A., Van Boom, J. H. & Rich, A. (1984b). A one- and two-dimensional NMR study of the B to Z transition of (m5dC- dG)3 in methanolic solution. *Nucleic Acids Res* **12**(2), 1243-63.

Fitzgerald, D. J. & Anderson, J. N. (1998). Unique translational positioning of nucleosomes on synthetic DNAs. *Nucleic Acids Res* **26**(11), 2526-35.

Flaus, A., Luger, K., Tan, S. & Richmond, T. J. (1996). Mapping nucleosome position at single base-pair resolution by using site-directed hydroxyl radicals. *Proc Natl Acad Sci U S A* **93**(4), 1370-5.

Flaus, A. & Richmond, T. J. (1998). Positioning and stability of nucleosomes on MMTV 3'LTR sequences. *J Mol Biol* **275**(3), 427-41.

Fletcher, M. C. & Fox, K. R. (1996a). Dissociation kinetics of echinomycin from CpG binding sites in different sequence environments. *Biochemistry* **35**(3), 1064-75.

Fletcher, M. C. & Fox, K. R. (1996b). Visualising the dissociation of sequence selective ligands from individual binding sites on DNA. *FEBS Lett* **380**(1-2), 118-22.

Fox, K. R. (1997). DNaseI Footprinting. In *Drug-DNA Interaction Protocols* 1 edit. (Fox, K. R., ed.), Vol. Methods in Molecular Biology: Volume 90. Humana Press.

Fox, K. R. & Cons, B. M. (1993). Interaction of mithramycin with DNA fragments complexed with nucleosome core particles: comparison with distamycin and echinomycin. *Biochemistry* **32**(28), 7162-71.

Fox, K. R., Cornish, A., Williams, R. C. & Waring, M. J. (1983). The use of radiolabelled triostin antibiotics to measure low levels of binding to deoxyribonucleic acid. *Biochem J* **211**(3), 543-51.

Fox, K. R., Gauvreau, D., Goodwin, D. C. & Waring, M. J. (1980). Binding of quinoline analogues of echinomycin to deoxyribonucleic acid. Role of the chromophores. *Biochem J* **191**(3), 729-42.

Fox, K. R., Harrison, N. L. & Waring, M. J. (1981a). Changes in contour length of polydeoxynucleotide fragments: direct evidence for bifunctional intercalative binding of antibiotic ligands. *FEBS Lett* **133**(2), 305-10.

Fox, K. R. & Kentebe, E. (1990). Echinomycin binding to the sequence CG(AT)nCG alters the structure of the central AT region. *Nucleic Acids Res* **18**(8), 1957-63.

Fox, K. R., Marks, J. N. & Waterloh, K. (1991). Echinomycin binding to alternating AT. *Nucleic Acids Res* **19**(24), 6725-30.

Fox, K. R., Wakelin, L. P. & Waring, M. J. (1981b). Kinetics of the interaction between echinomycin and deoxyribonucleic acid. *Biochemistry* **20**(20), 5768-79.

Fox, K. R. & Waring, M. J. (1984). Stopped-flow kinetic studies on the interaction between echinomycin and DNA. *Biochemistry* **23**(12), 2627-33.

Fox, K. R. & Waring, M. J. (1985). Kinetic evidence that echinomycin migrates between potential DNA binding sites. *Nucleic Acids Res* **13**(2), 595-603.

Galas, D. J. & Schmitz, A. (1978). DNAse footprinting: a simple method for the detection of protein-DNA binding specificity. *Nucleic Acids Res* **5**(9), 3157-70.

Gallego, J., Luque, F. J., Orozco, M., Burgos, C., Alvarez-Builla, J., Rodrigo, M. M. &
Gago, F. (1994). DNA sequence-specific reading by echinomycin: role of hydrogen bonding and stacking interactions. *J Med Chem* **37**(11), 1602-9.

Gallego, J., Ortiz, A. R. & Gago, F. (1993). A Molecular Dynamics Study of the Bis-Intercalation Complexes of Echinomycin with d(ACGT)2 and d(TCGA)2: Rational for Sequemce-Specific Hoogsteen Base Pairing. *J. Med. Chem.* **36**, 1548-1561.

Gao, X. & D.J., P. (1988). NMR Studies of Echinomycin Bisintercalation Complexes with d(A1-C2-G3-T4) and d(T1-C2-G3-A4) Duplexes in Aqueous Solution: Sequence-Dependent Formation of Hoogsteen A1-T4 and Watson-Crick T1-A4 Base Pairs Flanking the Bisintercalation Site. *Biochemistry* **27**(5), 1744-1751.

Gao, X. & Patel, D. J. (1989). Antitomour drug-DNA interactions: NMR studies of echinomycin and chromomycin complexes. *Quarerly Reviews of Biophisics* **22**, 93-138.

Gavathiotis, E., Sharman, G. J. & Searle, M. S. (2000). Sequence-dependent variation in DNA minor groove width dictates orientational preference of Hoechst 33258 in A-tract recognition: solution NMR structure of the 2:1 complex with d(CTTTTGCAAAAG)(2). *Nucleic Acids Res* **28**(3), 728-35.

Gilbert, D. E. & Feigon, J. (1991). The DNA sequence at echinomycin binding sites determines the structural changes induced by drug binding: NMR studies of echinomycin binding to [d(ACGTACGT)]2 and [d(TCGATCGA)]2. *Biochemistry* **30**(9), 2483-94.

Gilbert, D. E. & Feigon, J. (1992). Proton NMR study of the [d(ACGTATACGT)]2-2echinomycin complex: coformational changes between echinomycin binding sites. *Nuc. Acid. Res* **20**(10), 2411-2420.

Gilbert, D. E., Van der Marel, G. A., Boom, J. H. & Feigon, J. (1989). Unstable Hoogsteen base pairs adjecent to echinomycin binding sites within a DNA duplex. *Proc. Natl. Acad. Sci. USA* **86**, 3006-3010.

Godde, J. S. & Wolffe, A. P. (1996). Nucleosome assembly on CTG triplet repeats. *J Biol Chem* **271**(25), 15222-9.

Goodsell, D. & Dickerson, R. E. (1986). Isohelical analysis of DNA groove-binding drugs. *J Med Chem* **29**(5), 727-33.

Goto, H., Tomono, Y., Ajiro, K., Kosako, H., Fujita, M., Sakurai, M., Okawa, K., Iwamatsu, A., Okigaki, T., Takahashi, T. & Inagaki, M. (1999). Identification of a novel phosphorylation site on histone H3 coupled with mitotic chromosome condensation. *J Biol Chem* **274**(36), 25543-9.

Guo, X. W., Th'ng, J. P., Swank, R. A., Anderson, H. J., Tudan, C., Bradbury, E. M. & Roberge, M. (1995). Chromosome condensation induced by fostriecin does not require p34cdc2 kinase activity and histone H1 hyperphosphorylation, but is associated with enhanced histone H2A and H3 phosphorylation. *Embo J* **14**(5), 976-85.

Haq, I., Ladbury, J. E., Chowdhry, B. Z., Jenkins, T. C. & Chaires, J. B. (1997). Specific binding of hoechst 33258 to the d(CGCAAATTTGCG)2 duplex: calorimetric and spectroscopic studies. *J Mol Biol* **271**(2), 244-57.

Harp, J. M. Hanson, B. L. Timm, D. E. Bunick, G. J. (2001). Asymmetries in the nucleosome core particle at 2.5 A resolution. *Acta Crystallogr D Biol Crystallogr* **56** (12), 1513-34

Harshman, K. D. & Dervan, P. B. (1985). Molecular recognition of B-DNA by Hoechst 33258. *Nucleic Acids Res* **13**(13), 4825-35.

Hayes, J., Clark, J. & Wolffe, A. (1991a). Histone contributions to the structure of DNA in the nucleosome. *Biochemistry* **88**, 6829 - 6833.

Hayes, J. J., Bashkin, J., Tullius, T. D. & Wolffe, A. P. (1991b). The histone core exerts a
dominant constraint on the structure of DNA in a nucleosome. *Biochemistry* **30**(34), 8434-40.

Hayes, J. J., Tullius, T. D. & Wolffe, A. P. (1990). The structure of DNA in a nucleosome. *Proc Natl Acad Sci U S A* **87**(19), 7405-9.

Heinemann, U., Alings, C. & Bansal, M. (1992). Double helix conformation, groove dimensions and ligand binding potential of a G/C stretch in B-DNA. *Embo J* **11**(5), 1931-9.

Herrera, J. E. & Chaires, J. B. (1994). Characterization of preferred deoxyribonuclease I cleavage sites. *J Mol Biol* **236**(2), 405-11.

Hogan, M. E., Roberson, M. W. & Austin, R. H. (1989). DNA flexibility variation may dominate DNase I cleavage. *Proc Natl Acad Sci U S A* **86**(23), 9273-7.

Houssier, C., Depauw-Gillet, M. C., Hacha, R. & Fredericq, E. (1983). Alteration in the nucleosome and chromatin structures upon interaction with platinum coordination complexes. *Biochim Biophys Acta* **739**(3), 317-25.

Kimura, A. & Horikoshi, M. (1998). How do histone acetyltransferases select lysine residues in core histones? *FEBS Lett* **431**(2), 131-3.

Kralovics, R., Fajkus, J., Kovarik, A. & Bezdek, M. (1995). DNA curvature of the tobacco GRS repetitive sequence family and its relation to nucleosome positioning. *J Biomol Struct Dyn* **12**(5), 1103-19.

Kuo, M. H., Brownell, J. E., Sobel, R. E., Ranalli, T. A., Cook, R. G., Edmondson, D. G., Roth, S. Y. & Allis, C. D. (1996). Transcription-linked acetylation by Gcn5p

of histones H3 and H4 at specific lysines. *Nature* **383**(6597), 269-72.

Lahm, A. & Suck, D. (1991). DNase I-induced DNA conformation. 2 A structure of a DNase I-octamer complex. *J Mol Biol* **222**(3), 645-67.

Landt, O., Grunert, H. P. & Hahn, U. (1990). A general method for rapid site-directed mutagenesis using the polymerase chain reaction. *Gene* **96**(1), 125-8.

Larsen, T. A., Kopka, M. L. & Dickerson, R. E. (1991). Crystal structure analysis of the B-DNA dodecamer CGTGAATTCACG. *Biochemistry* **30**(18), 4443-9.

Laughton, C. & Luisi, B. (1998). The Mechanics of Minor Groove Width Variation in DNA, its Implications for the Accomodation of Ligands. *J. Mol. Biol* **288**, 953-963.

Lee, J. S. & Waring, M. J. (1978a). Bifunctional intercalation and sequence specificity in the binding of quinomycin and triostin antibiotics to deoxyribonucleic acid. *Biochem J* **173**(1), 115-28.

Lee, J. S. & Waring, M. J. (1978b). Interaction between synthetic analogues of quinoxaline antibiotics and nucleic acids. Changes in mechanism and specificity related to structural alterations. *Biochem J* **173**(1), 129-44.

Lee, K. M. & Hayes, J. J. (1997). The N-terminal tail of histone H2A binds to two distinct sites within the nucleosome core. *Proc Natl Acad Sci U S A* **94**(17), 8959-64.

Lee, S. & Hahn, S. (1995). Model for binding of transcription factor TFIIB to the TBP-DNA complex. *Nature* **376**(6541), 609-12.

Loontiens, F. G., McLaughlin, L. W., Diekmann, S. & Clegg, R. M. (1991). Binding of Hoechst 33258 and 4',6'-diamidino-2-phenylindole to self- complementary decadeoxynucleotides with modified exocyclic base substituents. *Biochemistry* **30**(1),

182-9.

Loontiens, F. G., Regenfuss, P., Zechel, A., Dumortier, L. & Clegg, R. M. (1990). Binding characteristics of Hoechst 33258 with calf thymus DNA, poly[d(A- T)], and d(CCGGAATTCCGG): multiple stoichiometries and determination of tight binding with a wide spectrum of site affinities. *Biochemistry* **29**(38), 9029-39.

Low, C. M., Drew, H. R. & Waring, M. J. (1984a). Sequence-specific binding of echinomycin to DNA: evidence for conformational changes affecting flanking sequences. *Nucleic Acids Res* **12**(12), 4865-79.

Low, C. M., Drew, H. R. & Waring, M. J. (1986a). Echinomycin and distamycin induce rotation of nucleosome core DNA. *Nucleic Acids Res* **14**(17), 6785-801.

Low, C. M., Fox, K. R., Olsen, R. K. & Waring, M. J. (1986b). DNA sequence recognition by under-methylated analogues of triostin A. *Nucleic Acids Res* **14**(5), 2015-33.

Low, C. M., Olsen, R. K. & Waring, M. J. (1984b). Sequence preferences in the binding to DNA of triostin A and TANDEM as reported by DNase I footprinting. *FEBS Lett* **176**(2), 414-20.

Lowary, P. T. & Widom, J. (1998). New DNA sequence rules for high affinity binding to histone octamer and sequence-directed nucleosome positioning. *J Mol Biol* **276**(1), 19-42.

Lowman, H. & Bina, M. (1990). Correlation between dinucleotide periodicities and nucleosome positioning on mouse satellite DNA. *Biopolymers* **30**(9-10), 861-76.

Luger, K., Mader, A. W., Richmond, R. K., Sargent, D. F. & Richmond, T. J. (1997).

Crystal structure of the nucleosome core particle at 2.8 A resolution [see comments]. *Nature* **389**(6648), 251-60.

Marchand, C., Bailly, C., McLean, M. J., Moroney, S. E. & Waring, M. J. (1992). The 2-amino group of guanine is absolutely required for specific binding of the anti-cancer antibiotic echinomycin to DNA. *Nucleic Acids Res* **20**(21), 5601-6.

Martin, R. F. & Holmes, N. (1983). Use of an 125I-labelled DNA ligand to probe DNA structure. *Nature* **302**(5907), 452-4.

McGhee, J. D. & Felsenfeld, G. (1980). Nucleosome structure. *Annu Rev Biochem* **49**, 1115-56.

McLean, M. J., Seela, F. & Waring, M. J. (1989). Echinomycin-induced hypersensitivity to osmium tetroxide of DNA fragments incapable of forming Hoogsteen base pairs. *Proc Natl Acad Sci U S A* **86**(24), 9687-91.

Mendel, D. & Dervan, P. B. (1987). Hoogsteen base pairs proximal and distal to echinomycin binding sites on DNA. *Proc Natl Acad Sci U S A* **84**(4), 910-4.

Mikhailov, M. V., Zasedatelev, A. S., Krylov, A. S. & Gurskii, G. V. (1981). [Mechanism of AT base pairs recognition by molecules of dye "Hoechst 33258"]. *Mol Biol (Mosk)* **15**(3), 690-705.

Murray, V. & Martin, R. F. (1988). Sequence specificity of 125I-labelled Hoechst 33258 damage in six closely related DNA sequences. *J Mol Biol* **203**(1), 63-73.

Murray, V. & Martin, R. F. (1994). Ultraviolet light-induced cleavage of DNA in the presence of iodoHoechst 33258: the sequence specificity of the reaction. *Nucleic Acids Res* **22**(3), 506-13.

Oefner, C. & Suck, D. (1986). Crystallographic refinement and structure of DNase I at 2 A resolution. *J Mol Biol* **192**(3), 605-32.

Ohsumi, K., Katagiri, C. & Kishimoto, T. (1993). Chromosome condensation in Xenopus mitotic extracts without histone H1. *Science* **262**(5142), 2033-5.

Park, J. Y. & Choi, B. S. (1995). NMR investigation of echinomycin binding to d(ACGTTAACGT)2: Hoogsteen versus Watson-Crick A.T base pairing between echinomycin binding sites. *J Biochem (Tokyo)* **118**(5), 989-95.

Parkinson, J. A., Barber, J., Douglas, K. T., Rosamond, J. & Sharples, D. (1990). Minor-groove recognition of the self-complementary duplex d(CGCGAATTCGCG)2 by Hoechst 33258: a high-field NMR study. *Biochemistry* **29**(44), 10181-90.

Patterton, H. G. & Hapgood, J. (1996). The translational placement of nucleosome cores in vitro determines the access of the transacting factor suGF1 to DNA. *Nucleic Acids Res* **24**(21), 4349-55.

Patterton, H. G. & Simpson, R. T. (1995). Modified curved DNA that could allow local DNA underwinding at the nucleosomal pseudodyad fails to position a nucleosome in vivo. *Nucleic Acids Res* **23**(20), 4170-9.

Pennings, S., Meersseman, G. & Bradbury, E. M. (1991). Mobility of positioned nucleosomes on 5 S rDNA. *J Mol Biol* **220**(1), 101-10.

Pennings, S., Muyldermans, S., Meersseman, G. & Wyns, L. (1989). Formation, stability and core histone positioning of nucleosomes reassembled on bent and other nucleosome-derived DNA. *J Mol Biol* **207**(1), 183-92.

Perez, J. J. & Portugal, J. (1990). Molecular modelling study of changes induced by netropsin binding to nucleosome core particles. *Nucleic Acids Res* **18**(13), 3731-7.

Pjura, P. E., Grzeskowiak, K. & Dickerson, R. E. (1987). Binding of Hoechst 33258 to the minor groove of B-DNA. *J Mol Biol* **197**(2), 257-71.

Polach, K. J., Lowary, P. T. & Widom, J. (2000). Effects of core histone tail domains on the equilibrium constants for dynamic DNA site accessibility in nucleosomes. *J Mol Biol* **298**(2), 211-23.

Polach, K. J. & Widom, J. (1995). Mechanism of protein access to specific DNA sequences in chromatin: a dynamic equilibrium model for gene regulation. *J Mol Biol* **254**(2), 130-49.

Polach, K. J. & Widom, J. (1996). A model for the cooperative binding of eukaryotic regulatory proteins to nucleosomal target sites. *J Mol Biol* **258**(5), 800-12.

Portugal, J., Fox, K. R., McLean, M. J., Richenberg, J. L. & Waring, M. J. (1988). Diethyl pyrocarbonate can detect a modified DNA structure induced by the binding of quinoxaline antibiotics. *Nucleic Acids Res* **16**(9), 3655-70.

Portugal, J. & Waring, M. J. (1986). Antibiotics which can alter the rotational orientation of nucleosome core DNA. *Nucleic Acids Res* **14**(22), 8735-54.

Portugal, J. & Waring, M. J. (1987a). Analysis of the effects of antibiotics on the structure of nucleosome core particles determined by DNAase I cleavage. *Biochimie* **69**(8), 825-40.

Portugal, J. & Waring, M. J. (1987b). Interaction of nucleosome core particles with distamycin and echinomycin: analysis of the effect of DNA sequences. *Nucleic Acids*

Res **15**(3), 885-903.

Portugal, J. & Waring, M. J. (1988). Assignment of DNA binding sites for 4',6-diamidine-2-phenylindole and bisbenzimide (Hoechst 33258). A comparative footprinting study. *Biochim Biophys Acta* **949**(2), 158-68.

Price, M. A. & Tullius, T. D. (1992). Using hydroxyl radical to probe DNA structure. *Methods Enzymol* **212**, 194-219.

Pruss, D., Hayes, J. J. & Wolffe, A. P. (1995). Nucleosomal anatomy--where are the histones? *Bioessays* **17**(2), 161-70.

Pruss, D. & Wolffe, A. P. (1993). Histone-DNA contacts in a nucleosome core containing a Xenopus 5S rRNA gene. *Biochemistry* **32**(27), 6810-4.

Quigley, G. J., Ughetto, G., van der Marel, G. A., van Boom, J. H., Wang, A. H. & Rich, A. (1986). Non-Watson-Crick G.C and A.T base pairs in a DNA-antibiotic complex. *Science* **232**(4755), 1255-8.

Quintana, J. R., Lipanov, A. A. & Dickerson, R. E. (1991). Low-temperature crystallographic analyses of the binding of Hoechst 33258 to the double-helical DNA dodecamer C-G-C-G-A-A-T-T-C-G-C-G. *Biochemistry* **30**(42), 10294-306.

Ramsay, N. (1986). Deletion analysis of a DNA sequence that positions itself precisely on the nucleosome core. *J Mol Biol* **189**(1), 179-88.

Ramsay, N., Felsenfeld, G., Rushton, B. M. & McGhee, J. D. (1984). A 145-base pair DNA sequence that positions itself precisely and asymmetrically on the nucleosome core. *Embo J* **3**(11), 2605-11.

Realini, C. A. & Althaus, F. R. (1992). Histone shuttling by poly(ADP-ribosylation).

J Biol Chem **267**(26), 18858-65.

Roberts, M. S., Fragoso, G. & Hager, G. L. (1995). Nucleosomes reconstituted in vitro on mouse mammary tumor virus B region DNA occupy multiple translational and rotational frames. *Biochemistry* **34**(38), 12470-80.

Rossetti, L., Cacchione, S., Fua, M. & Savino, M. (1998). Nucleosome assembly on telomeric sequences. *Biochemistry* **37**(19), 6727-37.

Satchwell, S. C., Drew, H. R. & Travers, A. A. (1986). Sequence periodicities in chicken nucleosome core DNA. *J Mol Biol* **191**(4), 659-75.

Sayers, E. W. & Waring, M. J. (1993). Footprinting titration studies on the binding of echinomycin to DNA incapable of forming Hoogsteen base pairs. *Biochemistry* **32**(35), 9094-107.

Searle, M. S. & Embrey, K. J. (1990). Sequence-specific interaction of Hoechst 33258 with the minor groove of an adenine-tract DNA duplex studied in solution by 1H NMR spectroscopy. *Nucleic Acids Res* **18**(13), 3753-62.

Shen, X., Yu, L., Weir, J. W. & Gorovsky, M. A. (1995). Linker histones are not essential and affect chromatin condensation in vivo. *Cell* **82**(1), 47-56.

Shimada, T., Inokuchi, K. & Nienhuis, A. W. (1986). Chromatin structure of the human dihydrofolate reductase gene promoter. Multiple protein-binding sites. *J Biol Chem* **261**(3), 1445-52.

Shrader, T. E. & Crothers, D. M. (1989). Artificial nucleosome positioning sequences. *Proc Natl Acad Sci U S A* **86**(19), 7418-22.

Shrader, T. E. & Crothers, D. M. (1990). Effects of DNA sequence and histone-histone interactions on nucleosome placement. *J Mol Biol* **216**(1), 69-84.

Shui, X., McFail-Isom, L., Hu, G. G. & Williams, L. D. (1998). The B-DNA dodecamer at high resolution reveals a spine of water on sodium. *Biochemistry* **37**(23), 8341-55.

Singh, U. C., Pattabiraman, N., Langridge, R. & Kollman, P. A. (1986). Molecular mechanical studies of d(CGTACG)2: complex of triostin A with the middle A - T base pairs in either Hoogsteen or Watson-Crick pairing. *Proc Natl Acad Sci U S A* **83**(17), 6402-6.

Sivolob, A. V. & Khrapunov, S. N. (1995). Translational positioning of nucleosomes on DNA: the role of sequence- dependent isotropic DNA bending stiffness. *J Mol Biol* **247**(5), 918-31.

Sriram, M., van der Marel, G. A., Roelen, H. L., van Boom, J. H. & Wang, A. H. (1992). Conformation of B-DNA containing O6-ethyl-G-C base pairs stabilized by minor groove binding drugs: molecular structure of d(CGC[e6G]AATTCGCG complexed with Hoechst 33258 or Hoechst 33342. *Embo J* **11**(1), 225-32.

Staffelbach, H., Koller, T. & Burks, C. (1994). DNA structural patterns and nucleosome positioning. *J Biomol Struct Dyn* **12**(2), 301-25.

Sternglanz, R. & Schindelin, H. (1999). Structure and mechanism of action of the histone acetyltransferase Gcn5 and similarity to other N-acetyltransferases [comment]. *Proc Natl Acad Sci U S A* **96**(16), 8807-8.

Strahl, B. D. & Allis, C. D. (2000). The language of covalent histone modifications.

Nature **403**(6765), 41-5.

Strahl, B. D., Ohba, R., Cook, R. G. & Allis, C. D. (1999). Methylation of histone H3 at lysine 4 is highly conserved and correlates with transcriptionally active nuclei in Tetrahymena. *Proc Natl Acad Sci U S A* **96**(26), 14967-72.

Suck, D., Lahm, A. & Oefner, C. (1988). Structure refined to 2A of a nicked DNA octanucleotide complex with DNase I. *Nature* **332**(6163), 464-8.

Suck, D. & Oefner, C. (1986). Structure of DNase I at 2.0 A resolution suggests a mechanism for binding to and cutting DNA. *Nature* **321**(6070), 620-5.

Sunnerhagen, M., Denisov, V. P., Venu, K., Bonvin, A. M., Carey, J., Halle, B. & Otting, G. (1998). Water molecules in DNA recognition I: hydration lifetimes of trp operator DNA in solution measured by NMR spectroscopy. *J Mol Biol* **282**(4), 847-58.

Suto, R. K. Clarkson, M. J., Tremethick, D. J. Luger, K. (2000). Crystal structure of a nucleosome core particle containing the variant histone H2A.Z. Nat Struct Biol **7**(12), 1121-4.

Tanaka, S., Zatchej, M. & Thoma, F. (1992). Artificial nucleosome positioning sequences tested in yeast minichromosomes: a strong rotational setting is not sufficient to position nucleosomes in vivo. *Embo J* **11**(3), 1187-93.

Tanner, K. G., Trievel, R. C., Kuo, M. H., Howard, R. M., Berger, S. L., Allis, C. D., Marmorstein, R. & Denu, J. M. (1999). Catalytic mechanism and function of invariant glutamic acid 173 from the histone acetyltransferase GCN5 transcriptional coactivator. *J Biol Chem* **274**(26), 18157-60.

Taquet, A., Labarbe, R. & Houssier, C. (1998). Calorimetric investigation of ethidium and netropsin binding to chicken erythrocyte chromatin. *Biochemistry* **37**(25), 9119-26.

Teng, M. K., Usman, N., Frederick, C. A. & Wang, A. H. (1988). The molecular structure of the complex of Hoechst 33258 and the DNA dodecamer d(CGCGAATTCGCG). *Nucleic Acids Res* **16**(6), 2671-90.

Thomson, S., Clayton, A. L., Hazzalin, C. A., Rose, S., Barratt, M. J. & Mahadevan, L. C. (1999). The nucleosomal response associated with immediate-early gene induction is mediated via alternative MAP kinase cascades: MSK1 as a potential histone H3/HMG-14 kinase. *Embo J* **18**(17), 4779-93.

Travers, A. A. & Klug, A. (1987). The bending of DNA in nucleosomes and its wider implications. *Philos Trans R Soc Lond B Biol Sci* **317**(1187), 537-61.

Travers, A. A. & Klug, A. (1990). Bending of DNA in Nucleoprotein Complexes, pp. 57-106. Cold Spring Harbor Laboratory Press.

Trievel, R. C., Rojas, J. R., Sterner, D. E., Venkataramani, R. N., Wang, L., Zhou, J., Allis, C. D., Berger, S. L. & Marmorstein, R. (1999). Crystal structure and mechanism of histone acetylation of the yeast GCN5 transcriptional coactivator [see comments]. *Proc Natl Acad Sci U S A* **96**(16), 8931-6.

Tullius, T. D. & Dombroski, B. A. (1985). Iron(II) EDTA used to measure the helical twist along any DNA molecule. *Science* **230**(4726), 679-81.

Tullius, T. D. & Dombroski, B. A. (1986). Hydroxyl radical "footprinting": high-resolution information about DNA- protein contacts and application to lambda repressor and Cro protein. *Proc Natl Acad Sci U S A* **83**(15), 5469-73.

Ughetto, G., Wang, A. H., Quigley, G. J., van der Marel, G. A., van Boom, J. H. & Rich, A. (1985). A comparison of the structure of echinomycin and triostin A complexed to a DNA fragment. *Nucleic Acids Res* **13**(7), 2305-23.

Usachenko, S. I., Bavykin, S. G., Gavin, I. M. & Bradbury, E. M. (1994). Rearrangement of the histone H2A C-terminal domain in the nucleosome. *Proc Natl Acad Sci U S A* **91**(15), 6845-9.

Van Dyke, M. M. & Dervan, P. B. (1984). Echinomycin binding sites on DNA. *Science* **225**(4667), 1122-7.

Vega, M. C., Garcia Saez, I., Aymami, J., Eritja, R., Van der Marel, G. A., Van Boom, J. H., Rich, A. & Coll, M. (1994). Three-dimensional crystal structure of the A-tract DNA dodecamer d(CGCAAATTTGCG) complexed with the minor-groove-binding drug Hoechst 33258. *Eur J Biochem* **222**(3), 721-6.

Verreault, A., Kaufman, P. D., Kobayashi, R. & Stillman, B. (1998). Nucleosomal DNA regulates the core-histone-binding subunit of the human Hat1 acetyltransferase. *Curr Biol* **8**(2), 96-108.

Viswamitra, M. A., Kennard, O., Cruse, W. B., Egert, E., Sheldrick, G. M., Jones, P. G.,
Waring, M. J., Wakelin, L. P. & Olsen, R. K. (1981). Structure of TANDEM and its implication for bifunctional intercalation into DNA. *Nature* **289**(5800), 817-9.

Wakelin, S. P. & Waring, M. J. (1976). The binding of echinomycin to deoxyribonucleic acid. *Biochem J* **157**(3), 721-40.

Walker, I. O. (1984). Differential dissociation of histone tails from core chromatin. *Biochemistry* **23**(23), 5622-8.

Wallrath, L. L., Lu, Q., Granok, H. & Elgin, S. C. (1994). Architectural variations of inducible eukaryotic promoters: preset and remodeling chromatin structures. *Bioessays* **16**(3), 165-70.

Wang, A. H., Ughetto, G., Quigley, G. J. & Rich, A. (1986). Interactions of quinoxaline antibiotic and DNA: the molecular structure of a triostin A-d(GCGTACGC) complex. *J Biomol Struct Dyn* **4**(3), 319-42.

Wang, Y. H., Gellibolian, R., Shimizu, M., Wells, R. D. & Griffith, J. (1996). Long CCG triplet repeat blocks exclude nucleosomes: a possible mechanism for the nature of fragile sites in chromosomes. *J Mol Biol* **263**(4), 511-6.

Wang, Y. H. & Griffith, J. D. (1996). The [(G/C)3NN]n motif: a common DNA repeat that excludes nucleosomes. *Proc Natl Acad Sci U S A* **93**(17), 8863-7.

Waring, M. J. (1979). Bis-Intercalative Binding to DNA of Diacridines and Quinoxaline Antibiotics. *Australian Journal of Pharmaceutical Sciences* **8**(3), 65-71.

Waring, M. J. & Wakelin, L. P. (1974). Echinomycin: a bifunctional intercalating antibiotic. *Nature* **252**(5485), 653-7.

Waring, M. J., Bailly, C.(1994). The purine 2-amino group as a critical recognition element for binding of small molecules to DNA. *Gene* 149 (1), 69-79

Waterloh, K. & Fox, K. R. (1991). Interaction of echinomycin with An.Tn. and (AT)n regions flanking its CG binding site. *Nucleic Acids Res* **19**(24), 6719-24.

Waterloh, K., Olsen, R. K. & Fox, K. R. (1992). Bifunctional intercalator [N-MeCys3,N-MeCys7]TANDEM binds to the dinucleotide TpA. *Biochemistry* **31**(27), 6246-53.

Wei, Y., Mizzen, C. A., Cook, R. G., Gorovsky, M. A. & Allis, C. D. (1998). Phosphorylation of histone H3 at serine 10 is correlated with chromosome condensation during mitosis and meiosis in Tetrahymena. *Proc Natl Acad Sci U S A* **95**(13), 7480-4.

Wei, Y., Yu, L., Bowen, J., Gorovsky, M. A. & Allis, C. D. (1999). Phosphorylation of histone H3 is required for proper chromosome condensation and segregation. *Cell* **97**(1), 99-109.

Weston, S. A., Lahm, A. & Suck, D. (1992). X-ray structure of the DNase I-d(GGTATACC)2 complex at 2.3 A resolution. *J Mol Biol* **226**(4), 1237-56.

Widlund, H. R., Cao, H., Simonsson, S., Magnusson, E., Simonsson, T., Nielsen, P. E., Kahn, J. D., Crothers, D. M. & Kubista, M. (1997). Identification and characterization of genomic nucleosome-positioning sequences. *J Mol Biol* **267**(4), 807-17.

Widom, J. (1998). Structure, dynamics, and function of chromatin in vitro. *Annu Rev Biophys Biomol Struct* **27**, 285-327.

Winston, F. & Allis, C. D. (1999). The bromodomain: a chromatin-targeting module? *Nature* **6**(7), 601-604.

Wolffe, A. P. & Hayes, J. J. (1999). Chromatin disruption and modification. *Nucleic Acids Res* **27**(3), 711-20.

Yager, T. D. & Van Holde, K. E. (1984). Dynamics and Equilibria of Nucleosomes at Elevated Ionic Strength. *J. Biol. Chem* **259**(7), pp. 4212-4222.

Young, M. A., Ravishanker, G. & Beveridge, D. L. (1997). A 5-nanosecond molecular dynamics trajectory for B-DNA: analysis of structure, motions, and solvation. *Biophys J* **73**(5), 2313-36.

Zhurkin, V. B., Lysov, Y. P. & Ivanov, V. I. (1979). Anisotropic flexibility of DNA and the nucleosomal structure. *Nucleic Acids Res* **6**(3), 1081-96.